JOURNAL OF GEOPHYSICAL RESEARCH

The continuation of

TERRESTRIAL MAGNETISM AND ATMOSPHERIC ELECTRICITY
(1896-1948)

An International Quarterly

VOLUME 62 December, 1957 NUMBER 4

CONTENTS

(Contents concluded on outside back cover)

Part one of two parts, December, 1957

Published at

THE WILLIAM BYRD PRESS, INC.

P. O. BOX 2-W, SHERWOOD AVE. AND DURHAM ST.

RICHMOND 5, VIRGINIA

Address all correspondence to

JOURNAL OF GEOPHYSICAL RESEARCH

5241 BROAD BRANCH ROAD, NORTHWEST

WASHINGTON 15, D.C., U.S.A.

SIX DOLLARS A YEAR SINGLE NUMBERS, TWO DOLLARS

JOURNAL OF GEOPHYSICAL RESEARCH

The continuation of

Terrestrial Magnetism and Atmospheric Electricity

(1896-1948)

An International Quarterly

Founded 1896 by L. A. BAUER *Continued 1928-1948 by* J. A. FLEMING

Fields of Interest

Terrestrial Magnetism
Atmospheric Electricity
The Ionosphere
Solar and Terrestrial Relationships
Aurora, Night Sky, and Zodiacal Light
The Ozone Layer
Meteorology of Highest Atmospheric Levels
The Constitution and Physical States of the Upper Atmosphere
Special Investigations of the Earth's Crust and Interior, including experimental seismic waves, physics of the deep ocean and ocean bottom, physics in geology
And similar topics

This Journal serves the interests of investigators concerned with terrestrial magnetism and electricity, the upper atmosphere, the earth's crust and interior by presenting papers of new analysis and interpretation or new experimental or observational approach, and contributions to international collaboration. It is not in a position to print, primarily for archive purposes, extensive tables of data from observatories or surveys, the significance of which has not been analyzed.

Forward *manuscripts* to one of the Associate Editors, or to the editorial office of the Journal at 5241 Broad Branch Road, Northwest, Washington 15, D.C., U.S.A. It is preferred that manuscripts be submitted in English, but communications in French, German, Italian, or Spanish are also acceptable. A brief abstract, preferably in English, must accompany each manuscript. A *publication charge* of $8 per page will be billed by the Editor to the institution which sponsors the work of any author; private individuals are not assessed page charges. Manuscripts from outside the United States are invited, and should not be withheld or delayed because of currency restrictions or other special difficulties relating to page charges. Costs of publication are roughly twice the total income from page charges and subscriptions, and are met by subsidies from the Carnegie Institution of Washington and international and private sources.

Back issues and *reprints* are handled by the Editorial Office, 5241 Broad Branch Road, N.W., Washington 15, D.C., U.S.A.

Subscriptions are handled by the Editorial Office, 5241 Broad Branch Road, N.W., Washington 15, D.C., U.S.A.

Second-class mail privileges authorized at Richmond, Virginia

Journal of

GEOPHYSICAL RESEARCH

The continuation of

Terrestrial Magnetism and Atmospheric Electricity

OLUME 62 DECEMBER, 1957 No. 4

SWEET'S MECHANISM FOR MERGING MAGNETIC FIELDS IN CONDUCTING FLUIDS*

BY E. N. PARKER

Enrico Fermi Institute for Nuclear Studies,
The University of Chicago, Chicago 37, Illinois

(Received June 4, 1957)

ABSTRACT

Sweet's mechanism for the merging of two oppositely directed magnetic fields in a highly conducting fluid is investigated in a semi-quantitative manner. It is shown that two oppositely directed sunspot fields with scales of 10^4 km could be merged by Sweet's mechanism, if shoved firmly together, in about two weeks; their normal interdiffusion time would be of the order of 600 years. It is suggested that Sweet's mechanism may be of considerable astrophysical importance: It gives a means of altering quickly the configuration of magnetic fields in ionized gases, allowing a stable field to go over into an unstable configuration, subsequently converting much of the magnetic energy into kinetic energy of the fluid.

I. INTRODUCTION

Sweet (1956) has recently pointed out that when two oppositely directed gnetic fields of scale L in a highly conducting medium are shoved against each er, an interesting situation arises in which the two fields will interdiffuse in es small compared to the usual diffusion time $L^2\sigma/c^2$; σ is the conductivity in . Sweet's mechanism may be of importance in rapidly altering the connectivity magnetic fields associated with activity in the solar atmosphere, etc.: For tance, a sunspot field, $L \cong 10^9$ cm, has an ordinary diffusion or decay time of

*Assisted in part by the Office of Scientific Research and the Geophysics Research Directorate, Force Cambridge Research Center, Air Research and Development Command, U.S. Air Force.

the order of 2×10^{10} sec, where the temperature is 10^4 degrees Kelvin and $\sigma \cong 1.8 \times 10^{13}$ esu; with Sweet's mechanism, it is conceivable that two such oppositely directed fields can be interdiffused and their lines of force reconnected in 10^6 seconds or less.

The rapid interdiffusion of two oppositely directed fields when they are pressed together by external forces arises from the fact that the field vanishes on the surface between the two oppositely directed regions, and the entire compressive stress falls on the conducting fluid. The fluid responds to the excess pressure by flowing out of the region along the lines of force, and the two oppositely directed magnetic fields approach each other more and more closely, according to the usual hydromagnetic equation

$$\frac{\partial \mathbf{B}}{\partial t} = \nabla \times (\mathbf{v} \times \mathbf{B}) \quad \ldots\ldots\ldots\ldots\ldots\ldots\ldots\ldots (1)$$

in a medium of large electrical conductivity. Consequently, the gradient in the field density across the neutral surface between the fields increases without limit, until no matter how large may be the electrical conductivity σ, the diffusion term $(c^2/4\pi\mu\sigma)\ \nabla^2\mathbf{B}$, omitted in (1), becomes comparable to the dynamical term $\nabla \times (\mathbf{v} \times \mathbf{B})$, and the two oppositely directed fields interdiffuse as rapidly as the efflux of fluid from between the fields allows them to approach each other. The process is shown schematically in Figure 1 for two bipolar sunspot fields at the same solar latitude. Initially, the fields are widely separated and have no interconnecting lines of force. In Figure 1(*a*), we imagine that suitable fluid motions in the dense gases beneath the photosphere have shoved the two fields together, with the distortion shown. The high electrical conductivity of the solar atmosphere prevents interconnection of the lines of force. However, with the outflow of the gas caught between the two fields, as indicated in Figure 1(*b*), the gradient in **B** across the neutral plane increases until rapid interdiffusion takes place and the lines of force reconnect, as shown in Figure 1(*c*).

If l is the characteristic length of the gradient in **B** across the neutral plane, then the decay time of the field in the region of this gradient is of the order of $l^2\sigma/c^2$. The velocity u with which the fields merge is $l/(l^2\sigma/c^2)$,

$$u \cong c^2/l\sigma$$

The fluid expelled along the lines of force over a front of width L achieves a velocity v, where

$$v \cong uL/l$$

based on geometrical considerations. The pressure $B^2/8\pi$ available for squeezing the fluid out along the lines of force leads to the conclusion that

$$\tfrac{1}{2}\rho v^2 \cong B^2/8\pi$$

from energy considerations; hence $v \cong C_0$, where C_0 is the characteristic hydromagnetic velocity $B/(4\pi\rho)^{1/2}$. Therefore, it follows that

$$u \cong c(C_0/L\sigma)^{1/2}$$

$$l/L \cong c/(C_0 L\sigma)^{1/2}$$

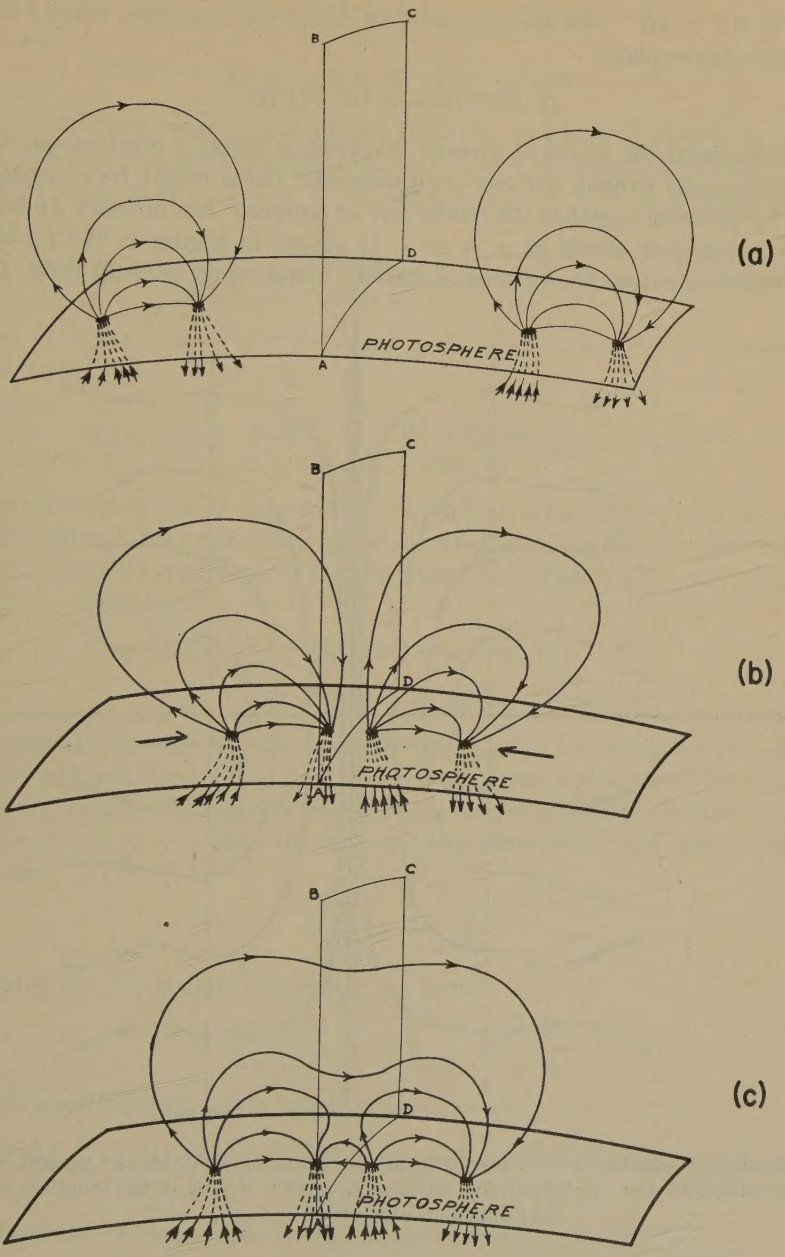

FIG. 1—(*a*) Two widely separated bipolar sunspot groups at the same solar latitudes
(*b*) The distortion of the bipolar fields as the groups are shoved together
(*c*) The reconnection of the lines of force in a week or so, as a consequence of Sweet's mechanism

thout Sweet's mechanism, the diffusion velocity would be $c^2/L\sigma$, which is equal $(l/L)u$. For the case of two bipolar sunspot fields of 1,000 gauss, $L \cong 10^9$cm, $\cong 1.8 \times 10^{13}$ esu, and $\rho = 10^{-8}$gm/cm^3, we have $C_0 \cong 100$ km/sec, $u \cong 7$ m/sec,

and $l/L \cong 0.7 \times 10^{-4}$. We see how thin, $10^{-4}L$, is the transition layer l in which the diffusion takes place.

II. EXPULSION OF FLUID

To understand the physical process involved in Sweet's mechanism, consider first how the fluid caught between two magnetic fields might be squeezed from between by pressing together the fields. Let us suppose that initially we have two infinitely conducting sheets at $x = \pm \epsilon$, as shown in Figure 2. We fill the thin layer between the two sheets with infinitely conducting inviscid fluid. Outside

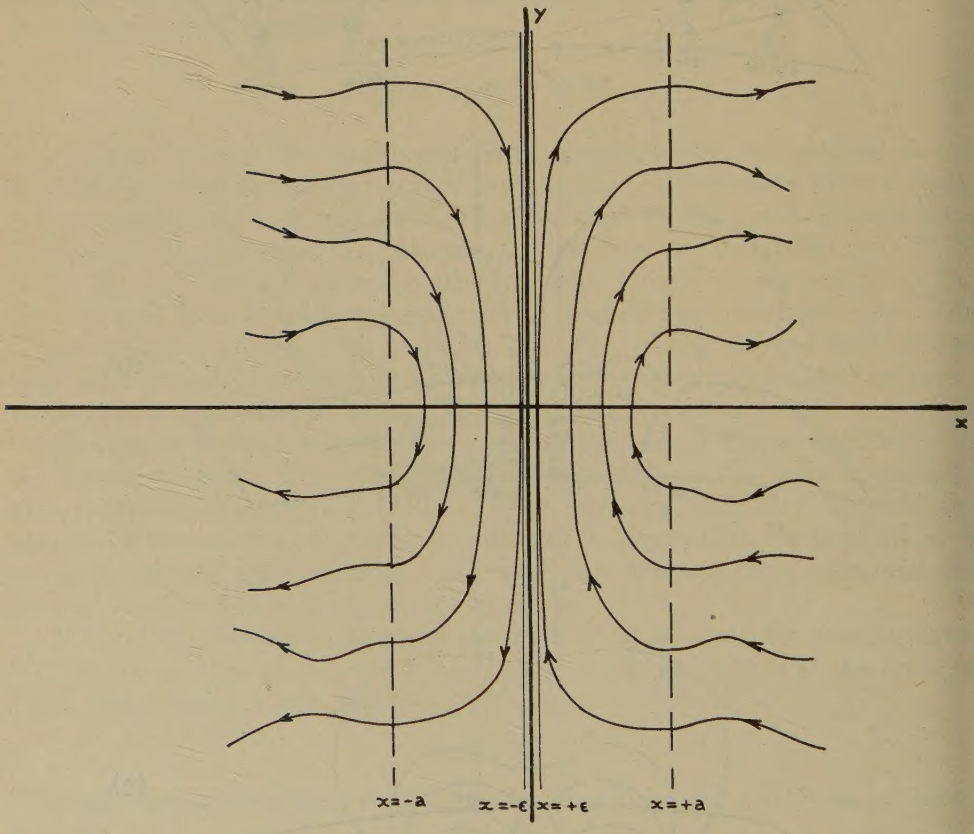

FIG. 2—Schematic diagram of two oppositely directed magnetic fields shoved against two superconducting sheets at $x = \pm \epsilon$ by suitable motions, beyond $x = \pm a$, of the infinitely conducting fluid outside the sheets at $x = \pm \epsilon$

the sheets, we introduce the magnetic field **B** with lines of force everywhere parallel to the xy-plane and expressible as the gradient of a scalar potential ψ,

$$\mathbf{B} = -\nabla\psi \quad \ldots\ldots\ldots\ldots\ldots\ldots\ldots\ldots\ldots\ldots\ldots\ldots (2)$$

so that **B** exerts no force on the conducting fluid there. To fix ideas, we suppose that the field **B** is in the grip of hydrodynamic forces in the conducting fluid beyond $x = \pm a$ and is held in such a way that $B_y = 0$ on $x = \pm a$ and

$$B_x = +B_0(y/b) \exp(-y^2/b^2)$$

t $x = +a$,

$$B_x = -B_0(y/b) \exp(-y^2/b^2)$$

t $x = -a$. As a consequence of the infinitely conducting sheets at $x = \pm \epsilon$ $\epsilon \ll a$), the field will not penetrate into $-\epsilon < x < +\epsilon$, and $B_x = 0$ on $x = \pm \epsilon$. With $\mathbf{B} = -\nabla\psi$ in $-a < x < -\epsilon$ and $+\epsilon < x < +a$, it is readily shown hat

$$\psi(x, y) = \pm\frac{B_0 b^2}{4\sqrt{\pi}} \int_{-\infty}^{+\infty} \frac{dk \sin ky}{\sinh ka} \cosh k(x \pm \epsilon) \exp(-k^2b^2/4) \quad \cdots\cdots (3)$$

where $\pm$ is $+$ for $-a < x < -\epsilon$ and $-$ for $+\epsilon < x < +a$. It follows that he field density at $x = \pm \epsilon$ is

$$B_y(\pm\epsilon, y) = \mp\frac{B_0 b^2}{4\sqrt{\pi}} \int_{-\infty}^{+\infty} \frac{dk\, k \cos ky}{\sinh ka} \exp(-k^2b^2/4)$$

f the forces beyond $x = \pm a$ press the two fields on either side of $x = \pm \epsilon$ together ufficiently firmly that the fields are considerably compressed in the x-direction nd $a \ll b$, then we may expand sinh ka about $k = 0$ and carry out the indicated ntegration, obtaining

$$\left.\begin{aligned} &B_y(\pm\epsilon, y) \sim (B_0 b/2a^2) \exp(-y^2/b^2) \\ &\times \{1 - \tfrac{1}{3}(a^2/b^2)(1 - 2y^2/b^2) + O^4(a/b)\} \end{aligned}\right\} \cdots\cdots (4)$$

The pressure exerted by the magnetic field on the two superconducting sheets t $x = \pm \epsilon$ is just $p = B_y^2(\pm\epsilon, y)/8\pi$. If we remove the superconducting sheets, o that the pressure is brought to bear directly on the field-free infinitely conducting uid in $-\epsilon < x < +\epsilon$, then the motion of an element of fluid with position $Y(t)$ s given by

$$\frac{d^2Y}{dt^2} = -\frac{1}{\rho}\frac{\partial p}{\partial y}$$

Multiplying by dY/dt and integrating, we have

$$\frac{1}{2}\left(\frac{dY}{dt}\right)^2 = -\int_{Y(0)}^{Y(t)} dy \frac{1}{\rho}\frac{\partial p}{\partial y}$$

or incompressible flow, ρ is a constant, and

$$\frac{dY(t)}{dt} = \frac{C_0 b}{2a}\left\{\exp\left[-\frac{2Y^2(0)}{b^2}\right] - \exp\left[-\frac{2Y^2(t)}{b^2}\right]\right\}^{1/2}\left\{1 + O^2\left(\frac{a}{b}\right)\right\}$$

here C_0 is the characteristic hydromagnetic velocity $B_0/(4\pi\rho)^{1/2}$.

To compute $Y(t)$ as a function of t and $Y(0)$, we expand $Y(t)$ in ascending owers of t. We may then carry out the integration, obtaining

$$\left.\begin{aligned} Y(t) = Y(0)\Bigg\{1 &+ \left(\frac{C_0 t}{a}\right)^2 \exp\left[-\frac{2Y^2(0)}{b^2}\right] \\ &+ \frac{1}{96}\left(\frac{C_0 t}{a}\right)^4\left[1 - \frac{4Y^2(0)}{b^2}\right]\exp\left[-\frac{4Y^2(0)}{b^2}\right] + O^6\left(\frac{C_0 t}{a}\right)\Bigg\} \end{aligned}\right\} \cdots\cdots (5)$$

The coefficient of the term $O^4(C_0t/a)$ is small because of the numerical factor 1/96; it vanishes when $Y(0) = \frac{1}{2}b$, and is negligible for $Y(0) > \frac{1}{2}b$ because of the exponential. Therefore, we may to good approximation neglect the term $O^4(C_0t/a)$, considering only the first two terms in the expansion. It follows that

$$\left.\begin{aligned} dY(t)/dt &\cong 2C_0[Y(0)/a](C_0t/a)\exp[-2Y^2(0)/b^2] \\ &= 2[Y(t) - Y(0)]/t \end{aligned}\right\} \quad \ldots\ldots\ldots (6)$$

$Y(0)$ may be expressed in terms of $Y(t)$, so that

$$Y(0) = Y(t)\left\{1 - \left(\frac{C_0t}{a}\right)^2 \exp\left[-\frac{2Y^2(0)}{b^2}\right] + O^4\left(\frac{C_0t}{a}\right)\right\} \quad \ldots\ldots\ldots (7)$$

Then, writing $v_y = dY(t)/dt$, $y = Y(t)$, we have

$$v_y = 2C_0(y/a)(C_0t/a)\exp(-2y^2/b^2) + O^3(C_0t/a) \quad \ldots\ldots\ldots (8)$$

We let $l(y, t)$ represent the width, in the x-direction, of the layer of field-free fluid at the position y and time t; we see that $l(y, 0) = 2\epsilon$. By integrating the equation of continuity $\nabla \cdot \mathbf{v} = 0$ for the fluid velocity from $x = -\frac{1}{2}\,l(y, t)$ to $x = +\frac{1}{2}\,l(y, t)$, we find that

$$\partial l(y, t)/\partial t + l(y, t)(\partial v_y/\partial y)_t = 0 \quad \ldots\ldots\ldots (9)$$

Hence, we find from equation (8) that

$$l(y, t) = l(y, 0)\left\{1 - \left(\frac{C_0t}{a}\right)^2\left(1 - 4\frac{y^2}{b^2}\right)\exp\left(-\frac{2y^2}{b^2}\right) + O^4(C_0t/a)\right\} \quad \ldots\ldots (10)$$

Near the x-axis, $y^2 \ll b^2$, and $l(y, t)/l(y, 0)$ is essentially independent of y; the field-free layer remains uniform as it decreases its thickness. For larger values of y^2/b^2, the decrease in thickness is not as rapid. No decrease occurs at $y^2 = b^2$, and for $y^2 > b^2$ the thickness increases; the fluid escaping from the high pressures in $y^2 < b^2$ inflates the low pressure region of $y^2 > b^2$, though, of course, the exponential factor $\exp(-2y^2/b^2)$ indicates that the inflation is not large.

III. MERGING OF FIELDS

Consider the rate at which two oppositely directed magnetic fields can merge, as a result of the squeezing out of the conducting fluid initially caught between them. Unfortunately, we are unable to solve simultaneously both the hydrodynamic equation for the motion of the fluid and the hydromagnetic equation for the magnetic field **B**. Since we have already discussed the hydrodynamic motions in a qualitative manner, we shall solve the equation for **B** in a formal manner, assuming an idealized form for the fluid motion based on the qualitative picture obtained in Section II. Thus, our final results will not be quantitative; we hope that they will represent a qualitative picture of the interdiffusion of **B**.

We shall restrict ourselves to steady-state conditions, so that $\partial/\partial t = 0$, and to the case considered in Section II, where the fields are pressed so closely together that $a \ll b$. Then, except in the region where $y^2 > b^2$, we have that v_x/v_y, B_x/B_y and $(\partial/\partial y)/(\partial/\partial x)$ are all small, $O(a/b)$. The x-component of the hydrodynamic

quation,

$$\partial \mathbf{v}/\partial t + (\mathbf{v}\cdot\nabla)\mathbf{v} = -(1/\rho)\nabla[p + B^2/8\pi] + (1/4\pi\rho)(\mathbf{B}\cdot\nabla)\mathbf{B} \quad \ldots\ldots(11)$$

ecomes

$$(\partial/\partial x)(p + B^2/8\pi) = O^2(a/b) \quad \ldots\ldots(12)$$

n Section I, we pointed out how thin is the transition layer, of thickness l, in hich the diffusion takes place between the two oppositely directed fields. For $^2 > l^2$, the field varies so slowly ($\partial/\partial x = O(1/a)$, as compared to $O(1/l)$, that or out present purposes we may regard $|\ \mathbf{B}\ (x, y)\ |$ as independent of x. Thus, e let

$$B(x, y) = B_y(\pm\epsilon, y)$$

or $x^2 > l^2$, where $B(x, y) = |\ \mathbf{B}(x, y)\ |$ and where $B_y\ (\pm\ \epsilon, y)$ is the field given n (4). We suppose that the hydrostatic pressure is p_0 at infinity. Therefore, upon ntegrating (12), we obtain

$$p(x, y) + B^2(x, y)/8\pi \cong p_0 + B_y^2(\epsilon, y)/8\pi \quad \ldots\ldots(13)$$

We cannot integrate the y-component of (11) because of the complications ntroduced by the non-linear term $v_x\partial v_y/\partial x$. However, in Section II, we found hat the expulsion of fluid from between the two fields proceeds in an orderly nd nearly uniform manner. In the region $y^2 < b^2$, we may expect to retain the ssential features of the expulsion if we introduce the qualitative argument that he elongation $\partial v_y/\partial y$ of a fluid element at a given point is proportional to the elocity which the excess pressure, $p - p_0$, at the point is capable of producing. e write

$$\frac{\partial v_y}{\partial y} = \left(\frac{p - p_0}{\rho}\right)^{1/2}\frac{1}{L}$$

is a constant of proportionality, and is $O(b)$. Using (13), we obtain

$$\frac{\partial v_y}{\partial y} = \left[\frac{B_y^2(\epsilon, y) - B^2(x, y)}{8\pi L^2\rho}\right]^{1/2} \quad \ldots\ldots(14)$$

We would like to demonstrate in our final calculations to what extent com- ressibility may enhance the merging of the two fields. The thinness of the ansition layer ($l \ll L, b$) in which the fluid is expelled suggests that it is not nreasonable to suppose that the compression may sometimes be essentially othermal; we write

$$\rho = \rho_0(p/p_0)$$

he equation of continuity under steady-state conditions becomes

$$\frac{\partial}{\partial x}(v_x p) = -p\frac{\partial v_y}{\partial y} - v_y\frac{\partial p}{\partial y}$$

t $y = 0$, $\partial v_y/\partial y$ is finite and v_y vanishes. Hence, for $y^2 < b^2$, we write

$$\frac{\partial}{\partial x}(v_x p) \cong -p\frac{\partial v_y}{\partial y} \quad \ldots\ldots(15)$$

The hydromagnetic equation

$$\frac{\partial \mathbf{B}}{\partial t} = \nabla \times (\mathbf{v} \times \mathbf{B}) + \frac{c^2}{4\pi\sigma}\nabla^2\mathbf{B}$$

may be written

$$\nabla \times [\mathbf{v} \times \mathbf{B} - (c^2/4\pi\sigma)\nabla \times \mathbf{B}] = 0$$

when $\partial/\partial t = 0$. Integrating, we find that

$$\mathbf{v} \times \mathbf{B} = (c^2/4\pi\sigma)\nabla \times \mathbf{B} + \nabla\Phi \quad \ldots\ldots(16)$$

where Φ is some scalar function of position. Since B_x and $\partial B_x/\partial y$ vanish at $y = 0$, it follows that (16) reduces to

$$v_x B_y = \frac{c^2}{4\pi\sigma}\frac{\partial B_y}{\partial x} + \nabla\Phi$$

in the region about $y = 0$. Since $v_x = 0$ at $x = 0$, we may evaluate $\nabla\Phi$ to be equal to $\partial B_y/\partial x$ at $x = 0$, or

$$v_x B_y = \frac{c^2}{4\pi\sigma}\left[\frac{\partial B_y}{\partial x} - \left(\frac{\partial B_y}{\partial x}\right)_0\right] \quad \ldots\ldots(17)$$

To determine the velocity with which the two oppositely directed fields are carried into each other, we must compute v_x outside the transition layer. Outside the transition layer, $\partial B_y/\partial x \cong B/L$ and is negligible. Hence, from (17), we find that the velocity v_∞ at which the fields merge is just

$$v_\infty = \frac{c^2}{4\pi\sigma B_y(\epsilon, y)}\left(\frac{\partial B_y}{\partial x}\right)_0 \quad \ldots\ldots(18)$$

We now use (14) to eliminate $\partial v_y/\partial y$, and (17) to eliminate v_x, from (15). We use (13) to eliminate p. Since we restrict ourselves to the region near $y = 0$, we may write $B = B_y$. We obtain

$$\left.\begin{aligned}\frac{\partial}{\partial x}\left\{\left[\frac{\beta^2(y) - B^2(x, y)}{B(x, y)}\right]\left[\frac{\partial B(x, y)}{\partial x} - \left(\frac{\partial B}{\partial x}\right)_0\right]\right\} \\ = -\eta\beta(y)[\beta^2(y) - B^2(x, y)]^{1/2}[B_\infty^2(y) - B^2(x, y)]^{1/2}\end{aligned}\right\} \quad \ldots\ldots(19)$$

where

$$B_\infty(y) \equiv B_y(\epsilon, y) \quad \ldots\ldots(20)$$

$$\beta^2(y) \equiv 8\pi p_0 + B_y^2(\epsilon, y) \quad \ldots\ldots(21)$$

$$\eta \equiv 4\pi\sigma p_0^{1/2}/c^2\rho_0^{1/2}L\beta(y) \quad \ldots\ldots(22)$$

For convenience, we let

$$\phi \equiv B(x, y)/B_y(\epsilon, y) \quad \ldots\ldots(23)$$

$$f(\phi) = (\partial B/\partial x)/(\partial B/\partial x)_0 \quad \ldots\ldots(24)$$

$$\xi \equiv B_y(\epsilon, y)/\beta(y) \quad \ldots\ldots(25)$$

treating ϕ as the independent variable in place of x. Then (19) may be rewritten

$$f\frac{df}{d\phi} - \frac{f(f-1)}{\phi}\left(\frac{1+\xi^2\phi^2}{1-\xi^2\phi^2}\right) + \frac{\Lambda}{\lambda}\frac{\phi(1-\phi^2)^{1/2}}{(1-\xi^2\phi^2)^{1/2}} = 0 \quad \ldots\ldots(26)$$

where the lengths Λ and λ are equal to $B_\infty/(\partial B/\partial y)_0$ and $(\partial B/\partial y)_0/\eta B_\infty^2$, respectively. We note from (23) that $\phi \leq 1$, since $B_v(\epsilon, y)$ is the value to which $B(x, y)$ rises as we leave the transition region, in the vicinity of $x = 0$. ξ is also less than or equal to unity.

We may expand $f(\phi)$ about $\phi = 0$ in ascending powers of ϕ. We obtain

$$\left.\begin{aligned} f(\phi) = 1 &- (\Lambda/\lambda)\phi^2 + \tfrac{1}{6}(\Lambda/\lambda)(1 - 5\xi^2 - 2\Lambda/\lambda)\phi^4 \\ &+ \tfrac{1}{4}(\Lambda/\lambda)[1 + 14\xi^2/3 - 97\xi^4/3 + (16/3)(\Lambda/\lambda)(1 - 3\xi^2) \\ &- (32/3)(\Lambda/\lambda)^2]\phi^6 + \cdots \end{aligned}\right\} \quad \ldots\ldots(27)$$

We cannot expand $f(\phi)$ in an ordinary power series about $\phi = 1$ ($B = B_\infty$) because it is not a regular point of the equation. We shall find, however, that when ϕ is close to unity, $f(f-1)/\phi$ is small in comparison to $f\mathrm{d}f/\mathrm{d}\phi$. Thus, we may solve the equation by reiteration. The zero-order function $f^{(0)}(\phi)$ satisfies

$$f^{(0)}\frac{\mathrm{d}f^{(0)}}{\mathrm{d}\phi} + \frac{\Lambda}{\lambda}\frac{\phi(1-\phi^2)^{1/2}}{(1-\xi^2\phi^2)^{1/2}} = 0 \quad \ldots\ldots(28)$$

We shall suppose that compressibility effects are small, $\xi^2 \ll 1$. Then, neglecting terms $O^4(\xi)$, we readily find that

$$f^{(0)}(\phi) = \left(\frac{2\Lambda}{3\lambda}\right)^{1/2}(1-\phi^2)^{3/4}\left\{1 + \frac{\xi^2}{20}(2 + 3\phi^2)\right\} + O^4(\xi) \quad \ldots\ldots(29)$$

Because $\partial B/\partial y$ essentially vanishes once we have left the transition region, we have the boundary condition $f(1) = 0$.

We now return to (26), using $f^{(0)}(\phi)$ in the term involving $f(f-1)/\phi$ and computing $f^{(1)}(0)$ from

$$f^{(1)}\frac{\mathrm{d}f^{(1)}}{\mathrm{d}\phi} - \frac{f^{(0)}(f^{(0)}-1)}{\phi}\left(\frac{1+\xi^2\phi^2}{1-\xi^2\phi^2}\right) + \frac{\Lambda}{\lambda}\frac{\phi(1-\phi^2)^{1/2}}{(1-\xi^2\phi^2)^{1/2}} = 0 \ldots\ldots(30)$$

Noting that

$$\int \mathrm{d}u(1-u)^{3/4}/u = 2\left\{\frac{2}{3}(1-u)^{3/4} + \arctan(1-u)^{1/4} - \operatorname{arctanh}(1-u)^{1/4}\right\}$$

we readily find that

$$\left.\begin{aligned} f^{(1)}(\phi) = &\left\{\left(\frac{2\Lambda}{3\lambda}\right)\left[\frac{5}{3}(1-\phi^2)^{3/2} + 2(1-\phi^2)^{1/2} - 2\operatorname{arctanh}(1-\phi^2)^{1/2}\right]\right. \\ &\left. - 2\left(\frac{2\Lambda}{3\lambda}\right)^{1/2}\left[\frac{2}{3}(1-\phi^2)^{3/4} + \arctan(1-\phi^2)^{1/4} - \operatorname{arctanh}(1-\phi^2)^{1/4}\right]\right\} \\ &+ \xi^2\left\{\left(\frac{2\Lambda}{3\lambda}\right)\left[2(1-\phi^2)^{1/2} + \frac{19}{6}(1-\phi^2)^{3/2} - \frac{61}{10}(1-\phi^2)^{5/2}\right.\right. \\ &\left. - 2\operatorname{arctanh}(1-\phi^2)^{1/2}\right] - \left(\frac{2\Lambda}{3\lambda}\right)^{1/2}\left[\frac{2}{3}(1-\phi^2)^{3/4} - \frac{43}{7}(1-\phi^2)^{7/4}\right. \\ &\left.\left. + \arctan(1-\phi^2)^{1/4} - \operatorname{arctanh}(1-\phi^2)^{1/4}\right]\right\}\end{aligned}\right\} \quad (30)$$

We note that $f^{(1)}(1) = 0$, as required.

We must now adjust Λ/λ in such a way that the series expansion about $\phi = 0$, given in (27), connects into the reiteration solution about $\phi = 1$, given by (30). We shall require that they meet at $\phi = 3/4$, which we shall find gives a smooth curve; both $f(\phi)$ and $df/d\phi$ appear to be continuous across $\phi = 0.75$. Equating $f(0.75)$ to $f^{(1)}(0.75)$ leads to a transcendental equation, requiring numerical solution. For the case of incompressibility, $\xi = 0$, we find that $\Lambda/\lambda = 0.820$; when $\xi = 0.316$, we find that $\Lambda/\lambda = 0.772$. $f(\phi)$ is shown as a function of ϕ in Figure 3.

FIG. 3—$\partial B/\partial x$ (in units of $\partial B/\partial x$ at $x = 0$) as a function of $B(x, y)$ (in units of the field density outside the transition region) for incompressible ($\xi = 0$) fluid motion and for slightly compressible ($\xi = 0.316$) fluid motion

From (20), (21), (22), and (25), it is readily shown that

$$\frac{1}{B_y(\epsilon, y)}\left(\frac{\partial B_y}{\partial x}\right)_0 = \left[\left(\frac{4\pi\sigma\xi}{c^2 L}\right)\left(\frac{p_0}{\rho_0}\right)^{1/2}\left(\frac{\lambda}{\Lambda}\right)\right]^{1/2}$$

(18) becomes

$$v_\infty = c\,\frac{\xi^{1/2}}{2\sqrt{\pi}}\left(\frac{\lambda}{\Lambda}\right)^{1/2}\left[\frac{(p_0/\rho_0)^{1/2}}{L\sigma}\right]^{1/2}$$

$$= \frac{c}{2^{5/4}\sqrt{\pi}}\left(\frac{\lambda}{\Lambda}\right)^{1/2}\left(\frac{C}{\sigma L}\right)^{1/2}(1-\xi^2)^{1/2}$$

C is the hydromagnetic velocity $B_y(\epsilon, y)/(4\pi\rho_0)^{1/2}$ outside the transition region.

Hence, when $\xi = 0$, we have

$$v_\infty = 0.263\, c(C/\sigma L)^{1/2} \quad (32)$$

when $\xi = 0.316$,

$$v_\infty = 0.253\, c(C/\sigma L)^{1/2} \quad (33)$$

(32) and (33) serve as crude estimates of the numerical factors omitted in the dimensional arguments presented in Section I. We see that, in terms of C, v_∞ decreases slightly with increasing compressibility: The gradient $(\partial B/\partial y)_0$ across the transition region tends to be enhanced by the compression, as indicated by the smaller value of Λ/λ, but the expulsion of the fluid is slower because of the increased density upon compression; the net effect is a slight decrease in v_∞ when related to the hydromagnetic velocity in the uncompressed gas. The net effect is slight. We must exercise caution, however, in applying our result, that compressibility slightly decreases the rate at which the fields merge, because the sign of the effect depends critically on the form of $\partial v_y/\partial y$ which we have assumed in constructing (19).

IV. CONCLUSION

Sweet's mechanism means that the reconnection of the lines of force of magnetic fields of scale L is not limited to the long time of $L^2\sigma/c^2$ and the slow merging velocity $c(c/\sigma L)$ which one would obtain from the diffusion equation

$$\frac{\partial \mathbf{B}}{\partial t} = \frac{c^2}{4\pi\sigma} \nabla^2 \mathbf{B}$$

When the velocity term $\nabla \times (\mathbf{v} \times \mathbf{B})$ is included, the merging velocity of two fields becomes of the order of $c(C/\sigma L)^{1/2}$, which may be very much larger. C is the hydromagnetic velocity $\mathbf{B}/(4\pi\rho)^{1/2}$. The ratio of Sweet's velocity of merging to the diffusion velocity is $(C/c)^{1/2}\,(\sigma L/c)^{1/2}$, which becomes large for large electrical conductivity, large scale, and/or large hydromagnetic velocity. Two fields need not be antiparallel for the Sweet's mechanism to work effectively: In Figure 4, we show schematically the process of merging two flux tubes which are perpendicular to each other; the process is to be compared with that computed from the diffusion equation alone (Parker and Krook, 1956).

We suggest that Sweet's mechanism may be of great importance in producing reconnection of the lines of force of a magnetic field into a configuration such that its energy becomes available for mechanical motions, etc. A solar flare may be an example of this (Parker, 1957).

We also suggest that the high electrical conductivity (Storey, 1954) of the gas within a few earth's radii of our planet does not necessarily exclude the penetration of exterior magnetic fields; $\sigma = 10^{13}$ esu, $L = 10^9$ cm, and a density of 10^{-21} gm/cm^3 leads to a merging velocity of the order of 0.1 km/sec: We suggest that the arguments we have presented elsewhere (Parker, 1956) against the Chapman-Ferraro ring-current model of the geomagnetic storm may lose some of their force.

Finally, we wonder if it is possible that Sweet's mechanism might modify somewhat the diffusion and dissipation of the magnetic field in hydromagnetic turbulence.

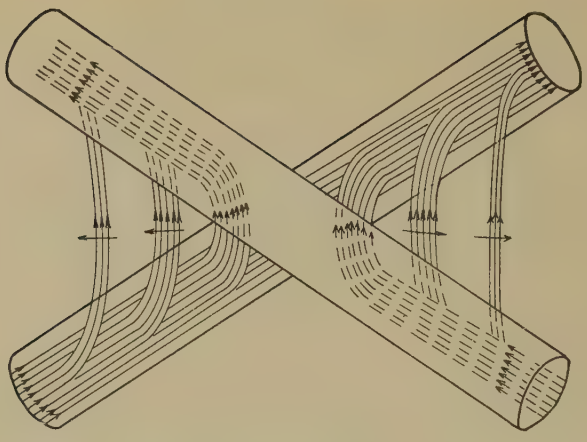

Fig. 4—Schematic drawing of the merging of two perpendicular flux tubes by Sweet's mechanism. The fluid squeezes out of the region of contact of the two tubes by flowing along the lines of force into the arms of the tubes. Following severing and reconnection of the lines of force, the tension in the reconnected lines tends to make them pull away from the region of contact and follow a shorter path between the tubes, as shown.

References

Sweet, P. A. (1956); Proceedings of the International Astronomical Union Symposium on Electromagnetic Phenomena in Cosmical Physics, Stockholm, 1956.

Parker, E. N., and M. Krook (1956); Astroph. J., **124**, 214.

Parker, E. N. (1957); Phys. Rev., **107**, 830 (1957).

Storey, L. R. O. (1954); Phil. Trans. R. Soc., A, **246**, 113.

Parker, E. N. (1956); J. Geophys. Res., **61**, 625.

HYDROGEN IN AURORAS*

BY C. W. GARTLEIN AND G. SPRAGUE

Physics Department, Cornell University, Ithaca, New York

(Received June 10, 1957)

ABSTRACT

Auroral spectrograms taken at Ithaca, New York, and Arnprior, Ontario, showing hydrogen lines have been studied. The velocity of incoming protons, as deduced from the Doppler shift, has been used to calculate the penetration of the protons into the atmosphere. The penetration appears possible to the 115-km level.

The intensity of hydrogen alpha has been obtained (1) by comparison with the known intensity of oxygen radiation 5577 of the normal night sky, (2) calculation from characteristics of the photographic emulsion, and (3) by calculation from the total intensity of auroral light. These methods agree within an order of magnitude. The H-alpha flux is about 10^{-4} erg per cm^2 column per steradian per second.

INTRODUCTION

It has long been known that hydrogen is sometimes observable in auroral displays [see 1, 2, and 3 of "References" at end of paper]. The question of the importance of hydrogen in the formation and behavior of auroras has been given prominence by more recent work [4, 5], which indicates that auroral hydrogen consists of solar protons entering along the lines of force of the earth's magnetic field. This evidence, combined with other relations between the sun and the aurora, suggests that hydrogen could be the immediate cause of an auroral display.

It is the purpose of this paper to present data and order of magnitude calculations which indicate that solar protons have sufficient energy, and number, to account for most of the observed radiations of the aurora. The following sections describe the results of various spectrographic investigations of the aurora, as they relate to hydrogen. Some of them have been briefly described elsewhere [6].

PROTON VELOCITY

The most prominent features of an aurora which are definitely ascribable to hydrogen are the H_α and H_β lines on auroral spectrograms. These lines are much broader than any other atomic lines observed, and when observed along the magnetic lines of force, as was done by Meinel [4] and by Gartlein [5], the center of the line is seen to be shifted from the normal position toward the violet. From measurements of the width and shift, it can be shown that the protons must have velocities of the order of at least two or three thousand kilometers per second. Such protons have a kinetic energy of about fifty thousand electron volts.

*The spectra were taken as part of the National Geographic Society–Cornell University Study of Aurora and the analysis was in part supported by the U. S. Signal Corps.

Assuming the earth's orbit around the sun has a radius of about 150 million kilometers, such protons would require 150,000,000/2,000 = 75,000 seconds, or about 21 hours to reach the earth from the sun. A time lag of 20 to 30 hours is customarily observed between the outbreak of a sudden magnetic disturbance and the onset of an aurora, a figure in satisfactory agreement with the estimate given above. (However, some of the observed protons are traveling faster than the figure used above—2,000 km/sec—and for these it is necessary to postulate some accelerating mechanism close to the earth, perhaps related to the Chapman-Ferraro ring-current.)

PROTON PENETRATION

It is possible, using range-energy relations for protons in air, to predict how far down into the atmosphere a proton of fifty thousand electron volts energy will penetrate. According to tables by the Atomic Energy Commission, the range is 0.082 cm in air at standard temperature and pressure [7]. Since the equivalent uniform atmosphere would be 8 km thick under these conditions, the protons will penetrate 0.082/800,000 of the atmosphere, or, in terms of the pressure, will penetrate to a depth where the pressure is

$$760 \times 0.082/800{,}000 = 7.7 \times 10^{-5} \text{ mm Hg}$$

According to the Rocket Panel Report [8], this pressure occurs at a height of 115 km. This is the average depth of penetration. Due to straggling,* the depth of penetration would vary from 105 to 125 km, centered at 115 km. Since the lower edge of an aurora is customarily at about 100 km, this figure is reasonable.

However, a serious error may result from applying atmospheric data obtained at New Mexico to the northern regions. Polar expeditions indicate that the troposphere is quite low in the extreme north, and a similar effect might be expected for the ionospheric region. If so, the protons might come lower. This fact, combined with the observed high velocities, and the sun-earth transit time, puts rather strict upper and lower limits on the value of the proton velocity, if it is to be considered the initiating agent for the aurora. These limits are, however, in agreement with the observations cited.

AMOUNT OF H_α RADIATION

The variety of auroral forms, and geographical variations in auroras, make the statement "amount of hydrogen in an aurora" somewhat meaningless. In the following, it is to be understood that statements refer to Ithaca, New York. Spectrograms obtained there have shown hydrogen concurrently with several auroral forms. The majority of auroras observed are glows, arcs, or rayed arcs in the northern sky. "Concurrently" in the previous sentence means that the spectrogram was taken at the same time the form was observed, but it cannot be assumed that no other form was present at the same time.

The amount of hydrogen in an aurora is related to the intensity of the H_α line

* According to [7], the straggling, measured by $(R_{extreme} - R_{av})/R_{av}$, decreases with increasing energy and at 1 KEV, it must be much greater than 3. Assuming the straggling is a factor of 3, then the extreme ranges will be 3/0.082 cm and 1/3/0.082 cm, and the corresponding pressures will be $3/7.7 \times 10^{-5}$ mm Hg and $1/3/7.7 \times 10^{-5}$ mm Hg. According to [8], these pressures correspond to heights of 104 km and 128 km.

ut the relationship is complex, and so this section gives estimates of the line ntensity, leaving the question of the amount of incident protons open. Calculations f the intensity from spectrograms are beset with many difficulties, and only ough estimates will be presented here.

Three methods of determining the intensity, and the related number of emitters n the aurora, are given below.

1. The simplest method is to compare the H_α line with the green oxygen line t 5577A. Since continuous monitoring of the sky is carried out at the Ithaca tation, there are many records available of the ordinary night sky and the ordinary reen line. This line is, of course, much enhanced in the aurora. Comparison of ecords, and correcting for different exposure times, shows that the H_α line in an verage aurora (neither weak nor strong, as seen from Ithaca) has about the me intensity as the oxygen green line in the normal night sky. Actual values of he ratio range from 0.50 to 2.3.

The energy flux from the oxygen green line has been measured by many authors. aking the value given by Rayleigh [9], the H_α flux, F, is

$$F = 7 \times 10^{-4} \text{ erg/cm}^2 \text{ column/steradian/sec}$$

his estimate neglects the change of quantum energy with wavelength and the ct that the oxygen data refer to a vertical column of the atmosphere, while the ectrograms are taken nearer horizontally. No more refined method is worth hile, in view of the rather ill-defined nature of an "average" aurora.

2. The intensity can also be estimated from the absolute calibration of the hotographic plate and the known spectrographic characteristics. An outline of he calculation follows.

The average density of the hydrogen line on the photographic plate is one, nd the plate sensitivity for a density of one (kindly supplied by the manufacturer) s about 10^{11} photons per square centimeter. For a one-hour exposure, and an image ize of 10^{-3} square centimeters, the spectrogram receives

$$10^{-3} \times 10^{11}/3{,}600 = 3 \times 10^4 \text{ quanta/sec}$$

These quanta come from the part of the aurora seen by the spectrograph and epresent the very small fraction of the radiation from this region which is inter- epted by the slit of the instrument (see Fig. 1). If H represents the quanta radiated er unit area of the aurora per second, and the aurora is 300 km away, then the adiation received at the plate is also given by

$$\text{quanta/sec} = H(\text{radiating area})\ (\text{slit area}/4\pi\ 300^2 \times 10^{10})$$

ll areas being in square centimeters. For the spectroscope used, the angle of cceptance was about 1°, which means that the radiating area effective at 300 m is about 25 km^2. The slit area is about one square centimeter. Substituting hese values and equating the two expressions gives

$$H = 1.5 \times 10^9 \text{ quanta/unit area/sec}$$

Converting to F,

$$F = 4 \times 10^{-4} \text{ erg/cm}^2 \text{ column/steradian/sec}$$

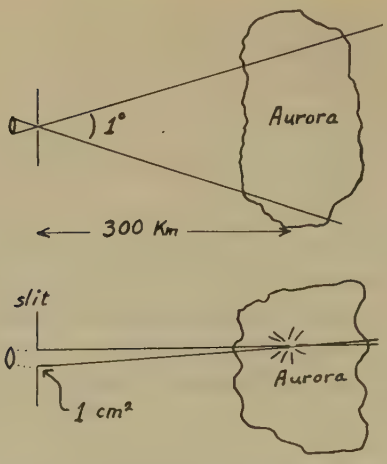

FIG. 1—Geometry of spectrograph and aurora
Upper: Portion of aurora seen by spectrograph
Lower: Portion of radiation intercepted by the slit

3. A third method is of special interest. It is based upon the following considerations:

(*a*) The H_α intensity is about 0.1 per cent of the total spectral energy, as estimated from spectrograms.

(*b*) An aurora is about 1/20 as bright as the full moon, and about 10,000 times as extensive.

(*c*) The sun is 14.2 magnitudes brighter than the moon, and has known surface energy flux.

From these rough data, Menzel [10] has calculated

$$F = 10^{-4} \text{ erg/cm}^2\text{/steradian/sec}$$

These three estimates agree very well, considering the approximations and assumptions. It must be remembered that they apply to average auroras seen from Ithaca, and to times when the three-hour magnetic K-index was about 5.

A Russian paper, reviewed in *Physics Abstracts* [11], gives

$$F = 3 \times 10^{-4} \text{ erg/cm}^2 \text{ column/steradian/sec}$$

THE AMOUNT OF HYDROGEN AND THE TOTAL ENERGY

Relatively simple arguments can be advanced to show that the hydrogen possesses enough energy to cause the observed visual auroral effects. The simplest comes from the third method of calculating the H_α flux outlined above. Since it agrees with the other methods, it is not unreasonable to assume that the data involved are reasonably accurate. In particular, the facts that auroral protons have energies of about fifty thousand electron volts, and that the H_α line constitutes only one-tenth of a per cent of the total visible auroral radiation, are sufficient to indicate that there is enough hydrogen present to cause an aurora. A fifty thousand volt proton has enough energy to produce over a thousand ion pairs, assuming that about thirty electron volts are required per ion pair. (This figure is fairly well established by the many range-energy studies made of high

energy particles.) If each recombination of an ion pair produced one visible photon and each proton captured an electron and radiated H_α line, the distribution of radiation would be accounted for. In actual fact, the recombination produces a whole series of visible radiations in the form of atomic and molecular radiations. In addition, many of the ultraviolet emissions which must result from, for instance, the nitrogen band system, will produce further excitations upon absorption, and thus contribute visible radiation. This would cause the percentage of H_α radiation to be lower than observed, on the present simple model.

The actual details of emission are still in doubt [12, 13] but if each proton (which becomes a hydrogen atom after electron capture) can turn four per cent of its energy (2,000 ev) into visible light for each H_α photon (2 ev) that it emits, then the observed protons have enough energy to be the energy supply for the aurora. This is not a very severe requirement, although it is certainly no proof that the protons do supply all the energy.

It is perhaps worth pointing out here that the hydrogen lines do not have to be visually prominent for the incoming hydrogen to be energetically important.

If the hypothesis of the importance of hydrogen as a primary energy supply is accepted, it is possible to calculate how many protons are needed to supply the total auroral energy, using again the figures in the estimate of H_α flux.

The auroral power, if supplied by 50,000 ev protons, would represent a current of I amperes, where

$$\text{Total power} = 50{,}000I \text{ watts}$$

(Of course, a neutralizing electron current must be somewhere nearby.)

The power per square centimeter at Ithaca can be estimated from the fact that, as already mentioned, the aurora is about 1/20 as bright as the full moon, which is, in turn, 10^{-6} (14.2 magnitudes) the brightness of the sun. Thus,

$$\text{Aurora power/cm}^2 \text{ at Ithaca} = (1/20)(10^{-6})(2 \times 4.18/60) \text{ watts/cm}^2 = 7 \times 10^{-9}$$

The factor 8.32/60 is the solar constant in watts/cm^2. The total power, assuming the aurora is a point source 300 km away, is related to the received power at Ithaca by

$$\text{Aurora power/cm}^2 = 50{,}000I/(4\pi)(3 \times 10^7)^2$$

Equating these two expressions gives

$$I \approx 10^3 \text{ amperes}$$

Currents of this order of magnitude are observed in the auroral zone during auroras, and may represent the recombination of the magnetically separated primary currents.

HYDROGEN DISTRIBUTION

The outstanding fact about the distribution of hydrogen in an auroral display is that it is, relative to other features, much more prominent in spectra taken by observers who are not underneath it. That is, Ithaca spectra show much more hydrogen than is observed from Canadian or Norwegian stations. Vegard [14, 15] has also indicated that hydrogen in spectra taken in northern Norway is more

intense when the spectroscope is pointed south than when it is pointed at an overhead aurora.

There are various possible interpretations of this fact. If charged particles enter the earth's atmosphere, the positive ones will be deflected to the south more than the negative ones [16]. This would still not explain the lack of hydrogen in auroras to the north of northern observers.

If greater southern extent is associated with greater concentrations of protons, some of the differences between northern and southern observers could be explained. However, most of the auroras seen at Ithaca are visible to many Canadian observers at the same time. Also, the very rare auroras which appear overhead at Ithaca do not seem to have the enormous amount of hydrogen this theory would suggest.

For the present, it seems that a reasonable view is that there is more hydrogen in southerly auroras, and that the hydrogen is distributed in a long horizontal layer. Looking diagonally through this would account for most of the observations reported above.

CONCLUSIONS

The outstanding features of this summary can be briefly outlined.

1. Protons enter the atmosphere with velocities and energies sufficient to penetrate to the 110-km level and supply the observed visual emissions. Part of this energy may be supplied by some mechanism outside the atmosphere but near the earth.

2. The H_α flux from an aurora is about 10^{-4} erg/cm^2 horizontal column/steradian/sec.

3. If the auroral energy is derived from protons of the maximum observed energy, a proton current of about ten thousand amperes is required.

4. These conclusions refer to auroras seen from Ithaca, New York, when the three-hour magnetic K-index was about 5.

References

[1] V. Carlheim-Gyllensköld, Expedition Polaire Suedoise, 1882-1883, Vol. II, p. 169 (1886).
[2] L. Vegard, Nature, **144**, 1089 (1939).
[3] C. W. Gartlein, International Union of Geodesy and Geophysics, Association of Terrestrial Magnetism and Electricity, Transactions of the Oslo meeting, Aug. 19-28, 1949, edited by J. W. Joyce (1950); p. 491.
[4] A. B. Meinel, Astroph. J., **113**, 50 (1951).
[5] C. W. Gartlein, Phys. Rev., **81**, 463-464 (1951).
[6] C. W. Gartlein and G. Sprague, Ottawa meeting of URSI, October 5, 1953.
[7] H. A. Bethe, Brookhaven National Laboratory, Pub. No. BNL-F7 (1949).
[8] Rocket Panel Report, Phys. Rev., **88**, 1027 (1952).
[9] Lord Rayleigh, Proc. R. Soc., A, **129**, 458 (1930).
[10] D. A. Menzel, Private communication (1951).
[11] I. S. Shklovskii, Doklady Akad. Nauk SSSR, **81**, 367 (1951).
[12] J. W. Chamberlain, Astroph. J., **120**, 360 (1954).
[13] J. W. Chamberlain, Astroph. J., **120**, 560 (1954).
[14] L. Vegard, Nature, **170**, 1120-1121 (1952).
[15] L. Vegard and G. Kvifte, Geofys. Pub., **19**, p. 10 (1954).
[16] C. Störmer, Arch. Sci. Phys., Geneva, **24**, pp. 5, 113, 221 (1907).

UHF RADAR OBSERVATIONS OF AURORA*

S. J. Fricker, R. P. Ingalls, M. L. Stone, and S. C. Wang

Lincoln Laboratory,
Massachusetts Institute of Technology,
Lexington 73, Massachusetts

(Received April 29, 1957)

ABSTRACT

Radar returns from aurora have been observed on a 412.85-Mcps pulsed bistatic radar, located at South Dartmouth, Massachusetts. Results obtained during two observational periods, 19 September to 6 October 1956, and 29 November to 21 December 1956, are given in terms of occurrence and position data, together with typical returns obtained on A-scope and range-time intensity modulated displays. Positions of observed returns are compared with positions computed on the basis of requiring beam perpendicularity to the earth's magnetic field. Indications are that returns may be obtained from regions which are 2° to 3° off perpendicular, and that returns at larger off-perpendicular angles may be limited by a height factor. The returns appear to be limited to the height range of 90 to 160 km approximately.

1. INTRODUCTION

The occurrence of visual aurora in northern latitudes is quite common, and has been the subject of considerable study in recent years. Data have been collected on its occurrence and on the type of display, and various theories have been suggested for the auroral mechanism.

A number of reports of radio reflections from aurora have been circulated from about the 1930 period. The frequencies concerned have been mainly in the HF-VHF bands, and often may have been complicated by the more usual ionospheric effects. Some effort has been made to collect the data available [see 1 of "References" at end of paper], and specific experiments have been carried out to gather more data [2, 3, 4]. Until quite recently, there were no indications that reflections had been observed in the UHF band, probably because of the lack of equipment of suitable power and sensitivity. Now that such equipment is becoming available, the effect of aurora on UHF transmissions is more amenable to experiment.

It is the object of this paper to present some results obtained with a 412.85-Mcps bistatic radar system, located at South Dartmouth, Massachusetts. Typical auroral returns obtained with this equipment are described in terms of time and position of occurrence. A small amount of polarization information also is available.

*The research in this document was supported jointly by the Army, Navy, and Air Force under contract with the Massachusetts Institute of Technology.

2. PHYSICAL CONSIDERATIONS

A simple view of the auroral mechanism is given by imagining that the sun ejects particles, some of which travel towards the earth in streamer form. These streams approach the earth in various complicated trajectories, and either directly or indirectly they cause considerable ionization activity in the region near the poles, during which the visual phenomena take place.

The formation of free electrons, and other particles, changes the effective dielectric constant of the region in which such phenomena occur, leading to the reflection or scattering (and absorption) of an incident radio wave. With the usual ionospheric theory in mind, it is to be expected that such effects at UHF will be rather slight, although the frequency dependence of the phenomenon is still an open question. Also it has been suggested that the free electrons will form clouds, of a thin ellipsoidal shape in general, with the long axis of the ellipsoid aligned with the direction of the earth's magnetic field. Such discontinuities would be aspect sensitive.

If one considers essentially specular partial reflection to take place, then the beam of a duplexed radar would have to be incident normally on the "reflector" for a return to be observed, that is, the beam would be normal to the earth's magnetic field [5]. If instead one thinks of the discontinuities as having scattering diagrams of small but finite angular width, then for returns to be observed, the beam must be almost normal to the earth's magnetic field in the auroral region. The term "almost normal" is vague, and is deliberately left so, as definite limits cannot be set at the moment.

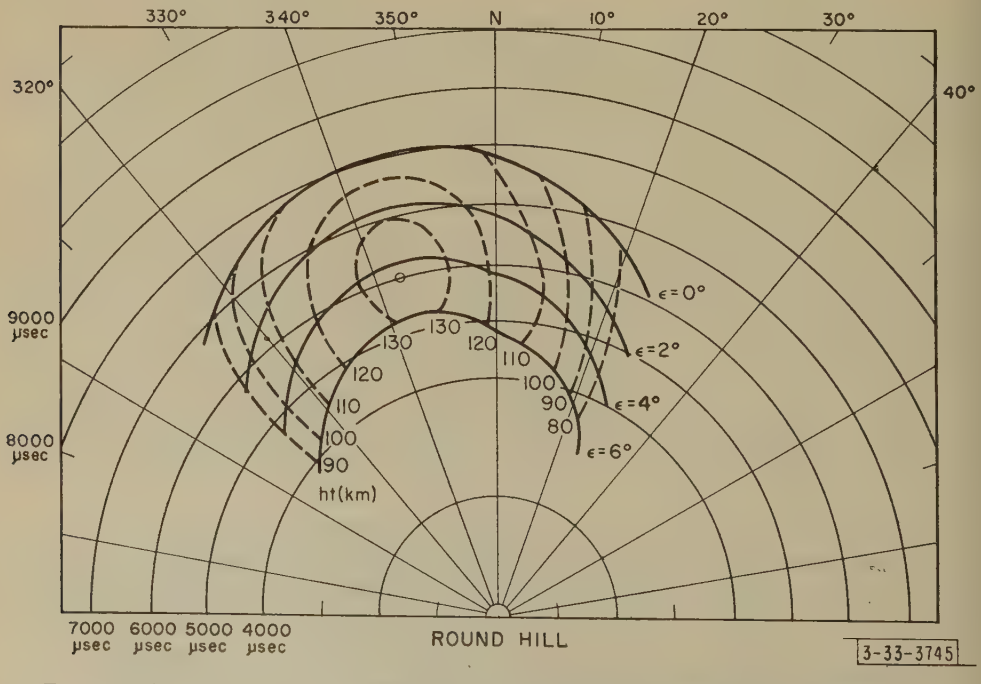

FIG. 1—Polar map for South Dartmouth, Massachusetts, showing loci of perpendicularity

The height at which the ionizing reactions occur also is limited. Thus, the region in space from which a radar at a given site may obtain auroral reflections is quite closely limited. The geometrical requirements may be expressed in a number of ways. Appendix A gives one convenient method, the results of which may be plotted on a polar presentation for a radar at a given location. Figure 1 was prepared for the South Dartmouth, Massachusetts, radar site, with the magnetic inclination and declination data taken from the Isoclinic and Isogonic Charts, Canada 1955 (Department of Mines and Technical Surveys). Constant range circles are shown in 1,000-μsec increments from 4,000 μsec to 9,000 μsec. The solid lines crossing the range circles are the loci of points where the beam is perpendicular to the earth's magnetic field at various elevation angles. The dotted lines are constant height loci (in kilometers). If upper and lower height bounds are placed on the auroral zone, then in combination with Figure 1 a region may be defined from which returns may be expected, provided of course that there is auroral activity in the region.

3. BISTATIC RADAR AT SOUTH DARTMOUTH, 412.85 MCPS

A bistatic arrangement was used to overcome the difficulty of duplexing, since a CW-type klystron (pulsed in its exciter) was used for the transmitter. The main parameters of the system were as follows:

(1) Peak transmitter power, approximately 10 kw
(2) Repetition rate, 50 c/s
(3) Pulse length variable, usually operated at 500 μsec
(4) Transmitting antenna, 28-foot diameter parabolic dish, polarization as noted in text
(5) Receiving antenna, 60-foot diameter parabolic dish, polarization as noted in text. Product of gains of transmitting and receiving antennas, $G_T G_R = 62$ db greater than isotropic.
(6) Receiver noise figure, approximately 5 db
(7) Receiver bandwidth, approximately 3,000 c/s
(8) Displays, (*a*) intensity modulated z-scope (with film recording); (*b*) normal A-scope

During the first observational period (September-October 1956), a single receiving channel was used for horizontal polarization. In the second period (November-December 1956), two identical channels were used, with dual displays, one for vertical polarization, the other for horizontal polarization.

4. METHOD OF OBSERVATION

The antenna mounts used in the system were not designed for continuous rotation, and the system was not set up to give a PPI type of presentation. The method adopted was to leave the two antennas pointed in the same direction for a given period of time, and then to shift to a different direction, repeating this periodically. The returns were used to give both A-scope and intensity modulated (with film recording) presentations. A reference pulse of known amplitude was injected into the antenna line and used for calibration. Range markers also were displayed on both presentations.

19 September to 6 October 1956 Period

The general procedure followed was to shift the antenna positions every 15 minutes, leaving the elevation of the antennas at approximately 1°. The particular azimuths chosen were decided upon after some initial observations of the extent of the aurora, plus the need to avoid picking up interpulse noise from the transmitter via the side lobes of the antennas.

29 November to 21 December 1956 Period

The main changes in this period were concerned with the polarization of the transmitting and receiving antennas. The feed horn in the transmitting parabola was arranged so that it could be rotated to give a linearly polarized signal at either 0°, 45°, or 90°. The 60-foot diameter receiving antenna was fitted with a dual polarization horn, mounted to receive two orthogonal linearly polarized signals, essentially vertical and horizontal. Table 1 gives the antenna settings, and the transmitter polarization used during the test.

TABLE 1

Date	Azimuth	Elevation	Trans. polarization
	°*true*	°	
29 Nov. to 6 Dec.	007	1	45°
6 Dec. to 10 Dec.	000	1	45°
11 Dec. to 17 Dec.	000	1	Horizontal
17 Dec. to 21 Dec.	000	1	Vertical

Azimuths and Transmitted Polarization During 29 November to 21 December

Each receiver channel had its own intensity modulated display and recording camera. A double-beam oscilloscope was used for the A-scope displays of both channels, and both channels had independently adjustable reference pulses injected in the antenna lines.

5. AURORAL OBSERVATIONS, DURING 19 SEPTEMBER TO 6 OCTOBER 1956

Some typical intensity modulated film recordings are shown in Figures 2(*a*), 2(*b*), 2(*c*), and 2(*d*). The time scale runs along the film direction, with marker gaps at 15-minute intervals. Range marks are in 300 nautical-mile intervals in Figure 2(*a*), and 150 nautical-mile intervals in Figures 2(*b*), 2(*c*), and 2(*d*). The reference pulse normally is shown between the 900 to 1,150 nautical-mile range marks. During quiet periods, the reference usually was set to a level about 3 db above the normal noise level of the receiver. Variations in the recorded level of the reference pulse are at times deliberate—when the amplitude was adjusted by the operator, and more frequently when the drift of the reference signal generator necessitated some retuning to put the reference pulse back in the 3-kc/s pass band.

The returns shown illustrate the typical observed behavior of auroral signals. Figure 2(*a*) shows the uniform appearance of the trailing edge of the returns at times. (The vertical striations are due to the oscilloscope; they are not auroral

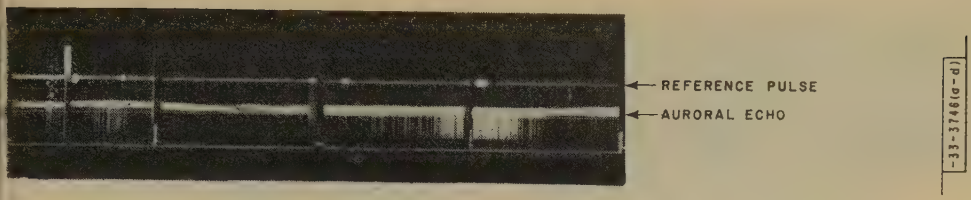

(a) 0100–0200, 20 September 1956.

(b) 2115–2215, 20 September 1956.

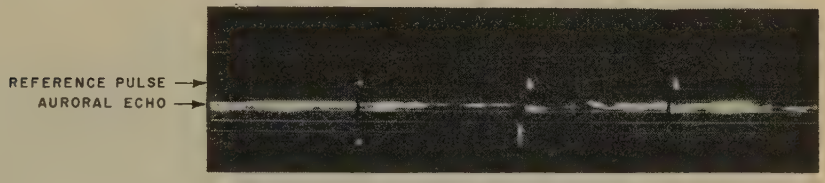

(c) 0400–0500, 22 September 1956.

(d) 0315–0415, 5 October 1956.

FIG. 2(*a*), (*b*), (*c*), (*d*)—Intensity modulated records, September-October 1956

returns.) In Figure 2(*b*), the returns are more patchy and varying in range. Figures 2(*c*) and 2(*d*) show some returns at different ranges, the definition being limited by the 500-μsec pulse length.

Some A-scope photographs are shown in Figures 3(*a*) through 3(*d*), with Figures 3(*a*), 3(*c*), and 3(*d*) taken during the displays shown in Figures 2(*a*), 2(*c*), and 2(*d*). The reference pulse is on the right in each case, with its amplitude approximately 14 db above noise in Figure 3(*a*), and approximately 20 db above noise in Figures 3(*b*), 3(*c*), and 3(*d*). The auroral returns are characterized by rapid fluctuations, their appearance on a A-scope presentation being quite different from the usual ground back-scatter signals observed at lower frequencies. The fluctuations are sufficiently rapid so that the return differs markedly from sweep to sweep (at 1/50 second repetition period). Figure 4 gives a portion of a fast recording made on 3 October 1956, showing portions of individual sweeps.

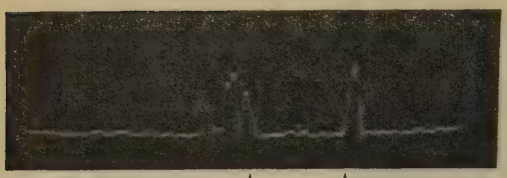

(a) 007°, 0145, 20 September 1956.

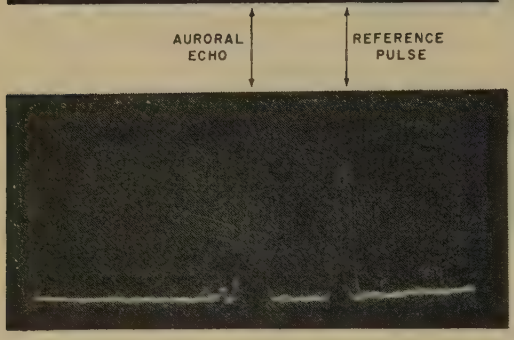

(b) 007°, 1557, 21 September 1956.

(c) 007°, 0355, 22 September 1956.

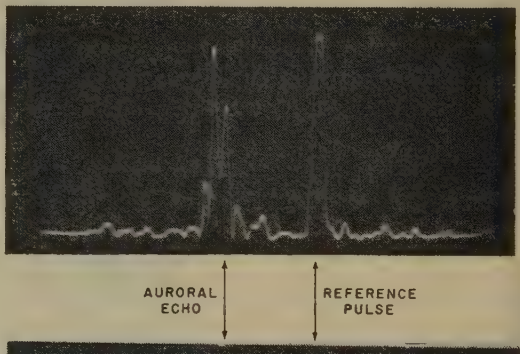

(d) 007°, 0356, 5 October 1956.

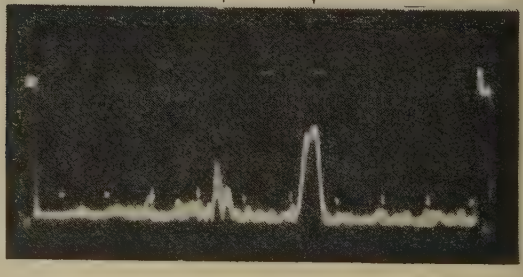

FIG. 3(*a*), (*b*), (*c*), (*d*)—A-scope records, September-October 1956

The usual level of the returns observed during this period was of the order of 10 to 20 db greater than noise, though occasionally signals would reach the 30-db level. At other times, of course, signals would just begin to show, and then fade into the noise again. Now it is not known how the returned signal is made up in total, but in order to attach some numbers to the returns for a given system, it is useful to regard the aurora as a simple scatterer with cross-section σ meters^2. The noise level then approximately corresponds to $\sigma = 30$ m^2 at a range of approximately 1,300 km, while the 30-db level corresponds to $\sigma = 30{,}000$ meters^2.

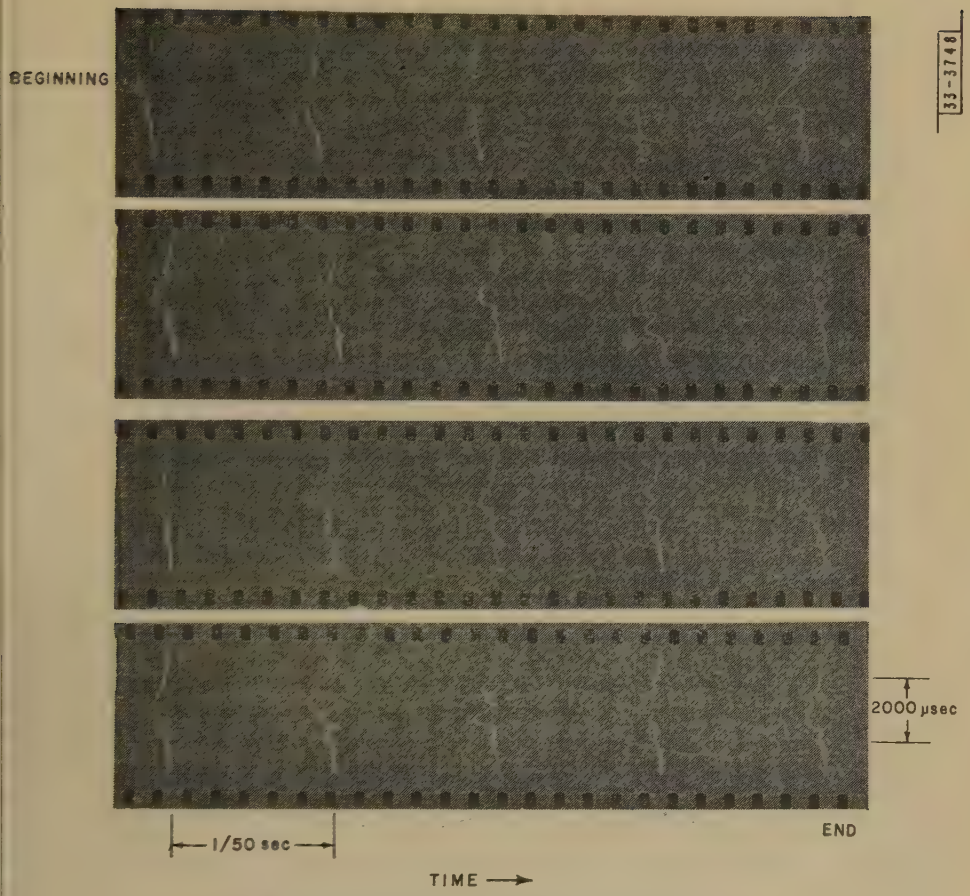

FIG. 4—Consecutive sweep video photographs

Figure 5 records the presence or absence of an auroral return, irrespective of azimuth and with no magnitude information. The same sort of information is presented in Figure 6 as a histogram of occurrence *versus* time of day, with time quantitized in 15-minute blocks.

On a number of occasions, when large returns were present, the system was used to search in azimuth and elevation to determine the approximate extent of the returns. In general, this was found to be within approximately 320° to 020° in azimuth, and from 0° to 7° in elevation. Often the returns were present only over a much more limited region, and sometimes these limits changed considerably in a period of a few minutes. The ranges of the returns varied between limits of 900 to 1,350 km. The outer limit was much more marked than the inner limit, although, as will be remarked later in Section 7, this could be due to a height limitation rather than any fundamental range limitation.

For the total period of 19 September to 6 October 1956, returns were observed approximately 4.8 per cent of the time. The distribution of occurrence among the various azimuths is given in Table 2.

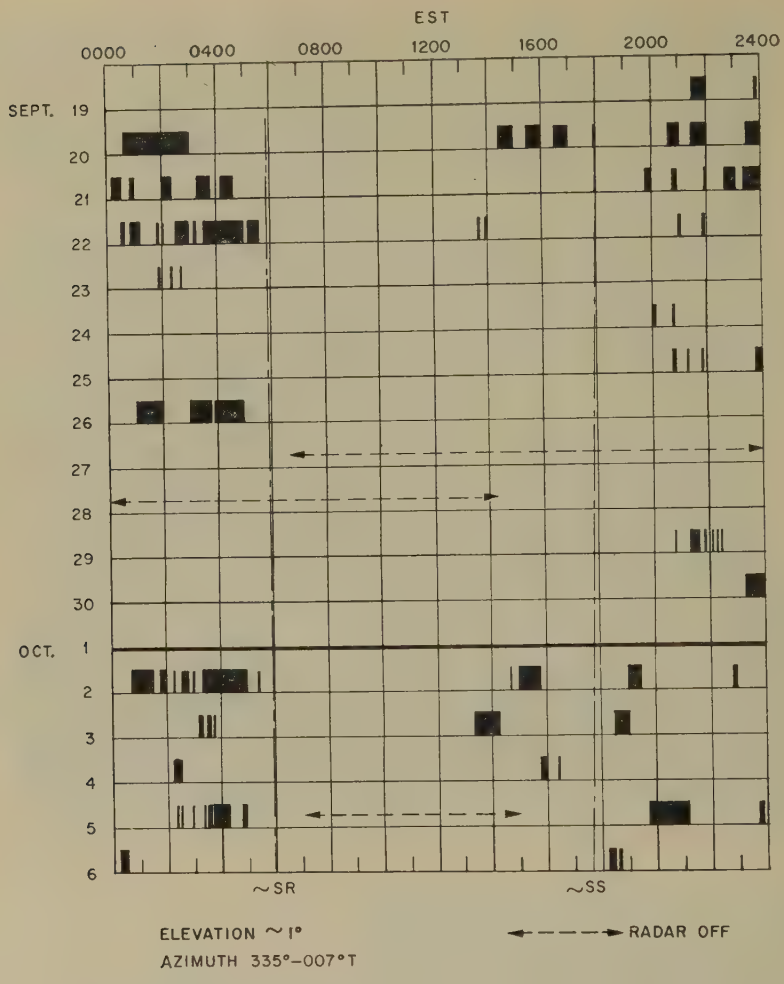

FIG. 5—Occurrence data, September 19 to October 6, 1956

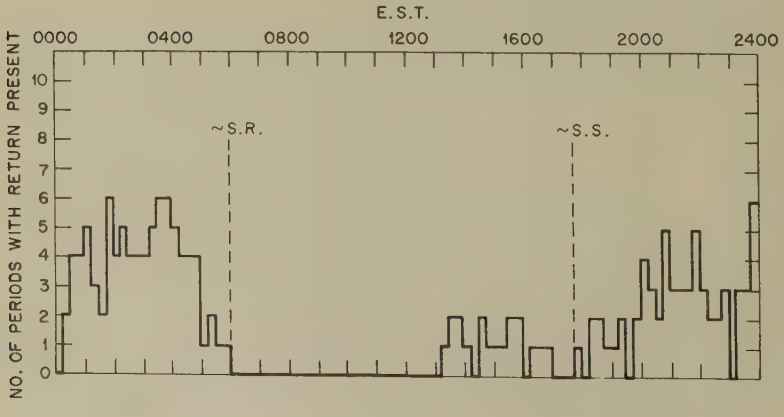

FIG. 6—Histogram for diurnal variation, September 19 to October 6, 1956

TABLE 2

Azimuth (°true)	335°	345°	335°	007°
Per cent of time returns were observed at indicated azimuth	3.6%	4.1%	5.4%	6.3%

Auroral Returns at Various Azimuths (19 September to 6 October 1956)

The direction of true north is obviously favored compared with magnetic north, although it is conceivable that more data would change this distribution. The diurnal variation shown in the histogram of Figure 6 similarly suffers from the small amount of data. A cut-off at sunrise appears to be fairly well defined, lasting until just after midday. The rate of occurrence of returns during the afternoon seems to be less than that during the hours of darkness, but the variations during the sunset to sunrise period may not be significant at the moment.

6. AURORAL OBSERVATIONS DURING 29 NOVEMBER TO 21 DECEMBER 1956

The bistatic radar was used for auroral monitoring during this period, with the polarization modifications described in Section 4, and the schedule given in Table 1. With both vertical and horizontal polarizations transmitted, the returns on the two receiver channels are exemplified by the portions of intensity modulated film shown in Figures 7(*a*) through 7(*d*). Figure 7(*a*) was obtained from the horizontal polarization channel, and Figure 7(*b*) from the vertical channel. The intensity settings are not quite the same on these two, and the horizontal signal is approximately 5 db greater than the vertical signal. Figures 7(*c*) and 7(*d*) similarly show the horizontal and vertical channels, at a time when the two signals were approximately equal [the reference pulse is rather intermittent in (7*c*) and (7*d*)]. Although some detail is lost in the prints, it is still fairly clear that the range-time structure of the two orthogonally polarized signals is the same. After 11 December 1956, when the transmitting horn was moved to give horizontally polarized transmission, received echoes appeared on the horizontal receiver channel only, until the signal amplitude became approximately 20 db above the noise level. At this point, the 20-db cross-coupling in the feed allowed the signal to appear on the orthogonal polarization receiver. Figures 8(*a*) and (*b*) show typical records obtained during a period when the horizontal channel displayed a signal with range variations and striations rather similar to those in Figure 7(*a*), though of weaker intensity. The echo amplitude was not large enough to allow a visible signal to leak through to the vertical channel.

The A-scope photographs shown in Figures 9(*a*), (*b*), 10(*a*) and (*b*) display the vertical return at the top, and the inverted horizontal return at the bottom. As before, the reference pulse is on the right. The photographs in Figures 9(*a*) and (*b*) were taken when both orthogonal polarizations were transmitted. Figure 9(*a*) has the horizontal channel reference pulse set at approximately 13 db above the noise level, with reduced receiver gain, and the vertical channel reference pulse set at approximately 8 db above the noise. In Figure 9(*b*), where both reference pulses are approximately 3 db above noise, the returns show different instantaneous values, though the average returns at this time were approximately equal.

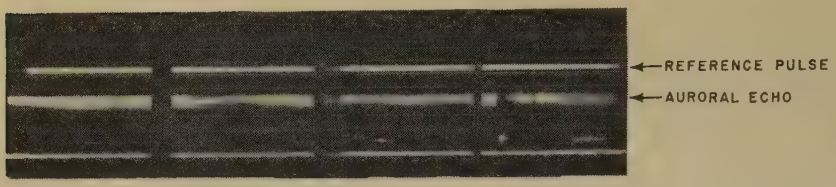

(a) Horizontal polarization, 1545–1645, 6 December 1956.

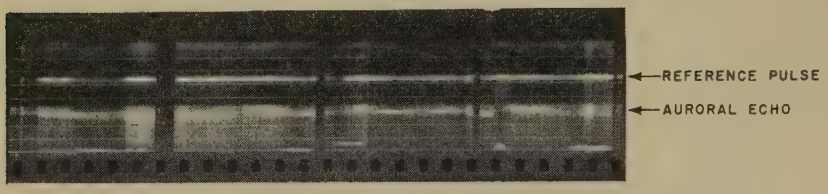

(b) Vertical polarization, 1545–1645, 6 December 1956.

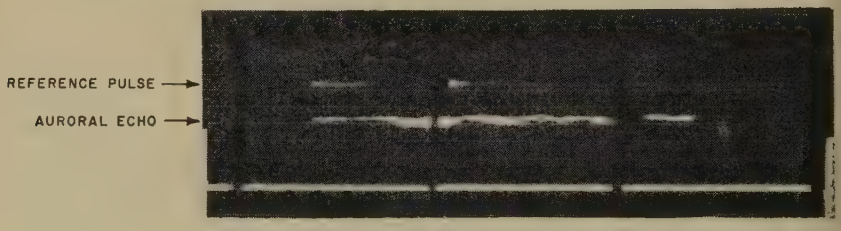

(c) Horizontal polarization, 0215–0300, 8 December 1956.

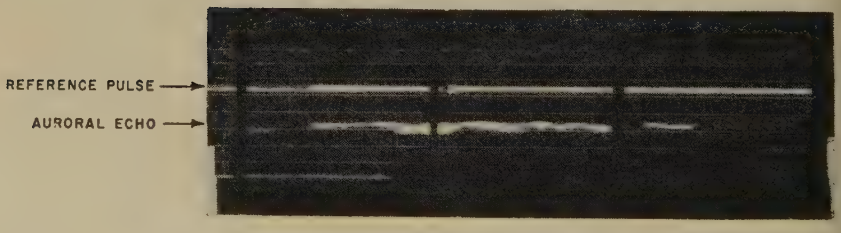

(d) Vertical polarization, 0215–0300, 8 December 1956.

FIG. 7(*a*), (*b*), (*c*), (*d*)—Intensity modulated records, November-December 1956

Figures 10(*a*) and (*b*) were obtained after the move to horizontal transmitted polarization. Figure 10(*a*) has the horizontal reference (at the bottom) set to 8 db above noise, and the vertical reference set to 3 db above noise. A return is visible only on the horizontal channel. A larger return is shown in Figure 10(*b*), where the reference pulses are set to 25 db and 4 db above noise and the horizontal (bottom) channel is operated at reduced gain. The leakage from the horizontal to the vertical channel is just becoming visible.

The auroral echoes observed during this second observational period were similar in appearance to the previously observed returns. Although the system was directed at 000° or 007° for most of the period, occasional searches with the system showed that returns were obtained from the same region as before, that is, during September-October.

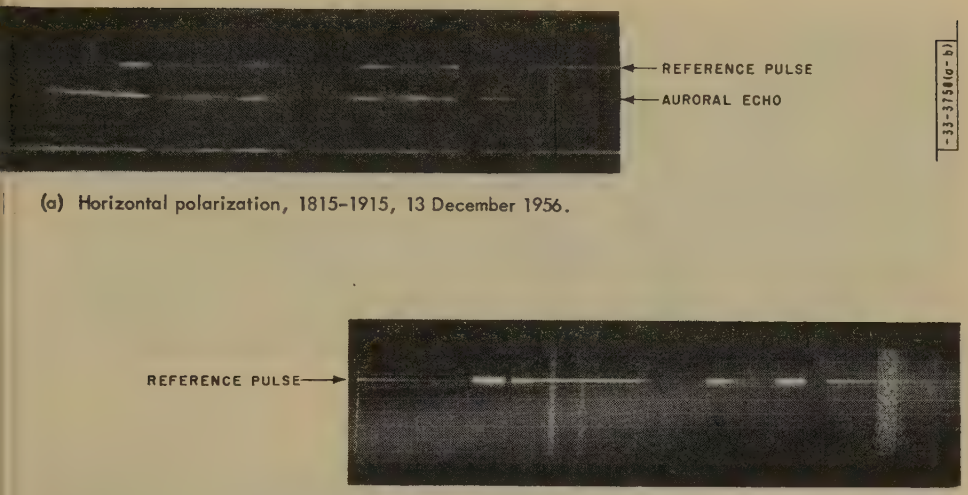

FIG. 8(*a*), (*b*)—Intensity modulated records, November-December 1956

Figure 11 shows an occurrence plot, similar to Figure 5 for the first period, and shows the same general characteristics. The cut-off at sunrise is marked as before, apart from one observation one hour after sunrise, and again lasts until 1300 to 1400 hours. A histogram of frequency of occurrence against time (in 15-minute periods), Figure 12, is slightly different from the histogram of Figure 6, in that the occurrence variations during the sunset to sunrise period are not the same in both cases. As mentioned before, this could well be due to insufficient data. The over-all percentage of time that returns were observed during the 29 November to 21 December period was 3.7 per cent compared with the previous figure of 4.8 per cent (Sect. 4*a*). The strong display on 12 December 1956 accounted for a large portion of the 3.7 per cent figure, but even so the rates of occurrence are not too different for the two periods.

7. REMARKS ON DATA GATHERED DURING BOTH PERIODS OF OBSERVATION

Polar Map Presentation

The map shown in Figure 1 forms a useful base for the general description of the geometry of the auroral returns. First, it is convenient to add more information to the map concerning height and the perpendicularity condition. The 2.5° receiving beam was set at a nominal 1° elevation angle, so that with this elevation angle the height of the beam above the surface at various ranges may be calculated (with a figure of 6,390 km used for the earth's radius). These heights are shown on the range curves in Figure 13. In addition to the loci of points where the perpendicularity condition is satisfied, loci could be plotted to show where the beam, at a given elevation angle, is at a fixed angle from perpendicular. However, rather than complicate the picture with too many curves, it is sufficient to note that in the region covered by the curves a range increment of 1,000 μsec corresponds to approximately 2° change in angle between the beam and the earth's

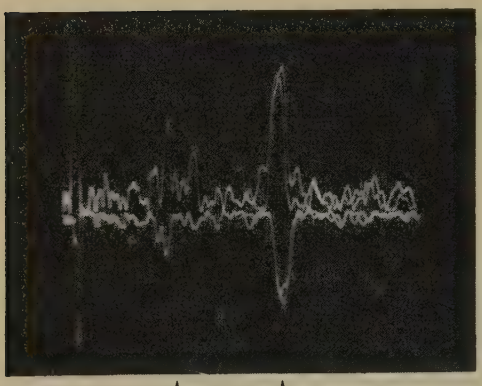

FIG. 9(*a*), (*b*)—A-scope records (horizontal and vertical polarizations transmitted)

magnetic field. Hence, the range curves may be regarded as giving approximate off-perpendicular angle information.

The maximum and minimum ranges of auroral echoes observed during both periods are shown in Figure 13. It is noticeable that the 9,000-μsec extreme range limitation is common to all azimuths, while the inner range limitation varies considerably with azimuth. Now the receiving beam may be assumed to fill the region between the two loci for elevation angles of 0° and 2°. Hence, if the perpendicularity condition were particularly stringent, the returns at various azimuths would be limited to this 2° segment. From Figure 13, it is apparent that returns are obtained from regions where the beam direction is as much as 2° to 3° from the perpendicular to the earth's magnetic field. From the uniform ranges of the extreme returns, it is possible that a height-dependent phenomenon may be the limiting factor here, rather than any geometrical requirement. It is also possible that the variations of the inner range limits would be smoothed if more data were collected. However, the fact that the innermost ranges in Figure 13 tend to follow the 2°

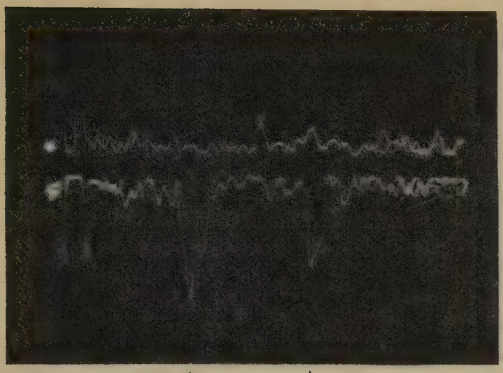

FIG. 10(*a*), (*b*)—A-scope records (horizontal polarization transmitted)

curve gives rise to suspicions that the geometry of the situation may have some considerable effect, perhaps in conjunction with some height dependence which becomes effective at 90 to 100 km.

Elevation Angle Versus Range Plots

An alternative viewpoint is afforded by constructing loci of constant height on an elevation angle *versus* range plot, and then using data from Figure 1 to superimpose the locus of points satisfying the perpendicularity condition, for particular azimuths. A typical plot is shown in Figure 14 for an azimuth of 007°. The range limits given in Figure 13, together with a beam coverage of approximately 0° to 2-1/2°, define vertical sections from which returns were obtained. For 007° azimuth, this region is shown as a box in Figure 14, and may be viewed as an indication of the resolution afforded by the system. Although this is not as fine as could be desired, it is evident that observations of returns at elevation angles of 3°, 5°, 7°, etc., may be useful for the determination of the character of the height dependence.

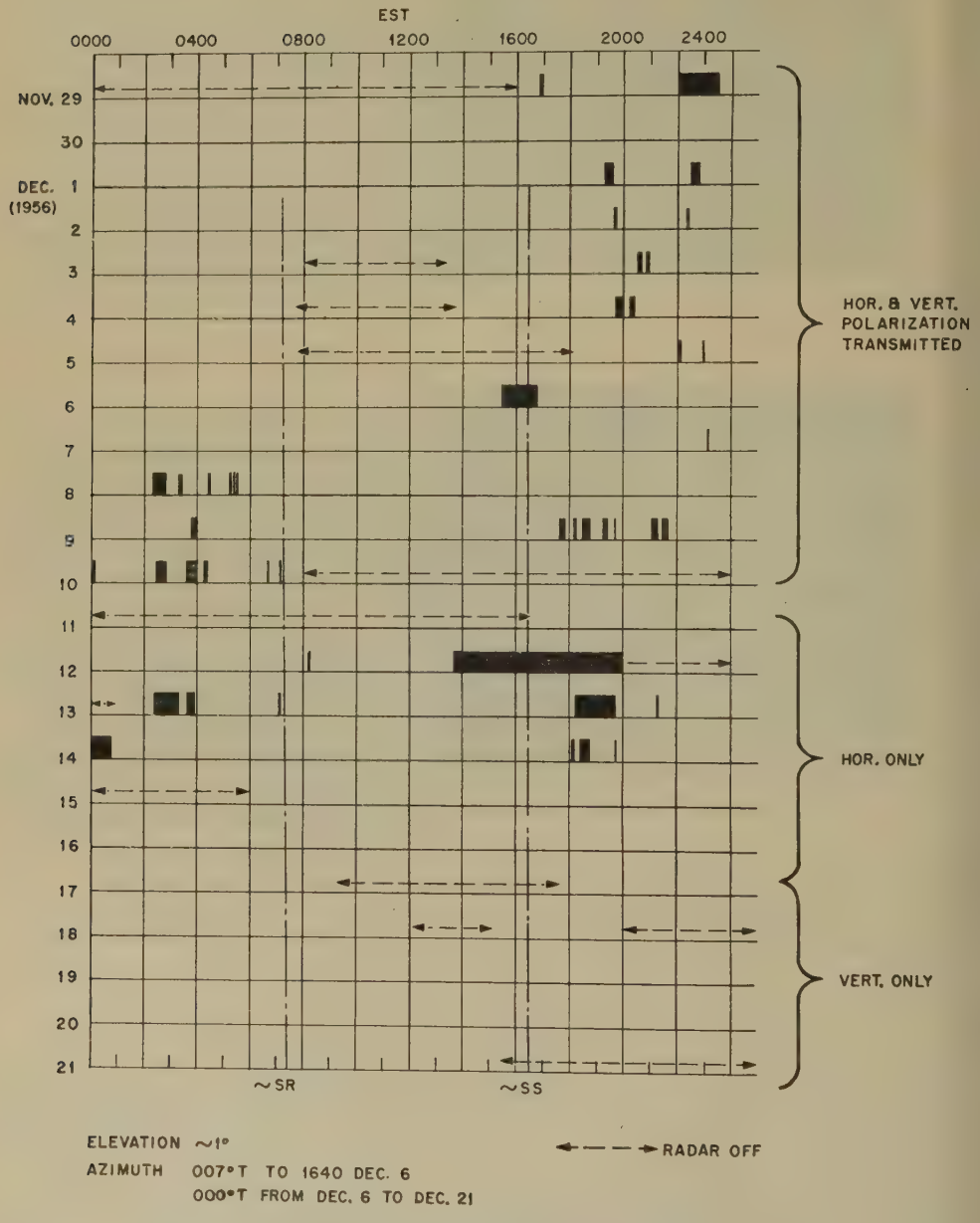

FIG. 11—Occurrence data, November 29 to December 21, 1956

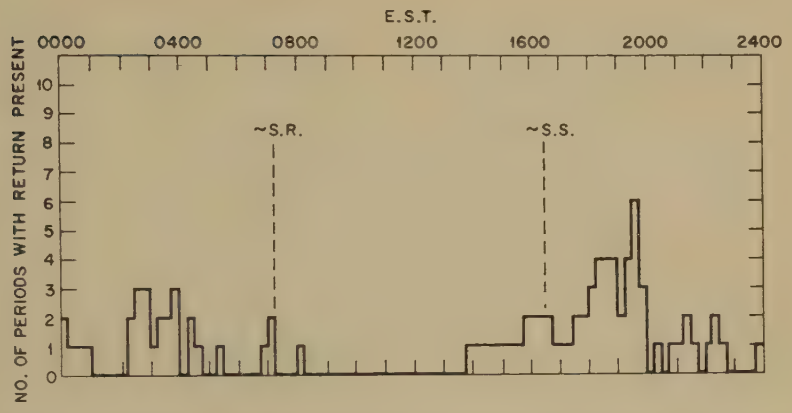

FIG. 12—Histogram for diurnal variation, November 29 to December 21, 1956

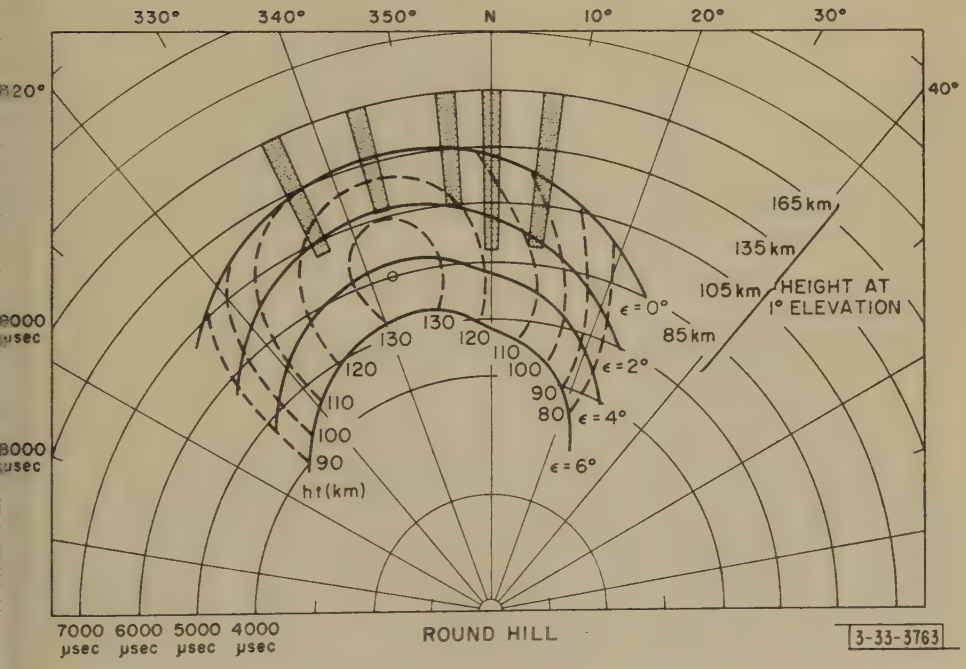

FIG. 13—Polar map with extreme range limits

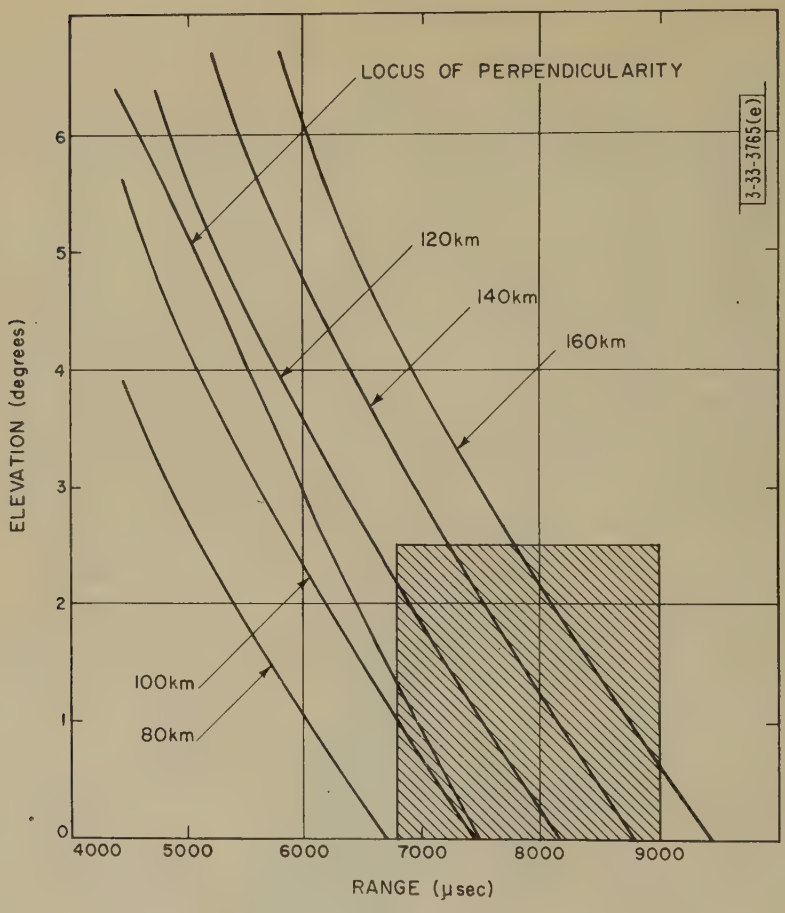

FIG. 14—Elevation angle *versus* range for 7° azimuth

Summary of Tentative Deductions from the Present Data

Location of Echo Areas at 400 Mcps

The geometrical requirements necessary for a radar beam to be perpendicular to the earth's magnetic field can be determined for any particular site. If there is sufficient auroral activity in the region, the returns may be expected from the area satisfying the geometry, plus a surrounding area where the beam is at least as much as 2° to 3° off perpendicular. Height limitations probably are superimposed upon the geometrical requirements; the upper height limit (in the Quebec region) may be of the order of 160 km.

Polarization of 400 Mcps Auroral Returns

The coarse structure of the signals on vertical and horizontal linear polarizations appears to be the same. The amplitudes are approximately equal most of the time, although for some periods the horizontally polarized signal was definitely the larger one, by 4 to 5 db. (This was at elevation angles of 1°; at other elevation angles, there are no data available at present.)

With the transmission horizontally polarized, the amount of depolarization in the propagation path and at the aurora was less than −20 db, for the relatively short period of observation.

Diurnal Variation

The results obtained so far have shown a striking lack of returns from sunrise to approximately 1300 hours. Returns during the afternoon hours, before sunset, occurred less frequently than during the hours of darkness. Peaks in the rate of occurrence may occur, but the present observations probably are not significant in this respect.

Seasonal Variations

It is well established that the equinoctial periods provide more frequent visual auroral displays than during the rest of the year. The figures of 4.8 per cent and 3.7 per cent for the percentage of time that 400-Mcps returns were seen during September-October and November-December agree with a similar trend for radar returns. The 3.7 per cent figure may be unduly inflated by the large display on 12 December 1956, and by the fact that the radar sometimes was not in operation during the daylight hours (see Fig. 12), when not too many returns would be expected.

Relation to Solar-Flare Activity

During the periods of observation, reports of solar-flare activity were noted. No direct correlation was evident with the occurrence of auroral returns. Sometimes returns were obtained approximately 30 hours after the flare eruption; at other times, after very intense flares, no auroral echoes at all were obtained for some time. It is possible that flares should fulfil certain position requirements on the sun before being considered as direct causes of increased auroral activity. Insufficient data are available at the moment to allow any postulations to be made on this subject.

(Magnetic index records also might be expected to show some correlation with auroral displays. This is under investigation, but at the time of writing no results are available.)

8. CONCLUSIONS

It has been demonstrated that radar reflections can be obtained from the aurora at a frequency of 412.85 Mcps. The general location of the reflecting regions may be predicted on the basis of the perpendicularity requirement. The actual reflecting region may overlap this by an amount which is not well determined, but where the perpendicularity requirement is not met by 3° or perhaps more. The height from which returns have been obtained appears to be approximately 90 to 160 km. The statistics of occurrence of the auroral returns are sufficient to give a general indication of the diurnal trend, namely, a very low occurrence rate from dawn to approximately 1300 hours, a somewhat greater rate from 1300 to sunset, and the greatest rate during the hours of darkness.

Further work is in progress with the bistatic radar system. More experimental verification is being obtained of the upper height limit of approximately 160 km, while the amount of depolarization observed appears to vary with time.

9. ACKNOWLEDGMENTS

Personnel from Lincoln Laboratory and from the M.I.T. Round Hill Field Station were responsible for the installation, operation, and maintenance of the bistatic radar system.

APPENDIX A

Mapping Procedure

The problem may be stated simply. Given a particular site, to determine the positions in space at which a beam from the site is perpendicular to the earth's magnetic field. If the earth's field is regarded as that of a dipole, the problem may be solved fairly conveniently [6]. For our purposes, however, the variations of the magnetic field from a simple dipole field are significant, and hence it is necessary to work from measured values of inclination and deviation. The values used were taken from the Canadian Isoclinic and Isogonic Charts, 1955. The site used was the South Dartmouth Field Station, at 41.5° north and 71° west. The only questionable part of the procedure lies in the assumption that the measured magnetic data on the earth's surface are unchanged at 100 to 200 km height.

The problem essentially is one involving spherical geometry, and the basic need is for some type of two-dimensional projection. This is developed in terms of the quantities α and A, as shown in Figure A-1. The site is at point P, on the

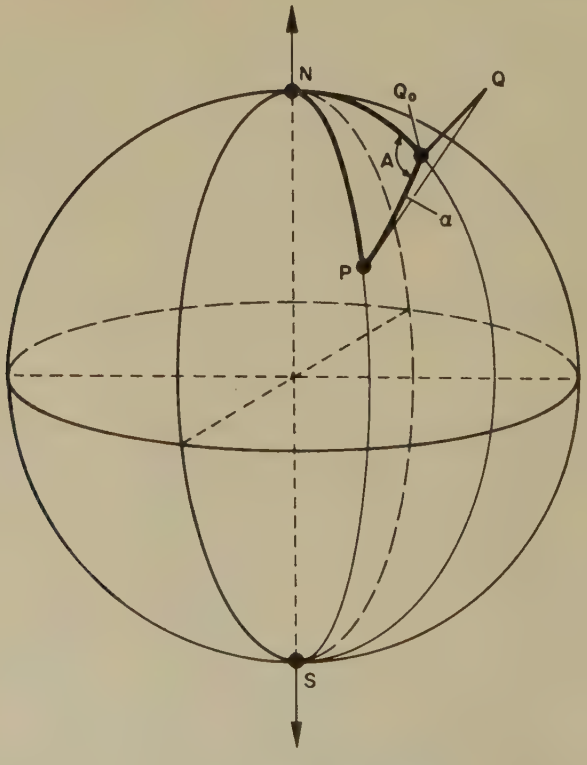

FIG. A-1—Geometrical model

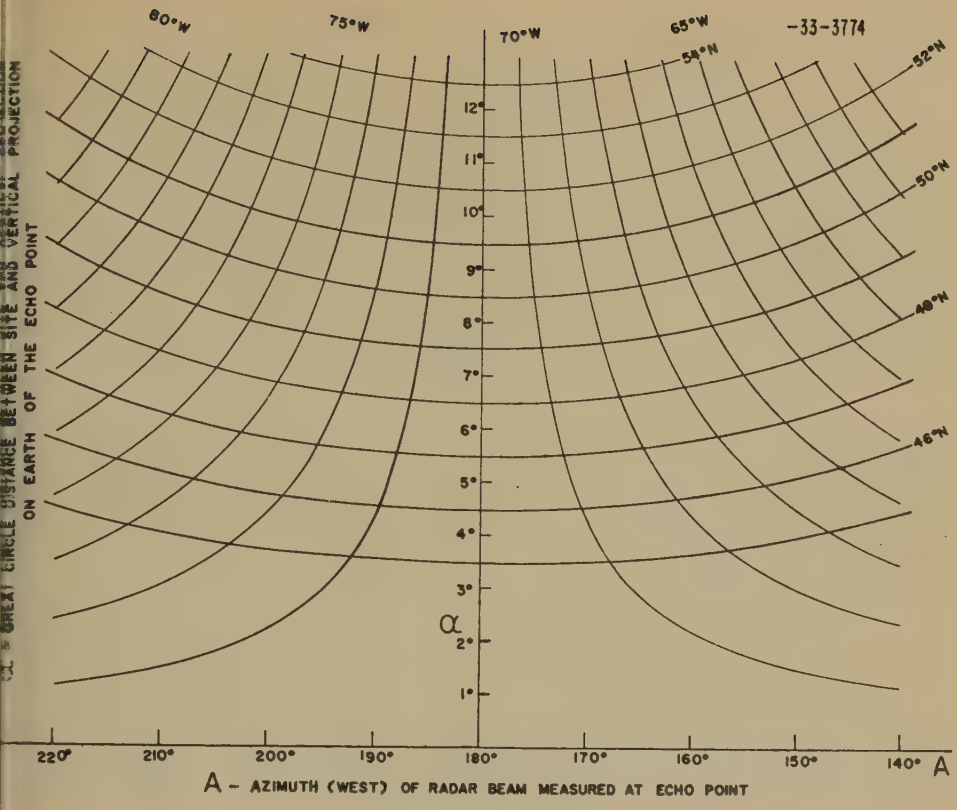

FIG. A-2—α-A plane

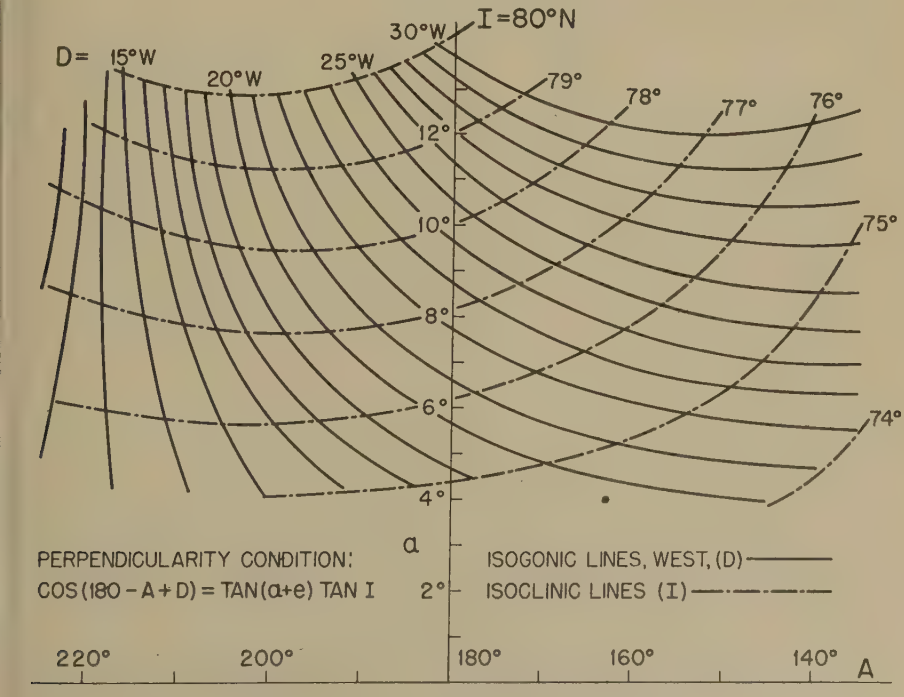

FIG. A-3—α-A plane with I and D contours

meridian NPS. Q is a point in the air above the surface, with Q_0 beneath Q on the surface. Thus, NQ_0S is a meridian, and the spherical triangle NQ_0P is formed. The side PQ_0 forms α, and the angle NQ_0P is A. Lines of constant latitude and longitude on the surface now may be described in terms of α and A measured from P. On the α-A plane for the site P, these latitude and longitude lines then appear as shown in Figure A-2. It is now a simple matter to transfer the isoclinic lines (constant inclination angle I) and isogonic lines (constant deviation angle D) to the α-A plane, giving the map shown in Figure A-3. With a beam elevation angle at P of $e°$, the perpendicularity condition may be written as

$$\cos (180 - A + D) = \tan I \tan (\alpha + e)$$

where westerly D values are taken as positive, and I is measured to the horizontal. Figure A-3 is used to determine values of A and α at which the above equation is satisfied for given e. The values of α and A are then transformed to give the normal radar range and bearing from the site P, these values being plotted to give the map shown in Figure 1.

References

[1] R. K. Moore, A VHF propagation phenomenon associated with aurora, J. Geophys. Res., **56**, 97-106 (1951).

[2] L. Harang, Scattering of radio waves from great virtual distances, Terr. Mag., **50**, 287-296 (1945).

[3] D. W. R. McKinley and P. M. Millman, Long duration echoes from aurora, meteors and ionospheric back-scatter, Can. J. Phys., **31**, 171-181 (1953).

[4] B. W. Currie, P. A. Forsyth, and F. E. Vawter, Radio reflections from aurora, J. Geophys. Res., **58**, 179-200 (1953).

[5] H. G. Booker, A theory of scattering by non-isotropic irregularities with application to radar reflections from the aurora, Cornell University, School of Electrical Engineering, T.R. No. 28 (Oct. 30, 1955).

[6] S. Chapman, The geometry of radio echoes from aurorae, J. Atmos. Terr. Phys., **3**, 1-29 (1952).

VHF RADAR ECHOES ASSOCIATED WITH ATMOSPHERIC PHENOMENA*

BY G. C. RUMI

Cornell University, Ithaca, New York
[*Present address:* Geophysical Institute, College, Alaska]

(Received March 25, 1957)

ABSTRACT

VHF radar observations during the summer and the fall of 1955 at Ithaca, New York, gave useful information not only about lightning, meteors, and aurora, but also about the possible existence and characteristics of "upward discharges" from the top of the troposphere to the bottom of the ionosphere.

A radar operated at 27.85 Mc/sec was used. A feature was the photographing from magnetic tape records that were played back to reproduce the original oscilloscope presentation. This technique proved to be useful in permitting more detailed analysis than had previously been possible. Photographs are presented that show examples of echoes (in an amplitude-*vs*-time display) that we have attempted to associate with "upward discharges." (Photographs of a simple meteor echo and of a meteor echo embedded in an auroral echo are also included.)

Detailed analysis led us to dissociate many of our echoes from meteors. Their rise and decay speeds, their duration, their flatness, their ranges of appearance, and the observed repetitions suggested that "upward discharges" from troposphere to ionosphere could have been responsible for the reflection of radio waves. Nevertheless, meteors cannot be ruled out of a complete picture of the phenomenon. Meteors may play a role in the generation of "upward discharges" as triggering agent.

INTRODUCTION

During observations at Ithaca, New York, in 1955, connected primarily with ne aurora and with meteors, echoes were obtained which did not seem to fit in ith either of these phenomena.

In the following pages, we shall present (*a*) the equipment used, (*b*) a repre-ntative selection of the data, and (*c*) a discussion of our interpretation of the xperimental results.

*This research was supported by the U. S. Signal Corps under Contract DA-56-039-sc-56748 nd by the National Science Foundation.

EQUIPMENT

The equipment used was a radar operating on 27.85 Mc/sec, with a peak power output of 200 kw, repetition rate of 50 pulses per second, and pulse width of 40 microseconds. The antenna used was a V antenna, fixed, horizontal, and pointing toward north.

A special feature was the photographing from magnetic tape records that were played back to reproduce the original A-scope presentation, of which only a selected slice was illuminated on the oscilloscope screen by means of intensity modulating circuits. The shutter of the oscillorecord camera was open in front of the screen, and the film was moved along the range axis of the A-type presentation. Successive pictures of the narrow gated slice were obtained and displayed side by side. Such a display is very useful when looking for fading of the various echoes.

The advantages of this technique over the direct filming of the original A-scope presentation are worth mentioning. First, the tape can be played back at a convenient reduced speed. Second, it is not necessary to use the discrete echo itself to trigger the camera and, in so doing, to lose the information contained in the first part of the life of the echo. Third, by isolating with a narrow gate the interesting spot on the A-scope display, we can eliminate the blurring of the film caused by multiple superimposition of the noise strip. Fourth, the information about the range of the echo is preserved.

REPRESENTATIVE SELECTION OF DATA

The general characteristics of the echoes we attribute to "upward discharges" are the following:

(*a*) They are discrete and generally last less than 0.5 second.

(*b*) They show no preferrred range. The maximum range observed in the absence of aurora was around 900 km.

(*c*) They sometimes rise from noise level to maximum value in two repetition periods of the radar, or 40 milliseconds. Calculations of the velocity required to produce the first Fresnel zone of a column of ionization (deduced from the rise time of the echo and its range) give values in some cases greater than 100 km/sec.

(*d*) They usually decay very rapidly from maximum amplitude (at least five times noise level) to less than noise level in 100 milliseconds. The decay is not exponential.

(*e*) They sometimes show a tendency to repeat themselves at the same range.

(*f*) They generally occurred for two hours around midnight, but did not occur every night. During the months of September, October, and November, 1955, they occurred on more than half the nights. Very few were observed during December. As many as 400 echoes in one hour were seen. No correlation with any known phenomenon was established.

The characteristics of these echoes are depicted by the examples here reproduced. In addition, for reference, a standard meteor echo and a case of a simultaneous meteor and auroral echo are shown. We shall introduce them with the following comments. (Later, we shall describe the measurement of speed.)

Echo 137 is a standard meteor echo composed of a specular and a turbulent ection.

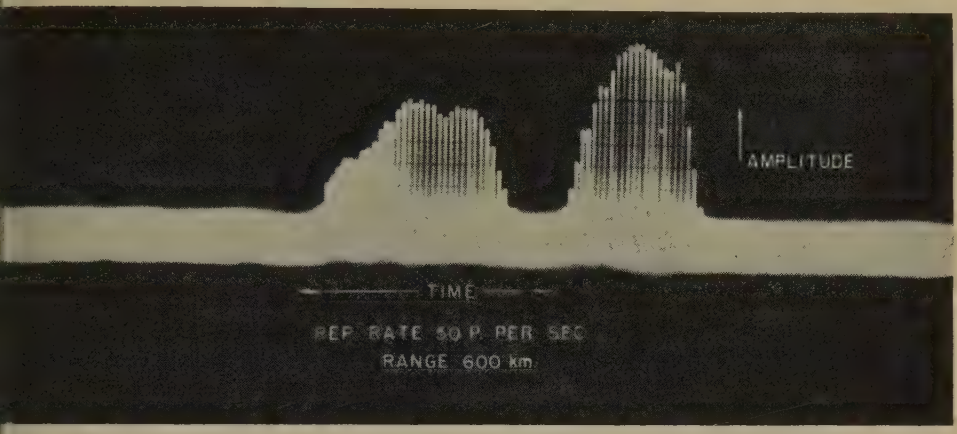

cho 137—Radar echo obtained at Ithaca, New York, on 27.85 Mc/sec, October 21, 1955, 2310-2415 hours EST

Echo 146 is typical because of its sharp rise of amplitude with time. The range 650 km. The ionized column that gives reflection is produced at a speed of bout 95 km/sec.

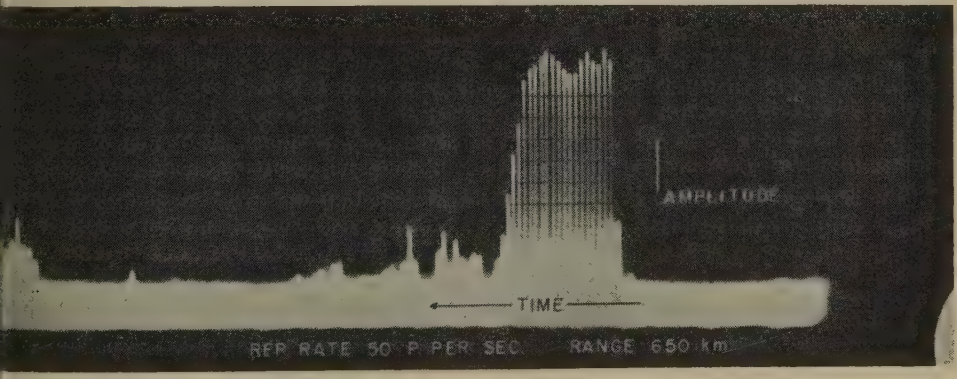

cho 146—Radar echo obtained at Ithaca, New York, on 27.85 Mc/sec, October 21, 1955, 2310-2415 hours EST

Echo 156 is typical for its steep rise of amplitude with time. The range is 750 km. The ionized column that gives reflection is produced at a speed of about 200 km/sec.

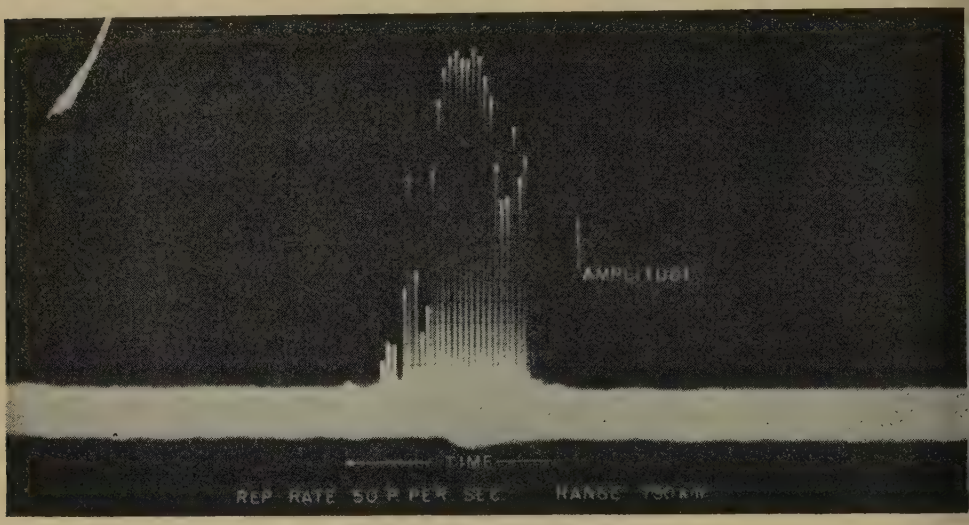

Echo 156—Radar echo obtained at Ithaca, New York, on 27.85 Mc/sec, October 21, 1955, 2310-2415 hours EST

Echo 150 is typical, not only for the steep rise, but also for the very flat horizontal top. It has to be emphasized that no saturation is limiting the amplitude. Indeed, the little rise at the left of the top indicates that there is still a possibility of increasing amplitude. Furthermore, a comparison with Echo 156 will show that larger pips with the same noise level can be recorded.

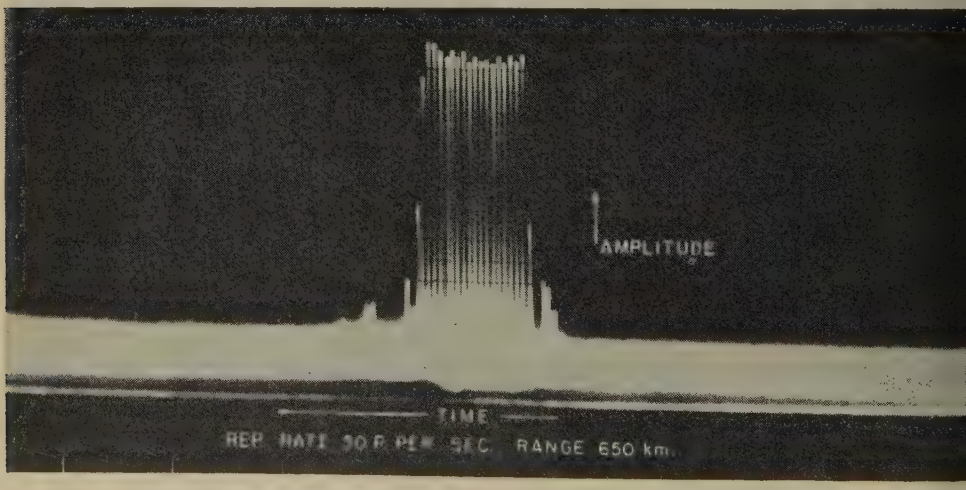

Echo 150—Radar echo obtained at Ithaca, New York, on 27.85 Mc/sec, October 21, 1955 2310-2415 hours EST

Echo 139 shows not only a fast rise and a flat top, but also a fast decay, with the point of maximum curvature at an amplitude of about 0.265 of its maximum amplitude.

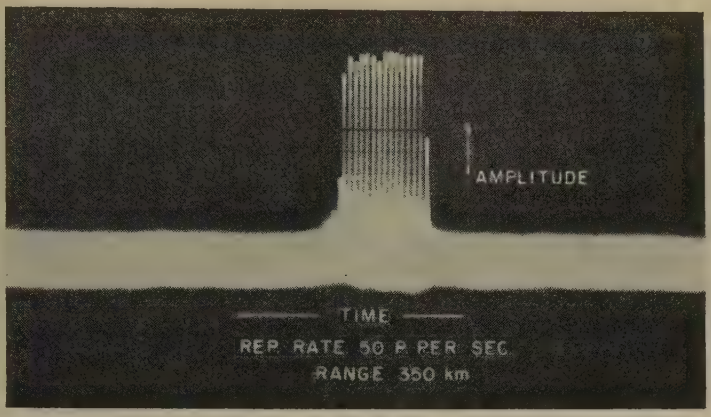

ECHO 139—Radar echo obtained at Ithaca, New York, on 27.85 Mc/sec, October 21, 1955, 2310-2415 hours EST

Echo 153 shows the same characteristics as Echo 139, but the decay is much slower. The point of maximum curvature is still at an amplitude of about 0.265 of its maximum.

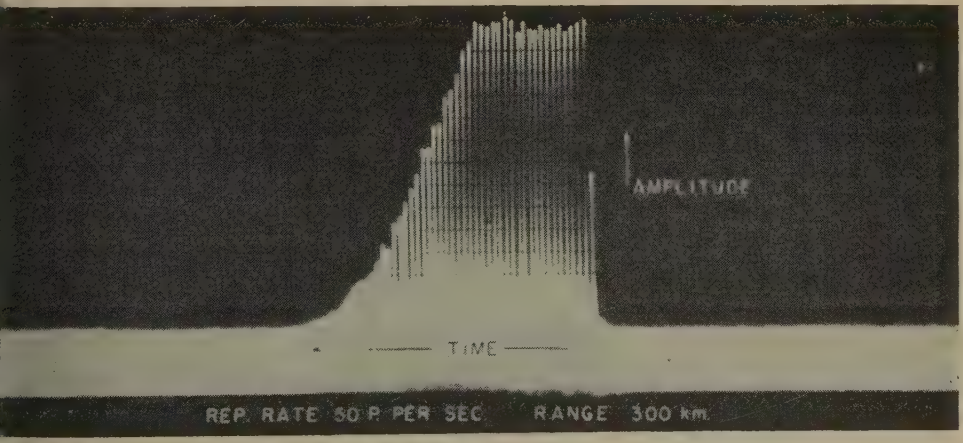

ECHO 153—Radar echo obtained at Ithaca, New York, on 27.85 Mc/sec, October 21, 1955, 2310-2415 hours EST

Echo 151 indicates a repetition of features after an interval of about 1.6 seconds. A fast rise is noticeable as well.

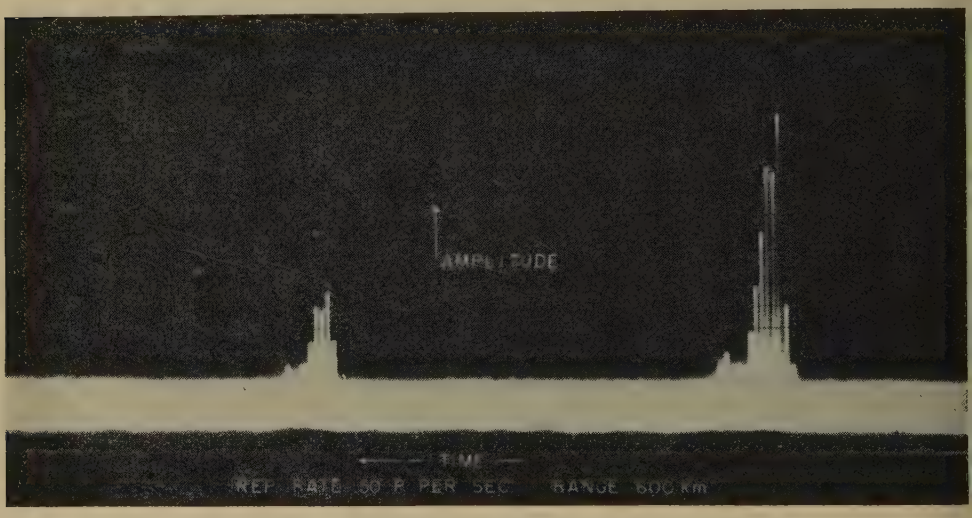

Echo 151—Radar echo obtained at Ithaca, New York, on 27.85 Mc/sec, October 21, 1955, 2310-2415 hours EST

Echo 154 has a long duration of about 4.3 seconds. It can be interpreted as a series of different echoes, or as a turbulent-type single echo. If it is the latter case, it decays according to a law roughly represented by $1/t$.

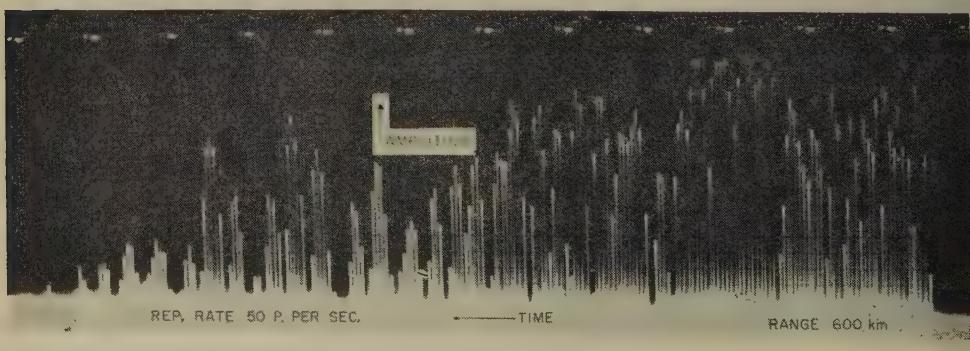

Echo 154—Radar echo obtained at Ithaca, New York, on 27.85 Mc/sec, October 21, 1955, 2310-2415 hours EST

Echo 173 presents double-feature characteristics. It appears to be a fast echo embedded in a meteor echo. Quite a number of echoes like this were collected.

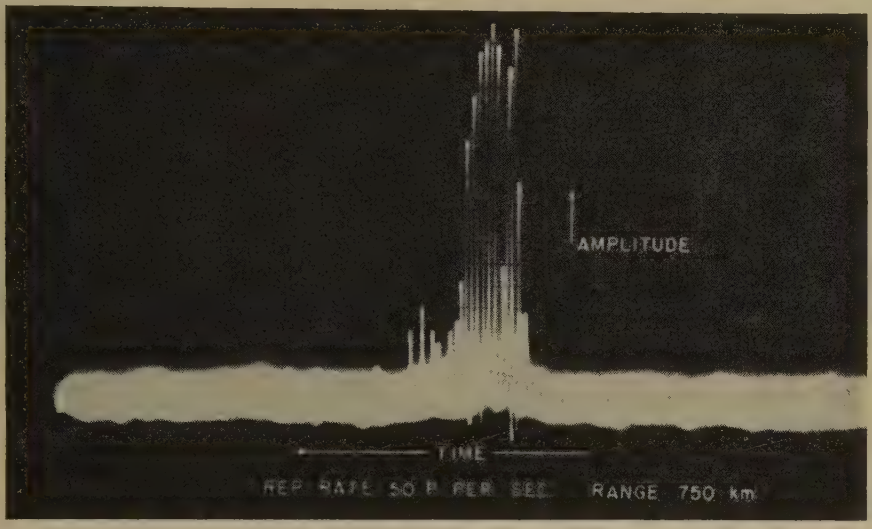

Echo 173—Radar echo obtained at Ithaca, New York, on 27.85 Mc/sec, November 2, 1955, 0100 hour EST

Echo 148 presents a deep fading right after the rise that can scarcely be attributed to noise.

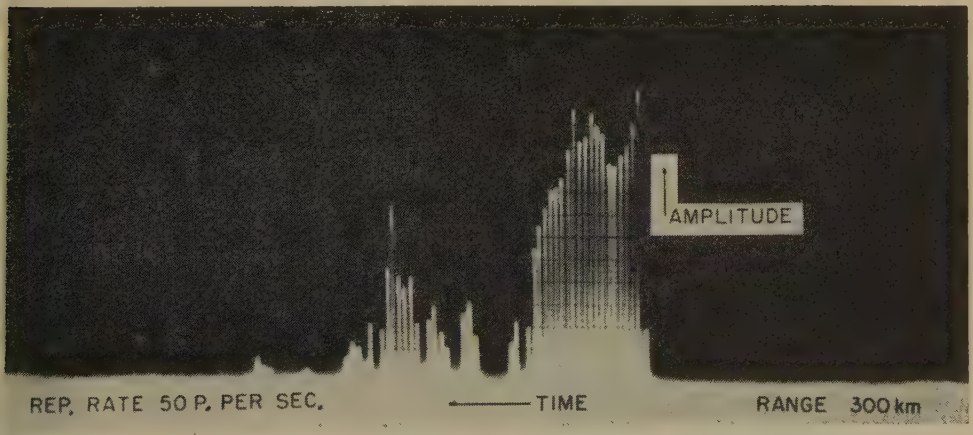

Echo 148—Radar echo obtained at Ithaca, New York, on 27.85 Mc/sec, October 21, 1955, 2310-2415 hours EST

Echo 171 is caused by a meteor accompanying an aurora.

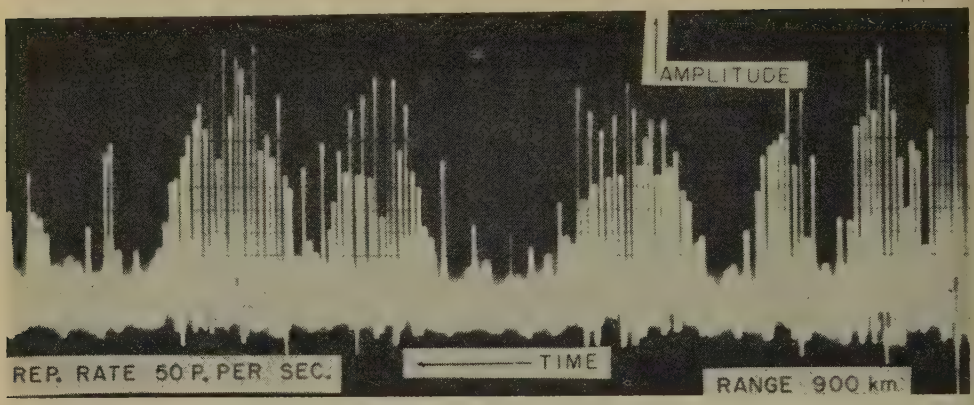

Echo 171—Radar echo obtained at Ithaca, New York, on 27.85 Mc/sec, November 2, 1955, 0100-0200 hours EST

DISCUSSION AND INTERPRETATION OF THE EXPERIMENTAL RESULTS

Echoes like the ones shown on these pages were observed on the screen of the 27.85-Mc/sec radar and recorded in great numbers during the fall of 1955 at Ithaca, New York.

They are similar to meteor echoes, but their characteristics are such that they cannot be attributed to meteors. Let us discuss these characteristics in some detail.

(*a*) *Speed*

The question of whether all meteors originate inside the solar system has not yet been given a definitive answer [see 1, 2, and 3 of "References" at end of paper]. The majority of astronomers, led by H. A. Newton and including Fisher, Watson, Wylie, and Whipple, support the hypothesis that all meteors have their origin inside the solar system. Consequently, they cannot have a speed greater than 72 km/sec. The grounds for such a position are that meteors do not show any preferred direction of approach to the sun, as one would expect for bodies coming into the solar system from outer space.

The remaining minority of astronomers, led by Von Niessel and including Hoffmeister, Opik, Boothroyd, Astapovitch, and La Paz, support the opposite idea. Their position is based on a number of experimental results obtained in the twenties and thirties which are not in agreement with H. A. Newton's theory. More recent work tends to reduce the significance of such experimental data because they are not sufficiently accurate [4].

A great improvement in the accuracy of speed measurements was brought about by radio methods. The approach as outlined in reference [5] makes use of the diffraction pattern produced by the incoming meteor as it is recorded in successive sweeps of an A-scope presentation.

The received intensity goes from a minimum to a maximum or *vice versa* as the head of the meteor crosses one Fresnel zone. The length of this zone is known

when the distance from the receiver of the ionized colum produced by the meteor is known. The time taken by the meteor to cross one of these zones is indicated by the number of pulses recorded between the entrance and the exit from the zone. Then the speed is deduced. Through the described procedure, the results published in reference [6], and many more since then, were obtained.

In general, only parabolic (that is, 72 km/sec) or elliptic (that is, less than 72 km/sec) speeds were recorded.

Our speed measurement followed the same approach, but contrary to what other workers have done, we concentrated our attention on the first Fresnel zone. That was possible, as indicated previously, because of the particular technique used, that is, the filming from magnetic tape records that are played back to reproduce the A-scope presentation. Thus, it was possible to study the life of the echo from its birth. The study of the first Fresnel zone facilitates accuracy because it is acting practically alone. The radio-wave reflection from the second Fresnel zone implies the presence of the first, the third one the presence of the first and the second, and so on.

A brief comment is required on the evaluation of the length of the first Fresnel zone. We used the expression of $\sqrt{2R\lambda}$, instead of $2\sqrt{\lambda R}$ used by Blackett and Lovell [7], or $\sqrt{(\lambda R)/2}$ used by Lovell and Clegg [8].

The derivation of this formula follows from the simple application of Pythagoras' theorem,

$$r^2 + R^2 = R^2 + \frac{\lambda^2}{16} + \frac{R\lambda}{2}$$

where r = radius of first Fresnel zone, R = range, and λ = wavelength. Since

$$\frac{\lambda^2}{16} \ll \frac{R\lambda}{2}$$

$$r^2 = \frac{R\lambda}{2}; \qquad d = 2r = \sqrt{2R\lambda}$$

There are some limitations on our measurements, as follows: (*a*) Should 1,000 km be the maximum detected range, that is, should 4.5 km be the largest detected first Fresnel zone, the repetition rate of 50 periods per second gives a maximum measurable speed of $4.5 \times 50 = 225$ kilometers per second. (*b*) Since $R = (1/2\lambda)(v/T)^2$, $\lambda = 10.8$ meters, and $T = 1/50$ second; then, if $v = 72$ km/sec, the minimum range useful for discriminating between hyperbolic and elliptic speed is $R_{min} = (1/2 \times 10.8)(72/50)^2 = 100$ km, and at ranges less than 100 km we cannot detect whether a speed is hyperbolic or elliptic. It would be very interesting to be able to lower this limit so that some statement about the height of the ionized column could easily be made.

Various speeds were measured from our recordings. The maximum speed measured was about 200 km/sec. How can we be sure that we are dealing with the entire first Fresnel zone? Is it not possible, theoretically speaking, that the columnar ionization stops before the central Fresnel zones are formed? The rise in echo amplitude due to the entire first Fresnel zone is very well characterized and cannot be mistaken. This statement becomes clear when one observes the amplitude contour for Fresnel diffraction at a straight edge.

(*b*) *Range*

No preference for any range was shown by these echoes during any of the observations. The interval of ranges was, of course, limited. The minimum recorded range was 120 km, a little above $R_{min} = 100$ km. Closer ranges were not recorded efficiently because of the spreading of the main bang. The maximum range, in the absence of aurora (that is, of spurious echoes), was about 900 km. On the other hand, standard meteor echoes were recorded up to ranges of about 1,100 km.

If we suppose that the maximum range recorded coincides with the maximum range detectable for this type of echoes, it will depend on the maximum height of the echo point.

In our case, the figure of 900 km leads to a height of 50 km. It appears that the height from which the echoes are returned is considerably less than that for meteors.

In addition, the fact that these echoes showed no range preference (while meteor-type echoes generally showed preferred ranges, especially during showers) leads us to conclude that our range observations are inconsistent with those expected from meteors.

(*c*) *Duration and shape*

The duration and the shape of these echoes are such that they can hardly be explained by present meteor theory. As shown by Booker [9], the data collected by Greenhow [10] prove that for the first 0.4 second meteor trails can be considered as non-turbulent. Then, during this interval, the meteor theory outlined by Kaiser and Closs [11] holds. Except in a few cases, our echoes were shorter than 0.4 second, and we have tried to fit them to the latter theory.

However, the tops of our echoes, when not affected by sudden jumps, are completely flat and horizontal. That means that we could not be dealing with the so-called underdense meteors requiring an exponential decay of the amplitude *vs* time right after the formation of the column, nor with the so-called overdense meteors requiring a rise in amplitude with time because of the enlargement of the "metallic" cylinder through diffusion.

(*d*) *Decay*

The decay of our echoes is not so abrupt as would be expected for overdense meteors, nor exponential as would be expected as a result of diffusion in the case of standard underdense meteors. (Note that we are not dealing with turbulence, since our echoes are shorter than 0.4 second.) The average decay time is about 0.1 second. The decay is not exponential because it does not present the properties of an exponential function. One of these properties is expressed by the following formula:

$$\frac{e^{-x} - e^{-(x+a)}}{e^{-(x+a)} - e^{-(x+2a)}} = e^{a} \qquad \ldots\ldots\ldots\ldots\ldots\ldots\ldots\ldots (1)$$

This means that if we take any succession of three pulses, the difference in amplitude between the first and the second pulse, divided by the difference in amplitude between the second and the third pulse, must be equal to e^a, that is, a constant. The echoes we are speaking about do not obey this law.

Furthermore, the derivative of the curvature of e^{-ax} can be shown to be

$$\frac{dK}{dx} = \frac{a^3 e^{-ax}(1 - 2a^2 e^{-2ax})}{(1 - a^2 e^{-2ax})^{5/2}} \quad \ldots\ldots\ldots\ldots\ldots\ldots\ldots\ldots (2)$$

The point of maximum curvature is given by

$$x_m = ln \frac{\sqrt{2a}}{a} \quad \text{and} \quad y_m = \frac{1}{\sqrt{2a}} \ldots\ldots\ldots\ldots\ldots\ldots\ldots\ldots (3)$$

Now let us observe Echo 139 and Echo 153. Let us accept the hypothesis that both echoes have an exponential decay with $a = 4k^2D$. It is clear that D is different in the two cases. D for Echo 139 would have a value of 12.4 m^2/sec and for Echo 153 a value of 2.33 m^2/sec. According to the preceding discussion, we should expect $y_m = 0.043$ for Echo 139 and $y_m = 0.225$ for Echo 153. But this is not true. In both cases, $y_m = 0.265$. Thus, the decay is not exponential.

On the other hand, a careful examination of our records showed that (*a*) the decay presents an S-shape with inversion of curvature, and (*b*) the point of maximum curvature of the decay appears at the same level of the point of maximum curvature of the rise. It seems that we are looking at a gradual disappearance of the ionized column with the characteristic diffraction pattern we should expect in the case of a receding edge. The speed of disappearance can be deduced by the same procedure that we have outlined for the speed of the rise.

(e) Time of occurrence

The 27.85-Mc/sec radar observations took place only in the second half of 1955. It was during this period that our echoes were noticed. Thus, we cannot make any general statement about seasonal variations, but we can report that a very definite trend in the frequency of occurrence was present. The maximum of this activity was noticed in October; it decreased slowly during November; and it was hardly noticeable in December and in the first half of January 1956.

The appearance of these echoes on the scope was not a regular one; nights of complete absence were randomly alternated with very active nights. These echoes were observed mostly at night, with a sharp peak around midnight.

We tried to correlate them with meteor showers, but without success. The first part of October does not regularly offer any meteor shower; in some years, we may expect the Giacobinid shower concentrated around October 10. Two significant meteoric showers are active at the end of October—Orionid and Taurid. Both are described by Lovell [12]. These two showers did not produce any noticeable enhancement of the frequency of appearance of our echoes; furthermore, the discontinuity between successive nights was always present

We may add that Orion and Taurus cross the meridian plane at Ithaca, New York, around 0300 during the month of October. Thus, we would expect a maximum number of echoes at this time. We observed a maximum around midnight.

As far as sporadic meteors are concerned, no better agreement between our observations and the expected sporadic meteor activity was found. It is true that the maximum efficiency of random meteors in producing radio echoes is expected to be during the fall, but, on the other hand, sudden discontinuities are

not to be expected. Furthermore, according to Villard, Eshleman, Manning, and Peterson [13], for a medium latitude, as in the case of Ithaca, New York, the maximum in the diurnal variation of radio occurrence is centered around 0600, not midnight.

(*f*) *Repetition*

A feature observed in our echoes that does not fit into the accepted idea of meteors is the tendency to repeat themselves. We have cases where the pattern of amplitude *vs* time is reproduced in succession with, in general, reduced amplitude. A classical example is shown in Echo 151.

But another variety of echoes has to be considered from this point of view. We refer to the group exemplified by Echo 154. At first glance, they appear to be long-duration echoes produced by turbulence. But if we examine their decay, we find that they do not obey the law $g(t) = (1/t)^3$, which, according to Booker [9], is required for such echoes. Echo 154, for example, decays as $1/t$. A more careful observation suggests that we have here a repetition of short echoes rather than a single echo lasting more than a few seconds.

(*g*) *Height*

On one occasion, we had a very complicated distribution of echoes on our A-scope screen. The situation recorded on November 5, 1955, is sketched in Figure 1, where *A* is the main bang, *B* is a fast fading auroral echo, *C* is a fast pip, and *D* is a low fading ground-scatter echo.

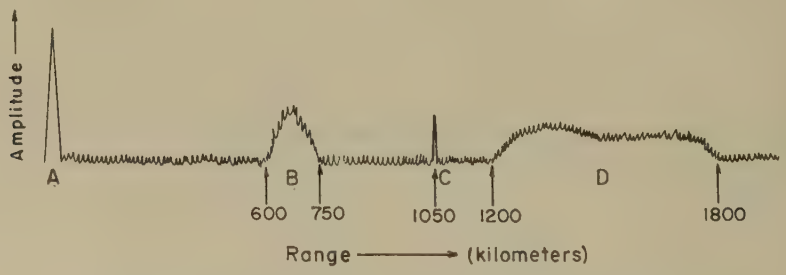

FIG. 1—Sketch of simultaneous echoes recorded on November 5, 1955

The amplitude-*vs*-time display of echo *C* indicates that the echo is connected with a speed measurement of more than 100 km/sec, and has a quasi-flat top and a

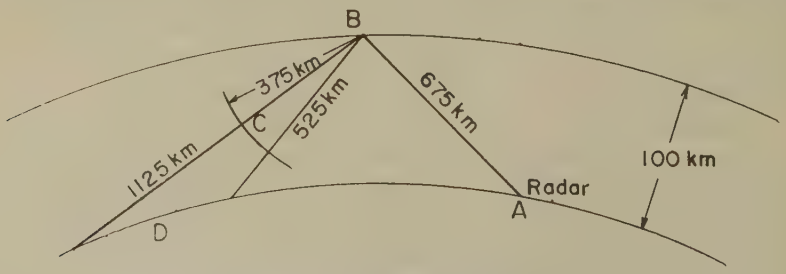

FIG. 2—Interpretation of echoes shown in Figure 1

sharp decay; furthermore, the top seems to be affected by a superimposed fading of the same type noticed in *B*. The fact that the range is quite long for this type of echo suggests an interpretation that is shown in Figure 2.

This leads us to state that the height of the relative echo points must have been between 20 and 60 km.

ADDITIONAL ARGUMENT FOR NON-METEORIC EXPLANATION OF ECHOES

In the foregoing discussion, we have shown that the speeds measured, the ranges, the flatness of the tops, the non-exponential decay, the time of the occurrence, the repetition, and the probable height lead to the conclusion that the echoes cannot be attributed to meteors. We obtain the same negative result when we use a synthetic approach.

Let us try to match our average echo with one of the amplitude-*vs*-time curves given by Kaiser and Closs [11]. We selected the curve corresponding to a line density of $\alpha = 5 \times 10^{14}$ electrons per meter, since it appears to resemble our echoes most closely. Now, we want to deduce what the expected duration for two possible meteoric speeds, namely, 36 and 60 kilometers per second, is.

We have $\alpha = 5 \times 10^{14}$ from the curve that we selected. Evans [14] gives a curve of altitude of maximum ionization (h_2) *vs* geocentric velocity for $\alpha = 2.3 \times 10^{13}$ electrons per meter. From it, for 36 km/sec, we read $h_2 = 93$ km; and for 60 km/sec, we read $h_2 = 103$ km.

From Herlofson [15], we know the relationship between two different heights of maximum ionization when the scale height and the values for the two maximum ionizations are given,

$$h_1 - h_2 = \tfrac{1}{3} H \ln \left(\frac{\alpha_2}{\alpha_1} \right)$$

In our case, according to Evans [14], $H = 7$ km, $\alpha_2 = 2.3 \times 10^{13}$, and $\alpha_1 = 5 \times 10^{14}$ electrons per meter. Then, for 36 km/sec, we have

$$h_1 = h_2 + \tfrac{1}{3} H \times 2.303 \log \left(\frac{\alpha_2}{\alpha_1} \right) = 85.8 \text{ km}$$

For 60 km/sec, we have $h_1 = 95.8$ km.

S. Evans and J. E. Hall [16] give a curve of atmospheric diffusion coefficient D *vs* height. From it, we read for 36 km/sec (that is, at a height of 86 km),

$$D = 1.023 \text{ m}^2/\text{sec}$$

and for 60 km/sec (that is, a height of 96 km),

$$D = 5.88 \text{ m}^2/\text{sec}$$

Kaiser and Closs [11] give an analytical expression for the duration of persistent echoes,

$$t = \frac{10^{-14} \alpha}{4k^2 D}$$

In our case, it follows then that for 36 km/sec, $t = 3.65$ seconds; and for 60 km/sec, $t = 0.64$ second. These two figures are somewhat large in comparison

with the durations measured by us. We infer that not even by a synthetic approach can we find agreement between meteor reflection theory and our observations.

EXPLANATION OF ECHOES AS CAUSED BY UPWARD DISCHARGES

Thus, we are left with the task of finding what is producing our echoes. An extensive examination of our records led us to the idea that upward atmospheric discharges from the top of the troposphere to the bottom of the ionosphere were responsible for the echoes we recorded. We shall try to explain on what evidence we constructed this explanation. From our records, the following conclusions are apparent:

(*i*) The echoes are discrete in range. We explain this observation by the fact that ionization has a columnar shape.

(*ii*) The ionization appears gradually at a speed that can be as high as 200 km/sec and disappears at lower speeds. We could assume that an unknown ionizing cause proceeds with the measured speed, and that after a short interval of a fraction of a second an again unknown de-ionizing cause moves along the column previously formed and destroys it. But it is simpler to conceive of the column as a train of ions moving along.

(*iii*) Diffusion, as indicated by the flatness of the echo amplitude-*vs*-time display, does not play an important role. Recombination contributes, but only as a second-order effect, to the destruction of the ionized column: indeed, the decay has a definite Fresnel diffraction aspect free of appreciable distortion. Diffusion and recombination, in fact, would not be very effective if the axial motion of ions described in (*ii*) above takes place and takes place at speeds of the order of magnitude quoted above.

(*iv*) The columns of ionization do not present a preferred direction (indeed, they do not show preferred range) and disappear at a height of about 50 km. They occur in the sub-ionospheric region.

(*v*) The speed at which the ionized column is produced is always larger than the speed at which the ionized column is destroyed. In other words, the cluster of ions that constitutes the head of our train has a larger speed than the cluster of ions that constitutes the tail. That is what one would expect if the voltage that caused the motion of the first cluster should decrease afterwards.

(*vi*) The ionization can be reproduced after short intervals with the same characteristics. In terms of what we have stated in point (*v*), this means that the applied voltage, after decreasing to zero, can rise again and repeat the cycle.

At this point, it does not seem unreasonable to call the physical agent that produced our echoes an "atmospheric discharge." These discharges should have been developing between the top of the troposphere and the bottom of the ionosphere. Speeds of the order of 110 km/sec characterized the streamers internal to a cloud which were studied by Miles [17].

Now, let us see what further evidence, both theoretical and experimental, we have for such discharges.

First of all, upward discharges to the *E*-layer are required as a necessary link in the charging processes that provide negative charges to the earth's surface. C. T. R. Wilson [18] has given a complete quantitative theoretical description of the phenomenon. The separation of charges created in a thundercloud generates

an electrostatic moment. Of course, the earth's qualities as a reflector must be taken into account. If M is the total electrostatic moment, the electric field vertically above the cloud is given by $2M/h^3$, where h is the height.

While the electric field caused by the thunderstorm falls off as h^3, the breakdown field, which for a given composition of the air is proportional to its density, falls off more rapidly. With experimental values for M and for the breakdown field, Wilson shows the practical possibility of triggering an upward discharge during a thunderstorm. It may even be unnecessary to have thunderclouds for this phenomenon. An ordinary cloud with an average moment of 2×10^4 coulomb-meters per square kilometer spread over an area 10 km in radius should be sufficient to produce upward discharges without other discharges internal or external to the cloud. It is important to notice that the field produced by the electrostatic moment does not decrease drastically as we move away from the vertical.

From the experimental point of view, we have the discharges described in two reports by Boys [19] and Malan [20]. Chalmers [21] writes that "there is some evidence that there is a discharge from the cloud to the ionosphere, shortly after the main stroke and taking the form of a continuous discharge."

Appleton and Chapman [22], after discussing the nature of atmospherics, conclude that "such a slow disturbance [long tail in photographic records, ed.] may possibly be due to an upward discharge from the top of the thundercloud to the ionosphere."

These quotations refer specifically to upward discharges. Other indirect evidence can be found in the scientific literature, especially in many studies of the association of thunderstorm activity and abnormal E-ionization; for example, the work of Ranzi [23] in 1932. Appleton and Naismith [24] in 1933 measured a correlation coefficient of 0.75. There were also the studies by Ratcliffe and White [25, 26] in 1933 and 1934. Good correlations between atmospheric perturbations and abnormal E were obtained in Calcutta [27] and in Australia [28].

It should be noted that a succession of experiments with positive results in favor of such an association was followed by a succession of experiments with negative results. The theory was then abandoned by most researchers around 1937. However, it is our impression that latitude plays an important role in this problem, and latitude should be taken into account, as has been indirectly suggested by E. Appleton and R. Naismith [29]. Furthermore, upward discharges, as pointed out by Wilson [18], are not necessarily connected with thunderstorms.

Last in the series of experimental evidence, we have the papers of Isted [30, 31]. Isted shows some correlation between lightning sferics and a succession of short signals from a distant television station, supposedly reflected by patches of ionization in the E-region that are produced by upward discharges.

ADDITIONAL CRITERION FOR DISCRIMINATION BETWEEN ECHOES FROM METEORS AND UPWARD DISCHARGES

An essential difference between the ionized column produced by a meteor and the ionized channel caused by an upward discharge is the curvature. Meteor trails do not present curvature, while discharges in the northern part of the sky must show a convexity toward east in the case of upward displacement of positive charges as an effect of the geomagnetic interaction.

The determination of such a curvature was outlined and solved by WatsonWatt, Wilkins, and Bowen [32]. Their equation for the radius of the curvature of the particle trajectory is $\rho = \mu V/300B$, where B is the magnetic field in gauss, μ is the permeability, and V is the applied voltage. For $B = 0.5$, horizontal and uniform, they give the curves shown in Figure 3, where it was taken into account that the path is in air, and not in free space.

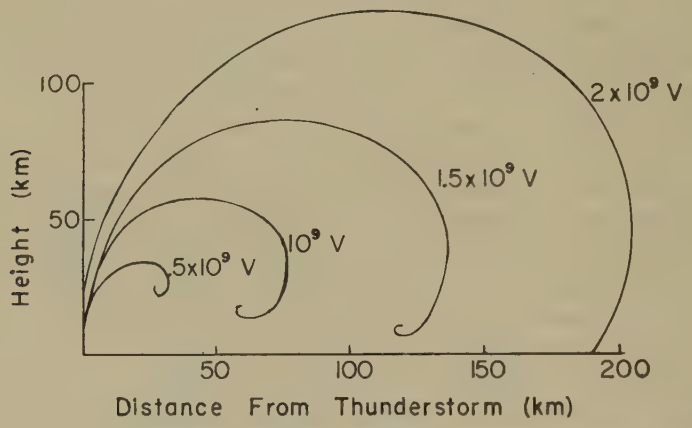

Fig. 3—Curvatures of upward discharges, produced by the geomagnetic interaction

A diffraction pattern different from the one due to an edge moving along a straight line should be expected, especially when the point of observation is contained in the plane of the curved trajectory. The difference should be an important argument for the discrimination between meteor echoes and upward discharge echoes.

Unfortunately, we were working with a fixed antenna pointing north, so that the effect of the curvature was greatly reduced. On the other hand, we were not operating with a pencil beam, but with a main lobe angular aperture of 20°, permitting observations in a direction not perpendicular to the plane of the trajectory.

It is possible that the deep groove appearing in Echo 148, right after the formation of the first Fresnel zone, must be attributed to the curvature already discussed.

POSSIBLE RELATION OF METEORS TO UPWARD DISCHARGES

Some evidence in our records suggests that probably meteors cannot be ruled out of a complete picture of the atmospheric phenomena we are studying. We have a good number of echoes, similar to Echo 173. A definite double pattern characterizes their amplitue-*vs*-time display. One feature may be related to the pattern of a meteor echo, and the second feature may be related to the aspect of an upward discharge echo.

At least 95 per cent of these hybrid echoes have both elements superimposed, and not appearing in sequence. The meteor aspects always precede the fast pip aspects. The delay in the appearance of the fast pips is of the order of 0.1 second. We suspect that the meteor triggered the discharge. The assumption is not at all

unreasonable if we consider a meteor trail as a lightning rod for an upward discharge. Under these circumstances, we can apply the theories of point discharge currents to this reverse aspect of a much observed phenomenon. It should be sufficient here to mention Wilson's [33] contribution to the study of this problem. He carried out experiments to determine "the magnitude of the potential gradient which has to be applied over the surface of a field of grass to make the tips of the grass blades come into action as point discharges" [18]. He proved effectively that even grass contributes to the generation of such discharges.

SUGGESTIONS FOR FURTHER STUDY

VHF radar observations during the summer and the fall of 1955 at Ithaca, New York, gave us useful information, not only about lightning, meteors, and aurora, but also about the existence and the characteristics of "upward discharges" leaving the top of the troposphere and moving toward the ionosphere. The existence of such discharges and their detectability create many new problems requiring further study. They have been outlined in this report, but much remains to be done, and better experimental and theoretical approaches are needed.

A basic repetition rate of 100 pulses per second would be more convenient than our 50 periods per second, because it would give a less spaced sampling of the Fresnel zones in the diffraction pattern that we observe.

A continuous recording system set up to record the number of pips appearing on the screen during each hour of the day would be very useful for the study of the time of occurrence.

An important consideration for any future experiment should be the design of the antenna. First of all, the most efficient antenna from our point of view is the one oriented normal to the meridian plane. A combination of two antennas giving information for two different orientations would be of interest. We suggest an orientation transverse to the meridian plane because the curvature of discharges lies in a plane approximately normal to the meridian plane and the curvature gives a more distorted Fresnel diffraction pattern when it is observed from a point of view contained in its own plane.

Finally, it would be desirable to set up an experiment using horizontal and vertical polarization. Two polarizations and eventually two frequencies in the VHF range should be a good source of information. They probably would give us four working points in the bifurcated region of the curves for metallic columnar reflection shown in reference [34]—two points on the upper curve and two points on the lower curve. From this approach, the diameter of the discharges could be determined.

ACKNOWLEDGMENTS

The present research was performed at the School of Electrical Engineering of Cornell University. The author is indebted for fruitful discussions, suggestions, and aid to Prof. Benjamin Nichols in particular and to the ionospheric research group directed by Prof. Henry G. Booker in general.

Special thanks are due to the National Science Foundation and to the United States Signal Corps, who supported this work.

References

[1] F. L. Whipple, Meteors, special supplement, J. Atmos. Terr. Phys., 149 (1955).
[2] J. P. M. Prentice, Rep. Progr. Phys. (Physical Society, London), **11**, 389 (1948).
[3] J. G. Porter, Rep. Progr. Phys. (Physical Society, London), **11**, 402 (1948).
[4] A. C. B. Lovell, Meteor Astronomy, Clarendon Press, Oxford (1954); Chaps. 8 to 12.
[5] D. C. Ellyett and J. G. Davies, Nature, **161**, 596 (1948).
[6] J. G. Davies and C. D. Ellyett, Phil. Mag., **40**, 614 (1949).
[7] P. M. S. Blackett and A. C. B. Lovell, Proc. R. Soc., A, **177**, 183 (1941).
[8] A. C. B. Lovell and J. A. Clegg, Proc. Phys. Soc., **60**, 491 (1948).
[9] H. G. Booker, URSI Spring Meetings, Washington, D. C., May 2, 1956.
[10] J. S. Greenhow, Proc. Phys. Soc., **65**, 169 (1952).
[11] T. R. Kaiser and R. L. Closs, Phil. Mag., **43**, 1 (1952).
[12] A. C. B. Lovell, Meteor Astronomy, Clarendon Press, Oxford (1954); Chap. 15.
[13] O. G. Villard, V. R. Eshleman, L. A. Manning, and A. M. Peterson, Proc. Inst. Radio Eng., **43**, 1473 (1955).
[14] S. J. Evans, Meteors, special supplement, J. Atmos. Terr. Phys., 86 (1955).
[15] N. Herlofson, Rep. Progr. Phys. (Physical Society, London), **11**, 444 (1948).
[16] S. Evans and J. E. Hall, Meteors, special supplement, J. Atmos. Terr. Phys., 18 (1955).
[17] V. G. Miles, J. Atmos. Terr. Phys., **3**, 258 (1953).
[18] C. T. R. Wilson, Proc. Phys. Soc., **37**, 32D (1925).
[19] C. V. Boys, Nature, **118**, 749 (1926).
[20] D. J. Malan, Paris, C.-R. Acad. sci., **205**, 812 (1937).
[21] J. A. Chalmers, Atmospheric Electricity, Clarendon Press, Oxford (1949); p. 151.
[22] E. V. Appleton and F. W. Chapman, Proc. R. Soc., A, **158**, 1 (1937).
[23] I. Ranzi, Nature, **130**, 368 (1932).
[24] E. V. Appleton and R. Naismith, Proc. Phys. Soc., **45**, 389 (1933).
[25] J. A. Ratcliffe and E. L. C. White, Proc. Phys. Soc., **45**, 399 (1933).
[26] J. A. Ratcliffe and E. L. C. White, Proc. Phys. Soc., **46**, 107 (1934).
[27] J. N. Bhar and P. Syam, Phil. Mag., **23**, 513 (1937).
[28] D. F. Martyn and O. O. Pulley, Proc. R. Soc., A, **154**, 455 (1936).
[29] E. V. Appleton and R. Naismith, Proc. Phys. Soc., **59**, 461 (1947).
[30] G. A. Isted, Marconi Rev., **17**, 37 (1954).
[31] G. A. Isted, Report of the Physical Society Conference on the Physics of the Ionosphere, Physical Society, Cambridge (1954); p. 150.
[32] R. A. Watson Watt, A. F. Wilkins, and E. G. Bowen, Proc. R. Soc., A, **161**, 181 (1937).
[33] C. T. R. Wilson, Phil. Trans. R. Soc., A, **221**, 73 (1920).
[34] J. Feinstein, J. Geophys. Res., **56**, 37 (1951).

AN APPRAISAL OF PHOTON COUNTER MEASUREMENTS OF UPPER ATMOSPHERE PARAMETERS

BY GUSTAVUS J. SIMMONS

Department of Physics, University of Oklahoma, Norman, Oklahoma

(Received July 5, 1957)

ABSTRACT

A model atmosphere is computed consistent with the measurements of O_2 concentration and ambient density between 100 and 125 km made by Byram, Chubb, and Friedman [see 1 and 2 of "References" at end of paper] of the Naval Research Laboratory and the parameters of the Rocket Panel model atmosphere [5] below 60 km. The resulting temperature gradient above 100 km is greater than can be supported by the atmosphere [4]. No physically reasonable alteration of the temperature profile in the 60 to 100 km region produces acceptable temperature gradients above 100 km.

It is concluded that the densities given by photon counting techniques are incompatible with other atmospheric information, and are probably consistently low; and, further, that if the general nature of the density variation as determined by this technique is correct, the resulting temperature segment above 100 km is essentially the same as derived by F. Johnson [4] from considerations of thermal conductivity.

INTRODUCTION

In computing the effects of the *E* layer of the ionosphere on radio wave propagation, it becomes necessary to know the collisional frequency of the electrons, since appreciable absorption of energy can take place in this relatively dense region of the ionosphere. A theoretical formula for the collisional frequency in a region in which oxygen is being dissociated has been used at this Laboratory,* which gives collisional frequency as a function of pressure, temperature, and the fraction of O_2 dissociated. The measurements of Byram, Chubb, and Friedman of ambient density and O_2 concentration seemed especially appropriate, since one of the three necessary atmospheric parameters was immediately available. An attempt was made to produce an atmospheric model consistent with these measurements giving pressures and temperatures between 100 and 130 km. The resulting model was found to have a temperature gradient greater than that which F. S. Johnson had shown the atmosphere capable of supporting [4]. This unexpected result prevented the original objective being achieved, but the method, results, and conclusions were thought to be of some interest.

*Lockheed Missile Systems Research Laboratory, Palo Alto, California. (The writer is now at the University of Oklahoma.)

OUTLINE OF METHOD EMPLOYED TO PRODUCE THE ATMOSPHERIC MODEL

Based on the measurements of density and O_2 concentration, a family of temperature segments between 100 and 130 km, dependent on assumed values of pressure at 100 km, was computed. The Rocket Panel values of the atmospheric parameters below 60 km were assumed correct, and this temperature segment was then fitted to the members of the family of possible temperature segments between 100 and 130 km. By integration along the resulting temperature profiles, the corresponding densities at 100 km were computed. An iterative program for this computation was carried out on an IBM 650 until a temperature profile was found which was compatible with both temperature segments, and which gave the measured density at 100 km.

COMPUTATION OF THE TEMPERATURE SEGMENTS BETWEEN 100 AND 130 KM

Recent rocket-borne instrumentation of atmospheric absorption in narrow spectral bands [1, 2], by workers at the Naval Research Laboratory, has given measurements of ambient density and oxygen concentration in O_2 form between 100 and 130 km. These data are self-consistent, since photon counting techniques were used in both instances, and have been extrapolated into an atmospheric model, primarily in an attempt to evaluate this system of instrumentation.

The density measurements made with Mylar and Glyptal window photon counters [2] have been chosen for use here, since these densities are relatively unaffected by the coronal temperature assumed (7×10^5 deg. K). A least mean square fit to a quadratic was made for the logarithms of the values of these two density profiles.

$$\rho = e^{(2.654-0.3291h_e+0.000,8273h_e^2)} \quad \ldots\ldots\ldots\ldots\ldots\ldots\ldots\ldots (1)$$

where h_e is height above the surface of the earth.

The three remaining density profiles, based on results obtained using aluminum window counters and assumed coronal temperatures of 7×10^5, 10^6, and 2×10^6 degrees Kelvin, can also be fitted to empirical quadratic exponentials with good precision; however, the results are considered to be less meaningful in the present application.

In an atmosphere in hydrostatic equilibrium, if the density between two levels is known to vary as a quadratic exponential, then the following development gives the variation of pressure in this interval:

$$\rho = e^{-(a+bh+ch^2)} \qquad 0 \leq h \leq \underline{h} \quad \ldots\ldots\ldots\ldots\ldots\ldots\ldots\ldots (2)$$

$$p = p_0 - \int_0^h \rho g \, dh \ldots\ldots\ldots\ldots\ldots\ldots\ldots\ldots\ldots\ldots\ldots (3)$$

Equation (3) is a general expression obtained by integrating the hydrostatic equation; p_0 being the pressure at the level $h = 0$.

$$g = g_0\left(\frac{r}{r+h}\right)^2$$

where r is the distance from the center of the earth to the level where $h = 0$, and

g_0 is the force of gravity at the level $h = 0$. If now $\underline{h} \ll r$, which is certainly the case here, where $\underline{h} \leq 30$ km and $r = 6{,}471$ km, equation (3) may be shown to be

$$\left.\begin{aligned} p = p_0 - \frac{2g_0e^{-a}}{rb}\left[\left(\frac{r}{2} - \frac{1}{b}\right) + e^{-bh}\left\{h - \left(\frac{r}{2} - \frac{1}{b}\right)\right\}\right] \\ - g_0e^{-a}\left[-\frac{1}{cr}(1 - e^{-ch^2}) + \frac{1}{2}\sqrt{\frac{\pi}{c}}\,\mathrm{erf}\,(h\sqrt{c})\right] \end{aligned}\right\} \quad (4)$$

It is of interest to note that if the density variation between the same levels is a linear exponential,

$$\rho = e^{-(a+bh)}$$

The corresponding pressure variation is

$$p = p_0 - \frac{2g_0e^{-a}}{rb}\left[\left(\frac{r}{2} - \frac{1}{b}\right) + e^{-bh}\left\{h - \left(\frac{r}{2} - \frac{1}{b}\right)\right\}\right]$$

which are the first two terms in equation (4). Since p_0 is unknown, that is, not measured by the techniques under consideration, it is convenient to define a variable, Δp, which is a known function.

$$\Delta p = p_0 - p \quad (5)$$

The values of Δp, computed from equation (4) at 1-km intervals, using

$$g_0 = 949.00 \text{ cm sec}^{-2}$$

and

$$\rho = e^{-(21.99+0.1637h-0.000{,}8273h^2)}$$

are tabulated in Table 1.

TABLE 1

h_e	Δp	h_e	Δp
101	0.024 7	116	0.157 5
102	0.045 7	117	0.159 8
103	0.063 6	118	0.161 8
104	0.078 9	119	0.163 5
105	0.092 0	120	0.165 0
106	0.103 3	121	0.166 3
107	0.113 0	122	0.167 5
108	0.121 3	123	0.168 5
109	0.128 5	124	0.169 4
110	0.134 7	125	0.170 3
111	0.140 0	126	0.171 0
112	0.144 6	127	0.171 6
113	0.148 5	128	0.172 1
114	0.152 0	129	0.172 6
115	0.155 0	130	0.173 1

The information available (density, O_2 concentration, and Δp) may be used to compute atmospheric parameters. For this purpose, the following relations are developed.

Given a mixture of X gases, a mean molecular weight $\bar{M}$ is defined.

$$\bar{M} = \frac{\sum_1^x n_i M_i}{\sum_1^x n_i} \qquad \text{.....(6)}$$

where n_i is the number of particles of the i^{th} gas of molecular weight M_i . In the case where two constituents form a dissociative-combination pair, and when the relative mass composition is invariant, that is, the atmosphere is a region in which diffusive separation has a long time constant and considerable turbulent mixing exists, the following formulas apply:

$$n_1 + \frac{n_2}{f} = kN$$

$$n_3 = lN, \text{ etc.}$$

where n_1 and n_2 are the dissociative-combinative pair, one particle of n_1 yielding f particles of n_2 , and k, l, etc., are the constants of mass composition. The atmosphere between 100 and 130 km may be considered such a system with O_2 and O as the only pair. D is defined to be the dissociation.

$$D = \frac{n_2}{2n_1 + n_2} = 1 - \frac{n_1}{kN}$$

$$n_1 = kN(1 - D)$$

$$n_2 = 2kND$$

Substituting these expressions into equation (6) yields

$$\bar{M} = \frac{1}{1 + kD}\bar{M}_0 = \frac{\rho N_0 \bar{M}_0}{\rho N_0(1 + k) - n_1 \bar{M}_0}$$

where $\bar{M}_0$ is the mean molecular weight when $D = 0$, N_0 is Avogadro's number, n_1 is the measured concentration of O_2 molecules, and ρ is the measured density. The working formula which involves only the experimentally measured quantities and a running parameter, p_0 , is

$$\left.\begin{aligned} T &= \frac{N_0 \bar{M}_0(p_0 - \Delta p)}{\rho(N_0 R)(1 + k) - n_1 \bar{M}_0 R} \\ (R &= 8.314 \times 10^7 \text{ erg deg}^{-1} \text{ mole}^{-1}) \end{aligned}\right\} \qquad \text{.....(7)}$$

A family of temperature profiles was computed using values of Δp between 0.1744 and 0.2725. Representative members have been plotted in Figure 1, along with temperature segments from several proposed atmospheric models [3, 4, 5]. It would appear that these results could be interpreted to support the atmospheric model proposed by F. Johnson [4], based on considerations of heat transfer and radiation.

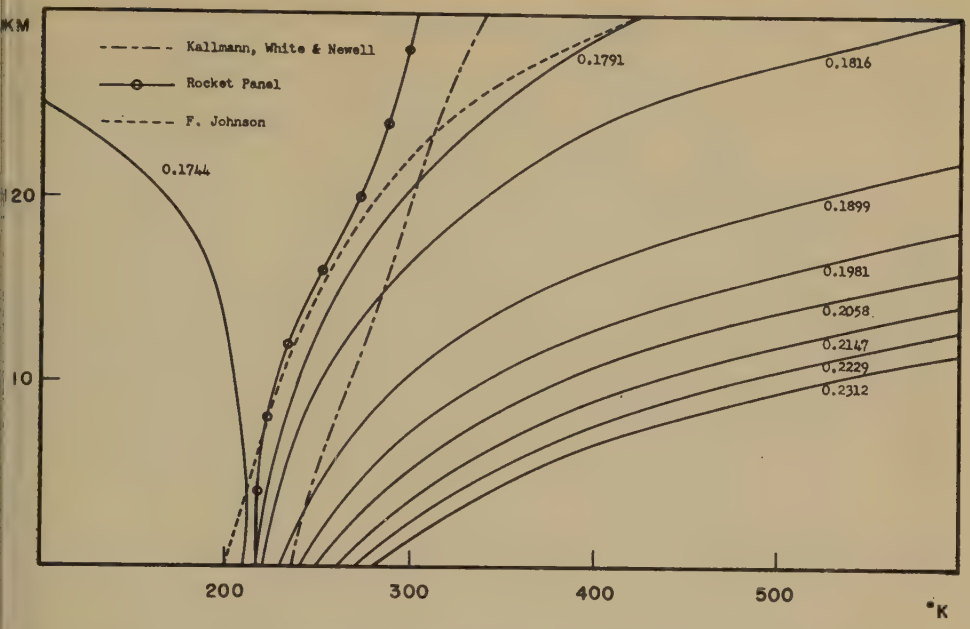

FIG. 1—Family of temperature profiles using values of Δp between 0.1744 and 0.2725

COMPUTATION OF THE ATMOSPHERIC MODEL

The temperatures proposed by the Rocket Panel for altitudes less than 60 km were derived from the firings of many rockets (26) and have remained in good agreement with later results. The Rocket Panel pressures, densities, and temperatures below 60 km were taken, therefore, for the lower atmospheric model. An arbitrary value of p_0 was substituted into equation (7), and the resulting temperatures at 100, 102, and 104 km used with the Rocket Panel temperatures at 56, 58, and 60 km to fit a fifth-order polynomial through these points, joining the temperature segments together. A numerical integration was then performed, and the following system solved for ρ at 100 km:

$$\Phi = \exp\left(-\int_{60}^{h} \frac{Mg}{RT}\,dh\right) \quad \ldots\ldots(8)$$

$$\rho = \rho_{60}\frac{T_{60}M}{TM_{60}}\Phi \quad \ldots\ldots(9)$$

The computed value of ρ at 100 km was compared with the measured value, and depending on the sign and magnitude of the error, a correction was made to the assumed p_0 . This computational scheme was programmed for an IBM 650 computer, which repeated the process until a temperature segment was found which fitted both pieces of the temperature profile as explained, and which gave the measured value of density at 100 km. The resulting temperature profile is shown in Figure 2.

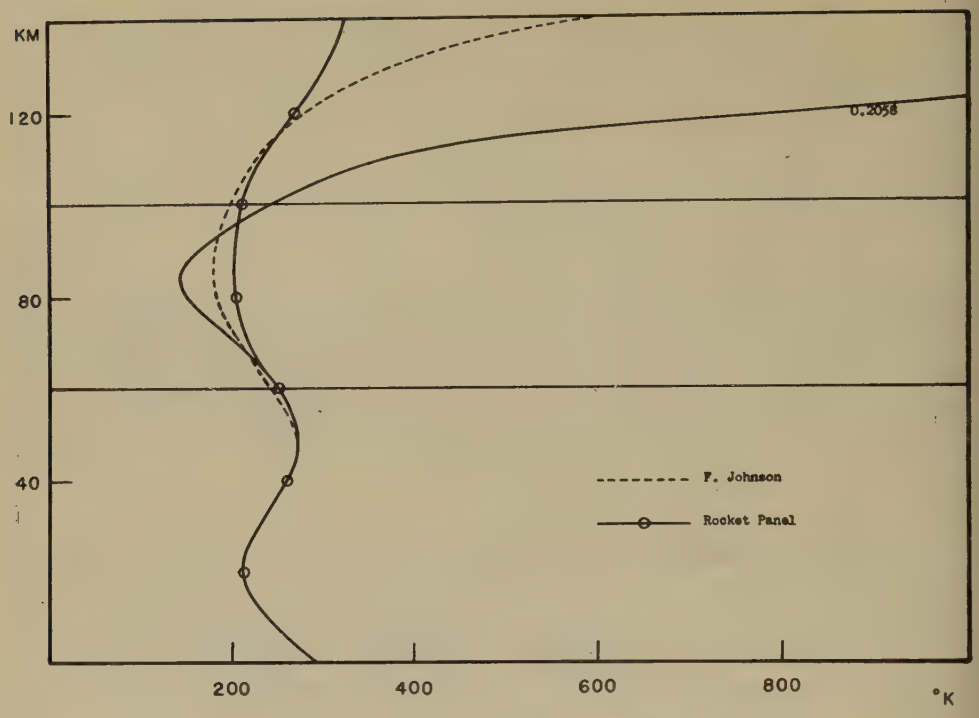

FIG. 2—Temperature profile resulting from computational scheme

APPRAISAL OF THE MODEL

The temperature gradient of the chosen profile is greater than can be supported by the atmosphere [3] between 100 and 130 km, and the temperature at 83 km (145.9°K) is lower than any measurements have shown it to be. Reference to Figure 1 shows that temperature profiles are available which are compatible with the theoretically derived temperature gradients in this region. However, the corresponding temperatures at 100 km are high enough that the only way equations (8) and (9) may be satisfied is by introducing an unrealistic protuberance in the temperature profile between 60 and 100 km, or else by assuming the Rocket Panel values below 60 km invalid. Neither of these procedures is physically justified.

CONCLUSIONS

It is conjectured, on the basis of this work, that the density at 100 km is significantly higher than found by photon counting techniques, and that quite probably the entire density profile is low. If, however, the general nature of the density variation as determined by this technique is correct, the resulting temperature segment is essentially the same as derived by F. Johnson [4].

The conclusions which have been reached are that a larger temperature gradient exists between 100 km and 200 km than has commonly been assumed [4, 5], and that the densities derived by photon counting techniques are rigorously incompatible with other atmospheric information and are probably consistently low.

ACKNOWLEDGMENTS

In conclusion, the author wishes to express his thanks to the Mathematical Services Group of Lockheed Missile Systems Division, and especially to Mr. Tom Jones for performing the computations indicated in this paper.

References

[1] E. T. Byram, T. A. Chubb, and H. Friedman, Dissociation of oxygen in the upper atmosphere, Phys. Rev., **98**, 1594-1597 (1955).

[2] E. T. Byram, T. A. Chubb, and H. Friedman, The solar x-ray spectrum and the density of the upper atmosphere, J. Geophys. Res., **61**, 251-263 (1956).

[3] H. K. Kallmann, W. B. White, and H. E. Newell, Jr., Physical properties of the atmosphere from 90 to 300 kilometers, J. Geophys. Res., **61**, 513-524 (1956).

[4] F. S. Johnson, Temperature distribution of the ionosphere under control of thermal conductivity, J. Geophys. Res., **61**, 71-76 (1956).

[5] The Rocket Panel, Pressures, densities, and temperatures in the upper atmosphere, Phys. Rev., **88**, 1027-1032 (1952).

MAGNETIC FIELDS IN A CONDUCTING FLUID SPHERE WITH VOLUME CURRENTS*

BY K. P. CHOPRA**

Physics Department, Delhi University, Delhi, India

(Received January 22, 1957)

ABSTRACT

The study of force-free and other equilibrium configurations of magnetic fields in a conducting fluid sphere with volume currents flowing in the interior of the sphere forms the subject matter of this note. In Part I, assuming the electrical conductivity of the sphere to be infinite, the general conditions governing the force-free and other equilibrium fields are derived, and their solutions obtained. It is found that a force-free field must be a suitable combination of a poloidal and a toroidal part. The magnetic energy is equally divided in its poloidal and toroidal components. The Part II of this note deals with the case of finite electrical conductivity. Here, the possibility of a current distribution is explored such that the corresponding magnetic field does not decay with time. It is concluded that it is difficult to imagine a poloidal configuration of the magnetic field, whereas a purely toroidal non-decaying magnetic field is certainly possible.

INTRODUCTION

Recently, the problem of equilibrium configurations of magnetic stars has been the subject of intensive investigation by Chandrasekhar and Fermi (1953) and Ferraro (1954). The present note deals with the study of some of the possible configurations of the magnetic fields in a conducting sphere in which body currents are assumed to flow. It is, however, assumed that there are no currents in the exterior of the sphere. The magnetic field **H** and the electric current density **j** are expressed in terms of two functions U and V. These functions are similar to Stokes' potential functions. The magnetic field components derived from U and V are called poloidal and toroidal, respectively. The abstract provides an adequate summary of the investigation.

*Since this paper was sent to the press, it has been pointed out to me that very recently S. Chandrasekhar (Astroph. J., 124, 232 and 571, 1956) has discussed a similar problem. I regret that I was not aware of these papers, which were not available here at the time of communication of this paper.

**The writer is now at the University of Maryland, Department of Physics.

I. INFINITE ELECTRICAL CONDUCTIVITY

I.1. *Fundamental Equations*—The magnetic field $\mathbf{H}$ in stars of infinitely conducting fluids, with electric currents $\mathbf{j}$ flowing in them, are governed by the Maxwell equations

$$\operatorname{div} \mathbf{H} = 0 \quad \ldots\ldots (1)$$

and

$$\operatorname{curl} \mathbf{H} = 4\pi\mathbf{j} \quad \ldots\ldots (2)$$

Further, if the electrodynamic forces are in hydrostatic equilibrium, then $\mathbf{j}$ and $\mathbf{H}$ should be such that

$$\operatorname{grad} (p + \rho\Omega) = \mathbf{j} \times \mathbf{H} \quad \ldots\ldots (3)$$

where p is the hydrostatic pressure, ρ is the fluid density, and Ω is the gravitational potential of the star. The last equation implies that the electrodynamic forces should be irrotational, and therefore we must have throughout the configuration

$$\operatorname{curl} (\mathbf{j} \times \mathbf{H}) = 0 \quad \ldots\ldots (4)$$

To these equations we may add a simplifying assumption of the axial symmetry, namely,

$$\frac{\partial \mathbf{H}}{\partial \varphi} = 0 \quad \ldots\ldots (5)$$

I.2. *Solution of Fundamental Equations*—By virtue of equations (1) and (5), the magnetic field $\mathbf{H}$ can be expressed in terms of the functions U and V, such that

$$H_r = \frac{1}{r^2 \sin\theta} \frac{\partial U}{\partial \theta}, \qquad H_\theta = \frac{1}{r \sin\theta} \frac{\partial U}{\partial r}, \qquad H_\varphi = \frac{V}{r \sin\theta} \quad \ldots\ldots (6)$$

where U and V are functions of r — and θ — only. The field components deriving from U and V are called "poloidal" and "toroidal," respectively.

Substitution of (6) in (2) gives for the components of the electric currents

$$4\pi\mathbf{j} = \frac{1}{r \sin\theta} \left[\frac{1}{r} \frac{\partial V}{\partial \theta} \hat{r} - \frac{\partial V}{\partial r} \hat{\theta} - \Delta U \hat{\varphi} \right] \quad \ldots\ldots (7)$$

where

$$\Delta U = \frac{\partial^2 U}{\partial r^2} + \frac{\sin\theta}{r^2} \frac{\partial}{\partial \theta} \left(\frac{1}{\sin\theta} \frac{\partial U}{\partial \theta} \right) \quad \ldots\ldots (8)$$

Equations (6) and (7) together give

$$4\pi\mathbf{L} = 4\pi\mathbf{j} \times \mathbf{H} = -\frac{1}{r^2 \sin^2\theta} \left[\left(\Delta U \frac{\partial U}{\partial r} + V \frac{\partial V}{\partial r} \right) \hat{r} + \frac{1}{r} \left(\Delta U \frac{\partial U}{\partial \theta} + V \frac{\partial V}{\partial \theta} \right) \hat{\theta} + \frac{1}{r} \frac{\partial (U, V)}{\partial (r, \theta)} \hat{\varphi} \right] \quad \ldots\ldots (9)$$

Now, equation (4) is satisfied if either (*i*)

$$\left(\Delta U \frac{\partial U}{\partial r} + V \frac{\partial W}{\partial r}\right)\hat{r} + \frac{1}{r}\left(\Delta U \frac{\partial U}{\partial \theta} + V \frac{\partial V}{\partial \theta}\right)\hat{\theta} + \frac{1}{r}\frac{\partial(U, V)}{\partial(r, \theta)}\hat{\varphi} = 0 \quad \ldots(10)$$

or (*ii*)

$$\left.\begin{aligned} &\frac{\partial}{\partial \theta}\left\{\frac{1}{\sin\theta}\frac{\partial(U, V)}{\partial(r, \theta)}\right\}\hat{r} - \frac{1}{\sin\theta}\frac{\partial}{\partial r}\left\{\frac{1}{r^2}\frac{\partial(U, V)}{\partial(r, \theta)}\right\}\hat{\theta} + \left[\frac{1}{\sin\theta}\frac{\partial}{\partial \theta}\right. \\ &\left.\left\{\frac{1}{r^2}\left(\Delta U \frac{\partial U}{\partial \theta} + V \frac{\partial V}{\partial \theta}\right)\right\} - \frac{\sin\theta}{r^2}\frac{\partial}{\partial \theta}\left\{\frac{1}{\sin^2\theta}\left(\Delta U \frac{\partial U}{\partial r} + V \frac{\partial V}{\partial r}\right)\right\}\right]\hat{\varphi} = 0 \end{aligned}\right\} \quad \ldots(11)$$

I.3. *Force-Free Fields*—Equation (10) leads to what are called the force-free fields. It is identically satisfied if

$$\left.\begin{aligned} \Delta U \frac{\partial U}{\partial r} + V \frac{\partial V}{\partial r} &= 0 \\ \Delta U \frac{\partial U}{\partial \theta} + V \frac{\partial V}{\partial \theta} &= 0 \\ \frac{\partial(U, V)}{\partial(r, \theta)} &= 0 \end{aligned}\right\} \quad \ldots(12)$$

and

The last equation in (12) is actually contained in the first two. A non-trivial simultaneous solution of the set of equations (12) is easily obtained if we put

$$V = kU \quad \ldots(13)$$

where k is a constant, and U is a solution of the equation

$$\Delta U + k^2 U = 0 \quad \ldots(14)$$

Outside the star, however, the functions U' and V' are such that

$$\Delta U' = 0, \quad \text{and} \quad V' = 0 \quad \ldots(15)$$

The solutions of (14) and (15) are

$$\left.\begin{aligned} U &= Cr^{1/2}J_{3/2}(kr)\sin^2\theta \\ V &= kCr^{1/2}J_{3/2}(kr)\sin^2\theta \end{aligned}\right\} \quad \ldots(16)$$

and

inside the sphere, ($r \leq R$); and

$$\left.\begin{aligned} U' &= (C'/r)\sin^2\theta \\ V' &= 0 \end{aligned}\right\} \quad \ldots(17)$$

outside the sphere ($r \geq R$), where R is the radius of the star, and C' is another constant to be determined from the condition of continuity of the magnetic field at the surface of the star. Hence, the components of the magnetic field inside the star are

$$\left.\begin{aligned} H_r &= 2Cr^{-3/2}J_{3/2}(kr)\cos\theta \\ H_\theta &= Cr^{-3/2}[J_{3/2}(kr) - krJ_{1/2}(kr)]\sin\theta \\ H_\varphi &= kCr^{-1/2}J_{3/2}(kr)\sin\theta \end{aligned}\right\} \quad \ldots(18)$$

and

while outside the star we have

$$\left.\begin{aligned} H'_r &= 2C(R^{1/2}/r)J_{3/2}(kR)\cos\theta \\ H'_\theta &= C(R^{1/2}/r)J_{3/2}(kR)\sin\theta \end{aligned}\right\} \quad \text{and} \quad H'_\varphi = 0 \qquad \ldots\ldots(19)$$

The corresponding current density j has the components

$$\left.\begin{aligned} j_r &= \frac{kC}{2\pi} r^{-3/2} J_{3/2}(kr)\cos\theta \\ j_\theta &= \frac{kC}{4\pi} r^{-3/2}[J_{3/2}(kr) - krJ_{1/2}(kr)]\sin\theta \end{aligned}\right\} \quad \text{and} \quad j_\varphi = \frac{k^2C}{4\pi} r^{-1/2}[J_{3/2}(kr)]\sin\theta \qquad \ldots\ldots(20)$$

Since the medium outside the star is assumed to be non-conducting, the normal component of the current density must vanish at the surface ($r = R$). This holds if

$$J_{3/2}(kR) = 0 \qquad \ldots\ldots(21)$$

The last equation has the roots

$$kR = 1.43\pi, 2.46\pi, 3.47\pi \qquad \ldots\ldots(22)$$

On application of the boundary condition (21), we finally have

$$\left.\begin{aligned} H_\theta &= -kCR^{-1/2}J_{1/2}(kR)\sin\theta \\ j_\theta &= -\frac{k^2C}{4\pi} R^{-1/2}J_{1/2}(kR)\sin\theta \end{aligned}\right\} \quad \text{and} \qquad \ldots\ldots(23)$$

at the surface ($r = R$), and

$$H'_\theta = -\frac{kCR^{5/2}}{r^3} J_{1/2}(kR)\sin\theta \qquad \ldots\ldots(24)$$

outside the star. All the other components of the magnetic field and the electric current density vanish at the surface of the star and outside it.

Let us now calculate the proportion in which the magnetic energy of a force-free field divides itself in its toroidal and poloidal parts. The magnetic energy M_T, corresponding to the toroidal part of the force-free magnetic field, is given by

$$M_T = \frac{1}{8\pi}\int_0^\pi \int_0^R H_\varphi^2 \cdot 2\pi r^2 \sin\theta \, d\theta \, dr \qquad \ldots\ldots(25)$$

which, with the help of (6) and (13), becomes

$$M_T = \tfrac{1}{4}k^2 \int_0^\pi \int_0^R \frac{U^2}{\sin\theta} \, d\theta \, dr \qquad \ldots\ldots(26)$$

On the other hand, the magnetic energy M_P, due to the poloidal part of the magnetic field, is

$$M_P = \frac{1}{8\pi}\int_0^{\pi}\int_0^{R} H_P^2 \cdot 2\pi r^2 \sin\theta \, d\theta \, dr$$

$$= \tfrac{1}{4}\int_0^{\pi}\int_0^{R}\left\{\frac{1}{r^4\sin^2\theta}\left(\frac{\partial U}{\partial\theta}\right)^2 + \frac{1}{r^2\sin^2\theta}\left(\frac{\partial U}{\partial r}\right)^2\right\} r^2 \sin\theta \, d\theta \, dr$$

$$= \pi\int_0^{\pi}\int_0^{R} U j_\varphi r \, d\theta \, dr \qquad \ldots\ldots(27)$$

But the equations (7) and (14) give for the currents corresponding to the poloidal part of the force-free field

$$j_\varphi = -\frac{\Delta U}{4\pi r\sin\theta} = \frac{k^2 U}{4\pi r\sin\theta} \qquad \ldots\ldots(28)$$

Hence, the poloidal magnetic energy is given by

$$M_P = \tfrac{1}{4}k^2\int_0^{\pi}\int_0^{R}\frac{U^2}{\sin\theta}\, d\theta \, dr \qquad \ldots\ldots(29)$$

On comparison of (26) and (29), it may be concluded that the magnetic energy of a force-free field is equally divided in its poloidal and toroidal parts.

I.4. *Other Equilibrium Fields*—Other equilibrium fields are provided by equation (11), which is satisfied if

$$\frac{\partial(U, V)}{\partial(r, \theta)} = 0 \qquad \ldots\ldots(30)$$

and

$$\frac{\partial\left(\frac{\Delta U}{r^2\sin^2\theta}, U\right)}{\partial(r, \theta)} + \frac{\partial\left(\frac{V}{r^2\sin^2\theta}, V\right)}{\partial(r, \theta)} = 0 \qquad \ldots\ldots(31)$$

The last equation is identically satisfied if inside the sphere we have

$$\Delta U = f(U) r^2 \sin^2\theta \qquad \ldots\ldots(32)^*$$

and

$$V = \kappa_2 r^2 \sin^2\theta \qquad \ldots\ldots(33)^*$$

where κ_2 is a constant, and $f(U)$ is an arbitrary function of U. The simplest solution of (32) would correspond to a constant value, say κ_1, for the function $f(U)$. Then,

$$\Delta U = \kappa_1 r^2 \sin^2\theta \qquad \ldots\ldots(34)$$

Since there are no currents outside the star, we must have

$$\left.\begin{aligned} \Delta U' &= 0 \\ \text{and} \qquad V' &= 0 \end{aligned}\right\} (r \geq R) \qquad \ldots\ldots(35)$$

The solution of (34) and (35) is [cf. Ferraro, 1954]

*Equations (32) and (33) satisfy (30) only if either $U = 0$ or $V = 0$. Therefore, the poloidal and toroidal solutions refer to two different cases. The properties of the hydrostatic fields are discussed elsewhere [Chopra, 1957].

$$U = \kappa_1\left(\frac{1}{10}r^4 - \frac{1}{6}R^2r^2\right)\sin^2\theta, \qquad (r \leq R) \quad \ldots\ldots\ldots\ldots (36)$$

and

$$U' = -\frac{1}{15}\kappa_1\left(\frac{R^5}{r}\right)\sin^2\theta, \qquad (r \geq R) \quad \ldots\ldots\ldots\ldots (37)$$

Finally, equations (6), (33), (35), (36), and (37) yield for the components of the magnetic field

$$\left.\begin{aligned} H_r &= -\kappa_1(\tfrac{1}{3}R^2 - \tfrac{1}{5}r^2)\cos\theta \\ H_\theta &= -\kappa_1(\tfrac{2}{5}r^2 - \tfrac{1}{3}R^2)\sin\theta \end{aligned}\right\} \quad \ldots\ldots\ldots\ldots (38)$$

and

$$H_\varphi = \kappa_2 r\sin\theta \quad \ldots\ldots\ldots\ldots (39)$$

inside the star, and

$$H_r' = -\frac{2\kappa_1R^5}{15r^3}\cos\theta, \qquad H_\theta = -\frac{\kappa_1R^5}{15r^3}\sin\theta, \qquad H_\varphi = 0 \quad \ldots\ldots (40)$$

outside the star. The corresponding current system is such that

$$j_r = \frac{\kappa_2}{2\pi}\cos\theta, \qquad j_\theta = -\frac{\kappa_2}{2\pi}\sin\theta, \qquad j_\varphi = -\frac{\kappa_1 r}{4\pi}\sin\theta \quad \ldots\ldots (41)$$

inside the star. Besides, the discontinuity in the toroidal component of the magnetic field at the surface of the star essentially requires the presence of surface currents j_s, given by

$$j_s = \frac{1}{4\pi}\kappa_2 R\sin\theta \quad \ldots\ldots\ldots\ldots (42)$$

These surface currents are essential to close the meridional electric currents flowing inside the star.

II. FINITE ELECTRICAL CONDUCTIVITY

II.1. *Formulation of the Problem; Basic Equations*—Investigated in this Section is the kind of a secularly constant (non-decaying) configuration of a magnetic field subject to the condition of hydrostatic equilibrium of the electrodynamic forces that is possible when electric currents flow in a sphere of finite electrical conductivity. The basic equations involved in the present case are the Maxwell equations

$$\left.\begin{aligned} \operatorname{curl}\mathbf{H} &= 4\pi\mathbf{j} \\ \operatorname{div}\mathbf{H} &= 0 \\ \operatorname{curl}\mathbf{E} &= -\frac{d\mathbf{H}}{dt} = 0 \\ \operatorname{div}\mathbf{E} &= 0 \\ \mathbf{j} &= \sigma\mathbf{E} \end{aligned}\right\} \quad \ldots\ldots\ldots\ldots (43)$$

and the equilibrium condition

$$\operatorname{curl}(\mathbf{j}\times\mathbf{H}) = 0$$

To these equations, we may add the simplifying assumption of axial symmetry (5).

II.2. *Solution of the Problem*—Assuming that the electrical conductivity σ is constant and finite throughout the configuration, it follows from (7) and (43) that

$$\text{curl } \mathbf{E} = -\frac{1}{4\pi\sigma r \sin\theta}\left[\frac{1}{r}\frac{\partial}{\partial\theta}(\Delta U)\hat{r} - \frac{\partial}{\partial r}(\Delta U)\hat{\theta} + \Delta V\hat{\phi}\right] \quad \ldots\ldots(44)$$

The right-hand side of (44) vanishes when

$$\Delta U = \text{const} \quad \ldots\ldots(45)$$

and

$$\Delta V = 0 \quad \ldots\ldots(46)$$

But for poloidal fields, the equilibrium condition requires that

$$\Delta U = f(U)r^2 \sin^2\theta \quad \ldots\ldots(47)$$

Hence, it may be concluded that it is difficult to imagine a secularly constant poloidal magnetic field subject to the condition of hydrostatic equilibrium of the electrodynamic forces.

On the other hand, for toroidal fields, we have a solution of (46),

$$V = Cr^2 \sin^2\theta \quad \ldots\ldots(48)$$

where C is a constant. The magnetic field is given by

$$H_\varphi = Cr \sin\theta \quad \ldots\ldots(49)$$

which results from a current distribution,

$$j_r = \frac{C}{2\pi}\cos\theta, \qquad j_\theta = -\frac{C}{2\pi}\sin\theta \quad \ldots\ldots(50)$$

Such a configuration satisfies the equilibrium condition (26). Hence, it is concluded that a purely toroidal configuration of non-decaying magnetic field is possible which simultaneously satisfies the condition of hydrostatic equilibrium of the electrodynamic forces.

References

[1] S. Chandrasekhar and E. Fermi, Astroph. J., **118**, 116 (1953).
[2] V. C. A. Ferraro, Astroph. J., **119**, 407 (1954).
[3] K. P. Chopra, University of Maryland Tech. Rep. No. 90 (1957).

THE EFFECT OF SOLAR FLARES ON THE GEOMAGNETIC FIELD

By R. PRATAP*

The Dominion Observatory,
Department of Mines and Technical Surveys,
Ottawa, Canada

(Received June 10, 1957)

ABSTRACT

The dynamo equation is solved for a conductivity produced by solar-flare ultraviolet radiations from the sun. The crochet amplitudes in horizontal field components are then computed and compared with observed results. It is found that fair agreement exists between the theoretical and experimental values only if the seat of the crochet current system is within a few kilometers of the current system producing the quiet-day solar variation.

INTRODUCTION

The phenomena of crochets and their dependence on solar flares have been studied by Fleming [see 1 of "References" at end of paper], McNish [2], and others. McNish concludes that no measurable crochet amplitudes exist beyond 90° of the sub-solar point. He has also shown that the crochet effect is due to an augmentation of the S_q field produced by an increase in the electrical conductivity of the ionosphere under the influence of enhanced ultraviolet radiation from the sun. Further evidence has been provided by Newton [3], who has discussed 23 major crochets recorded on Abinger magnetograms. He observed that the amplitudes of these crochets in the horizontal field ΔH were always negative and the amplitudes ΔV when present were also negative, whereas the amplitudes $H\Delta D$ change direction during the day, being easterly before and westerly after about 10.7 hours local time. The amplitudes of ΔH and ΔD vary in the same manner as the S_q variation in the respective elements, in agreement with the conclusions of McNish [2]. Recently, Nagata [4] has studied statistically the crochets from Huancayo, Kakioka, and Watheroo and found crochet amplitudes at Huancayo to be abnormal compared to those at other low-latitude stations. Thus, the most frequent crochet amplitude at Kakioka was 7.2 gammas, while that at Huancayo was 25.8 gammas. However, the ratio $\Delta H/R_h$, where R_h is the range of the S_q variation in H at the time of maximum crochet, was found to be the same for all the above-mentioned stations and equal to about 0.3. Furthermore, the times from the start to the maximum perturbation T_1 and from the maximum to recovery T_2 were found to be much the same for all three stations. Nagata has also observed that the angle between the ΔH and R_h vectors is negligible, and the maximum

*Permanent address: Geophysical Laboratories, Bengal Engineering College, Howrah, India.

number of crochets occur near local noon. Nagata, however, did not take into account such important parameters as the intensity of the flare and the epoch of its occurrence. Forbush [5] has shown that there exists a correlation between ΔH and R_h, and that this can be explained on the assumption of variation in the strength of the wind pattern. Further evidence is provided by Ellison [6] and others [7], who have suggested that the probable seat of the current system producing the crochet effect may be below the E layer and at about the 80-km level.

It is the purpose of the present paper to calculate theoretically the changes in the geomagnetic field at the surface of the earth associated with a growth and decay of ionospheric conductivity. The results of the calculations are then compared with the observed effects of flares. The method used in solving the dynamo equations is the same as that used by Chakrabarty and Pratap [8] in discussing the quiet-day solar diurnal variations.

EXPRESSION FOR THE IONOSPHERIC CONDUCTIVITY

The change in the ionospheric conductivity associated with the solar flare is taken as a function of the zenith distance of the sun. Then the integrated conductivity due to a solar flare can be written as

$$(\rho e) = \sum_{s=0}^{\infty} a_s \cos^s \chi \exp\left[-\alpha \sin^2 (t - t_0)\right] \quad \ldots\ldots\ldots\ldots\ldots\ldots (1)$$

where

$$\cos \chi = \sin \delta \cos \theta + \cos \delta \sin \theta \cos t$$

t_0 is the time of maximum of the crochet, α and a_s are constants, δ being the declination of the sun, θ the colatitude, and t the local time, measured from the midday meridian. We confine our attention to the region of t defined by

$$-\pi/2 \leq t \leq +\pi/2$$

since the phenomenon is observed only on the daylit hemisphere. It may be mentioned here that the ionospheric conductivity is independent of the position of the flare on the sun's disk [6]. α is a constant depending on the growth and decay of the flare, as well as combination and recombination in the upper atmosphere.

Equation (1) can be expressed in the form of Fourier series as

$$(\rho e) = \sum_{s=0}^{\infty} f_s \cos st \exp\left[-\alpha \sin^2 (t - t_0)\right] \quad \ldots\ldots\ldots\ldots\ldots\ldots (2)$$

where f_s are functions of a_s, δ, and θ.

DYNAMO EQUATION AND ITS SOLUTION

The dynamo equation is given by

$$a(\rho e)^2\left[\frac{\partial}{\partial \phi}(vH_z) + \frac{\partial}{\partial \theta}(uH_z \sin \theta)\right] = (\rho e)\left[\frac{1}{\sin \theta}\frac{\partial^2 R}{\partial \phi^2} + \frac{\partial}{\partial \theta}\sin \theta \frac{\partial R}{\partial \theta}\right] - \left[\frac{1}{\sin \theta}\frac{\partial R}{\partial \phi}\frac{\partial (\rho e)}{\partial \phi} + \sin \theta \frac{\partial R}{\partial \theta}\frac{\partial (\rho e)}{\partial \theta}\right] \quad \ldots\ldots (3)$$

If we take the earth as a dipole, we have

$$H_z = C \cos \theta \quad \ldots\ldots(4)$$

where C is a constant (about -0.6 gauss); we can also take the velocity potential of the atmospheric oscillation as

$$\psi_\sigma^\tau = \sum_\sigma \sum_\tau K_\sigma^\tau P_\sigma^\tau \sin (\tau t + \beta) \quad \ldots\ldots(5)$$

and in substituting equations (2), (4), and (5) in equation (3) we get after reductions as in [8] and using the same notation

$$\left.\begin{aligned} \sum_\sigma \sum_\tau CK_\sigma^\tau \frac{(-\sin \theta)}{2\sigma + 1} [\sigma(\sigma + 2)(\sigma - \tau + 1)P_{\sigma+1}^\tau + (\sigma^2 - 1)(\sigma + \tau)P_{\sigma-1}^\tau] \\ \times \sum_{s'=-\infty}^{\infty} g_{s'} \sin [(\tau + s')t + \beta] \exp [-2\alpha \sin^2 (t - t_0)] \end{aligned}\right\} \ldots\ldots(6)$$

On the R.H.S., we can assume a current function of the form

$$\left.\begin{aligned} R = \sum_\sigma \sum_\tau CK_\sigma^\tau \sum_n \sum_m P_n^m \{p_n^m \sin (mt + \beta_m) + q_n^m \cos (mt + \beta_m)\} \\ \times \exp [-\alpha \sin^2 (t - t_0)] \end{aligned}\right\} \ldots\ldots(7)$$

Substituting this in equation (3), we can write the coefficient of $\sin [(m + s)t + \beta_m]$ as

$$\left.\begin{aligned} \sum_{n=0}^{\infty} [Q_n^{m-2}(s)(Ap_n^{m-2} + Bq_n^{m-2})(m - s) \\ + p_n^m R_n^m(s) + Q_n^{m+2}(s)(-Ap_n^{m+2} + Bq_n^{m+2})(m - s)] \end{aligned}\right\} \ldots\ldots(8)$$

and that of $\cos [(m + s)t + \beta_m]$ as

$$\left.\begin{aligned} \sum_{n=0}^{\infty} [Q_n^{m-2}(s)(-Bp_n^{m-2} + Aq_n^{m-2})(m - s) \\ + q_n^m R_n^m(s) + Q_n^{m+2}(s)(Aq_n^{m+2} + Bp_n^{m+2})(s - m)] \end{aligned}\right\} \ldots\ldots(9)$$

where

$$R_n^m(s) = \left[n(n + 1) - \frac{ms}{\sin^2 \theta}\right] f_s P_n^m + \frac{\mathrm{d}f_s}{\mathrm{d}\theta} \frac{\mathrm{d}P_n^m}{\mathrm{d}\theta}$$

$$Q_n^m(s) = \frac{f_s P_n^m}{\sin^2 \theta}$$

and $A = (\alpha/2) \cos 2t_0$ and $B = (\alpha/2) \sin 2t_0$.

For the actual computations of the solution, we have taken $s = 0, \pm 1$ and we have confined our calculations to the equinoctial epochs, thus putting $\delta = 0$. Furthermore, we have written the phase β in equation (6) as

$$\beta = \beta' + \epsilon$$

and equation (6) was written as the sum of two terms in

$$\sin [(\tau + s')t + \beta'] \text{ and } \cos [(\tau + s')t + \beta']$$

Thus, this combined with equations (8) and (9) gave us two sets of simultaneous

equations giving the coefficients p_n^m and q_n^m (on equating $\tau + s' = m + s$ and $\beta_m = \beta'$).

When we confine to $s = 0, \pm 1$, we have $s' = \pm 2, \pm 1, 0$, and hence we have five groups of equations giving the necessary value of p_n^m and five groups of equations giving q_n^m. In each group, there were residuals, but the residuals were not more than 10 per cent. The coefficients are given in Table 1.

TABLE 1—*Table of coefficients*

$p_4^3 = \frac{1}{140} a_1 \cos \epsilon$	$q_4^3 = \frac{1}{140} a_1 \sin \epsilon$
$p_3^2 = \frac{2}{15} a_0 \cos \epsilon$	$q_3^2 = \frac{2}{15} a_0 \sin \epsilon$
$p_4^1 = -\frac{3}{70} a_1 \cos \epsilon$	$q_4^1 = -\frac{3}{70} a_1 \sin \epsilon$
$p_2^1 = \frac{1}{7} a_1 \cos \epsilon + \frac{3\alpha}{56} a_1 \cos (\epsilon - 2t_0)$	$q_2^1 = \frac{1}{7} a_1 \sin \epsilon + \frac{3\alpha}{56} a_1 \sin (\epsilon - 2t_0)$
$p_4^{-1} = 0$	$q_4^{-1} = 0$
$p_2^{-1} = \frac{65}{42} a_1 \cos \epsilon + \frac{9\alpha}{28} a_1 \cos (\epsilon - 2t_0)$	$q_2^{-1} = \frac{65}{42} a_1 \sin \epsilon + \frac{9\alpha}{28} a_1 \sin (\epsilon - 2t_0)$

It may be seen that on writing $P_n^m [p_n^m \sin (mt + \beta_m) + q_n^m \cos (mt + \beta_m)]$ we can write them as sine series without involving the arbitrary parameter ϵ. We can thus compute the results without involving ϵ and the results are presented in graphical form. In making the numerical computations, we have taken $a_1 = 2.45\, a_0$ and $\beta = 275°$. The value of $\beta = 275°$ was found to be the best fitting phase for the S_q current system [9]. We have also taken $\alpha = 10$, which was found to be a value which reduces the amplitude to about half in one hour.

RESULTS AND DISCUSSION

In Figure 1, the maximum crochet amplitudes are plotted against the time of maximum occurrence for Abinger and for a low-latitude station such as Alibag. The Abinger curves are for ΔH and $H\Delta D$, and on a normalized scale Newton's results are plotted. The numbers against each point plotted correspond to the reference numbers given in Newton's paper, and the values have been normalized for the one given by 16 in Newton's paper. It can be seen that the observed values of ΔH and $H\Delta D$ agree reasonably well with the calculated curves. It may be noted that ΔD changes from easterly to westerly in direction at about 11.7 hours, whereas Newton has given this value as 10.7 hours. If, however, we take the equinoctial cases from Newton's table, there is much better agreement with the results presented here.

The curve for the low-latitude station shows that all the ΔH amplitudes are positive except in the early morning and late evening hours. These very small negative amplitudes are generally not measurable. This result has been demon-

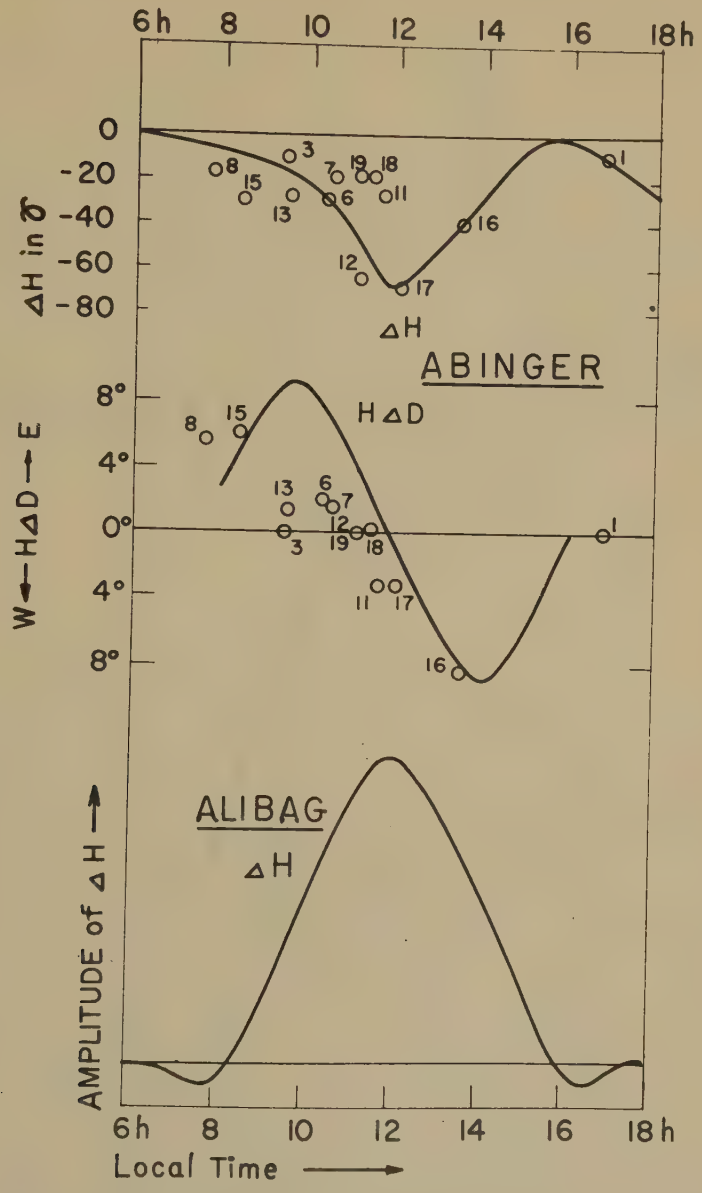

IG. 1—The maximum crochet amplitudes plotted against the time of maximum occurrence

rated by Forbush for crochets at Huancayo. Figure 2 gives a typical crochet r Abinger that would occur with the maximum time of occurrence at local noon. he main characteristic is that the crochet is negative throughout as shown by ewton; but it may be mentioned that in the figures given by Newton many of ie crochets have a sudden decrease and a slow recovery, while those given by llison [6] are to a fair degree symmetrical about the amplitude at the maximum the crochet. From the analysis, it can be seen that this difficulty can be rectified taking suitable values of α before and after the maximum time. This can be

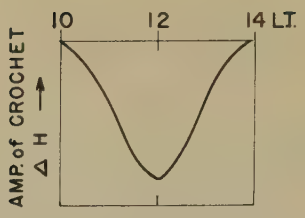

FIG. 2—A typical crochet that would take place at Abinger with the maximum of occurrence at 12 hours local time—starting at 10 hours local time and ending at 14 hours local time

used to discuss the phenomena of ionization and recombination in the ionospheric level of crochet occurrence.

In Figure 3, we have calculated the latitude and longitude distribution of ΔH (crochet amplitudes). The sub-solar point is at (0, 0) and Figure 3*a* gives the

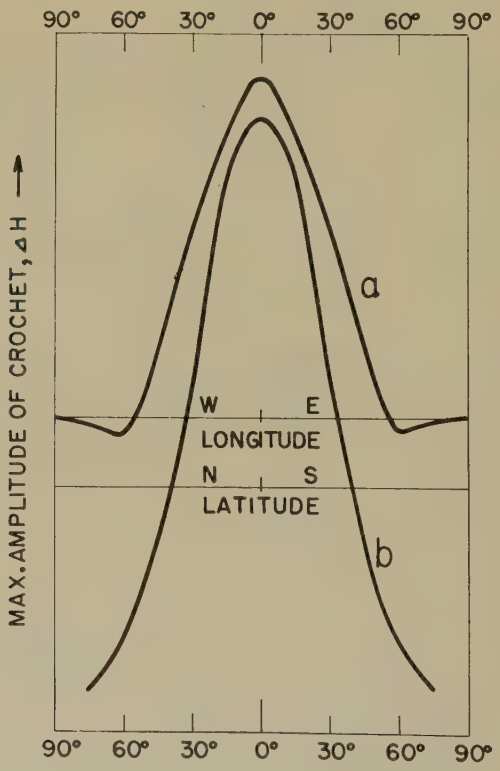

FIG. 3—Maximum crochet amplitudes plotted (*a*) as a function of longitude, and (*b*) as a function of latitude. The sub-solar point is at (0, 0).

longitude distribution. It can be seen that the amplitudes beyond 60° are very small and so are not measurable. The latitude distribution along the noon meridian is given in Figure 3*b*. The amplitude here again is reduced by a factor of three as we go to 60° latitude, which can be seen from the arbitrary scale. This agrees well with the observations of McNish and Newton.

HEIGHT OF THE FLARE REGION

In calculating the above curves, we have taken the height as 100 km and a phase of 275°, while Ellison [6] and others place the seat of the current system at a height of 60 to 70 km. Weekes [7] places the region at about 95 km.

Taking a nodal plane at 30 kms and a phase value of 275° at a height of 100 km, we obtain a phase of about 200° at a height of 80 km, assuming a linear relationship. We have computed the ΔH and $H\Delta D$ (Fig. 4) for Abinger (crochets),

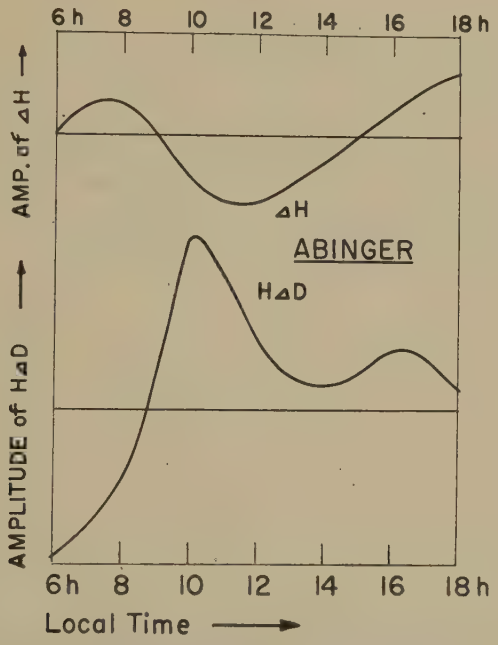

FIG. 4—Maximum crochet amplitudes for Abinger plotted against the maximum time of occurrence with the phase 200° for the atmospheric oscillation

and we observe that there is not good agreement between the observed and the calculated curves. This may be because of our assumption of a linear relation between the phase and height, or it may be because that at the height of 100 km the phase may be $(2\pi n + 275)$. We cannot, however, determine n from these calculations. Greenhow and Neufeld [10] find a linear relationship between the phase and height and a value of about 5° km^{-1}, but from the harmonic expressions given in that paper it is difficult to write an expression for the velocity potential, since the phases for the V_{NS} and V_{EW} do not agree. It may, however, be explained as due to a non-potential part in the velocity components. Hence, from such calculations as these, it is difficult to determine uniquely the height at which the crochet current system exists, but calculations demonstrated in Figure 4 suggest that a decrease in height of more than about 15 km is unlikely.

ACKNOWLEDGMENTS

I am greatly indebted to Dr. S. K. Chakrabarty for the discussions I had in

the early part of this work and to Dr. Kenneth Whitham of this laboratory for many useful discussions. It is a pleasure to acknowledge the advice and encouragement given by Dr. C. S. Beals and Mr. R. G. Madill. The work was made possible through a postdoctorate Research Fellowship awarded by the National Research Council of Canada.

References

[1] J. A. Fleming, Terr. Mag., **41**, 404 (1936).
[2] A. G. McNish, Terr. Mag., **42**, 109 (1937).
[3] H. W. Newton, Mon. Not. R. Astr. Soc., Geophys. Sup., **5**, 200 (1948).
[4] T. Nagata, J. Geophys. Res., **57**, 1 (1952).
[5] S. E. Forbush, J. Geophys. Res., **61**, 93 (1956).
[6] M. A. Ellison, Pub. Royal Observatory, Edinburgh, Vol. 1, 4 (1950).
[7] Geophysical Discussion, Observatory, **75**, 61 (1955).
[8] S. K. Chakrabarty and R. Pratap, J. Geophys. Res., **59**, 1 (1954).
[9] R. Pratap, Proc. Nat. Inst. Sci. India, **20**, 3, 252 (1954).
[10] J. S. Greenhow and E. L. Neufeld, Phil. Mag., **1**, 1157 (1956).

SUDDEN COMMENCEMENTS OF MAGNETIC STORMS AND ATMOSPHERIC DYNAMO ACTION

BY T. OBAYASHI† AND J. A. JACOBS*

Geophysics Laboratory, University of Toronto, Toronto 5, Canada

(Received June 13, 1957)

ABSTRACT

A statistical investigation of world-wide sudden commencements of magnetic storms has been carried out using data from over 30 magnetic observatories distributed all over the world. An appreciable diurnal change in the amplitude of SC's has been found, and the average electric current system for the *Ds* field shows conspicuous current concentrations in the polar regions. The pattern of this current system is similar to that caused by an electric doublet centered on the highly conducting region near the geomagnetic pole, and hence it is probable that the current system exists within the earth's atmosphere. On the other hand, the *Dst* field of SC's seems more likely to be of extraterrestrial origin.

An atmospheric dynamo theory has been applied to interpret this *Ds* current system, on the assumption that the main source of electromotive force generation is due to the enhancement of electrical conductivity in the polar region. The change at a SC is so abrupt (within a few minutes) that it is reasonable to assume that the wind system in the ionosphere will not change. Thus, using the wind system estimated from the *Sq* field, the current system at the time of commencement of the storm has been computed, assuming an appropriate change in the electrical conductivity. Good agreement with observed results has been obtained, and it suggests that a dynamo action in the upper atmosphere is the dominant cause of geomagnetic variations during disturbances. Moreover, there has been found a consistent wind system which can produce the observed geomagnetic variations both for quiet and disturbed conditions with a reasonable range of conductivity changes in the polar regions. This wind system consists of both a diurnal and a semidiurnal term, and the estimated order of magnitude agrees with recent ionospheric measurements.

1. INTRODUCTION

Recently, several investigators [see 1 to 4 of "References" at end of paper] have pointed out that there is an appreciable local time change in the amplitude of sudden commencements (SC's) of magnetic storms in high-latitude zones. An

†On leave from Radio Research Laboratory, Kokubunji, Tokyo, Japan.
*Now at Department of Physics, University of British Columbia, Vancouver 8, Canada.

outstanding daytime enhancement of SC's at Huancayo has also been found [5], and Forbush and Vestine [6] have shown that the effect is possibly associated with known *Sq* electrojets confined within the earth's atmosphere along the geomagnetic equator. On the other hand, Nagata [7] has shown that even the preliminary reverse impulse SC* must be due to atmospheric sources. Thus, it appears likely that the geomagnetic change at a SC must in part be due to atmospheric current systems flowing in the ionosphere.

Since any existing corpuscular theory of magnetic storms has postulated the cause of the SC to be of extraterrestrial origin, it is possible by such theories to account for those observed effects which originate within the earth's atmosphere. Thus, it is highly important to investigate the detailed behavior of SC's in order to make further advances in the theory of magnetic storms.

It was thus decided in the first place to carry out a comprehensive statistical analysis of SC's of magnetic storms using data from world-wide geomagnetic observatories. Some of the results have already been reported previously (Jacobs and Obayashi, [8] and [9]); average electric current systems of the storm time variation *Dst* and the disturbance diurnal variation *Ds* for the SC have been obtained, and it has been found that a conspicuous *Ds* current system exists in the polar regions. Further extensions of this analysis are made in the present paper, and the possible origin of these current systems is discussed.

An interpretation of the cause of the *Ds* current system for the SC is also attempted. Since it is likely that this current system exists within the earth's atmosphere, it may be produced by an enhanced dynamo action due to a sudden increase in the electrical conductivity of the ionosphere at the time of a SC. Using the dynamo theory developed by Schuster [10] and Chapman [11], the current system for the SC is computed in the same way that Fukushima [12] has applied this theory to explain the *Ds* field of the main phase of magnetic storms. Since the change at a SC is abrupt, it seems reasonable to assume that the wind system, which is responsible for the dynamo action, does not change during this time. Therefore, the change from the *Sq* field to the disturbance may be considered as due only to a conductivity change in the polar regions caused by the corpuscular invasion into the earth's upper atmosphere. A consistent wind system which can produce the current system both for the *Sq* and *Ds* fields has been determined, assuming reasonable changes in the conductivity at each stage of the disturbance. The current systems calculated from this wind system agree well with data obtained from actual geomagnetic variations.

2. AVERAGE CURRENT SYSTEMS OF SC'S OF MAGNETIC STORMS

For the present analysis, a knowledge of the world-wide characteristics of geomagnetic variations is required. A considerable amount of data on SC's, well distributed in different latitudes, has been collected for this purpose. The distribution of stations whose data have been used in this study is given in Figure 1, the period of analysis covering the years from 1949 to 1953.

Examining world-wide storm data, it has become evident that individual SC's observed simultaneously at different stations show a considerable local time inequality. Figure 2 is typical of the observations of a particular SC at high-latitude stations, which are arranged according to the longitude of each station.

FIG. 1—Distribution of magnetic observatories whose data are used in this analysis

A systematic change in the shape of SC's exists with geographic longitude; that is, the amplitude of SC's is strongly dependent on the local time of occurrence,

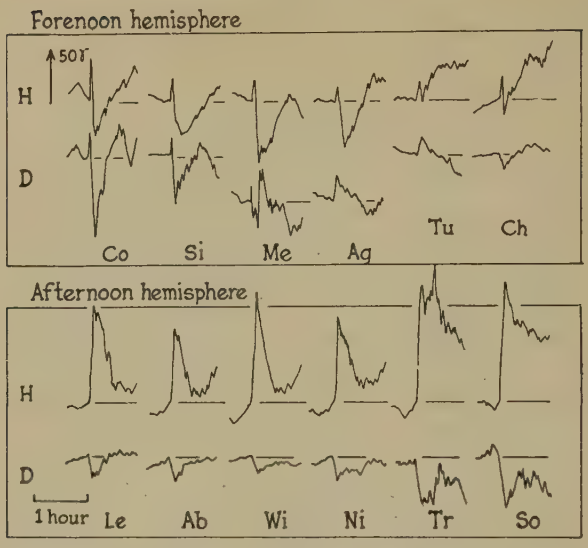

FIG. 2—Local time inequality of SC's at $17^h\ 01^m$ GMT on June 17, 1951. Systematic changes of SC's with respect to the local time (longitude) are evident.

tending to depress or reverse in the horizontal component in the forenoon hemisphere, while it is enhanced in the afternoon hemisphere. Though the shape of SC's is more or less the same for any station in low latitudes, it is thus clear that the local time effect is predominant in the polar regions.

This local time dependence of SC's can be seen more clearly when a statistical examination of a large number of SC's is carried out at each station. The average local time variations of SC's have thus been obtained, and curves for the $X'm$, $Y'm$, and $Z'm$ components† are shown in Figure 3.

It is clear that systematic local time variations of SC's exist all over the world. The diurnal curves of the $X'm$ component indicate a broad minimum in the morning hours and a maximum in the afternoon; the amplitude is very large in the polar regions and decreases towards the lower latitudes. Huancayo, on the geomagnetic equator, behaves very differently from other stations; its anomalous daytime enhancement of SC's has already been discussed in detail by Forbush and Vestine [6].

From these curves, it is possible to draw the equivalent electric current system which would produce such world-wide geomagnetic variations. To construct the current system, the geomagnetic variations are divided into two parts—the storm time variation Dst and the disturbance diurnal variation Ds. Thus, the disturbance field D is expressed as

$$D(\lambda s;\ tst) = Dst(tst) + Ds(\lambda s;\ tst)$$

where tst is the storm time, reckoned from the commencement of the storm, and λs the longitude with reference to the sun (that is, local time, without reference to any fixed point of the earth). Dst is the variation which is averaged over λs

†Details of the statistical method of this analysis are described by Jacobs and Obayashi [8]. $X'm$, $Y'm$, $Z'm$ are normalized values.

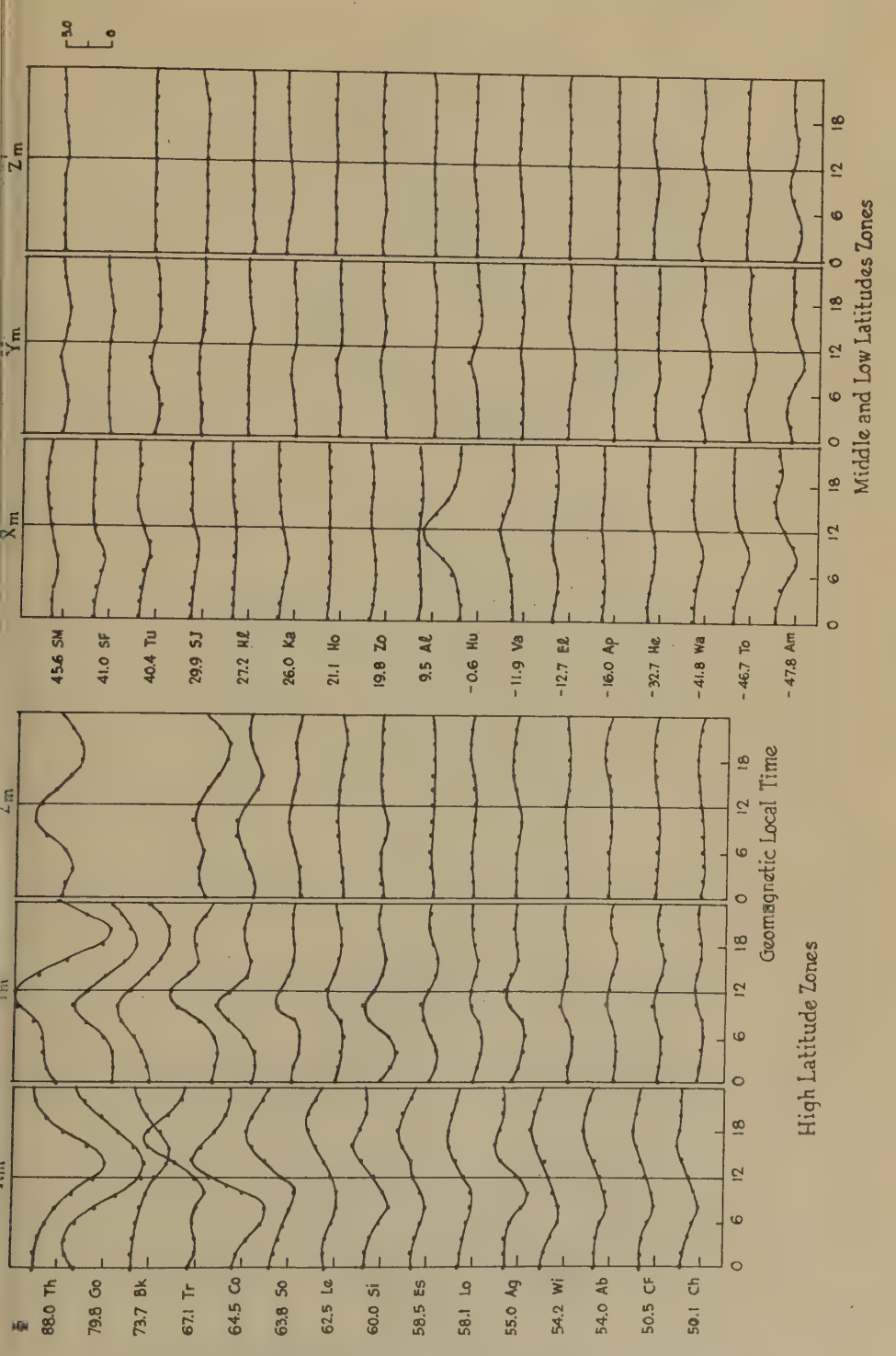

FIG. 3—Average diurnal variations of $X'm$, $Y'm$, and $Z'm$

FIG. 4—Electric current systems of Dst^c, Ds^c, and D^c fields for sudden commencements of magnetic storms (viewed from above the pole; 10,000 amp flow between successive stream lines)

around each parallel of latitude and is essentially symmetrical about the earth's axis, while *Ds* represents the variation of the diurnally varying part of the storm.

The current systems for these Dst^c, Ds^c, and D^c fields (superscript *c* denotes the field for the SC) are shown in Figure 4, on maps viewed from above the geomagnetic north pole. That part of the geomagnetic horizontal component of external origin is estimated as about two-thirds of the magnitude observed on the earth's surface, and the stream lines on the maps are so drawn that a total of 10,000 amperes flows in the direction of the arrows between successive lines.

The Dst^c current system consists of currents which are everywhere in the same direction, eastward along circles of latitude. Currents are concentrated with greater intensity along the auroral zone and the geomagnetic equator. The diurnal part Ds^c is composed of two main current systems located in the inner polar region and the equator. In the polar region, it bears some resemblance to the *Ds* current system for the main phase of the magnetic storm, but has considerable differences in middle and low latitudes. The total amount of current across the polar region is of the order of 150,000 amperes. Currents flow toward the meridian of about 10 hours local time and are supposed to complete their paths along the outer auroral zone. At the equator, the eastward current prevails during daytime.

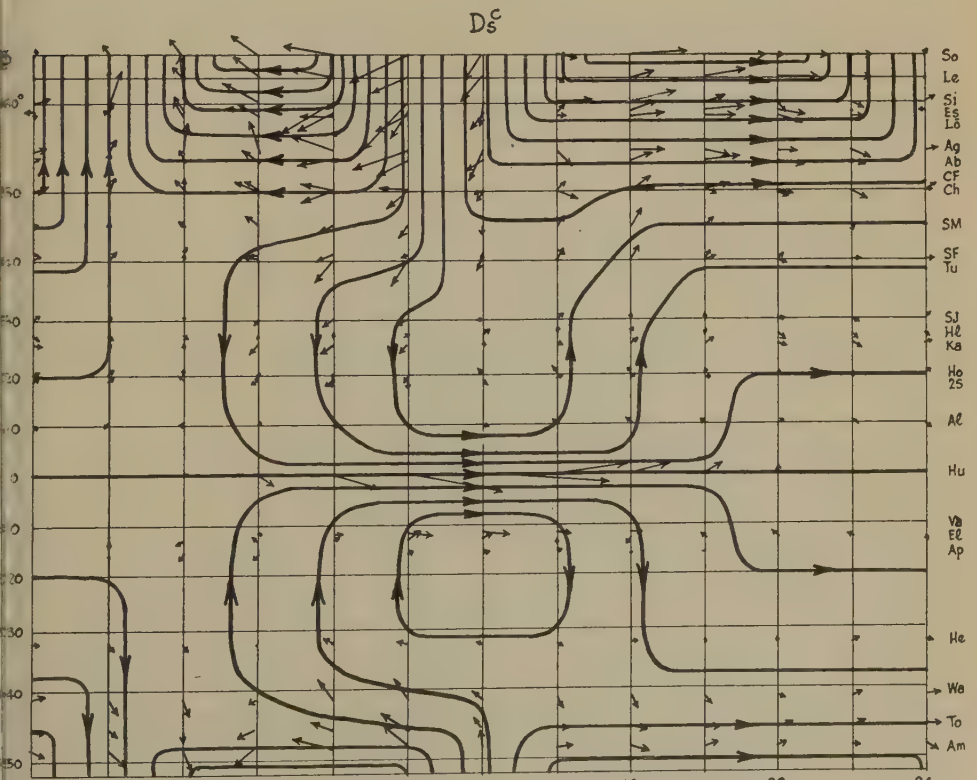

FIG. 5—Average electric current vectors and the current system of the Ds^c field (Mercator's projection in geomagnetic coordinates)

This current must be highly concentrated, flowing in the ionosphere in a rather narrow zone along the geomagnetic equator. It is also of interest that the current system in the middle- and low-latitude zones seems to indicate a slight augmentation of the *Sq* field; weak streams of current are flowing towards the north on the evening side and towards the equator on the morning side. These characteristics are more clearly shown in Figure 5, where the Ds^c current system is drawn on a map of Mercator's projection in geomagnetic coordinates. The complete current system D^c is the combination of the Dst^c and Ds^c systems, and represents the average features of world-wide SC's of magnetic storms.

Although the above-mentioned current systems are the average of many SC's, current systems for individual SC's have also been examined. In Figure 6, magnetic records of the SC at 17^h51^mUT, on June 14, 1951, are shown, and the equivalent current system derived from these magnetic variations is drawn in Figure 7. The change of shape of SC's with longitude (local time) is very pronounced, and well-defined inverted SC's can be seen on the American hemisphere. The current system indicates that the *Ds* field predominates in polar regions, while the *Dst* field prevails in low latitudes.

Another example at 20^h12^mUT, on October 13, 1949, is shown in Figure 8. The current system for the main impulse of this SC is illustrated in Figure 8(*b*), while that for the preliminary reverse impulse SC* is shown in Figure 8(*a*). The SC* current system is quite similar to that for the main impulse of the SC, although the current is much less intense and flows in the opposite direction. This result agrees with the analysis of SC* by Nagata and Abe [13].

3. POSSIBLE ORIGIN OF CURRENT SYSTEMS

In the thory of magnetic storms based on a neutral stream of charged particles ejected from the sun, the SC of a magnetic storm is interpreted as the compression of the magnetic field due to the approach of the conducting corpuscular front towards the earth. The magnetic field produced by this advancing stream must be fairly uniform in the vicinity of the earth, because the effect originated far outside the earth, and it may be assumed that the external part of the SC is composed chiefly of the P_1 (cos θ) term in its potential.

In order to examine whether the Dst^c field could be responsible for this, actual latitude distributions of $Dst^c(X'm)$ and $Dst^c(Z'm)$ were made and are illustrated in Figures 9. The distribution curves seem to indicate some of the tendencies predicted by the theory, though the $Z'm$ component shows a rather irregular distribution from place to place. The reason for this irregularity in $Dst^c(Z'm)$ is not certain, but may be due to the effect of the induced current inside the earth where distribution of electrical conductivity may be considerably heterogeneous.

There is another fact which may support the extraterrestrial origin of the Dst^c part. This is indicated by the relation between the value of $Dst^c(Y'm)$ and the *geomagnetic declination* $D - \Psi$ (that is, the magnetic declination referred to the geomagnetic meridian) of the relevant station. A graph of the amplitude of $Dst^c(Y'm)$ against $(D - \Psi)$ is shown in Figure 10. It indicates that the eastward (positive) change of the Y component of a SC is observed at a station whose magnetic north is deviated westward from the geomagnetic meridian and conversely. Since the effect of an additional magnetic field due to the approaching

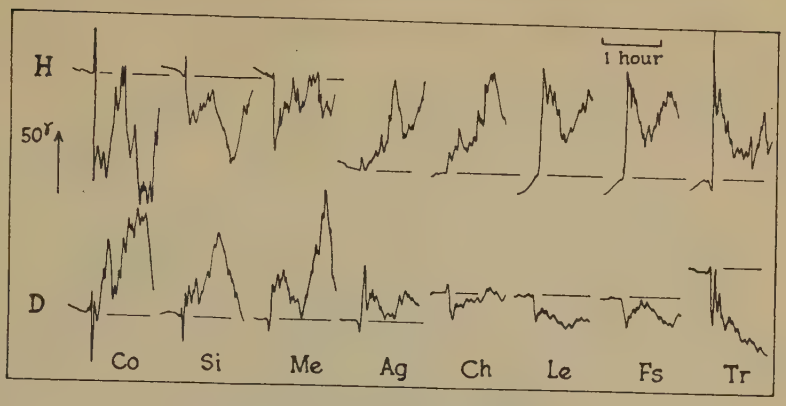

FIG. 6—World-wide pattern of SC's at 17^h51^m on June 14, 1951

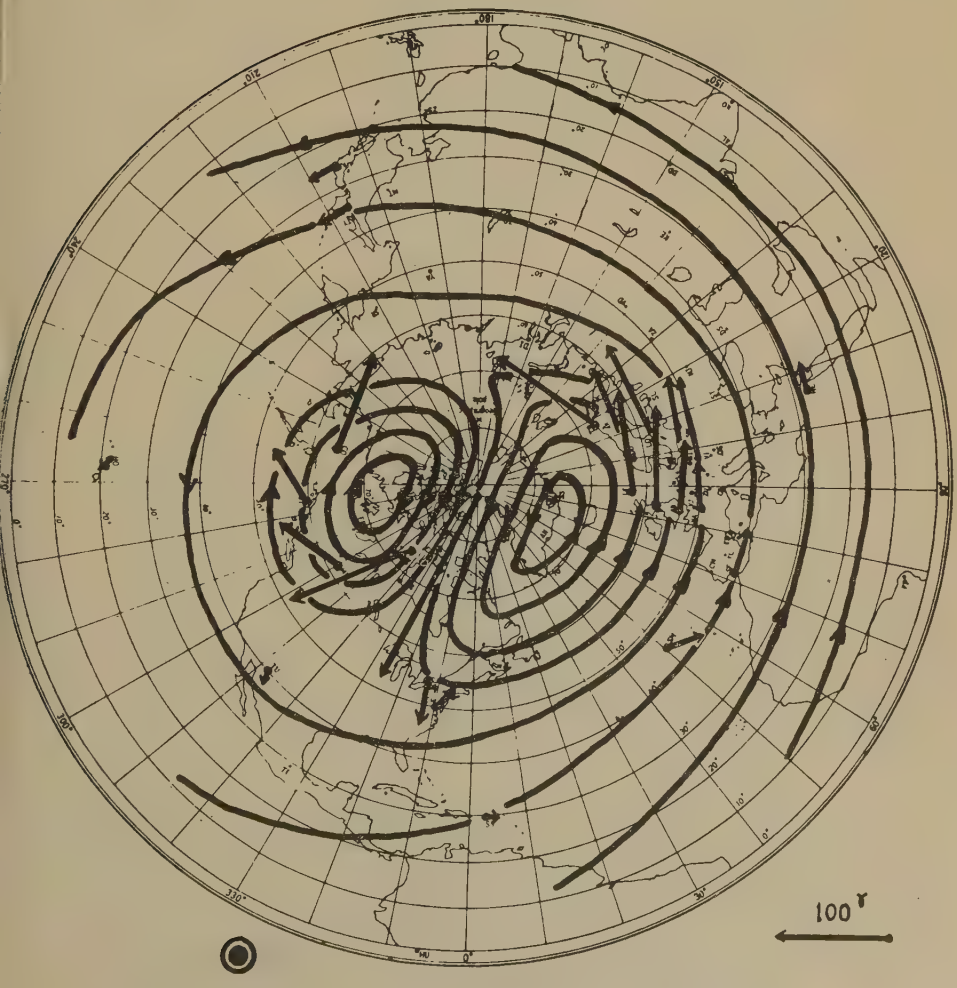

FIG. 7—The current system of SC at 17^h51^m on June 14, 1951

FIG. 8—Current systems of SC*(*a*) and SC(*b*) at 20^h12^m on October 13, 1949

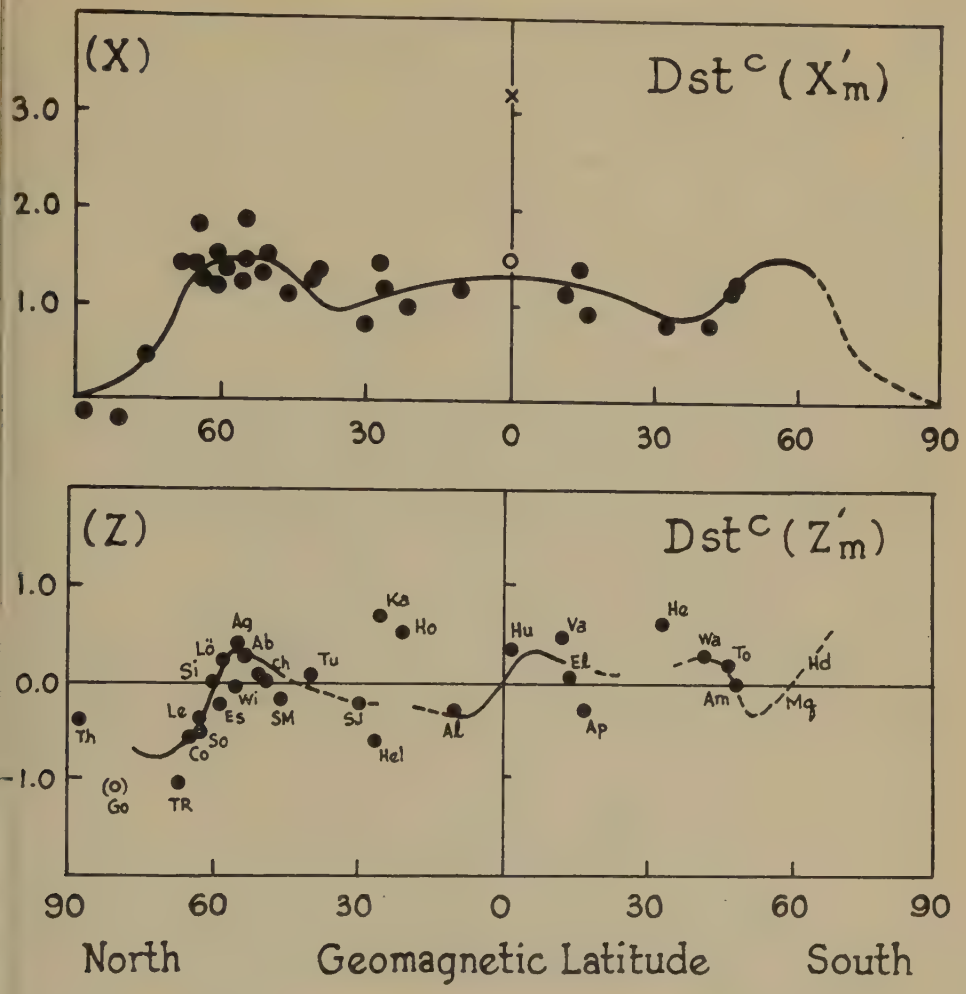

FIG. 9—Latitude distributions of $Dst^c(X'm)$ and $Dst^c(Z'm)$

orpuscular front into the earth's magnetic dipole-field is essentially the same as hat of the image dipole induced inside the corpuscular stream, the impressed nagnetic field near the earth should be parallel to the geomagnetic axis. The bserved facts are consistent in this respect, and hence it suggests that the Dst^c eld may be attributed to an extraterrestrial origin. However, an anomalous *Dst* ield in the auroral zone is more likely to have originated in the earth's upper tmosphere.

The Ds^c current system consists of two main parts, with current concentrations n the equatorial and polar regions. Forbush and Vestine [6] pointed out that the quatorial current system must be associated closely with the electrojet effect esponsible for the large *Sq* variation at the geomagnetic equator and that SC's an be explained as the sudden enhancement of this electrojet.

On the other hand, the pattern of the polar current system is very similar to

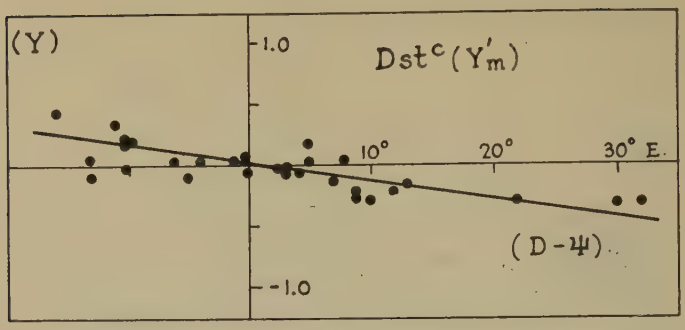

FIG. 10—Relation between $Dst^c(Y'm)$ and geomagnetic declination $(D - \Psi)$

that caused by an electric doublet situated in the highly conducting region near the pole. Since it is highly probable that this Ds^c current system exists within the earth's atmosphere, one possible cause may be an enhanced dynamo action at the time of the SC. As shown in Figure 11, the intensity of the Ds^c field is very

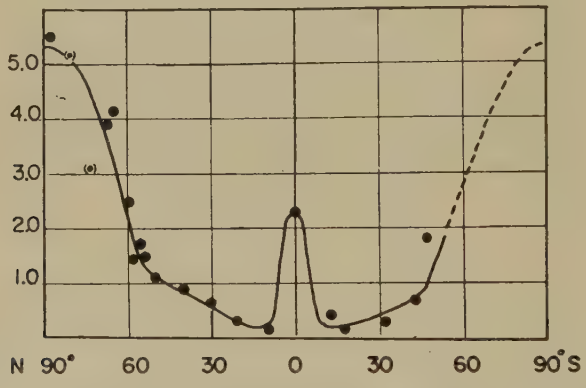

FIG. 11—Latitude distribution of amplitude of Ds^c $(\sqrt{X'^2m + Y'^2m})$

large in the polar regions, decreasing markedly with latitude, being practically zero at low latitudes. If the cause of the Ds current system is attributed to a dynamo action in the upper atmosphere, this curve represents to some extent the latitude distribution of the enhanced electrical conductivity.

In order to assume such a high conductivity in the polar regions, however, a branch stream of incoming corpuscles must arrive in the earth's atmosphere at the time of the SC. Nagata [13] suggested that such a branch stream may exist, since that part of the corpuscular stream approaching the earth along lines of magnetic force is scarcely affected by the retarding force, so that part of the stream arrives in the polar regions at the same time as the front surface of the main stream near the geomagnetic equator begins to cause the SC of a storm. Details of the physical interpretation of the Ds^c current system by a dynamo theory are given in the subsequent Sections.

4. DYNAMO ACTION IN THE UPPER ATMOSPHERE

It was first suggested by Balfour Stewart that geomagnetic variations might

be due to electric currents flowing in the upper atmosphere, produced by motion of electrically conducting air across the lines of force of the geomagnetic field. This so-called dynamo theory was developed by Schuster [10] and Chapman [11], and is the only adequate theory which can readily account for the *Sq* and *L* fields.

Since the dynamo theory has also been quite successful in interpreting various phenomena, such as a solar-flare effect [14] and the change in the geomagnetic field at a solar eclipse [15], it is natural to consider that the disturbance field may also be in part due to a dynamo action in the upper atmosphere. In 1927, Chapman [16] pointed out that atmospheric winds could produce the disturbance diurnal variation *Ds* if the conductivity in the polar regions were enhanced. The first theoretical calculation of the disturbance field based on a dynamo theory was made by Rikitake [17], who assumed a highly conducting region around the auroral zone. This study was later extended by Fukushima [12], who successfully explained the current systems for polar magnetic storms.

The present problem is the application of this dynamo theory to the interpretation of the current system at the SC of magnetic storms. Since the theory should also be able to explain the *Sq* field and the *Ds* field of magnetic storms, an attempt is made to formulate a consistent theory for all these magnetic variations.

In the mathematical theory of the atmospheric dynamo action [18], fundamental equations governing electric currents, produced by motions of the conductive air in the earth's magnetic field, are derived. The rigorous mathematical treatment of this problem is extremely complicated. However, assuming a given *steady* air motion which seems likely to lead to an atmospheric dynamo, it is possible to

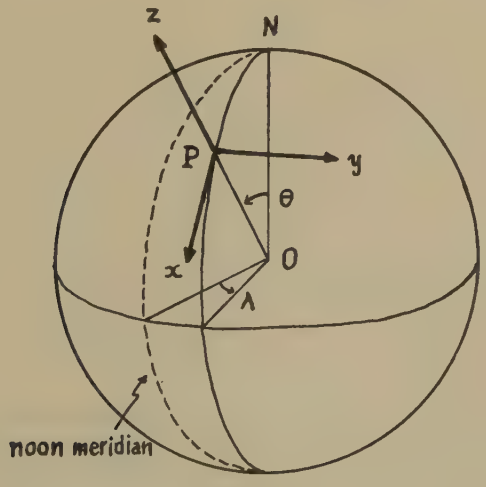

FIG. 12

determine a solution in terms of the current function J where

$$i_\theta = \frac{\partial J}{a \sin\theta \, \partial\lambda}, \qquad i_\lambda = -\frac{\partial J}{a \, \partial\theta} \qquad \text{.....(1)}$$

Assuming the ionosphere to be a thin spherical shell of radius a and conductivity σ, and the air motion $v(u, v, 0)$ to be purely lateral, the dynamo equation is

$$\frac{1}{\sin\theta}\frac{\partial}{\partial\lambda}\left(\frac{1}{\sigma}\frac{\partial J}{\partial\lambda}\right)+\frac{\partial}{\partial\theta}\left(\frac{\sin\theta}{\sigma}\frac{\partial J}{\partial\theta}\right)=a\left\{\frac{\partial}{\partial\lambda}(vZ)+\frac{\partial}{\partial\theta}(uZ\sin\theta)\right\} \quad \ldots\ldots(2)$$

where $Z = -2GP_1(\cos\theta)$, the vertical component of the geomagnetic field, and $G = 0.3\ \Gamma$.

If the air motion is irrotational, it can be derived from a velocity potential Ψ, where

$$u = -\frac{\partial\Psi}{a\,\partial\theta}, \qquad v = -\frac{\partial\Psi}{a\sin\theta\,\partial\lambda} \quad \ldots\ldots(3)$$

The conductivity σ is expressed in the form [19]

$$\sigma = \sigma_0 + \sigma^* = \sigma_0(1 + \gamma\cos\chi) \quad \ldots\ldots(4)$$

where σ_0 is a constant term, σ^* a function of χ, the solar zenith angle, and γ a numerical factor ($\gamma \leq 1$).

Expressing Ψ and J in terms of surface spherical harmonics,

$$\Psi = \sum_N\sum_M \Psi_N^M = \sum_N\sum_M k_N^M P_N^M(\cos\theta)\sin(M\lambda+\alpha_N^M) \quad \ldots\ldots(5)$$

$$J = \sum_n\sum_m j_n^m = \sum_n\sum_m j_n^m P_n^m(\cos\theta)\sin(m\lambda+\alpha_n^m) \quad \ldots\ldots(6)$$

the dynamo action can be solved by perturbation methods. Dividing the current function J into a main term J_0 and a perturbation term J^*, the solution for the current function corresponding to Ψ_N^M is given by

$$\left.\begin{aligned}\sum_n\sum_m \frac{n(n+1)}{\sigma_0}J_{0n}^m &= \frac{2Gk_N^M}{2N+1}\{[(N+1)^2-1][(N+1)^2-M^2]^{1/2}P_{N+1}^M(\cos\theta)\\ &\quad + [N^2-1][N^2-M^2]^{1/2}P_{N-1}^M(\cos\theta)\}\sin(M\lambda+\alpha_N^M)\end{aligned}\right\} \quad \ldots\ldots(7)$$

and

$$\left.\begin{aligned}\sum_n\sum_m \frac{n(n+1)}{\sigma_0}J_n^{*m} = -\frac{\gamma}{\sigma_0\sin\theta}\sum_\mu\sum_\nu\Bigg\{&\frac{\partial}{\partial\lambda}\left(\cos\lambda\frac{\partial J_{0\nu}^\mu}{\partial\lambda}\right)\\ &+\frac{\partial}{\partial\theta}\left(\sin^2\theta\frac{\partial J_{0\nu}^\mu}{\partial\theta}\right)\cos\lambda\Bigg\}\end{aligned}\right\} \quad \ldots\ldots(8)$$

where $\sum_\mu\sum_\nu$ is a summation over integers which are specified as n and m in the solution of J_0 given by (7). Since the magnetic effects of the different harmonic terms in Ψ are additive, they can be calculated separately for individual components of the wind system.

The above solution, although a good approximation in the case of the *Sq* variation, cannot apply in the case of a magnetic disturbance, since the electrical conductivity may be very different in the auroral zones and polar caps. The ionosphere is thus divided into five zones with different conductivities, namely, the polar caps, the auroral zones, and the equatorial regions. In the present analysis, the following conductivity distribution was adopted:

I—Northern polar cap	$(\theta = 0° \sim 15°)$,	$\sigma = a\sigma_0(1 + \gamma_1 \cos \chi)$
II—Northern auroral zone	$(\theta = 15° \sim 25°)$,	$\sigma = b\sigma_0 (1 + \gamma_2 \cos \chi)$
III—Equatorial region	$(\theta = 25° \sim 155°)$,	$\sigma = c\sigma_0 (1 + \gamma_3 \cos \chi)$
IV—Southern auroral zone	$(\theta = 155° \sim 165°)$,	$\sigma = b\sigma_0 (1 + \gamma_2 \cos \chi)$
V—Southern polar cap	$(\theta = 165° \sim 180°)$,	$\sigma = a\sigma_0 (1 + \gamma_1 \cos \chi)$

At the equinoxes, the conductivity distribution is assumed symmetrical with respect to the equator, so that regions I and II are identical with V and IV, respectively. From the particular solutions obtained in equations (7) and (8), the general solution for the current functions can be derived. The dominant harmonics of geomagnetic variations such as the *Sq* and *Ds* fields are diurnal and semidiurnal, and these fields are also approximately symmetrical with respect to the equator. Thus, possible wind systems responsible for such current systems are

$$\left.\begin{aligned} \Psi &= \Psi_1^1 + \Psi_3^1 + \Psi_5^1 + \cdots \text{(diurnal term)} \\ \Psi &= \Psi_2^2 + \Psi_4^2 + \Psi_6^2 + \cdots \text{(semidiurnal term)} \end{aligned}\right\} \quad (9)$$

Actual calculations were carried out for the cases Ψ_1^1, Ψ_3^1, and Ψ_2^2. The solutions for these wind systems are as follows:

$$\Psi = k_N^M P_N^M (\cos \theta) \sin (M\lambda + \alpha_N^M)$$

$$\begin{aligned} J_i = 2Gk_N^M\sigma_i[&\{Q_N^M + A_p u(\theta)^M + A_q v(\theta)^M\} \sin (M\lambda + \alpha_N^M) \\ &+ \{\gamma_i R_N^{M+1} + B_p u(\theta)^{M+1} + B_q v(\theta)^{M+1}\} \sin (\overline{M+1}\lambda + \alpha_N^M) \\ &+ \{\gamma_i S_N^{M-1} + C_p u(\theta)^{M-1} + C_q v(\theta)^{M-1}\} \sin (\overline{M-1}\lambda + \alpha_N^M)] \end{aligned}$$

where $u(\theta)^m = \tan^m \frac{\theta}{2}$ $(m \neq 0)$, $= 1$ $(m = 0)$

$v(\theta)^m = \cot^m \frac{\theta}{2}$ $(m \neq 0)$, $= ln \tan \frac{\theta}{2}$ $(m = 0)$

i = regions I, II, III$\cdots$

Case	Q_N^M	R_N^{M+1}	S_N^{M-1}
Ψ_1^1	$\frac{1}{2\sqrt{3}} P_2^1$	$\frac{1}{3\sqrt{15}} P_3^2$	$\frac{3}{20} P_1^0 - \frac{1}{15} P_3^0$
Ψ_2^2	$\frac{2}{3\sqrt{5}} P_3^2$	$\frac{1}{2}\sqrt{\frac{3}{70}} P_4^3$	$\frac{8}{63} P_3^1 - \frac{1}{14}\sqrt{\frac{3}{10}} P_4^1$
Ψ_3^1	$\frac{8\sqrt{2}}{21} P_2^1 + \frac{3\sqrt{15}}{28} P_4^1$	$\left(\frac{16\sqrt{10}}{315} - \frac{5\sqrt{10}}{224}\right) P_3^2 + \frac{1}{\sqrt{70}} P_5^2$	$\frac{4\sqrt{6}}{35} P_1^0 + \left(\frac{25}{56\sqrt{6}} - \frac{16\sqrt{6}}{315}\right) P_3^0 - \frac{\sqrt{6}}{21} P_5^0$

i	σ_i	γ_i	A_p	A_q	B_p	B_q	C_p	C_q
J_{I}	$a\sigma_0$	γ_1	A_1	0	B_1	0	C_1	0
J_{II}	$b\sigma_0$	γ_2	A_2	A_3	B_2	B_3	C_2	C_3
J_{III}	$c\sigma_0$	γ_3	A_4	$-A_4$	B_4	$-B_4$	C_4^*	$-C_4$

*for $M = 1$ $\quad C_4^* = 0$

Groups of arbitrary constants A, B, and C must be determined from the condition that the normal component of electric current and the tangential component of electric field given respectively by

$$\frac{\partial J}{a \sin\theta \, \partial\lambda}, \qquad \frac{1}{\sigma} \frac{\partial J}{a \, \partial\theta}$$

are continuous along the boundaries of the zones.

5. GEOMAGNETIC CURRENT SYSTEM DERIVED FROM THE DYNAMO-THEORY OBSERVED CURRENT SYSTEMS FOR THE *Sq*, *Ds*^{c}, AND *Ds* FIELDS

There are three main geomagnetic variations which must be explained consistently by the dynamo theory. These are the *Sq*, *Ds*^{c}, and *Ds* fields. Brief descriptions of the observed geomagnetic current systems for these fields are given below.

The current system for the *Sq* field consists of two main vortices: a strong one situated over the sunlit hemisphere, the other extending over the night area. There is also a weak current system in the polar regions. Nagata and Mizumo [20] and Whitham and Loomer [21] have shown that this polar current system is substantially the residual part of the *Ds* field and that on absolutely quiet days ($Kp = 0$) it will disappear. The *Sq* current system (northern hemisphere) based on Vestine's analysis [22] is illustrated in Figure 13*a*.

The *Ds*^{c} current system which has been obtained in the present analysis has strong current concentrations in the polar regions, as shown in Figure 13*b*. Currents flow towards the meridian of about 10^h local time, completing their paths along the outer auroral zone in opposite directions in the forenoon and afternoon hemispheres. The current system for the preliminary reverse impulse of SC's (namely, SC*) is similar to that for the *Ds*^{c} field, but the currents flow in opposite directions.

During magnetic storms, an intense *Ds* current system appears in the polar regions. The current system derived from Vestine's analysis is shown in Figure 13*c*. The pattern is similar to that for the *Ds*^{c} field, but there is a more pronounced concentration of currents along the auroral zone, with return flows in the middle latitudes.

Possible wind systems for geomagnetic variations

There have been several attempts to estimate the wind systems in the upper atmosphere which are responsible for geomagnetic variations. Chapman [11] in his theory of the *Sq* field proved that diurnal and semidiurnal winds (Ψ_1^1 and Ψ_2^2) are dominant. Recently, Chakrabarty and Pratap [23] have shown that a

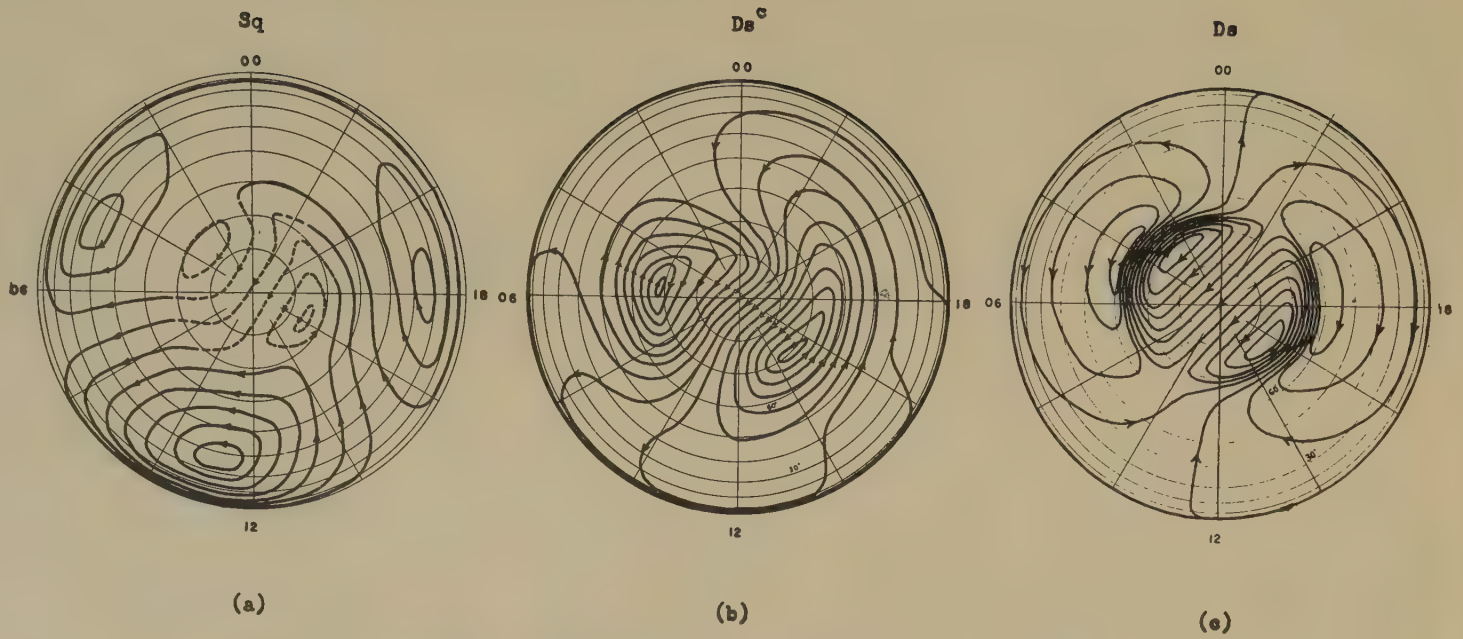

FIG. 13—Observed electric current systems of *Sq*, *Ds*^{c}, and *Ds* fields, viewed from above the pole

semidiurnal wind system can set up a current system which accounts fairly satisfactorily for the observed *Sq*. Maeda and others [24, 25, 26], on the other hand, have shown that the required wind system is predominantly diurnal, with a velocity of the order of 50 m/sec. Possible modes of wind systems related to geomagnetic disturbances have also been discussed by Vestine [27]. Fukushima [12] showed that, assuming a Ψ_1^1 wind system, the current system for the *Sq* and the *Ds* fields can be produced simultaneously if the conductivity in the auroral zones becomes very high at the time of magnetic storms. However, as he himself has pointed out, the calculated *Ds* current system is far too weak and its phase is almost the reverse of that observed.

In considering a dynamo action for the *Ds* field, it is important to determine whether the electromotive force, from which *Ds* current system derives, arises mainly in the auroral zone itself or over the polar cap. In the former case, as has been shown by Fukushima, the auroral zone currents are the primary ones and the currents bordering on them are return flows. On the other hand, in the latter case, the polar cap currents are the primary ones. In this case, the discrepancy in phase between the wind systems of the *Sq* and *Ds* fields is removed and the total current intensity of the system can be raised without an excessive increase in conductivity in the polar regions, because of the larger area of electromotive force generation. There are also several other reasons for adopting this point of view. Statistical results of magnetic disturbances inside the polar cap show that the *Ds* field has fairly regular and large amplitudes, and that its phase does not change even on very quiet days [21]. Moreover, as has already been pointed out, the Ds^c current system also shows a strong concentration of currents over the inner polar region. All these facts favor a polar cap origin for the *Ds* current system. Taking the above considerations into account, tentative wind systems are estimated and the corresponding current systems are calculated using an electronic computor. Since Ψ has the form given by (9), the following wind systems were used in the present analysis:

$$\left.\begin{aligned} \Psi_1^1 &= k_1^1 P_1^1 (\cos\theta) \sin(\lambda + \alpha_1^1) \\ \Psi_2^2 &= k_2^2 P_2^2 (\cos\theta) \sin(2\lambda + \alpha_2^2) \\ \Psi_3^1 &= k_3^1 P_3^1 (\cos\theta) \sin(\lambda + \alpha_3^1) \end{aligned}\right\} \quad \ldots\ldots\ldots\ldots\ldots\ldots (10)$$

The stream lines and equipotentials for these wind systems are illustrated in the upper half of Figure 14. The wind velocity due to Ψ_1^1 and Ψ_3^1 is a maximum at the pole, although there is no wind across the pole due to Ψ_2^2. The corresponding (calculated) electric current systems for the case of uniform conductivity over all regions are shown in the lower half of Figure 14. It can be seen that currents are concentrated in the polar regions in the case of Ψ_1^1 and Ψ_3^1, while for Ψ_2^2 they flow mainly in middle latitudes. Thus, if the conductivity is raised in the polar regions, the current systems due to Ψ_1^1 and Ψ_3^1 will be enhanced, but not those due to Ψ_2^2.

Since polar cap currents for the disturbance field rotate, relative to the earth, with a 24-hour period and the direction of the flow is approximately towards 10^h local time meridian, the diurnal term Ψ_1^1 or Ψ_3^1 plays the main role in the polar regions during disturbances and the relevant wind system must have its phase

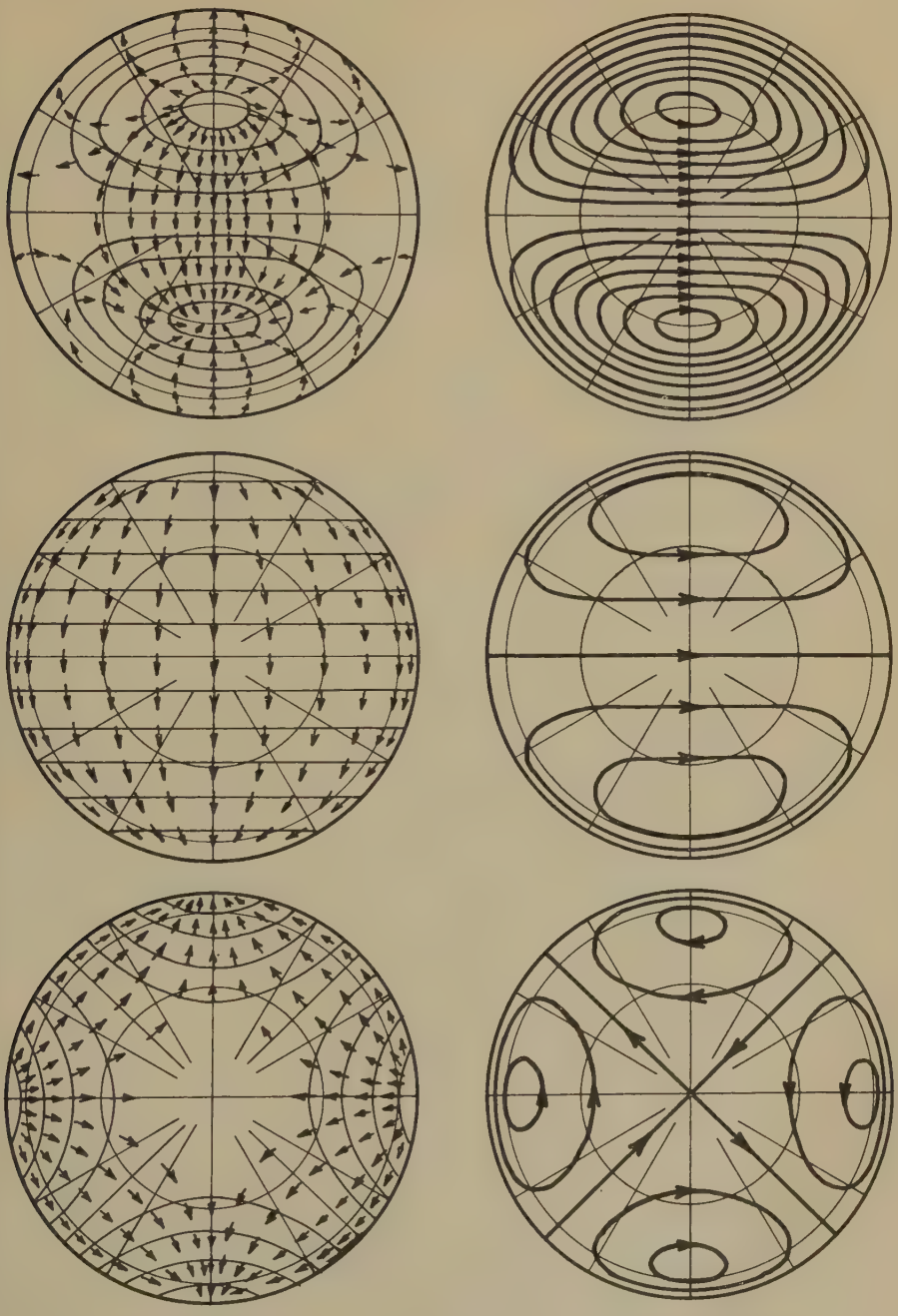

FIG. 14—Wind systems and corresponding current systems (view from the north pole)

α_1^1 or α_3^1 about 30° (that is, the wind should flow from 16^h to 04^h local time across the pole). On the other hand, a consideration of the *Sq* field shows that the semi-diurnal term Ψ_2^2 is important and its phase α_2^2 must be about 120° (that is, source point at 11^h). Thus, a resultant wind system which is consistent for both quiet and disturbed geomagnetic variations will be of the form

$$\Psi = \Psi_2^2 + p\Psi_1^1 \quad \ldots\ldots\ldots\ldots\ldots\ldots\ldots\ldots\ldots\ldots (12)$$

or

$$\Psi = \Psi_2^2 + p\Psi_3^1 \quad \ldots\ldots\ldots\ldots\ldots\ldots\ldots\ldots\ldots\ldots (13)$$

where p is a combination factor, that is, the ratio of a diurnal to a semidiurnal term.

In the first place, calculations were made for the Sq field, assuming that the conductivity in all region was given by

$$\sigma = \sigma_0(1 + \cos\chi)$$

that is, $a = b = c = 1$ and $\gamma_1 = \gamma_2 = \gamma_3 = 1$. To find the best value of p, the following procedure was adopted. Values of the current function were calculated for the two cases given by (12) and (13), and curves of their latitude variations were drawn along the meridians of 05^h, 11^h, and 17^h local time (which are the most representative of the Sq distribution) for values of $p = 2, 1, \frac{1}{2}, \frac{1}{4} \cdots$ These are shown in the top two curves of Figure 15, where the actual observed Sq current system is shown by dotted lines. The scale is adjusted so that the maximum value along the 11^h meridian is the same as that calculated for $p = 0.2$. An examination of these curves shows that the most suitable values of p are 0.5 and 0.2 for the cases (12) and (13), respectively.

The extension for the case of geomagnetic disturbances was made on the following considerations. The change at a sudden commencement is so abrupt (within a few minutes) that it is reasonable to assume that the wind system does not change during that time. Hence, the wind system for the Sq and Ds^c fields should be identical, and the difference between them should be due only to a change in the conductivity of the ionosphere. In other words, if a reasonable change of conductivity is assumed in the polar regions at the time of a SC, the problem is reduced to finding a consistent wind system which could produce the observed current systems for both the Sq and the Ds^c fields. Furthermore, on the assumption of even higher conductivities in the polar regions, it may be possible that this wind system could also account for the Ds field.

Calculations have been made for the cases.

Case	a	b	c	
1	1	1	1	
2	1.5	2	1	for the Sq field
3	5	10	1	
4	10	1	1	
5	10	20	1.2	for the Ds^c field
6	25	25	1.5	
7	50	100	2	for the Ds field

where in the

Polar cap $(\theta = 0° \sim 15°)$, $\sigma = \sigma_0 (a + \cos\chi)$
Auroral zone $(\theta = 15° \sim 25°)$, $\sigma = \sigma_0 (b + \cos\chi)$
Equatorial zone $(\theta = 25° \sim 90°)$, $\sigma = \sigma_0 (c + \cos\chi)$

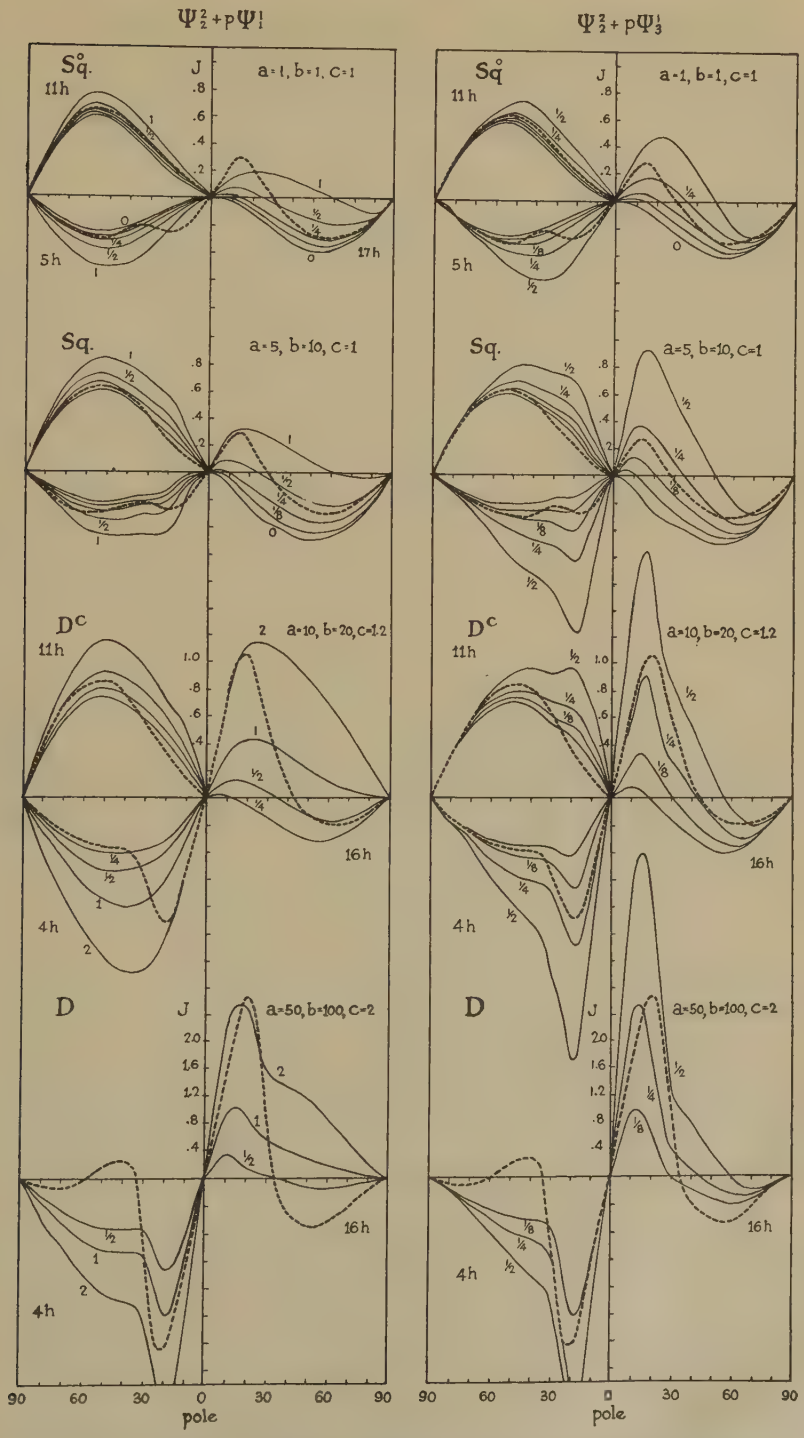

FIG. 15—Calculated current functions for various conductivity distributions

For the first model of the *Sq* field, the value of γ was taken as unity in all regions. For other conductivity distributions, since the enhancement should appear in the constant term only and not depend on cos χ, the coefficient of cos χ was kept the same, that is, $\gamma_1 = 1/a$, $\gamma_2 = 1/b$, and $\gamma_3 = 1/c$. Some of these cases are illustrated in Figure 15. In the case of disturbances, observed curves of (*Sq* + *Ds*) are shown in the Figure by dotted lines, since the calculated current function represents the resultant of both the *Sq* and *Ds* fields.

Examining these and other diagrams, it was found impossible to obtain good agreement between observed values and those calculated from the wind system (12). On the other hand, for the wind system (13), namely, $\Psi_2^2 + p\Psi_3^1$, a consistent wind system can be obtained with reasonable changes of conductivity from quiet to disturbed conditions, if p has the value 0.2. This result is shown more clearly

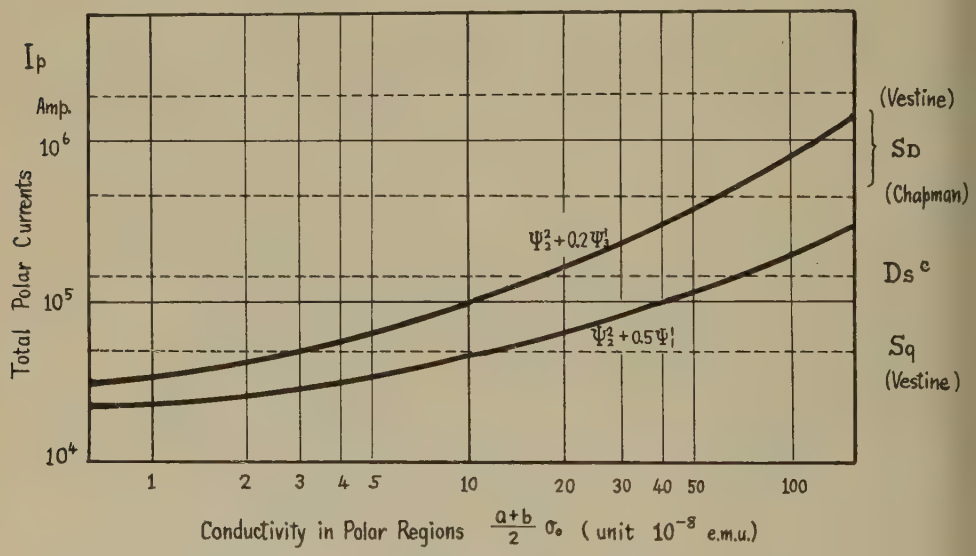

FIG. 16—The relation of the total polar currents and the conductivity for two wind systems

in Figure 16, where the total intensity *Ip* of the polar currents is plotted against corresponding values of the conductivity expressed by $\frac{1}{2}(a + b)\sigma_0$ for the two cases $\Psi_2^2 + 0.5\Psi_1^1$ and $\Psi_2^2 + 0.2\Psi_3^1$ The observed intensity of the polar current system is given in Table 1 and indicated by dotted lines in Figure 16.

TABLE 1—*Intensity of polar current system*

Name	Current system	Intensity
		(10^4 *amp*)
Chapman (1935)	*SD* field	45
Nagata (1951)	*SD* field	32
Vestine (1947)	*Ds* field	180
Obayashi (1956)	*Ds*^{c} field	15
Vestine (1947)	(*Sq* field)	5

For the wind system (12), it is necessary to raise the conductivity by a factor $\simeq 100$ in order to obtain sufficient current intensity even for the Ds^c field. The wind system (13), on the other hand, can account for the required intensity with far more reasonable conductivity change ($a \simeq 10 \sim 20$). Thus, the wind system which best explains both geomagnetically quiet and disturbed fields is

$$\Psi_2^2 + 0.2\Psi_3^1$$

and the ratio of the conductivity in the polar regions for quiet-day sudden commencements and main phase of magnetic storms is approximately 1:5:25 (assuming the best value of a for the Sq field is approximately $2 \sim 4$).

Current systems derived from the dynamo theory

Current systems for the Sq, Ds^c, and Ds fields were obtained using the above-mentioned wind system, namely,

$$\Psi = \Psi_2^2 + p\Psi_3^1 = k_2^2 P_2^2 \sin(2\lambda + 120°) + k_3^1 P_3^1 \sin(\lambda + 30°)$$

where $k_3^1 = 0.2\, k_2^2$, and conductivity distributions

$a = 1$	$b = 1$	$c = 1$	(Sq field)
$a = 10$	$b = 20$	$c = 1.2$	(Ds^c field)
$a = 50$	$b = 100$	$c = 2$	(Ds field)

Observed current systems are compared with those calculated from the dynamo theory and are illustrated in Figure 17. It can be seen that, except for some minor discrepancies, agreement is excellent. For the Sq field, the main current vortex in the sunlight hemisphere shows up well in the calculated field, although there is no polar current system. Thus, this model of the conductivity ($a = b = c = 1$) may represent very quiet day conditions. The actual conductivity in the polar regions (during international quiet days) is slightly higher than that assumed. The calculated Ds^c current system agrees both in phase and magnitude with that observed, and it thus appears that the conductivity change in the polar regions for a SC is several times that during quiet days. During the main phase of magnetic storms, agreement is less satisfactory, except in the polar regions. However, there is no guarantee that during this stage of magnetic storms the wind system will remain unchanged. Strong current flows which will interact with the geomagnetic fields may alter the wind system, so that precise agreement cannot be expected. The good agreement in the polar regions is encouraging and indicates that a dynamo action is probably the most important factor in an interpretation of the Ds field of magnetic storms.

Since the current intensity is determined by $2G\sigma_0 k_N^M$, the values of σ_0 and k_N^M may be chosen so that the current intensity agrees with that observed. Comparing the results of the Sq field, the best agreement is obtained if $2G\sigma_0 k_2^2 \simeq 5 \times 10^4$ (e.m.u.). Taking $\sigma = 10^{-8}$ e.m.u. as a representative value (Nagata, [8]), $k_2^2 \simeq 2.\times 10^{12}$, wind velocity

$$u = -\frac{\partial \Psi}{a\, \partial \theta} = -\frac{k_N^M}{a} \frac{\partial P_N^M}{\partial \theta} \sin(M\lambda + \alpha_N^M)$$

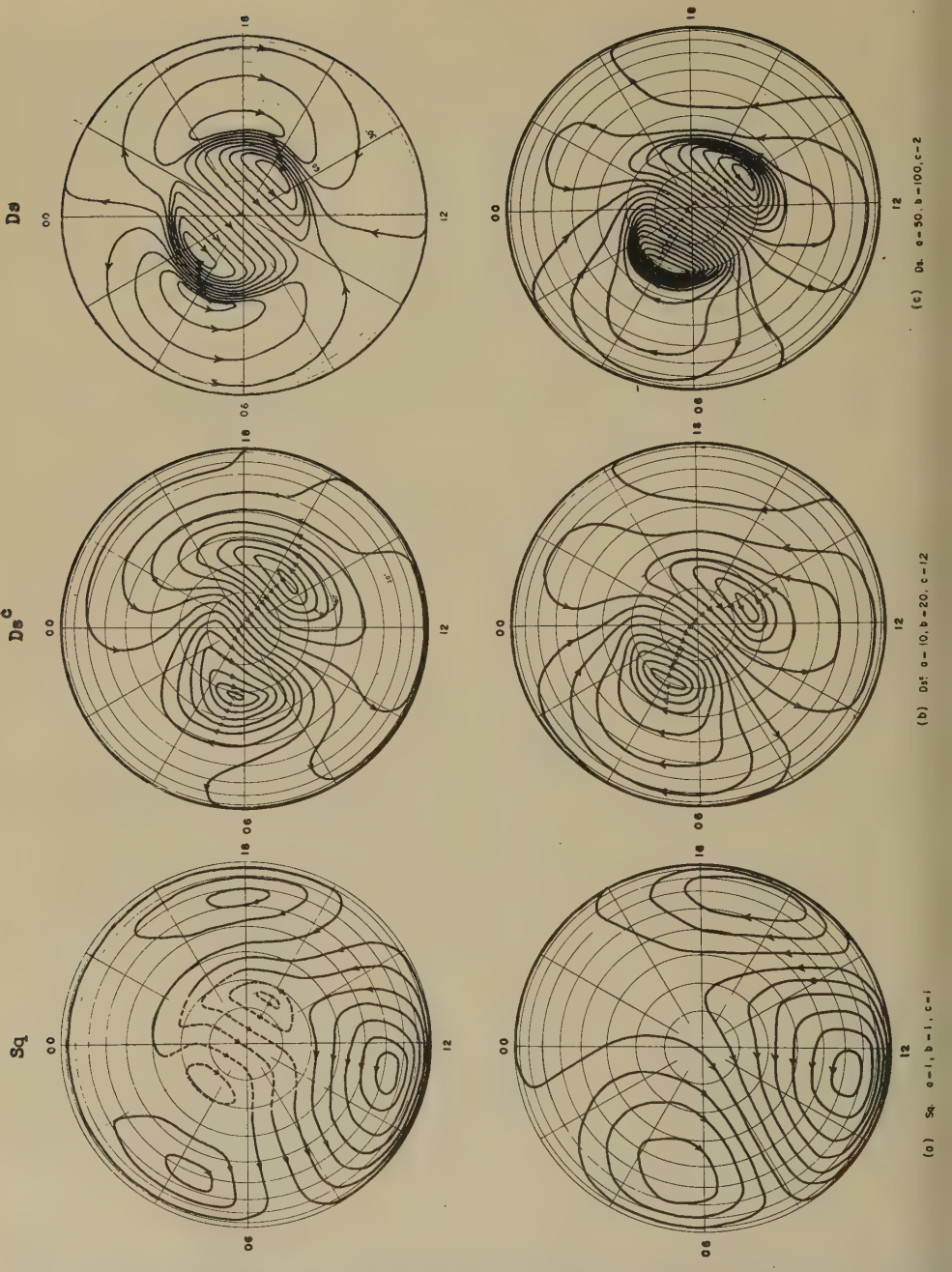

FIG. 17—Observed and computed Sq, Ds^c, and Ds fields [viewed from above the pole; electric currents between successive stream lines are 10,000 amp for (a) and (b), 25,000 amp for (c)] so that

$$| u_2^2 |_{\max} = \frac{\sqrt{3}}{2} \frac{k_2^2}{a} | \sin 2\theta |_{\theta=45^\circ} \simeq 20 \text{ m/sec}$$

and

$$| u_3^1 |_{max} = \frac{\sqrt{6}}{16} \frac{pk_2^2}{a} | 15 \cos 3\theta + \cos \theta |_{\theta=0^\circ} \simeq 10 \text{ m/sec}$$

These are exactly the right order of magnitude as obtained by radio observations of the ionosphere (Briggs and Spencer, [29]).

The wind system in the upper atmosphere obtained by various authors both from theoretical and experimental researches is summarized in Table 2. The velocity and phase have been determined by a dynamo theory of geomagnetic

TABLE 2—*Wind system in the upper atmosphere*

Name	Source of data	Diurnal term		Semidiurnal		Remarks
		v_1	t_{01}*	v_2	t_{02}*	
		m/s	*hour*	*m/s*	*hour*	
Chapman, 1905	*Sq* field	0.5	10.4	0.3	17.3	Dynamo theory of the uniform conductivity model
Chapman, 1905	*L* field	...	...	...	9.4	
McNish, 1936	*Sq* field	...	...	...	12.7	Dynamo theory only for Ψ_2^2 wind
Chakrabarty, 1954	*Sq* field	...	...	...	12.2	
Maeda, 1955	*Sq* field	30	15	10	13.5	Dynamo theory
Hirono and Kitamura, 1956	*Sq* field	25	13	14	13	Scaloidal wind
		100	13	30	13	Toroidal wind
Fukushima, 1953	*SD* field	...	0~3	...	...	Dynamo theory
Whitham, 1956	*Sq* and *SD*	5	16	2.5	10	Dynamo theory in the polar region
	Resolute Bay Observatory ($\theta = 7°$)					
Obayashi, 1957	*Sq*, *Ds*^{c}, *Ds* combined	10 Polar region	16	20 Low latitudes	11	Dynamo theory
Bartels, 1928	Atmospheric pressure	...	...	0.3	13	Tidal oscillation
Weekes and Wilkes, 1949	.....	...	...	...	19	Oscillation theory
	Ionospheric observations in the E region					
Briggs and Spencer, 1954	Radio wave fadings	...	...	25	15	At Cambridge, England
Chapman, 1953	"	...	...	40	15.3	At Ottawa, Canada
Burtt, 1953	"	...	...	42	17	At New Zealand
Elford and Robertson, 1953	Meteor echoes	20	6±2	20	18±2	At Adelaide
Weiss, 1955	"	21	5	...	...	.....

*t_0 = local time of the maximum poleward wind velocity (v_N maximum in the northern hemisphere and v_S maximum in the southern hemisphere).

variations, tidal oscillations of the atmosphere, and ionospheric movements measured by radio waves. Comparing these values with the wind system given in the present analysis, the magnitude is fairly consistent, although the phase is

almost opposite to that observed. However, this is not regarded as serious, since it is known from ionospheric observations that there is a marked variation of phase with height [30]. The pattern of the stream lines of the wind system obtained in the present analysis is illustrated in Figure 18.

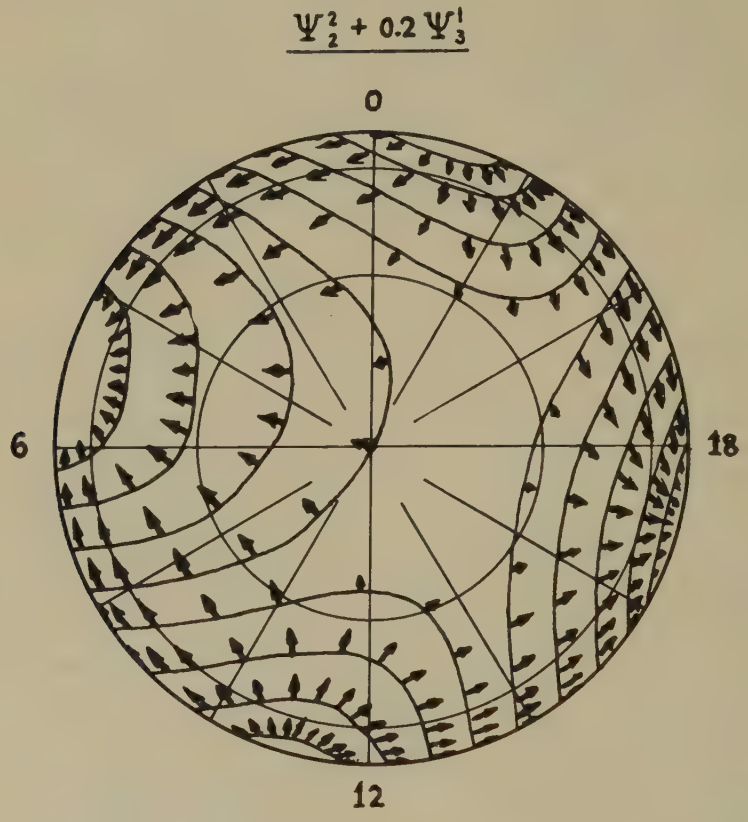

FIG. 18—The wind system derived from the dynamo theory (viewed from above pole)

It thus appears that the geomagnetic disturbance variations Ds^c and Ds can be explained by a dynamo theory consistent with that for the Sq field, assuming a reasonable conductivity change in the polar regions. It is also of interest that the current system for the preliminary reverse impulse SC* can be accounted for on the assumption that the wind system is reversed in the higher regions of the ionosphere where solar charged corpuscles first penetrate so that the conductivity of that region may be enhanced before the Ds^c current system has had time to develop in the lower regions of the ionosphere.

6. CONCLUSIONS

In the present study, the world-wide morphology of SC's of magnetic storms has been carried out in detail. The dynamo theory has been applied to explain the geomagnetic disturbance fields Ds^c and Ds, and a consistent wind system in the upper atmosphere which is responsible for the dynamo action of both geo-

magnetically quiet and disturbed fields has been found. The following conclusions were obtained:

1. From statistical investigations, it has been confirmed that there exists a remarkable local time change of SC's in high latitudes. The average electric current system for SC's of magnetic storms was derived, and it was found that there is a conspicuous current concentration in the polar regions.
2. The origin of SC's is due partly to the effect of the approaching solar corpuscular stream, and partly to conditions within the earth's atmosphere. The dynamo theory was applied to explain this atmospheric part of magnetic storms, and it was concluded that a dynamo action is the most important cause of the Ds^c field.
3. As a result of this analysis, a consistent wind system has been obtained which could produce current systems both for magnetically quiet and disturbed days. This wind system consists of both diurnal and semidiurnal terms and is of the same order of magnitude as that indicated by actual ionospheric observations.

There still remains, however, several problems which must be solved in order to have a complete understanding of SC's of magnetic storms. The mechanism of the corpuscular invasion into the earth's atmosphere at the time of commencement is not well understood, and there is no satisfactory explanation connecting the polar *Ds* current system and the equatorial electrojet during the SC. The interpretation of SC* should also be consistent with that of the main SC. It is also desirable to obtain more comprehensive experimental measurements of ionospheric movements which can be used to confirm or disprove the wind system estimated from the dynamo theory of magnetic disturbances.

7. ACKNOWLEDGMENTS

In concluding, the authors wish to express their thanks to Prof. B. A. Griffith and Mrs. B. Gertner for their suggestions and cooperation in the mathematical computations.

Data used in this study have been supplied from various observatories all over the world, and the authors' appreciations are due to all who have sent geomagnetic information, especially Mr. R. G. Madill and Dr. K. Whitham, of the Dominion Observatory, Ottawa.

The research was aided by a grant from the U.S. Air Force, Cambridge Research Center, Contract No. AF19(604)2147.

References

[1] H. W. Newton, Mon. Not. R. Astr. Soc., Geophys. Sup., **5**, 159 (1948).
[2] V. C. A. Ferraro, W. C. Parkinson, and H. W. Unthank, J. Geophys. Res., **56**, 177 (1951).
[3] D. H. McIntosh, J. Atmos. Terr. Phys., **1**, 223 (1951).
[4] G. Ishikawa and M. Kadena, Rep. Ionosphere Res. Japan, **5**, 144 (1951).
[5] M. Sugiura, J. Geophys. Res., **58**, 558 (1953).
[6] S. E. Forbush and E. H. Vestine, J. Geophys. Res., **60**, 299 (1955).
[7] T. Nagata, Rep. Ionosphere Res. Japan, **5**, 134 (1951).

[8] J. A. Jacobs and T. Obayashi, Can. J. Phys., **34**, 876 (1956).
[9] J. A. Jacobs and T. Obayashi, Geofisica pura e appl., Milano, **34**, 21 (1956).
[10] A. Schuster, Phil. Trans. R. Soc., A, **208**, 163 (1908).
[11] S. Chapman, Phil. Trans. R. Soc., A, **218**, 1 (1919).
[12] N. Fukushima, J. Fac. Sci. Tokyo Univ., Sec. 2, Vol. 8, pt. 5 (1953).
[13] T. Nagata and S. Abe, Rep. Ionosphere Res. Japan, **9**, 39 (1955).
[14] A. G. McNish, Terr. Mag., **42**, 109 (1937).
[15] T. Nagata, Y. Nakata, T. Rikitake, and I. Yokoyama, Rep. Ionosphere Res. Japan, **9**, 121 (1955).
[16] S. Chapman, Proc. R. Soc., A, **115**, 242 (1927).
[17] T. Rikitake, Rep. Ionosphere Res. Japan, **2**, 57 (1948).
[18] S. Chapman and J. Bartels, Geomagnetism, Clarendon Press, Oxford (1940); Chap. 23, pp. 750-798.
[19] T. Nagata, Rep. Ionosphere Res. Japan, **4**, 155 (1950).
[20] T. Nagata and H. Mizumo, J. Geomag. Geoelectr., **7**, 69 (1955).
[21] K. Whitham and E. I. Loomer, Characteristics of magnetic disturbances at the Canadian arctic observatories, Pub. Dominion Observatory, Ottawa (1956).
[22] E. H. Vestine, L. Laporte, I. Lange, and W. E. Scott, Washington, D. C., Carnegie Inst. Pub. 580 (1947).
[23] S. K. Chakrabarty and R. Pratap, J. Geophys. Res., **59**, 1 (1954).
[24] H. Maeda, J. Geomag. Geoelectr., **7**, 121 (1955).
[25] S. Kato, J. Geomag. Geoelectr., **8**, 24 (1956).
[26] M. Hirono and T. Kitamura, J. Geomag. Geoelectr., 8, 9 (1956).
[27] E. H. Vestine, J. Geophys. Res., **59**, 93 (1954).
[28] T. Nagata, J. Geophys. Res., **57**, 1 (1952).
[29] B. H. Briggs and M. Spencer, Rep. Progr. Phys., **17**, 245 (1954).
[30] B. H. Briggs, private communication (December 1956).

JOURNAL OF GEOPHYSICAL RESEARCH VOLUME 62, No. 4 DECEMBER, 1957

AIRBORNE MEASUREMENT OF ATMOSPHERIC POTENTIAL GRADIENT

BY JOHN F. CLARK

*U. S. Naval Research Laboratory, Washington 25, D. C., and University of Maryland, College Park, Maryland**

(Received June 8, 1957)

ABSTRACT

Grounded-rotor induction-type electric field meters are mounted horizontally at the wing tips and vertically at the bottom of the fuselage of a P4Y airplane for the airborne measurement of the fair weather atmospheric potential gradient. The measurement has been corrected for the electric field distortion due to the aircraft itself by comparing observed values of potential gradient and conductivity at the earth's surface and at altitude during low-altitude flights over a portable ground station. A typical altitude distribution of potential gradient observed during clear weather at 67° north latitude is integrated to obtain a value of atmospheric potential at a 6-km altitude of 220 kv relative to the earth's surface.

I. INTRODUCTION

The earth's atmosphere has been considered a leaky dielectric of approximately 200 ohms resistance, through which flows about 1,800 amperes of current [see 1 of "References" at end of paper]. It is believed that the necessary positive upper atmospheric potential of some 360 kv relative to the earth's surface is maintained by world-wide thunderstorm activity [2, 3]. However, the lack of quantitative potential gradient measurements, even in fair weather at altitudes above the exchange layer, has left considerable uncertainty regarding the absolute value of atmospheric potential as a function of position and time.

In 1954, in order to fill such observational gaps, a P4Y aircraft (Fig. 1) was instrumented [4] to measure simultaneously the atmospheric potential gradient and other atmospheric electric and meteorological variables. From measurements between 0.03 and 6 km, the altitude distributions of these, and of derived quantities such as atmospheric potential and space charge density, are obtained and correlated with universal (world-wide) and local (meteorological) effects. It is the purpose of this paper to describe the airborne instrumentation system and techniques which are used to measure the fair weather atmospheric potential gradient, free from disturbing effects created by the aircraft.

*Part of this work was submitted to the University of Maryland in partial fulfillment of the requirements for the Doctor of Philosophy degree in Physics. Other portions of the dissertation will be published separately.

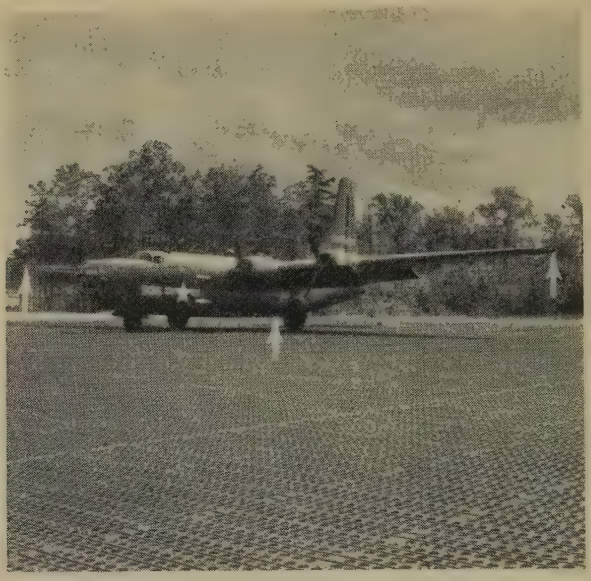

FIG. 1—P4Y atmospheric electricity research airplane. Arrows point to electric field meter locations.

II. THE ELECTRIC FIELD METER

A grounded-rotor induction-type electric field meter (EFM) was selected for use in the airplane installation. A review of the evolution of various types of field meters has been given by Mapleson and Whitlock [5]. The chosen type had already demonstrated its ruggedness and dependability while operating in several types of airborne vehicles. The present EFM evolved from instruments which had been designed at the U.S. Naval Research Laboratory for airplane use in the Joint Precipitation Static Research Program [6], and were developed further for rocket use in the Upper Atmosphere Research Program [7].

Two of the present field meters and their associated dual-channel amplifier are shown in Figure 2. Each EFM is 6 inches in diameter, 6 inches long, and weighs 7 pounds. The stator-exposure frequency is approximately 500 cps. With

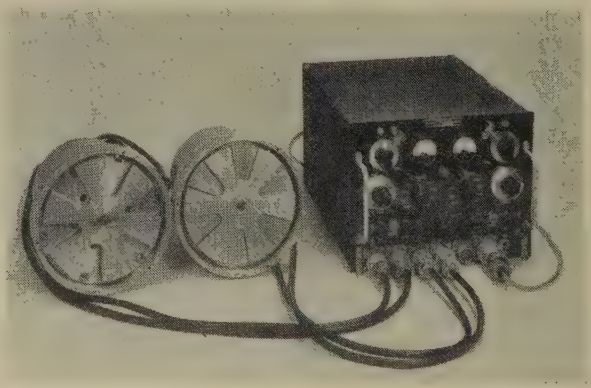

FIG. 2—Two electric field meters and associated dual-channel amplifier

a stator input resistance of 10 megohms shunted by a 500 $\mu\mu$f capacitor, its stator voltage sensitivity is roughly 2×10^{-5}v for a field of 1 v/m. Its "residual field" or "residue," the fairly steady field of some 50 v/m which is indicated by the EFM for zero incident field, is eliminated by connecting the stator return to an adjustable dc bias source. The effect of the drift in this residue, at a maximum rate of perhaps 0.1 v/m per minute, is minimized by special flight measurement techniques described in Section VIII. The higher frequency peak-to-peak noise level of this EFM is equivalent to a field of about 1 v/m, which is negligible compared to the minimum field amplitudes encountered at the aircraft locations.

Figure 3 is a block diagram of an EFM and one of the two duplicate channels of the associated amplifier. Nine ranges of sensitivity are provided, with full-scale readings of 10, 30, 100, 300, $\cdots$, 100,000 v/m. An auxiliary synchronous

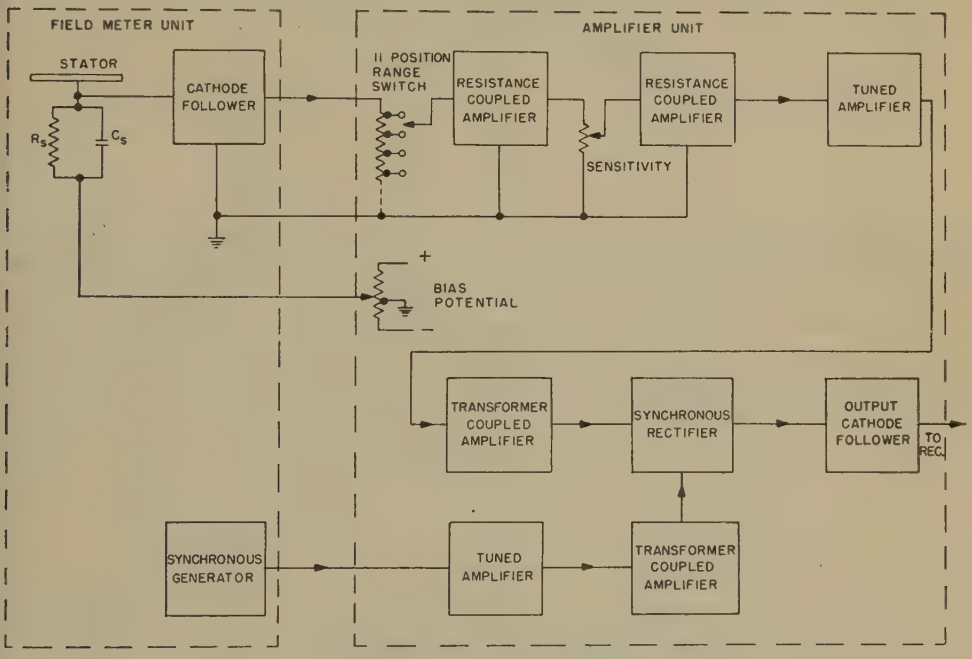

FIG. 3—Block diagram of single EFM channel

voltage, derived from an electromagnetic generator on the rotor shaft, is combined with the smaller amplified signal in the synchronous rectifier. The amplifier output to the recorder is thus a dc voltage, which is proportional to the incident field and of the same polarity.

III. AIRPLANE IN ATMOSPHERIC POTENTIAL GRADIENT

Consider the measurement of the fair weather atmospheric potential gradient from an airplane whose coordinate system is defined in Figure 4. The electric field strength at the port wing tip is

$$E_p = p_y E_y + p_z E_z \quad \ldots\ldots\ldots\ldots\ldots\ldots\ldots\ldots (1)$$

where E_y is the ambient atmospheric electric field component parallel to the

y axis of the aircraft and p_y is the constant positive dimensionless geometric augmentation factor by which E_y is multiplied at the conducting aircraft wing tip. The reciprocal of this augmentation factor is known as the reduction factor [8]. The quantity E_q is the field strength which would be developed by the net

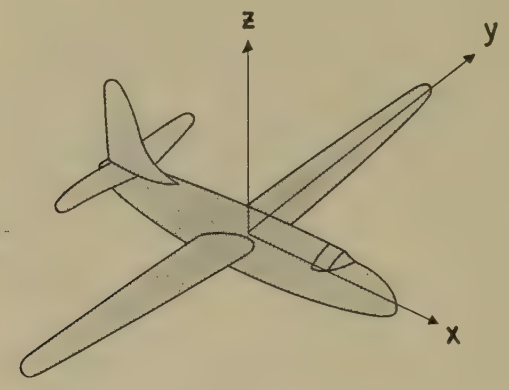

FIG. 4—Airplane coordinate system

airplane charge q at every point on the surface of an isolated sphere whose capacity equals that of the aircraft. Consequently, the geometric charge augmentation factor p_q is the ratio of field strength developed by q at the wing tip location to E_q.

An expression similar to Eq. (1) may be given for the starboard wing tip. Because of the symmetry of the aircraft about the xz plane, the respective wing tip augmentation factors are equal, and the sum and difference of E_p and E_s may be solved for E_q and E_y:

$$E_q = \frac{E_p + E_s}{2p_q} \quad \ldots\ldots\ldots\ldots\ldots\ldots\ldots\ldots\ldots\ldots (2)$$

$$E_y = \frac{E_p - E_s}{2p_y} \quad \ldots\ldots\ldots\ldots\ldots\ldots\ldots\ldots\ldots\ldots (3)$$

Another expression similar to Eq. (1) for the bottom of the fuselage in the xz plane of symmetry (see Fig. 1) may be combined with Eq. (2) to obtain the ambient field component parallel to the z aircraft axis:

$$E_s = -\frac{E_b}{b_z} + \frac{b_q(E_p + E_s)}{2p_q b_z} \quad \ldots\ldots\ldots\ldots\ldots\ldots\ldots\ldots (4)$$

Gunn and Parker [9] termed the ratio p_q/b_q the "multiplier" of a selected point on the airplane with respect to a reference position on the fuselage bottom.

An angle of bank θ may be defined as the elevation angle of the y axis (port wing) above the horizontal while the x axis (fuselage) remains horizontal. From Eq. (4), the fair weather (vertical) atmospheric potential gradient is given by

$$\frac{\partial V}{\partial Z} = \frac{1}{b_z \cos\theta}\left[E_b - \frac{b_q}{p_q}\frac{(E_p + E_s)}{2}\right] \quad \ldots\ldots\ldots\ldots\ldots\ldots\ldots\ldots (5)$$

or from Eq. (3),

$$\frac{\partial V}{\partial Z} = \frac{E_s - E_p}{2p_v \sin \theta} \quad \ldots\ldots\ldots\ldots\ldots\ldots\ldots\ldots\ldots\ldots\ldots\ldots (6)$$

where Z is the altitude. The potential gradient may be obtained from Eq. (5) during straight and level flight, where cos θ is unity. Alternatively, $\partial V/\partial Z$ may be obtained from Eq. (6) during a precision turn in which the angle of bank and the altitude are maintained constant.

IV. THE AIRBORNE EFM SYSTEM

A block diagram of the airborne EFM system and its associated multi-channel recorder is given in Figure 5. It is, in effect, a computer for producing continuous solutions of Eqs. (2), (3), and (4) in the form of recorder galvanometer deflections which are proportional to E_q , E_y , and E_z , respectively. A voltage proportional to the average value of E_p and E_s is obtained by the use of the two identical re-

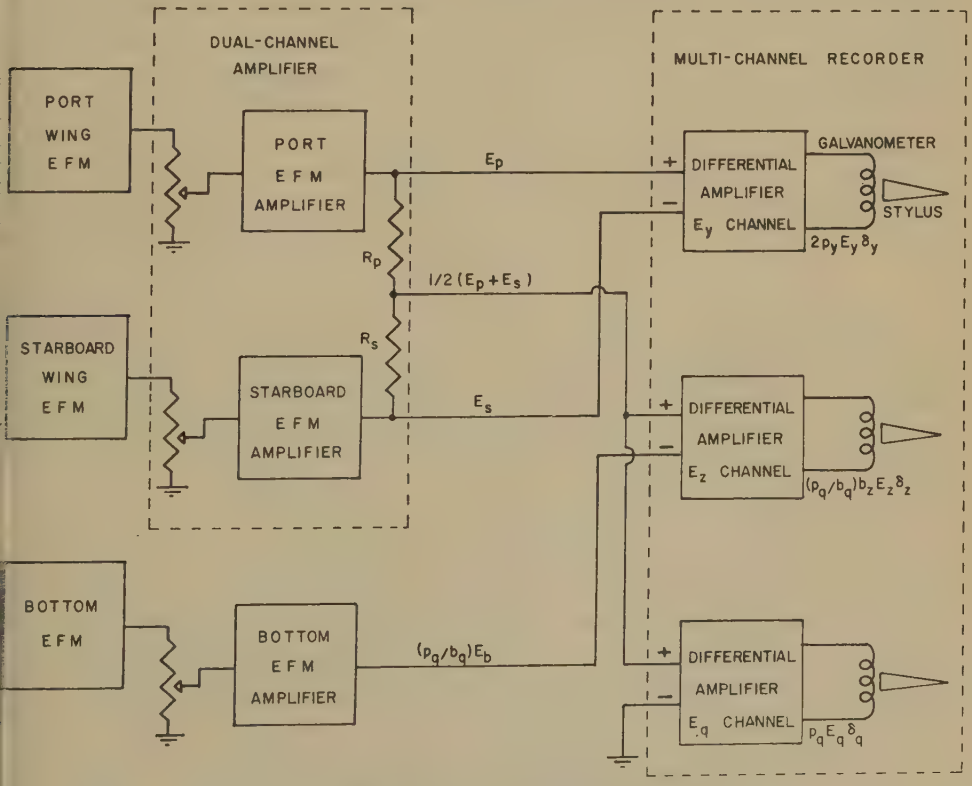

FIG. 5—Block diagram of airborne EFM system and recorder

sistances R_p and R_s . Voltage differences are obtained by use of the differential amplifiers of the conventional multi-channel recorder. Orthogonal, linear deflections up to ± 25 mm are obtained with each galvanometer-driven hot-wire stylus, at all frequencies from dc to 10 cps (limited by the present EFM response), at a normal paper speed of 1 mm per second.

Prior to each flight, the differential amplifier gains of each recorder channel are equalized. An artificial field is applied to the port EFM alone and its associated gain potentiometer is adjusted to obtain the standard recorder deflection sensitivity δ_y (in millimeters deflection for 1 v/m field strength). The same artificial field is applied to the starboard EFM and its amplifier potentiometer is set to produce a gain equal to that of the port channel. After these adjustments, Eq. (3) becomes

$$E_y = \frac{E_p - E_s}{2p_y} = \frac{D_y}{2\delta_y p_y} \quad \ldots\ldots\ldots\ldots\ldots\ldots\ldots\ldots (7)$$

where D_y is the deflection of the E_y channel in millimeters. Similarly, Eq. (2) becomes

$$E_q = \frac{E_p + E_s}{2p_q} = \frac{D_q}{\delta_q p_q} \quad \ldots\ldots\ldots\ldots\ldots\ldots\ldots\ldots (8)$$

Finally, an artificial field is applied to the bottom EFM and its amplifier potentiometer is adjusted to provide a gain of p_q/b_q times that of the port channel. Eq. (4) becomes

$$E_z = \frac{D_z}{\delta_z b_z (p_q/b_q)} \quad \ldots\ldots\ldots\ldots\ldots\ldots\ldots\ldots (9)$$

where

$$\frac{D_z}{\delta_z} = -\frac{p_q}{b_q} E_b + \frac{E_p + E_s}{2} \quad \ldots\ldots\ldots\ldots\ldots\ldots\ldots\ldots (10)$$

To check the gain balance of the EFM system in flight, some engine condition (usually the fuel mixture ratio) is changed to produce several variations in the potential of the airplane. The same value of D_y before and after each change in E_q indicates equality between the port and starboard EFM channel gains, while the same D_z indicates the proper ratio p_q/b_q of bottom to port EFM channel gains.

V. EXPERIMENTAL DETERMINATION OF AUGMENTATION FACTORS

The ratio of charge augmentation factors p_q/b_q and the augmentation factor b_z must be known before the potential gradient can be determined on an absolute basis from Eq. (5). Similarly, the value of p_y is needed to compute the gradient using Eq. (6). These dimensionless geometric constants were obtained experimentally in the order p_q/b_q , p_y/b_z , and b_z .

The ratio p_q/b_q was obtained in flight by producing variations in E_q , checking the equality between the port and starboard EFM channel gains, and then adjusting the bottom EFM gain until no change in D_z was observed before and after each change in airplane potential. From Section IV, the ratio of the adjusted bottom EFM channel gain to that of the port channel is p_q/b_q . The value 17.54 $\pm$ 0.26 was obtained from six such determinations.

The ratio p_y/b_z was also obtained in flight, by comparing relative values of $\partial V/\partial Z$ determined simultaneously from Eqs. (5) and (6) during precision turns. The value 31.3 $\pm$ 1.4 was obtained from nine such double turns in which the angle of bank was held at 45°, first in one direction and then in the opposite one.

In order to obtain b_z experimentally, a level meadow free of trees was selected in Kingman State Park, Kansas, for the measurement of absolute values of atmospheric potential gradient and total conductivity at the earth's surface. An electric field meter was flush-mounted at the center of a conducting ground plane 1 m square and calibrated by the application of an artificial field. This assembly was placed in a shallow hole so that its top was flush with the ground surface, to insure that the potential gradient measurement was on an absolute basis.

On November 29, 1955, from 1419 to 1446 GMT, seven low-altitude passes were made by the P4Y aircraft over this ground site, at altitudes of 30, 30, 30, 15, 15, 30, and 60 m, respectively. Figure 6 shows the absolute surface potential gradient $\partial V/\partial Z$ observed at the ground site and the relative gradient $(\partial V/\partial Z)/b_z$ observed above the ground site during these passes. No change in the surface potential gradient was observed as the airplane passed overhead. It is apparent that the potential gradient was varying more with time than with altitude below 60 m. Furthermore, the average total conductivity values on the ground and in the air were the same within 2 per cent, although rapid variations attributed by Kraakevik [10] to triboelectric charging of the inner electrodes of the conductivity chambers by dust caused variations of some individual readings by as much as 20 per cent from the mean. Therefore, it was assumed that the average potential gradient at the surface was the same as that between 15 and 60 m above the ground. A value of b_z was computed for each pass from the ratio of the surface to airborne gradient. On the basis of the seven passes of Figure 6, b_z equals 1.69 ± 0.13.

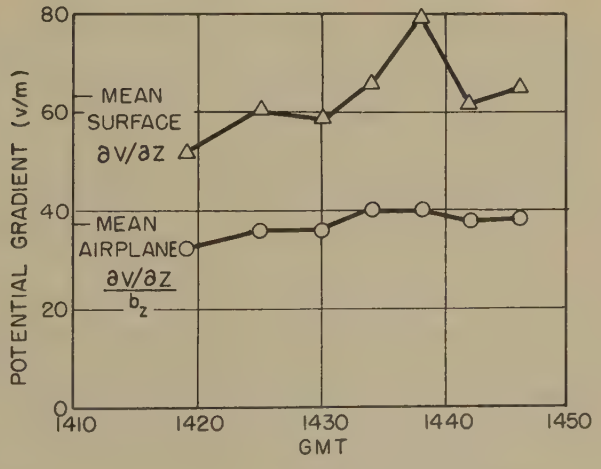

Fig. 6—Determination of airplane bottom augmentation factor

An independent check of this value was made some two hours later, as shown in Figure 7. All airborne values of potential gradient were computed using the value 1.69 for b_z . Passes over the ground site were made at 135, 30, and 15 m within a period of nine minutes, during which time the average surface potential gradient was 91.2 v/m. The solid straight line in Figure 7 is drawn between the average surface value and the 135 m point. The agreement between this interpolation and the measured gradient at 15 and 30 m is excellent.

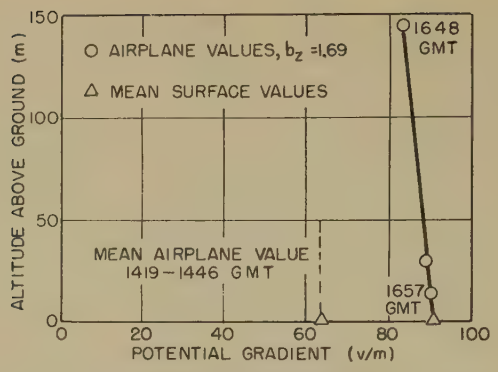

FIG. 7—Check of bottom augmentation factor

The value of p_v as computed from p_v/b_z and b_z is 52.9. Gish and Wait measured the vertical field component above thunderstorms from an airplane by means of two field meters, one on the top wing surface looking upward and one directly beneath it, about 8 feet from the wing tip. The augmentation factors were 1.7 and 1.2, respectively [11]. Chapman cites a similar system of four field meters, using two locations similar to those of Gish and Wait on each wing [12]. It is the contrast between such low factors and that of 52.9 attainable at the wing tips looking horizontally which led to the choice of the latter EFM locations for the present fair weather, small potential gradient investigation.

VI. ANALYTIC DETERMINATION OF AUGMENTATION FACTORS

An estimate of b_z was made by noting that the P4Y airplane fuselage at the bottom EFM location is 1.33 times as high as it is wide. Its yz cross-section at this point is intermediate between a rectangle and an ellipse. Thus, b_z should lie between unity at the sides of a rectangle and 2.33, established by the augmentation factor $(1 + a/b)$ at the ends of the major elliptic axis [13], where a/b is the major to minor axis ratio. The experimental value of 1.69 lies near the center of this range.

The wing may be approximated by a prolate spheroid of axis ratio 11.6, where the mean value of its wing root chord and thickness is used as the minor axis. Unpublished expressions for the augmentation factors of a prolate spheroid at its pole (p_v) and along its equator (b_z) have been derived by Spitz:

$$p_v = \frac{2c^3}{-2b^2c + ab^2 ln \frac{a+c}{a-c}}, \qquad b_z = \frac{4c^3}{2a^2c - ab^2 ln \frac{a+c}{a-c}} \quad \ldots\ldots (11)$$

where a is the semimajor and b the semiminor spheroid axis, and c equals $(a^2-b^2)^{1/2}$. From Eq. (11), the experimental value for p_v of 52.9 corresponds to an axis ratio a/b of 10.5, in satisfactory agreement with 11.6 considering the wing approximation employed.

Expressions for analogous prolate spheroid polar and equatorial charge augmentation factors are derived in the Appendix:

$$p_q = \left[\frac{2c}{b \ln \frac{a+c}{a-c}}\right]^2, \qquad b_q = \frac{b}{a} p_q \ldots\ldots\ldots\ldots\ldots\ldots (12)$$

If the airplane wing is approximated by a prolate spheroid whose axis ratio is 10.5, as required for agreement between the experimental and analytic values of p_v, then from Eq. (12) p_q equals 11.8.

VII. THE MEASUREMENT OF AIRPLANE CHARGE AND POTENTIAL

The capacity C of the isolated P4Y airplane is approximately 740 $\mu\mu$f (0.22 times its wingspread in centimeters [14]). Consequently, for this airplane,

$$E_q = 2.0 \times 10^8 q \ldots\ldots\ldots\ldots\ldots\ldots (13)$$

From Eqs. (2) and (13), using the analytic value of 11.8 for p_q, the net airplane charge

$$q = 4.2 \times 10^{-10} \frac{E_p + E_s}{2} \ldots\ldots\ldots\ldots\ldots\ldots (14)$$

in coulombs. The corresponding airplane potential

$$V_q = 0.57 \frac{E_p + E_s}{2} \ldots\ldots\ldots\ldots\ldots\ldots (15)$$

that is, its potential in volts is numerically equal to 57 per cent of the average field in volts per meter at the wing tips.

At an altitude of roughly 2 km, using normal cruising power, the airplane potential from Eq. (15) was ordinarily several hundred volts negative. Changing the fuel mixture from "lean" to "rich" resulted in a more negative potential of some 200 v in 5 seconds. The average net current

$$I_d = -C \frac{dV_q}{dt} \ldots\ldots\ldots\ldots\ldots\ldots (16)$$

discharged by the exhaust during this interval was 3.0×10^{-8} ampere.

VIII. EXPERIMENTAL ACCURACY

The relatively small but steady potential gradient which usually exists above 2 km was measured during precision turns using Eq. (6). Negligible error was introduced by wing tip EFM residual drift during the 30 seconds required for this measurement. At lower altitudes, the gradient changes rapidly with position and a constant angle of bank is difficult to maintain in turbulent air. Here the potential gradient was measured in straight and level flight using Eq. (5), with $\cos\theta$ equal to unity. Variations of θ about zero by as much as 8° cause less than one per cent error in this measurement. The bottom EFM was provided with a remotely actuated shutter to provide a zero incident field between measurements at each altitude, to compensate for the residual field drift of this instrument.

Considering instrumental stability and the accuracy of b_z, p_v, p_q/b_q, and θ, the absolute accuracy of each potential gradient measurement is approximately $\pm$ 10 per cent. However, values of aircraft potential, charge, and exhaust current,

which depend upon the approximate analytical value of p_a, are probably accurate only to within ± 20 per cent.

IX. POTENTIAL GRADIENT DISTRIBUTION ABOVE GREENLAND FJORD

The measurements at 67° north latitude above Söndre Strömfjord, Greenland, at 1100 GMT, 11 September 1955, are representative of cloudless weather and clean air. The hour is near that of the diurnal mean value of surface atmospheric potential gradient. The ascent to 6 km required 50 minutes. The time of the altitude distribution, or "profile," is defined as the quarter-hour nearest the midpoint of the 70-minute descent. Figure 8 is a plot of this atmospheric potential gradient profile on a semilogarithmic scale. Above 0.1 km, the straight line

$$\partial V/\partial Z = 15.8 \exp [(6 - Z)/4.0] \text{ v/m} \quad \ldots\ldots\ldots\ldots\ldots\ldots (17)$$

where V is the atmospheric potential in kilovolts and Z is the altitude in kilometers, is fitted by the experimental data with a standard deviation of 3.7 per cent.

The atmospheric potential at 6 km obtained by integration of the potential gradient profile of Figure 8 is 220 kv. Extrapolating upward on the assumption that Eq. (17) is valid at all higher altitudes yields a value for the potential of the upper atmosphere with respect to the earth's surface of 283 kv.

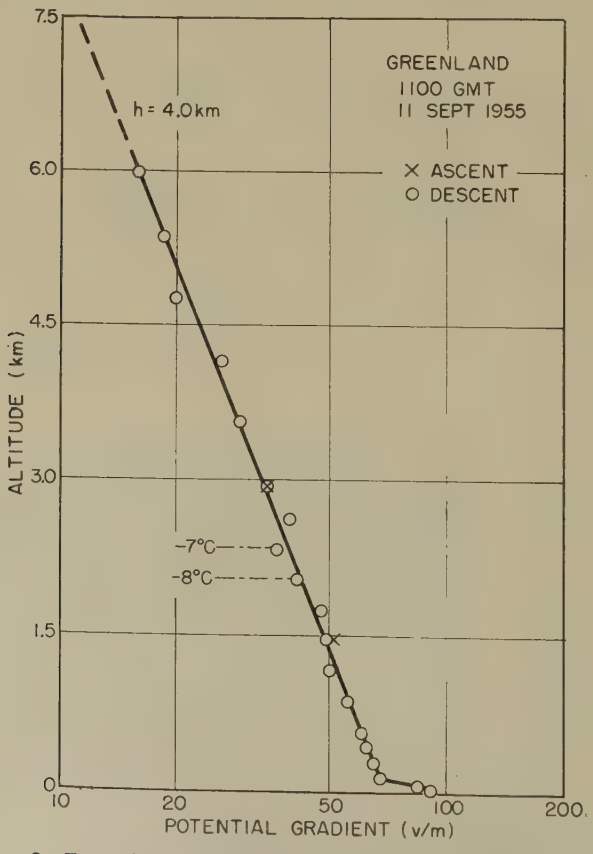

FIG. 8—Potential gradient distribution above Greenland fjord

X. SUMMARY AND CONCLUSIONS

Grounded-rotor induction-type electric field meters are used to measure the electric field normal to the conducting surface of a P4Y airplane at the two wing tips and at the bottom of the fuselage. The resultant data are automatically processed in flight to obtain continuous recorded values of the ambient atmospheric electric field component E_z perpendicular to the wing and fuselage axes; the component E_y parallel to the wing axis; and the net airplane charge. The measurement has been corrected for the electric field distortion due to the aircraft itself by comparing observed values of atmospheric potential gradient and conductivity at the earth's surface and at altitude during low-altitude flights over a portable ground station. Within the exchange layer, E_z is used to obtain the more accurate average value of the fair weather atmospheric potential gradient. At higher altitudes up to the airplane's ceiling (6 km), E_y is used in sustained precision turns to obtain values of the smaller, more constant potential gradient free of instrumental drift effects. The estimated accuracy of any one airborne measurement of the absolute atmospheric potential gradient is approximately $\pm$ 10 per cent.

The potential gradient observed during clear weather at altitudes up to 6 km above Söndre Strömfjord, Greenland, at 67° north latitude, decreased exponentially with altitude above 0.1 km. Integration of this altitude distribution yields a 6-km potential of 220 kv relative to the earth's surface.

XI. ACKNOWLEDGMENTS

The author is indebted to Dr. J. H. Kraakevik for sharing the responsibility for the airborne data collection and reduction, and for supervising the surface measurements and providing the airborne conductivity data in connection with the experimental determination of the airplane augmentation factors. He is equally indebted to Mr. R. E. Bourdeau, who provided helpful criticism of this manuscript, for his major role in the development of the field meter and in its successful integration into the airborne system. Thanks are also due to Mr. H. Spitz for the use of Eq. (11); and to Prof. Jules de Launay, of the University of Maryland, who supervised the thesis.

APPENDIX: THE POLAR AND EQUATORIAL CHARGE AUGMENTATION FACTORS OF A PROLATE SPHEROID

The potential of an isolated conducting prolate spheroid having a net charge q is

$$V_a = \frac{q}{8\pi\epsilon c} \ln \frac{a+c}{a-c} \quad \ldots\ldots\ldots\ldots\ldots\ldots\ldots\ldots (18)$$

and its surface charge density in the absence of an external field is [15]

$$\sigma = \frac{q}{4\pi a b^2} \left[\frac{x^2}{a^4} + \frac{y^2+z^2}{b^4} \right]^{-1/2} \quad \ldots\ldots\ldots\ldots\ldots\ldots\ldots\ldots (19)$$

The resultant electric field strengths at the pole $(a, 0, 0)$ and along the equator $(0, 0, b)$ are, respectively,

$$E_{qa} = \frac{q}{4\pi\epsilon b^2}\,; \qquad E_{qb} = \frac{q}{4\pi\epsilon ab} \quad \ldots\ldots\ldots\ldots\ldots\ldots (20)$$

From Eq. (18), the capacity of the prolate spheroid is

$$C = \frac{q}{V_q} = \frac{8\pi\epsilon c}{ln\,\dfrac{a+c}{a-c}} \quad \ldots\ldots\ldots\ldots\ldots\ldots (21)$$

The radius of the sphere having the same capacity is

$$R = \frac{2c}{ln\,\dfrac{a+c}{a-c}} \quad \ldots\ldots\ldots\ldots\ldots\ldots (22)$$

Consequently, the polar charge augmentation factor of a prolate spheroid is

$$p_q = \frac{E_{qa}}{E_q} = \left[\frac{R}{b}\right]^2 = \left[\frac{2c}{b\ ln\,\dfrac{a+c}{a-c}}\right]^2 \quad \ldots\ldots\ldots\ldots\ldots\ldots (23)$$

where

$$E_q = \frac{q}{4\pi\epsilon R^2} \quad \ldots\ldots\ldots\ldots\ldots\ldots (24)$$

The ratio of polar to equatorial charge augmentation factors is

$$\frac{p_q}{b_q} = \frac{E_{qa}}{E_{qb}} = \frac{a}{b} \quad \ldots\ldots\ldots\ldots\ldots\ldots (25)$$

References

[1] O. H. Gish, Compendium of Meteorology (edited by T. F. Malone), American Meteorological Society, Boston (1951); p. 107.
[2] F. J. W. Whipple, Q. J. R. Met. Soc., 55, 1 (1929).
[3] O. H. Gish and G. R. Wait, J. Geophys. Res., 55, 473 (1950).
[4] J. H. Kraakevik and J. F. Clark, Report of NRL Progress (March 1957); p. 1.
[5] W. W. Mapleson and W. S. Whitlock, J. Atmos. Terr. Phys., 7, 61 (1955).
[6] R. C. Waddel, R. C. Drutowski, and W. N. Blatt, Proc. Inst. Radio Eng., 34, 162P (1946).
[7] J. F. Clark, Instruments, 22, 1007 (1949).
[8] O. H. Gish and G. R. Wait, J. Geophys. Res., 55, 475 (1950).
[9] R. Gunn and J. P. Parker, Proc. Inst. Radio Eng., 34, 241 (1946).
[10] J. H. Kraakevik, The electrical conductivity and current density in the troposphere, University Microfilms, Ann Arbor, Michigan, 1957; Doctoral Dissertation Series, Pub. No. 21,526, p. 80.
[11] O. H. Gish and G. R. Wait, J. Geophys. Res., 55, 475 (1950).
[12] R. E. Holzer and W. E. Smith, Editors, Proceedings of the Conference on Atmospheric Electricity, Air Force Cambridge Research Center, Bedford, Massachusetts, Geophys. Res. Papers No. 42, 121 (1955).
[13] J. F. Clark, The fair weather atmospheric electric potential and its gradient, University Microfilms, Ann Arbor, Michigan, 1956; Doctoral Dissertation Series, Pub. No. 19,655, p. 139.
[14] R. Gunn and J. P. Parker, Proc. Inst. Radio Eng., 34, 243 (1946).
[15] J. A. Stratton, Electromagnetic Theory, McGraw-Hill Book Co., Inc., New York (1941); p. 209.

GEOMAGNETIC AND SOLAR DATA

INTERNATIONAL DATA ON MAGNETIC DISTURBANCES, SECOND QUARTER, 1957

This report continues the series which has appeared regularly in the JOURNAL since Vol. 54, No. 3, 295 (1949). Please refer to that first report for an explanation of the data given, and to Vol. 59, No. 3, 423 (1954) for the definition of *Ap*.

Preliminary Report on Sudden Commencements

S.c.'s given by five or more stations are in italics. Times given are mean values, with special weight on data from quick-run records.

Sudden commencements followed by a magnetic storm or a period of storminess (s.s.c.)

1957 April *15d 20h 48m*: thirty-four (s.f.e.: Hu).—*17d 11h 36m*: forty-five.—*18d 15h 08m*: twelve.—*18d 15h 38m*: seven.

1957 May *21d 09h 10m*: eighteen.—*30d 08h 22m*: forty-four.

1957 June 03d 04h 57m: Me Ag.—*15d 13h 58m*: thirteen.—*24d 03h 40m*: fifteen.—*25d 00h 46m*: forty-one.—*30d 05h 28m*: thirty-six.

Sudden commencements of polar or pulsational disturbances (p.s.c.)

1957 April 02d 00h 43m: SM Ta Hr.—02d 01h 00m: Te El.—*02d 18h 47m*: eight.—03d 18h 24m: Qu El.—*03d 22h 50m*: twenty-six.—04d 01h 55m: Sm Ta Te.—05d 01h 18m: Es SM Ta.—05d 07h 07m: Cm Fu Bi Ap.—05d 22h 51m: CF Te Bi.—*05d 23h 16m*: twenty.—*06d 02h 14m*: six.—06d 22h 50m: Tl Bi El.—*08d 21h 32m*: twelve.—08d 23h 32m: Wn Pr.—09d 20h 33m: Wn Pr IK.—09d 23h 46m: Tr Cm Vl.—10d 01h 23m: Va Hr.—11d 21h 13m: Tr So Cm Bi.—*11d 22h 37m*: eight.—12d 06h 58m: Ag Te.—12d 15h 45m: Ka Qu.—12d 17h 14m: Hb Qu.—*12d 23h 31m*: nine.—13d 01h 31m; CF Tl SM.—*14d 17h 50m*: five.—15d 11h 04m: Me Ap.—*15d 23h 07m*: fifteen.—*16d 21h 32m*: seven.—19d 01h 28m: SM Hr.—20d 02h 10m: SM Va.—20d 07h 00m: Ag Te.—20d 23h 50m: CF Eb Tl.—23d 01h 03m: Cm Tl.—23d 13h 56m: Vl Hb (s.f.e.?: Eb).—*23d 23h 41m*: five.—24d 02h 27m: Me Ag Te.—26d 02h 01m: Si Te.—*27d 00h 27m*: fourteen.—27d 04h 11m: SM Te Hr.—28d 20h 12m: Qu Bi.—*28d 21h 17m*: fourteen.—*29d 03h 25m*: six.—30d 03h 49m: Ag SM.—30d 20h 54m: Do Hr.

1957 May 01d 01h 40m: SM Hr.—*03d 20h 55m*: nine.—03d 21h 35m: Ma Hb Tl.—03d 21h 53m: Do Me Pr SM.—04d 23h 26m: CF Hr.—05d 00h 16m: Ci Ta.—05d 22h 52m: Do CF El Hr.—*05d 23h 50m*: five.—07d 17h 36m: So Hb.—08d 07h 42m: Me Ag.—08d 09h 15m: Cm SM.—08d 22h 03m: IK SM Te.—*08d 22h 45m*: ten.—*11d 20h 49m*: five.—*11d 21h 35m*: fourteen.—13d 00h 17m: Vl CF Eb Bi.—13d 10h 25m: Me Te Ap.—14d 04h 13m: Ag Ci SM Hr.—*15d 21h 22m*:

TABLE 1—*Geomagnetic planetary three-hour-range indices Kp, preliminary magnetic character-figures C, average amplitudes Ap (unit 2γ), and final selected days, April to June, 1957*

April 1957									
E	1	2	3	4	5	6	7	8	Sum
1	4o	4+	4o	3+	3o	3+	4−	4−	29+
2	4+	2−	3o	3o	2+	2+	3+	3+	23+
3	3o	2o	3−	3+	3o	3o	4o	5o	26o
4	4o	4+	3o	2+	3o	3+	3+	3o	26+
5	4o	3+	3+	5+	6−	5o	3−	5o	34+
6	6−	5o	5−	5−	3−	2−	1o	1−	26o
7	1o	1+	2−	1o	0+	1−	0+	1o	7+
8	2o	2+	3o	3−	3o	2o	3−	3o	21−
9	3−	4+	4o	3o	4+	4−	4−	5−	30+
10	5+	7−	7−	6−	5−	5+	3+	2o	40−
11	3o	2+	2−	5−	5−	2+	2o	3o	24−
12	2o	3−	4−	1+	2o	3o	3o	2o	20−
13	3+	3−	4−	2o	3−	2−	1−	1+	18o
14	1−	1o	0+	0+	0o	2o	1+	1+	7o
15	0+	2o	2o	3o	3+	2o	3+	6−	22−
16	4+	4o	2+	2+	3−	3+	3−	3+	25o
17	3+	4o	3+	4+	5+	4o	6o	8−	38o
18	6+	4−	3o	4−	2+	6−	5+	5o	35o
19	6+	6+	7−	4+	5−	5o	5−	4o	42o
20	4o	4o	3o	2o	2o	3−	3−	2+	23−
21	3+	4−	3o	3−	4−	4o	3−	2+	25+
22	1o	0+	0+	0+	1−	2−	2o	1o	7+
23	3−	3o	2o	2−	3+	1+	2o	3o	19o
24	4o	3o	3−	4−	5−	5−	4−	5−	31o
25	3o	2−	2−	2o	3−	3o	2+	2−	18o
26	2o	3o	3+	4o	5−	5−	4o	3o	29−
27	5o	4o	4−	3+	3+	2+	2o	3−	26+
28	2−	2−	2+	3−	4−	5−	4−	4o	24+
29	3+	4o	2o	3o	3o	3o	2o	1−	21o
30	2o	4−	2o	2o	2o	3o	3o	3+	21o
31									

May 1957									
1	2	3	4	5	6	7	8	Sum
4o	4+	4o	3+	2+	2+	1+	1o	23−
2o	3o	3+	3o	3−	1o	1o	2o	18o
2−	2+	1+	3−	2o	3−	3−	4o	19+
1+	1+	2+	2+	3−	3−	3−	3−	18o
3−	2o	1+	2−	2o	2o	1+	3−	16−
3−	3−	2+	4+	3o	2−	2−	2+	21−
3−	4−	3−	2o	2o	3−	2+	1o	19o
0+	1o	3−	3−	2+	3−	3−	4o	18+
4−	5−	5−	4−	3+	3o	3o	2−	28−
2−	2+	2−	2+	2o	1+	3+	4−	18+
2+	2o	1o	1+	2−	1+	2o	3+	15o
2+	1o	1+	2−	1o	2−	0+	2o	11+
3−	3−	2−	3−	3−	3−	3o	2+	20+
2−	2+	1o	1+	1+	1o	2o	1+	12o
1+	0+	1−	1+	2−	1+	1+	2+	10+
0+	0+	1−	1−	0+	1+	2+	1o	7o
1−	2o	2−	2−	1o	3o	2o	2o	14o
2−	1+	2−	1+	2−	1o	2o	2o	13−
2−	1−	2−	2−	3+	3+	3+	3+	19o
3o	4−	3+	3o	3+	4−	3+	2+	26−
2+	3o	3−	4−	3+	2+	2+	2o	22−
2−	2+	2−	2o	1+	2o	1−	1−	12+
2+	2−	3−	1+	2o	2+	3−	1+	16+
1o	1−	2o	3o	2−	1o	1o	0+	11−
2−	2+	3o	3o	3o	2o	2+	3+	21−
4−	4−	4+	5o	4−	5−	3+	4−	32o
2+	2+	3o	3−	2o	1+	1o	2−	16+
2−	1o	2+	2o	2−	2+	1o	2o	14o
1o	1+	2+	1o	1+	2o	1o	1+	11+
3−	1+	3o	5+	5−	5−	5−	3o	29+
3−	4−	2−	3−	1o	1o	2+	2+	17+

June 1957									
E	1	2	3	4	5	6	7	8	Sum
1	0+	1−	1+	1o	3−	2o	0+	1o	9+
2	1o	2+	1o	1+	1o	1o	1o	2o	11−
3	2−	4−	3o	5−	4+	4+	6−	5o	32+
4	5−	5+	4−	4o	3o	5−	5−	6−	36−
5	6−	4−	3o	3−	2+	4o	4o	5+	31−
6	4+	5o	5−	4+	3+	3−	4+	5o	34−
7	4+	2o	1+	2−	1−	1−	1−	3o	14+
8	3−	3o	2o	2−	2+	1o	1o	1+	15o
9	1−	1+	1+	0+	1−	1o	2−	1−	8−
10	1o	0o	0+	1−	0+	1−	1−	2o	6−
11	1o	1o	1−	1−	1−	1−	1−	1+	7−
12	2o	1o	2−	0+	3−	3−	1o	2−	13o
13	1o	1o	2−	3o	1+	2−	3−	3+	16−
14	2−	2−	1+	2−	2+	1+	3−	2−	14+
15	3−	3o	3−	2+	4−	5o	4−	2+	25+
16	2−	1−	1+	1+	2−	1+	1o	2+	11+
17	2o	4o	4o	3−	4−	2+	2o	4−	24+
18	5−	5−	4o	3−	3+	2o	3o	4o	28+
19	5−	5−	3o	3+	5+	3+	2o	3−	29o
20	3o	3+	3−	1+	2o	4−	4−	2+	22o
21	2+	3o	3+	3−	1+	2+	4o	3−	22−
22	3+	2−	2+	5−	4+	2o	2o	2+	23−
23	2o	1+	1−	2−	2+	2−	3+	2o	15o
24	4o	3+	4−	3o	2o	2−	2−	2+	22−
25	5−	4−	3+	5o	5−	5−	6−	5+	37o
26	5o	6o	6+	7−	7o	7−	5−	5+	48−
27	3o	2o	3o	3+	4o	3−	2+	4+	25−
28	3o	3o	4o	4−	4+	3+	3−	2o	26o
29	1o	1o	1o	1+	2o	1o	1o	2+	11−
30	3o	6+	5+	8−	8o	8o	8o	8+	55−
31									

Preliminary *C*, 1957			Average amplitude *Ap*		
Apr.	May	June	Apr.	May	June
1.0	0.7	0.2	23	16	5
0.8	0.4	0.2	15	10	5
1.0	0.7	1.3	20	11	33
0.8	0.5	1.3	19	10	38
1.3	0.4	1.1	37	8	29
1.1	0.8	1.2	27	13	33
0.1	0.7	0.6	4	11	9
0.6	0.9	0.3	12	11	8
1.1	1.0	0.2	25	22	4
1.5	0.6	0.0	58	10	3
0.8	0.6	0.1	17	8	4
0.8	0.2	0.2	11	5	7
0.5	0.6	0.5	11	11	9
0.1	0.3	0.4	4	6	7
1.0	0.2	0.9	18	5	19
1.0	0.2	0.2	17	4	5
1.6	0.4	0.9	55	7	17
1.5	0.2	1.1	42	6	23
1.6	0.6	1.0	60	12	26
0.7	0.9	0.8	14	17	14
0.9	0.8	0.8	17	13	13
0.2	0.4	0.9	4	6	16
0.6	0.4	0.4	11	8	8
1.1	0.2	0.9	27	6	14
0.4	0.8	1.5	10	12	41
1.1	1.2	1.7	23	28	84
0.9	0.4	1.0	20	8	17
0.9	0.4	1.0	18	6	18
0.8	0.2	0.1	13	5	5
0.8	1.3	2.0	12	28	150
	0.5			10	

TABLE 1—(Concluded)—*Final magnetically selected days, April to June, 1957*

Month	Five quiet days	Ten quiet days	Five disturbed days
1957			
April	7 13 14 22 25	7 8 12 13 14 22 23 25 29 30	5 10 17 18 19
May	12 15 16 24 29	12 14 15 16 17 18 22 24 28 29	1 9 20 26 30
June	1 2 9 10 11	1 2 8 9 10 11 12 14 16 29	4 6 25 26 30

five.—17d 16h 57m: Ka Wa.—19d 20h 07m: Wn CF Hb IK.—20d 19h 16m: Tr Do.—21d 01h 03m: Ag Ta El.—21d 19h 01m: So Do.—25d 03h 56m: Ag Te.—25d 21h 26m: Vl CF Eb.—*26d 02h 20m*: ten.—28d 06h 49m: Ag Te.—*28d 22h 28m*: thirteen.—28d 22h 43m: Ta El.—*30d 00h 16m*: eight.—31d 02h 09m: CF Tl.

1957 June 02d 15h 00m: Fu IK (s.f.e.?: Ks).—*03d 21h 53m*: five.—*04d 22h 16m*: eight.—05d 01h 17m: Eb SM El Hr.—05d 22h 51m: Eb Tl.—*07d 21h 35m*: sixteen.—07d 21h 53m: Ta Bi.—12d 00h 27m: CF Fu.—*12d 21h 29m*: five.—*13d 20h 24m*: five.—*13d 21h 35m*: fourteen.—14d 04h 46m: Me Ag.—14d 12h 26m: Me Ap.—15d 14h 38m: Me Ap Wa To.—*15d 23h 11m*: eleven.—*17d 21h 08m*: seven.—17d 21h 44m: IK Te.—18d 03h 43m: SM Te Va.—18d 22h 47m: Vl Tl Bi Hr.—*18d 23h 21m*: five.—19d 02h 57m: IK Ta.—*20d 01h 53m*: five.—20d 04h 35m: Me Ag SM.—20d 04h 52m: Ag Ci.—21d 05h 28m: SM Hr.—*21d 19h 24m*: fifteen.—22d 01h 28m: Vl SF.—23d 20h 04m: So Cm Bi.—*24d 01h 05m*: nine.

Sudden impulses found in the magnetograms (s.i.)

1957 April *05d 14h 36m*: seventeen (s.s.c.? p.s.c.? s.f.e.: Hu).—06d 10h 47m: So Le Ap Hr.—09d 05h 05m: Qu Am.—11d 11h 43m: Wn Ma Hb.—11d 13h 03m: Vl Te.—15d 21h 44m: Ma Db Cm.—15d 21h 51m: Ma Db.—16d 05h 25m: El Va Hr.—*17d 23h 32m*: eighteen.—*24d 14h 28m*: eight.—26d 10h 24m: IK Te Am (s.f.e.: El).

1957 May: None.

1957 June 04d 09h 00m: Ks Bi El Tn (s.f.e.: Hr).—05d 23h 19m: Hb IK Ci Va.—*06d 20h 29m*: thirty.—*20d 17h 11m*: eight.—20d 19h 19m: So Hb Te Bi.—*25d 11h 17m*: fifteen.—25d 19h 06m: Tr So?—*26d 10h 36m*: eight.—27d 12h 21m: Wn IK Hr.—*27d 23h 26m*: nine.—*28d 12h 02m*: seven.—28d 15h 34m; Wi Fu.—29d 23h 45m: Si Te.—30d 22h 18m: Wn IK.

Preliminary Report on Solar-flare Effects

Effects confirmed by ionospheric or solar observations are in italics.

1957 April 04d 09h 44m–10h 06m: El (s.i.: SM).—*05d 14h 37m*: Hu (s.i., s.s.c., p.s.c.: seventeen).—*06d 14h 53m–15h 23m*: Es.—*07d 14h 59m*: Wn Mn? Hb Eb Hu.—*09d 14h 18m–14h 42m*: Le Es (s.i.: SM).—14d 11h 04m: IK.—*14d 17h 11m*: Hu.—15d 09h 48m–10h 18m: El.—*15d 13h 55m–14h 30m*: Le Es Hu Hr (p.s.c.: Ta).—*15d 20h 49m*: Hu (s.s.c.: thirty-four).—16d 05h 12m–05h 24m: Tn?—*16d 10h 43m–12h 00m*: Le Es Wn? Wi Cm Ab Ma? Vl CF IK Gi Ks Hr (p.s.c.: six).—*17d 10h 09m–10h 50m*: Es Hr.—*17d 14h 59m–15h 30m*: Le Hu.—*18d 13h 05*m–*13h 20m*: Le Wn Hr.—22d 14h 22m: Eb?—24d 14h 50m: Hu.—26d 10h 25m: El (s.i.: three).

1957 May 05d 09h 53m–10h 08m: El.—07d 08h 59m–09h 37m: El.—13d 06h 45m–06h 55m: Hr.—*13d 11h 32m*: Le Es.—*14d 14h 18m*: Eb.—*14d 14h 35m–14h 50m.*—Wn Hb Eb Tl Hr.—*14d 18h 38m–* Hu (s.i.: Te).—*15d 18h 13m*: Hu.—*16d 12h 43m–13h 30m*: Le Es Wn CF Hb *Eb* Ci? Tl Gi Ks IK Hu Va Hr (s.c.: SF).—*18d 08h 10m–08h 30m*: Wn CF Hb Eb Tl Tn? Hr (s.c.: El).—25d 14h 55m: *Es.*—27d 12h 02m: Hu.

1957 June *01d 12h 55m*: Wn IK Gi Ks? Hr (p.s.c.: SF).—*02d 15h 11m–15h 19m*: Es Wn.—03d 03h 50m–04h 00m: Tn?—03d 07h 50m–09h 00m: Tn?—03d 09h 22m: Ks? (s.c.?: Tn).—*03d 10h 44m*: Hr.—03d 18h 36m: Vl.—*04d 09h 01m*: Hr (s.i.: four).—04d 10h 08m–10h 34m: El.—04d 10h 43m–11h 08m: El.—04d 14h 25m: Hu.—*05d 13h 27m–13h 56m*: Le Es Wn Gi (s.i.: Vl Fu IK; s.c.: Ma SF).—05d 15h 05m: Ks (s.s.c.: Ma; s.i.: Hu).—05d 15h 40m–15h 49m: Te.—16d 13h 15m–13h 25m: Te.—19d 02h 26m–03h 28m: Te.—*19d 16h 09m–17h 10m*: Le Es (p.s.c.: Vl Ta).—28d 04h 00m–07h 00m: Tn??

Ionospheric or solar disturbances without clear geomagnetic effect

1957 April: None

1957 May: None.

1957 June: None.

Minor disturbances reported by one station only are listed in the De Bilt quarterly circular, but omitted here.

Table 2—*Monthly mean values of Ci, Cp, and Ap*

Index	April 1957	May 1957	June 1957
Mean *Ci*	0.89	0.56	0.76
Mean *Cp*	0.93	0.55	0.78
Mean *Ap*	21	11	22

Errata: In Vol. 62, No. 2 (June 1957), p. 312, "International Data on Magnetic Disturbances," Preliminary Report on Sudden Commencements, the data given as 1956 July 24d 00h 12m: Ci Ta Bi Hr, 26d 00h 31m: Me Ag Eb, and *31d 10h 16m*: twenty-eight, occurred actually in August.

Committee on Rapid Variations and Earth Currents
A. Romañá, *Chairman*, Observatorio del Ebro, Tortosa, Spain

Committee on Characterization of Magnetic Disturbances

J. Bartels, *Chairman*
University
Göttingen, Germany

J. Veldkamp
Kon. Nederlandsch Meteorologisch Instituut
De Bilt, Holland

PROVISIONAL SUNSPOT-NUMBERS FOR JULY TO SEPTEMBER, 1957

(Dependent on observations at Zurich Observatory and its stations at Locarno and Arosa)

Day	July	Aug.	Sep.
1	187	150	257
2	204	148	230
3	208	178	201
4	269	166	166
5	216	147	184
6	257	162	160
7	194	167	137
8	147	141	175
9	167	121	250
10	135	88	265
11	110	95	255
12	96	118	264
13	96	120	260
14	140	135	263
15	169	170	265
16	200	198	283
17	210	189	258
18	218	197	295
19	225	185	317
20	244	170	294
21	250	144	334
22	290	147	302
23	285	114	268
24	272	104	239
25	232	138	234
26	206	164	220
27	173	182	227
28	158	222	249
29	142	244	249
30	171	255	229
31	152	282	
Means.....	194.3	162.6	244.3
No. days.....	31	31	30

Mean for quarter: 199.9 (92 days)

M WALDMEIER

SWISS FEDERAL OBSERVATORY
Zurich, Switzerland

FREDERICKSBURG THREE-HOUR-RANGE INDICES *K* FOR JULY TO SEPTEMBER, 1957

[$K9 = 500\gamma$; scale-values of variometers in γ/mm: $D = 2.7$; $H = 2.5$; $Z = 2.9$]

Gr. day	July 1957		August 1957		September 1957	
	Values *K*	Sum	Values *K*	Sum	Values *K*	Sum
1	6664 2476	41	2341 2233	20	6643 3123	28
2	2145 6554	32	4322 1233	20	3655 5576	42
3	5443 4123	26	2122 2444	21	7566 7765	49
4	1001 1135	12	4321 2212	17	3522 7986	42
5	5755 2234	33	2111 2233	15	8964 3355	43
6	3332 2234	22	3454 3234	28	4523 5433	29
7	2321 2232	17	4432 1122	19	3413 2233	21
8	3231 2223	18	2232 2133	18	2012 2213	13
9	3121 1222	14	3331 4233	22	3343 2221	20
10	2211 1121	11	5322 0113	17	1121 1232	13
11	2102 2001	8	2111 2222	13	1132 1221	13
12	3331 2123	18	3333 4343	26	1212 2423	17
13	2101 0221	9	5554 2232	28	6699 6544	49
14	1112 2223	14	1212 2232	15	3345 5334	30
15	3101 0012	8	4221 1133	17	3311 2232	17
16	1043 3223	18	2311 1122	13	4311 1221	15
17	3202 2132	15	0000 1211	5	2212 3332	18
18	2332 2223	19	3203 2123	16	4321 2333	21
19	4333 4433	27	4334 2111	19	1111 1112	9
20	2322 2123	17	1213 3333	19	2011 1223	12
21	2212 2123	15	4633 2321	24	3116 5655	32
22	2443 3244	26	1211 1122	11	4454 7755	41
23	3521 1113	17	1000 1111	5	6976 5554	47
24	3132 3223	19	0001 1112	6	5444 4232	28
25	3222 1222	16	0111 1233	12	4453 4222	26
26	2211 1011	9	2101 3233	15	1332 2111	14
27	1101 1244	14	3433 3243	25	0011 1112	7
28	3221 2222	16	2332 2233	20	2321 0132	14
29	2433 2222	20	3011 2266	21	4443 7776	42
30	1311 1122	12	6445 2332	29	5445 3343	31
31	2111 2223	14	2231 2455	24		

ROBERT L GEBHARDT
Observer-in-Charge

FREDERICKSBURG MAGNETIC OBSERVATORY
Corbin, Virginia, U. S. A.

PRINCIPAL MAGNETIC STORMS

(Advance knowledge of the character of the records at some observatories as regards disturbances)

Observatory (Observer-in-Charge)	Greenwich date	Storm-time GMT of begin.	Storm-time GMT of ending[1]	Sudden commencement Type[2]	Amplitudes[3] D	H	Z	C-figure, degree of activity[4]	Maximal activity on K-scale 0 to 9 Gr. day	Gr. 3-hr. period	K-index	Ranges D	H	Z
(1)	(2)	(3)	(4)	(5)	(6)	(7)	(8)	(9)	(10)	(11)	(12)	(13)	(14)	(15
	1957	*h m*	*d h*		′	γ	γ					′	γ	γ
College (C. J. Beers)	July 2	08 57	3 15	s.c.*	7	66	−9	ms	2	5,6,7	6	150	1390	74
									3	5	6			
	July 5	00 43	5 17	s.c.*	−34	409	−92	ms	5	4	7	230	1630	113
	Aug. 3	15 57	4 10	s.c.*	−42	134	−39	ms	3	6	6	90	730	41
	Aug. 5	15 00	7 18	.....	....	....	....	ms	6	3	7	170	1280	96
	Aug. 12	02 00	13 24	.....	....	....	....	ms	13	3	7	280	1930	134
	Aug. 29	11 35	30 21	s.c.*	−5	−23	17	ms	29	7,8	6	180	490	116
									30	4	6			
	Aug. 31	12 00	1 16	.....	....	....	....	ms	31	7	7	110	1630	50
	Sep. 2	03 00	4 06	.....	....	....	....	s	3	5	8	460	2750	165
	Sep. 4	13 00	7 05	.....	....	....	....	s	4	5,6	8	470	2460	164
	Sep. 12	24 00	15 07	.....	....	....	....	s	13	4	8	400	2700	224
	Sep. 21	08 00	25 16	.....	....	....	....	s	23	4	8	480	2850	170
	Sep. 29	00 16	1 06	s.c.*	−8	−14	472	s	29	6	9	750	3310	166
Sitka (J. L. Bottum)	July 2	08 58	3 15	s.c.	−5	+98	+20	s	2	5	9	176	1333	82
	July 5	00 43	6 02	s.c.*	−16	+123	+36	s	5	2	8	118	1208	64
	July 22	04 19	23 06	s.c.	−2	+10	+4	m	22	4	5	42	216	30
									23	2	5			
	Aug. 3	15 57	4 07	s.c.*	−16	+49	+19	m	3	6,7	5	55	186	13
	Aug. 5	23 ..	7 14	.....	....	....	....	ms	6	3,4	7	70	669	53
	Aug. 13	01 ..	13 21	.....	....	....	....	s	13	3,4	8	177	1260	86
	Aug. 20	13 ..	21 18	.....	....	....	....	ms	21	2	6	40	373	37
	Aug. 29	19 21	30 12	s.c.	+2	+60	0	ms	29	7,8	6	79	435	33
									30	1,4	6			
	Aug. 31	12 ..	1 15	.....	....	....	....	ms	31	7	6	59	493	34
									1	3	6			
	Sep. 2	03 15	4 06	s.c.	−2	+35	+8	s	3	5,6	9	241	1683	100
	Sep. 4	13 00	7 05	s.c.*	−22	+140	+53	s	4	5,6,7	9	302	2644	144
	Sep. 13	00 47	15 06	s.c.*	−34	+202	+41	s	13	2,3,4	9	277	3766	10
	Sep. 21	08 40	24 21	s.c.	−3	+9	0	s	21	4	9	330	2606	15
									22	5,6	9			
									23	2,4,5	9			
	Sep. 25	03 ..	25 15	.....	....	....	....	ms	25	4,5	6	44	301	3
	Sep. 29	00 16	1 05	s.c.*	−9	+98	+23	s	29	5,6	9	419	2907	13
Witteveen (D.van Sabben)	July 1	16 00	1 22	.....	....	....	....	ms	1	7	7	15	260	
	July 2	08 57	3 15	s.c.*	+5	+24	−1	ms	2	5	7	30	255	1
	July 5	00 42	5 15	s.c.	−5	+30	0	ms	5	2	6	30	185	
	July 22	04 19	23 06	s.c.	+2	+22	0	ms	22	7	6	30	180	
	Aug. 3	15 57	4 02	s.c.*	−10	+162	−5	ms	3	6	6	35	225	
									4	1	6			
	Aug. 6	05 08	6 24	s.c.*	−4	−18	0	m	6	3,5,7,8	5	25	160	
	Aug. 29	19 22	30 19	s.c.*	+8	+114	−3	ms	29	7	7	30	290	
	Aug. 31	13 00	1 15	.....	....	....	....	ms	31	7	7	30	255	
	Sep. 2	03 15	3 24	s.c.*	−7	+30	0	s	3	6	9	85	600	3
	Sep. 4	12 59	5 23	s.c.*	−9	+96	−3	s	4	6	9	110	980	6
	Sep. 6	11 22	6 20	s.c.*	+2	+42	0	ms	6	6	6	25	145	
	Sep. 13	00 46	13 22	s.c.*	−15	+70	0	s	13	4	9	55	770	2
	Sep. 21	10 05	22 07	s.c.*	+4	+80	−5	ms	21	4,5,6,8	6	35	220	1
	Sep. 22	13 44	24 14	s.c.	−3	+32	−4	s	22	6	8	75	615	5
									23	1,2	8			
	Sep. 29	00 16	30 24	s.c.*	−5	+34	0	s	29	6	9	110	725	6

[1]Approximate time of ending of storm construed as the time of cessation of reasonably marked disturbance movements in traces; more specifically, when the *K*-index measure diminished to 2 or less for a reasonable period.

[2]s.c. = sudden commencement; s.c.* = small initial impulse followed by main impulse (the amplitude in this case is that of *main impulse only*, neglecting the initial brief pulse); ... = gradual commencement.

[3]Signs of amplitudes of *D* and *Z* taken algebraically; *D* reckoned positive if towards the east and *Z* reckoned positive if ve cally downwards.

[4]Storm described by three degrees of activity: *m* for moderate (when *K*-index as great as 5); *ms* for moderately severe (w *K* = 6 or 7); *s* for severe (when *K* = 8 or 9).

PRINCIPAL MAGNETIC STORMS—Continued

Observatory (Observer-in-Charge)	Greenwich date	Storm-time GMT of begin.	Storm-time GMT of ending[1]	Sudden commencement Type[2]	Amplitudes[3] D	H	Z	C-figure, degree of activity[4]	Maximal activity on K-scale 0 to 9 Gr. day	Gr. 3-hr. period	K-index	Ranges D	H	Z
(1)	(2)	(3)	(4)	(5)	(6)	(7)	(8)	(9)	(10)	(11)	(12)	(13)	(14)	(15)
	1957	*h m*	*d h*		′	γ	γ					′	γ	γ
Hericksburg (E.Gebhardt)	July 1	16 ..	1 22	.....	.....	.....	.....	ms	1	7	7	11	211	36
	July 2	08 57	3 15	s.c.*	−5	+46	−8	ms	2	5	6	33	200	174
	July 4	19 ..	5 14	.....	.....	.....	.....	ms	5	2	7	51	204	219
	Aug. 12	02 40	13 14	.....	.....	.....	.....	m	13	1,2,3	5	27	122	90
	Aug. 29	19 00	30 14	.....	.....	.....	.....	ms	29	7,8	6	28	215	116
									30	1	6			
	Sep. 2	03 15	4 06	s.c.	+1	+34	−6	ms	2	7	7	50	481	522
									3	1,5,6	7			
	Sep. 4	13 00	7 05	s.c.*	+7	+21	+7	s	4	6	9	181	884	854
									5	2	9			
	Sep. 13	00 46	15 06	s.c.	.....	.....	.....	s	13	3,4	9	104	1344	626
	Sep. 21	10 05	.. ..	s.c.*	+5	+69	−10	s	23	2	9	154	926	748
	Sep. 22	13 45	25 15	s.c.*	−14	−18	−7	...	..	...	...	...	...	...
	Sep. 29	00 16	1 05	s.c.	−1	+38	−5	ms	29	5,6,7	7	55	444	282
son (F. White)	July 1	17 46	1 24	.....	.....	.....	.....	ms	1	7	6	10	90	30
	July 2	8 57	3 15	s.c.	−2	+65	+3	ms	2	5	6	16	117	86
	July 5	00 43	5 15	s.c.	−2	+63	+4	ms	5	2	7	21	162	19
	(*Note:* Disturbance preceded s.c. Started at about $18^h\ 40^m$)													
	July 22	04 18	23 07	s.c.	−1	+29	+2	m	23	2	5	16	122	40
	Aug. 3	15 57	4 09	s.c.	−2	+30	+2	m	3	6	5	15	138	49
									4	1	5			
	Aug. 6	05 08	6 15	s.c.	−1	+32	+2	m	6	2,3,4	5	11	41	16
	Aug. 12	01 ..	13 06	.....	.....	.....	.....	m	12	3	5	15	111	44
	Aug. 13	06 19	13 13	s.c.	+1	+47	+2	ms	13	3	6	16	85	13
	Aug. 26	15 ..	27 24	.....	.....	.....	.....	m	27	2	5	19	106	49
	Aug. 29	19 21	30 15	s.c.*	−1	+50	+3	ms	30	1	7	22	168	62
	Aug. 31	14 ..	1 09	.....	.....	.....	.....	...	..	...	...	...	...	...
	Aug. 31	18 12		s.i.	+1	−33	−7	m	31	7,8	5	17	139	50
									1	1,2,3	5			
	Sep. 2	03 15	4 09	s.c.	+1	+32	+2	s	3	6	8	48	256	83
	Sep. 4	13 00	6 08	s.c.	+2	+27	+3	s	4	6	8	42	391	219
									5	2	8			
	Sep. 6	11 21	7 09	s.c.	+0	+17	+1	m	6	2,5,6	5	19	59	41
	Sep. 13	00 48	15 06	s.c.	−3	+88	+7	s	13	3,4	8	40	471	92
	Sep. 21	10 05	.. ..	s.c.	+1	+89	+5	ms	21	4	7	18	275	80
	Sep. 22	13 45	.. ..	s.c.	−14	+50	−3	s	23	2	8	40	262	104
	Sep. 23	02 36	25 15	s.i.	+9	+65	+5	...	..	...	...	...	...	...
	Sep. 29	00 17	1 09	s.c.	−1	+29	+2	ms	29	5,6	7	30	288	124
Juan Vazquez)	July 5	00 42	5 13	s.c.	−0	+29	−5	m	5	2,3	6	12	114	15
	Aug. 29	19 20	30 07	s.c.*	+0	+60	−10	m	29	8	6	6	174	35
									30	1	6			
	Sep. 2	03 15	4 06	s.c.	−0	+20	−5	ms	2	8	7	21	254	75
	Sep. 4	13 00	6 06	s.c.	+1	+19	−10	ms	4	6	7	19	320	114
	Sep. 13	00 44	15 05	s.c.	−0	+62	−15	ms	13	2,3,4	7	21	453	50
	Sep. 21	10 05	22 07	s.c.	+1	+31	−11	ms	21	4,6,8	6	22	243	47
	Sep. 22	13 44	23 21	s.c.*	−2	+23	−10	ms	23	2	7	13	177	71
	Sep. 29	00 17	1 05	s.c.	....	+19	−5	ms	29	5	7	16	329	57
olulu (L. Cleven)	July 5	00 45	5 13	s.c.	−	+	+	ms	5	2	7	3	180	35
	Aug. 29	19 21	30 20	s.c.	+	+	+	ms	30	1	6	4	120	40
	Sep. 2	03 15	4 06	s.c.	−	+	+	ms	2	8	6	11	180	55
									3	3,5	6			
	Sep. 4	13 00	7 05	s.c.	+	+	+	ms	4	6	7	13	340	75
									5	1,3	7			
	Sep. 13	00 47	14 14	s.c.	+	+	+	s	13	3	9	11	460	100
	Sep. 21	10 05	24 14	s.c.	+	+	+	ms	23	2	7	12	400	85
	Sep. 29	00 17	1 05	s.c.	−	+	+	ms	29	5,6,7	6	17	240	90
									30	1	6			

PRINCIPAL MAGNETIC STORMS—Continued

Observatory (Observer-in-Charge)	Greenwich date	Storm-time GMT of begin.	Storm-time GMT of ending[1]	Sudden commencement Type[2]	Amplitudes[3] D	H	Z	C-figure, degree of activity[4]	Maximal activity on K-scale 0 to 9 Gr. day	Gr. 3-hr. period	K-index	Ranges D	H	Z
(1)	(2)	(3)	(4)	(5)	(6)	(7)	(8)	(9)	(10)	(11)	(12)	(13)	(14)	(15
	1957	*h m*	*d h*		′	γ	γ					′	γ	γ
Apia	June 29	20 44	3 14	.....	....	....	....	ms	30	7,8	6	8	269	7
(A.A. Thomson)	July 4	21 ..	5 14	.....	....	....	....	ms	5	2	7	4	197	4
	Aug. 6	05 09	7 01	s.c.	−0	+8	−4	m	6	4	5	4	87	2
	Aug. 12	04 ..	13 13	.....	....	....	....	ms	13	2	6	4	186	2
	Aug. 25	04 40	28 09	.....	....	....	....	m	27	2	5	8	107	2
	Aug. 29	19 21	30 20	s.c.	−1	+24	−5	ms	30	1	6	8	153	3
	Sep. 2	03 13	4 07	s.c.	−0	+23	−11	ms	2	2	6	9	206	4
									3	3,5	6			
	Sep. 4	13 00	8 00	s.c.	+0	+17	−7	s	4	6	8	12	418	5
	Sep. 9	05 26	9 15	.....	....	....	....	m	9	4	5	1	44	1
	Sep. 13	00 47	14 15	s.c.*	+1	+50	−24	s	13	3	9	11	636	9
	Sep. 21	10 05	22 13	s.c.	+0	+45	−22	ms	21	4	7	5	185	4
	Sep. 22	13 44	25 15	s.c.	+0	+61	−24	ms	23	2	7	12	370	6
Hermanus	July 1	17 47	1 22	s.c.	+0	+3	+2	m	1	7	5	8	53	4
(A.M.van Wijk)	July 2	08 58	2 21	s.c.	+2	+14	+14	m	2	5,6	5	17	114	6
	July 3	01 45	3 15	s.c.	....	....	....	m	3	1	5	13	73	4
	July 4	22 59	5 13	s.c.	....	....	....	ms	5	2	6	27	95	7
	July 19	08 ..	20 00	.....	....	....	....	m	19	6	5	12	132	8
	July 22	04 19	23 06	s.c.	+2	+9	+11	m	22	4	5	16	104	7
	Aug. 3	15 58	4 02	s.c.*	+2	+27	+11	ms	3	6	6	15	98	9
	Aug. 6	05 09	7 01	s.c.	+4	+10	+16	m	6	2	5	25	98	9
	Aug. 12	04 14	14 00	.....	....	....	....	m	12	4	5	22	125	7
	Aug. 21	02 48	21 08	s.c.	....	....	....	m	21	2	5	14	22	5
	Aug. 29	19 21	30 12	s.c.	+2	+45	+35	ms	29	7,8	6	23	118	15
	(*Note:* S.c. heralded by slow movements at 19^h 09^m, Aug. 29)													
	Aug. 31	12 ..	1 15	.....	....	....	....	m	31	7	5	16	74	6
	(*Note:* Sharp impulses at 18^h 12^m, Aug. 31)													
	Sep. 2	3 15	4 10	s.c.	+3	+12	+15	ms	3	1	7	49	251	23
	Sep. 4	13 00	7 00	s.c.*	+4	+35	+29	s	4	6	8	68	353	39
	Sep. 13	00 47	14 17	s.c.	+6	+44	+40	ms	13	3,4	7	41	466	27
	Sep. 21	10 05	22 ..	s.c.*	+2	+68	+35	ms	21	4,6,7	6	28	315	23
	Sep. 22	13 45	24 14	s.c.	+4	+7	+10	ms	23	1,2	7	35	293	21
	(*Note:* Strong impulse at 02^h 37^m, Sep. 23)													
	Sep. 29	00 16	1 09	s.c.	+2	+9	+10	ms	29	5,6,7	7	45	320	30
	(*Note:* The s.c.'s of Aug. 6, Sep. 2, Sep. 13, and Sep. 29 showed small initial impulses in *D* only													
Amberley	July 2	08 57	3 15	s.c.	1	42	6	ms	2	5	6	29	137	6
(A. L. Cullington)	July 5	00 45	5 12	s.c.	2	49	8	ms	5	2	6	24	174	10
	Aug. 6	05 09	7 06	s.c.*	+2	+17	−5	m	6	3,4	5	19	106	5
	Aug. 12	01 ..	13 15	.....	....	....	....	ms	13	3	6	24	128	5
	Aug. 29	19 21	30 12	s.c.	+7	+38	−25	m	29	7,8	5	21	167	5
									30	1,2	5			
	Aug. 31	18 13	1 15	s.c.	+7	+37	−17	m	31	7	5	18	125	5
	Sep. 2	03 16	4 08	s.c.	+3	+69	−20	ms	3	3,4,5,6	6	57	299	24
	Sep. 4	13 00	7 06	s.c.	+4	+43	−15	s	4	6	9	34	580	67
	Sep. 13	00 46	14 18	s.c.	−9	+130	+24	s	13	3	9	64	760	43
	Sep. 21	10 06	22 13	s.c.*	+1	+95	−9	ms	21	7	6	26	260	12
	Sep. 22	13 43	24 17	s.c.	−4	+120	−7	ms	22	6	7	45	400	45
									23	1,2,3	7			
	Sep. 29	00 18	1 12	s.c.	−1	+45	−6	ms	29	6	7	36	380	21

PRINCIPAL MAGNETIC STORMS—Continued

bservatory (Observer-n-Charge)	Green-wich date	Storm-time GMT of begin.	Storm-time GMT of ending[1]	Sudden commencement Type[2]	Amplitudes[3] D	H	Z	C-figure, degree of activity[4]	Maximal activity on K-scale 0 to 9 Gr. day	Gr. 3-hr. period	K-index	Ranges D	H	Z
(1)	(2)	(3)	(4)	(5)	(6)	(7)	(8)	(9)	(10)	(11)	(12)	(13)	(14)	(15)
	1957	*h m*	*d h*		′	γ	γ					′	γ	γ
				Reports added in galley-proof:										
abethville/ avia (Alexandre)	Mar. 29	03 36	30 04	s.c.	−1	+43	+2	ms	29	3,4,5	...	14	275	40
	Apr.	Pas d'orage important												
	May	Pas d'orage important												
	June 30	05 28	1 05	s.c.	−1	+51	−3	s	30	4,5	...	13	346	46
		(*Note:* Heures approchées: marque-temps en panne)												
	July	Pas d'orage important												
	Aug. 29	19 20	30 12	s.c.*	+1	+64	−3	ms	29	7,8	...	11	176	38
	Sep. 2	03 14	3 24	s.c.	−2	+19	+1	s	3	5,6	...	18	331	49
	Sep. 4	13 00	5 24	s.c.	−1	+35	−2	s	4	6,7	...	28	513	56
	Sep. 13	00 46	14 12	s.c.	−1	+91	−2	s	13	3,4	...	20	520	59
	Sep. 21	10 05	22 02	s.c.	−3	+86	−5	s	21	4,5,6,7	...	13	449	52
	Sep. 22	13 44	23 24	s.c.	+1	+21	−2	ms	23	2,3	...	18	230	28
	Sep. 29	00 16	30 24	s.c.	+1	+15	−2	s	29	6,7	...	12	520	58
heroo (F. Tillett)	July 2	08 57	3 14	s.c.*	−1	+16	−5	ms	2	5	7	18	150	124
	July 4	20 00	5 12	...	...	...	...	ms	5	1,2	6	17	177	94
	Aug. 3	15 57	4 08	s.c.*	+2	+49	+13	m	3	6,7	5	14	98	77
									4	1	5			
	Aug. 6	05 08	6 24	s.c.*	−3	+6	−10	m	6	7	5	13	80	82
	Aug. 29	19 21	30 13	s.c.*	+5	+64	+34	ms	29	7	6	18	159	96
									30	1	6			
	Aug. 31	16 00	1 16	...	....	....	....	m	31	7,8	5	14	107	78
									1	1	5			
	Sep. 2	3 15	4 06	s.c.*	−3	+20	−15	ms	2	7	7	36	238	250+
									3	4,5	7			
	Sep. 4	13 00	6 20	s.c.*	+2	+23	+10	s	4	6	8	40	343	215+
	Sep. 13	00 46	14 17	s.c.*	−6	0	−25	s	13	2,4	8	51	438	270+
	Sep. 21	10 05	.. ..	s.c.*	−1	+70	0	ms	21	4	7	18	237	142
	Sep. 22	13 45	.. ..	s.c.*	−7	+60	−25	ms	22	5	7	23	158	136
	Sep. 22	20 00	24 21	s.c.	+9	+39	+50	ms	23	1,5	7	30	230	216
	Sep. 29	00 16	2 04	s.c.*	−3	+9	−13	ms	29	5,6	7	31	291	232
angi	June 30	05 27	1 10	s.c.*	+3	−54	−2	ms	30	7	7	52	290	143
3.	July 2	08 58	3 14	s.c.*	−4	+36	+1	m	2	5,6	6	31	190	65
veringham)	Sep. 2	03 15	4 08	s.c.*	+4	....	+5	ms	3	4,5,6	7	57	302	108
	Sep. 4	13 00	5 23	s.c.	+2	+54	+6	s	4	6	9	55	458	372
	Sep. 13	00 46	14 20	s.c.*	−10	+51	+5	s	13	2,3	8	65	560	533
	Sep. 21	10 06	22 13	s.c.*	−7	+92	+13	ms	21	4	7	21	280	102
	Sep. 22	13 44	.. ..	s.c.*	−8	+115	+21	ms	22	6	7	36	310	102
	Sep. 23	02 36	24 16	s.c.	−10	+70	+16	ms	23	1,2,3,4	7	56	360	276
	Sep. 29	00 17	.. ..	s.c.	−4	+23	+6	ms	29	6	7	36	382	159
		(*Note:* Storm still continuing on Sep. 30)												
	1956													
son McGregor)	Mar. 2	17 ..	4 17	.....	....	....	....	s	3	3,8	8	134	1432	946
	Mar. 21	00 15	23 08	.....	....	....	....	s	22	1,2	8	147	1104	1324
	Apr. 20	19 ..	22 12	.....	....	....	....	ms	22	1,2,3	7	106	816	1155
	Apr. 26	20 30	28 10	.....	....	....	....	s	27	2	8	202	1276	1254
		(*Note:* Record incomplete Apr. 27)												
	Apr. 28	19 ..	1 19	.....	....	....	....	s	29	2	8	204	1269	1397
									30	2	8			
	May 11	22 40	13 14	.....	....	....	....	ms	13	2	7	117	653	776
	May 13	22 55	17 15	.....	....	....	....	s	15	5	8	171	1439	1174
	May 20	06 37	21 09	s.c.*	+27	+197	−173	ms	20	8	7	81	863	838
	May 23	07 ..	25 11	.....	....	....	....	s	24	8	8	195	1642	1423
	June	None												
		(*Note:* Mawson concluded on next page)												

PRINCIPAL MAGNETIC STORMS—Concluded

Observatory (Observer-in-Charge)	Greenwich date	Storm-time GMT of begin.	Storm-time GMT of ending[1]	Sudden commencements Type[2]	Amplitudes[3] D	H	Z	C-figure, degree of activity[4]	Maximal activity on K-scale 0 to 9 Gr. day	Gr. 3-hr. period	K-index	Ranges D	H	Z
(1)	(2)	(3)	(4)	(5)	(6)	(7)	(8)	(9)	(10)	(11)	(12)	(13)	(14)	(1
	1957	h m	d h		′	γ	γ					′	γ	γ
Mawson —Continued (P. McGregor)	July 25	20 30	29 11	.....	....	....	....	ms	26	8	7	211	1070	10
									28	7,8	7			
									29	3	7			
	Aug. 22	19 ..	26 21	.....	....	....	....	s	24	1	8	199	1205	14
									25	8	8			
	Sep. 2	02 ..	3 20	.....	....	....	....	s	2	2,3	8	168	1191	15
	Sep. 20	03 45	22 20	.....	....	....	....	ms	20	2	7	126	762	7
									22	7	7			
	Oct. 2	04 45	4 05	.....	....	....	....	ms	2	8	6	98	583	8
									3	6	6			
	Oct. 20	03 30	22 05	.....	....	....	....	ms	20	2,3	7	130	988	7
	(*Note:* Beginning time uncertain; record incomplete to 03[h], Oct. 20)													
	Oct. 26	13 11	28 15	s.c.	+8	−44	−2	ms	26	8	6	123	579	7
									27	2,7	6			
									28	3	6			
	Nov. 9	14 30	13 ..	.....	....	....	....	s	10	8	8	290	1332	12
	(*Note:* Record incomplete Nov. 12 and 13)													
	Nov. 14	.. ..	18 16	.....	....	....	....	s	14	3	8	221	1492	13
	(*Note:* Record incomplete Nov. 14; beginning time unknown; ranges are approximate)													
	Nov. 20	06 ..	23 ..	.....	....	....	....	ms	23	2	7	169	677	9
	(*Note:* Record incomplete Nov. 23)													
	Dec. 10	03 30	11 04	.....	....	....	....	ms	10	2,4,5	6	120	978	8
	Dec. 24	18 ..	26 12	.....	....	....	....	ms	25	7	7	171	733	9
									26	2,3	7			
	Dec. 27	10 30	31 05	.....	....	....	....	ms	27	6	7	126	821	10
	1957													
	Jan. 2	09 09	3 05	s.c.*	+23	+158	−44	ms	2	7	7	138	866	5
	Jan. 8	01 ..	11 15	.....	....	....	....	ms	10	3,7,8	7	154	893	12
	Jan. 21	04 ..	25 08	.....	....	....	....	s	24	7	8	239	1417	10
	Jan. 29	13 13	31 03	s.c.	−2	−71	−17	ms	30	2	7	158	870	12

LETTERS TO EDITOR

DISCUSSION OF THE WHEELON PAPER,"RADIO FREQUENCY AND SCATTERING ANGLE DEPENDENCE OF IONOSPHERIC SCATTER PROPAGATION AT VHF

Being somewhat familiar with the fields of radio wave propagation and atmospheric turbulence, I am deeply concerned by the possible effects of some of the theoretical work which has been reported in the past two years. Consequently, I should like to submit the following brief criticism of Dr. A. D. Wheelon's paper, "Radio frequency and scattering angle dependence of ionospheric scatter propagation at VHF," published in Vol. 62, No. 1, of this JOURNAL.

In Section 4 of his recent paper,[1] Wheelon concludes that the spectrum of mean square fluctuations produced by turbulent mixing of an established gradient is proportional, in the inertial subrange, to k^{-3}. There is a sizable body of radio data[2,3,4,5] which, on the basis of scatter propagation theory, has been interpreted[6] as being in agreement with such a law; and Wheelon's analysis, together with the similar result previously published by Villars and Weisskopf,[7] has been taken by many investigators as theoretical confirmation of the experimental findings, thus tending to *close the book* on this aspect of the subject. This is most unfortunate, since Wheelon's work contains a contradiction which, when fully appreciated, places the whole of the k^{-3} theory in grave doubt. Moreover, experimental studies of the spectrum of refractive index fluctuations support a $k^{-5/3}$ law.[8]

As for the inconsistency in Wheelon's development, he assumes *a priori* that, in the inertial subrange, the spectrum is independent of the molecular diffusivity, k being taken to be much smaller than k_s , the viscosity cutoff. By dimensional arguments, he then arrives at his k^{-3} result. However, this implies the spectrum of molecular "dissipation," $2Dk^2B(k)$ in his notation, is proportional to k^{-1}. Thus, the spectral distribution of molecular effects has its maximum at a wave-number which is much smaller than the range of values he is considering. Therefore, molecular diffusion cannot be neglected in this range, in contradiction with his *a priori* assumption.

Wheelon claims for his treatment that it accounts for the fluctuation contribution to each wave-number interval as a result of the mixing of the mean gradient

[1]A. D. Wheelon, J. Geophys. Res., **62**, 93-112 (1957).
[2]L. G. Trolese, Proc. Inst. Radio Eng., **43**, 1300-1305 (1957).
[3]J. H. Chisholm, *et al.*, Proc. Inst. Radio Eng., **43**, 1317-1335 (1955).
[4]K. Bullington, *et al.*, Proc. Inst. Radio Eng., **43**, 1306-1316 (1955).
[5]J. H. Chisholm, *et al.*, paper read before General Session, URSI, Washington, D. C., May 23-25, 1957.
[6]K. A. Norton, *et al.*, Proc. Inst. Radio Eng., **43**, 1488-1526 (1955).
[7]F. Villars and V. F. Weisskopf, Proc. Inst. Radio Eng., **43**, 1232-1239 (1955).
[8]R. Bolgiano, Jr., paper read before Comm. II, URSI, Washington, D. C., May 23-25, 1957; to be published.

by all size eddies simultaneously, whereas he implies that both Silverman's[9] and Batchelor's[10] analyses are less satisfactory in this respect, in that they employ a k-independent external source of turbulent input. However, Bolgiano[11] has shown, by extending Batchelor's work to include the effect of the presence of an established gradient, that, even when in-mixing by a whole hierarchy of eddies is considered, one is still led to the $k^{-5/3}$ law in the inertial subrange. Hence, contrary to Wheelon, so-called "mixing-in-gradient" is not at variance with Batchelor's result; and the radio data *cannot* be explained on the grounds of turbulent mixing of mean gradients as Villars and Weisskopf and Wheelon have proposed.

Ralph Bolgiano, Jr.

Cornell University,
School of Electrical Engineering,
Ithaca, New York, August 26, 1957
(Received August 30, 1957)

[9]R. A. Silverman, J. Appl. Phys., **27**, 699-705 (1956).

[10]G. K. Batchelor, Cornell University, School of Electrical Engineering, Res. Rep. EE-262 (Sept. 15, 1955).

[11]R. Bolgiano, Jr., Cornell University, School of Electrical Engineering, Res. Rep. EE-334 (April 30, 1957).

OCCURRENCE OF SOFT RADIATION DURING THE MAGNETIC STORM OF 29 AUGUST 1957

On 29 August 1957, there occurred a quite intense geomagnetic storm as observed at Fort Churchill, Manitoba, Canada, and associated with it was a marked Forbush-type decrease in the cosmic-ray intensity. Earlier on this same day, a balloon carrying cosmic-ray instrumentation was launched from Fort Churchill and it reached ceiling altitude about five hours before onset of the storm. Several events of interest occurred in the cosmic-ray detectors at high altitude and in a variety of ground-level detectors, operated by the Defense Research Northern Laboratory. The temporal sequence of these events will first be given.

(1) The balloon reached ceiling altitude at 1420 UT at an atmospheric depth of 8.3 gm-cm^{-2}. From this time, the cosmic-ray intensity steadily increased until approximately 1730 UT. The increase observed between these hours was 3.7 per cent in the ion chamber (I.C.) and 4.5 $\pm$ 0.7 per cent in the single counter (S.C.). This change in intensity is believed to be part of the daily variation, although some of the effect being due to changing geographic position cannot with certainty be ruled out. However, several other flights having somewhat different trajectories show a quite similar behavior. The amplitudes of the variation which occurred on 29 August preceding the cosmic-ray decrease do not seem to be abnormally large, since a larger effect was observed on a quiet day.

(2) At 1909 $\pm$ 04 UT, the I.C. and S.C. began to increase their response quite markedly above the cosmic-ray level observed previous to this time. The increase became quite rapid and reached a peak amplitude of 19 per cent above the normal cosmic-ray level in the I.C. and 24 $\pm$ 3 per cent in the S.C. at 1925 UT. After this time, the radiation quickly fell away, the full width of this peak at half height being about five minutes. At 1908 UT, a magnetic storm was observed[1] to begin at Fredericksburg, Virginia, but little or no magnetic disturbance was present at Fort Churchill at this time.

(3) At about 1930 UT, the vertical component of the earth's magnetic field at Fort Churchill began rapidly decreasing, while the I.C. and S.C. in the balloon-borne equipment showed a response above the cosmic-ray level that followed the field changes closely for several minutes. The vertically directed threefold counter telescope (C.T.) counted at the cosmic-ray rate during this time. The magnetic field changes were at least as large as four or five hundred gammas, indicating a quite intense geomagnetic storm.

(4) At 2045 UT, an intense burst of 30-Mc radio noise was observed at the Fort Churchill Defense Research Northern Laboratory.

(5) At 2050 $\pm$ 05 UT, the C.T. at high altitude abruptly decreased its counting rate, indicating a cosmic-ray decrease. The chance that the decrease occurred outside the time interval stated above is one in 19,000.

(6) Beginning at 2356 UT, the I.C. pulse rate increased by 18 per cent within a period of 90 seconds, then remained nearly constant until 0135 UT on 30 August, when the sun set on the balloon and it began descending rapidly. This sudden increase was accompanied by a large and rapid decrease in the vertical component

[1]U.S. Coast and Geodetic Survey, Washington, D.C.

of the earth's magnetic field as measured by the Defense Research Northern Laboratory. The events were simultaneous to within the accuracy that the magnetic records can be read, which is about two minutes.

(7) From about 0300 UT on 30 August, visual observations[2] of aurora could be made. An inactive surface of intensity 1 was recorded, indicating that no unusual auroral activity was present. On the next night, a very active and bright display of rayed bands was present.

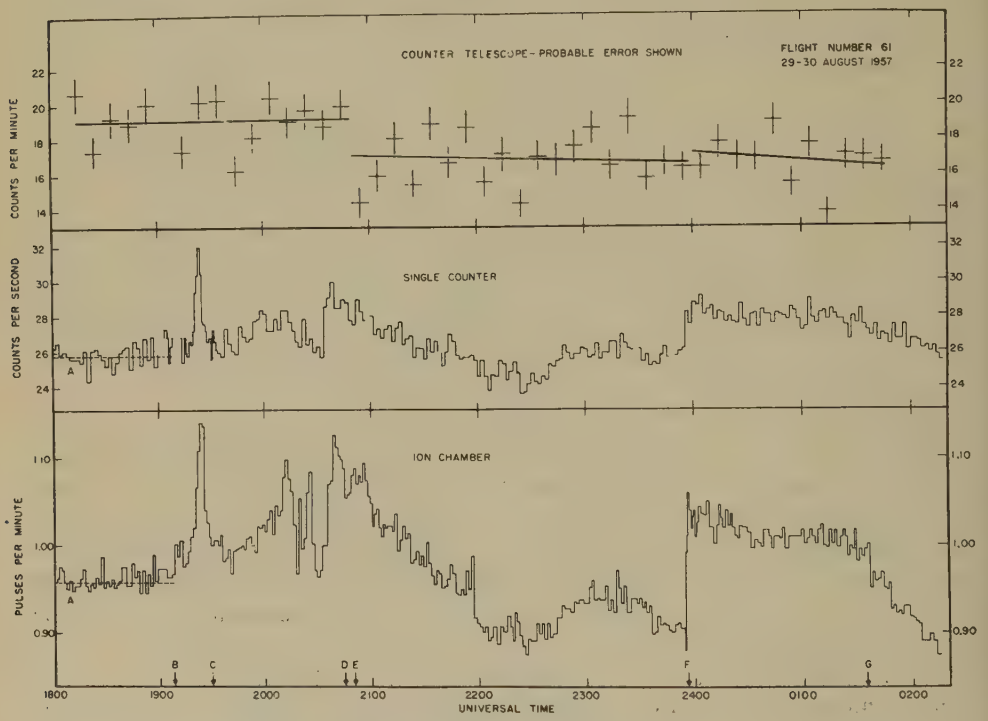

FIG. 1—Cosmic-ray and soft radiation intensities during the magnetic storm of 29 August 1957:

A. Steady pre-storm cosmic-ray level

B. Soft radiation begins to appear and magnetic storm begins outside of auroral zone

C. Magnetic storm begins at Churchill

D. Intense burst of 30-Mc radio noise received at Churchill

E. Cosmic-ray decrease begins

F. Very sharp increase of soft radiation and sudden decrease in vertical component of earth's magnetic field

G. Sun sets on balloon and it begins sinking rapidly

Considerable information about the nature of the excess radiation appearing at high altitude during the magnetic storm can be deduced from the characteristics of the three cosmic-ray detectors. The first point is that the wall thickness of the ion chamber is greater than the stopping power of the counter telescope, these being 0.5 and 0.2 gm-cm^{-2}, respectively. Secondly, no effect except that due to

[2]H. Lutz, Defense Research Northern Laboratory, private communication.

cosmic rays is observed in the vertical counter telescope, while in both the omnidirectional detectors appreciable effects occur. Therefore, the possibility that the enhanced counting rates are due to charged particles entering near the zenith can be ruled out. The observations could be accounted for by postulating a beam of high-energy charged particles arriving outside the solid angle of the telescope. However, it is believed that no evidence exists which would support this assumption. The observations can also be explained if the extra radiation incident on the detectors is taken to be X-rays of energy less than 700 kev, since then the recoil electrons produced at the Compton edge would not have sufficient energy to penetrate the counter telescope. There is precedence for such a view in the rocket experiments of the Iowa group[3] carried out on the soft radiation in the northern auroral zone. Further support is given to this hypothesis by carrying out simulation experiments with beams of γ-rays from radioactive sources. These show that the relative response of the I.C. and S.C. during the flight can be reproduced by γ-rays of approximately 100 kev energy. There is no conclusive evidence at present that the extra radiation present at balloon altitude during the magnetic storm and that originally observed by Winckler[4] during an auroral display should be identified as soft radiation, as defined by the Iowa rocket experiments.[3] However, it is convenient to use as a general term and it will be tentatively adopted here.

Using the observed counting rate produced in the single counter by the soft radiation and reasonable values for its efficiency and effective solid angle, one obtains a figure for the X-ray flux of roughly 20 photons cm^{-2}-$sterad^{-1}$-sec^{-1} from the vertical direction. Assuming these 100-kev X-rays are produced by *bremsstrahlung* from 300 kev electrons, then their production must occur high in the atmosphere and an absorption correction needs to be made. This gives an initial X-ray flux of 75 photons cm^{-2}-$sterad^{-1}$-sec^{-1}. Using some figures given by Kasper,[5] the original electron intensity must have been 3×10^5 particles cm^{-2}-$sterad^{-1}$-sec^{-1}, giving an energy flux of about 0.1 erg in the same units. If lower energy electrons are chosen, the energy flux incident on the atmosphere goes up rapidly, due to the strong dependence of the *bremsstrahlung* efficiency on energy. Since lower energy radiation is quite effectively shielded by the 9 gm-cm^{-2} of atmosphere remaining above the balloon, the total energy involved in the soft radiation may well be several factors larger than the estimate given above.

There are two features of the soft radiation data which strongly suggest that its acceleration, at least into the kilovolt region, takes place locally, that is, the electrons presumed to give rise to the X-rays are accelerated within a few earth radii of the earth's surface rather than on the sun. These are:

(1) The short time required for the radiation to markedly change its intensity. For example, at 2356 UT, the X-ray intensity increases several fold within an interval of 30 seconds.

(2) The simultaneous changes in the soft radiation intensity and the large storm-type decreases in the earth's magnetic field.

If the electron hypothesis for the production of the observed X-rays is pursued,

[3] J. A. Van Allen, Proc. Nation. Acad. Sci., **43**, 57 (1957).

[4] J. R. Winckler, to be published.

[5] J. E. Kasper, unpublished.

then in order to originate on the sun the electrons must be very nearly monoenergetic in order to account for the short rise times involved. If the X-rays themselves originate on the sun, the objections imposed by the rise times vanish, but then the second point just raised becomes very difficult to understand.

Kinsey A. Anderson

State University of Iowa,
Iowa City, Iowa, November 23, 1957
(Received November 25, 1957)

COMMENTS ON THE VILLARD-STEIN-YEH PAPER, "STUDIES OF TRANSEQUATORIAL IONOSPHERIC PROPAGATION BY THE SCATTER-SOUNDING METHOD"

In reading the above article,[1] I find that the authors verified, by means of a good experiment, the existence of propagation paths over the geomagnetic equator which traverse much longer distances than the nominal 4,000-km one-hop limiting distance without touching the ground and behave systematically. The general idea that the evening echoes might follow trajectories of the type drawn in Figure 11 can be inferred from the virtual-height plots of Figure 9. Apparently, the authors have been able to obtain close quantitative agreement in at least one instance by a method of determining refractive-index values for the ionosphere and tracing ray paths through the medium. If this is a rigorous treatment including magnetic field and collisions, it would be desirable for the details to be available so that others could apply it in similar cases.

I know of two instances where very-long-range echoes of the evening type have been observed in the past upon repeated occasions, although in neither case was a systematic pattern of behavior described in a paper.

Probably the first long-range echoes of this type to be noted by a United States experimenter were observed in 1953 by W. L. Hartsfield[2] (ref. 2, Fig. 3) on several evenings, using a 13.7-Mc transmitter beamed to the southeast of Washington, D.C. Mr. Hartsfield and I called these echoes "two-hop without one-hop" and offered two explanations of the phenomenon. The first was that reflection of the assumed first hop was from the upper side of a smooth E layer. One of the features of Figure 3, which did not reproduce in printing, is described in the middle of page 56. At half the range to the long distance echo at 00:00 were a group of dots of the meteor-trail type. In retrospect, this suggests a wave going through a portion of the E region near the middle of its trajectory, which would be possible on a trajectory such as shown by Villard, *et al.*, in Figure 11. The other explanation was that the first reflection point was on an unusually calm sea. Mr. Hartsfield suggested a program of comparing these echoes with meteorological data for the Caribbean area.

Another instance of observations at about the same time is reported by E. D. R. Shearman.[3] I believe this is the report which the authors perhaps intended as their reference [7] on the matter of the *normal* one-hop echo. (Their reference to a companion paper by the same author, in the same issue of the Proceedings of the Institute of Electrical Engineers, does not appear to be pertinent.) In the apparently correct reference, Shearman notes echoes at distances of 4,000 to 6,000 km while observing from Slough in the direction of Malaya. He also states that "it is possible

[1] O. G. Villard, Jr., S. Stein, and K. C. Yeh, J. Geophys. Res., **62**, 399 (1957).

[2] W. L. Hartsfield, Observations of distant meteor-trail echoes followed by ground scatter, J. Geophys. Res., **60**, 53 (1955).

[3] E. D. R. Shearman, A study of ionospheric propagation by means of ground backscatter, Proc. Inst. Elec. Eng., **103**, Pt. B, 203 (1956).

that this very long trajectory, apparently without ground-reflection point, was made possible by two successive reflections from the layer, appropriate tilts being present at the reflection points."

R. Silberstein

National Bureau of Standards,
Boulder, Colorado, November 22, 1957
(Received November 25, 1957)

NOTES

(33) *Russian satellite launched*—On October 5, 1957, the Soviet Union announced that it had launched the earth's first man-made satellite some hundreds of miles out in space, encircling the earth approximately every 96 minutes at a speed of around 18,000 miles per hour. Radio transmissions from the Soviet device were broadcast on 20 and 40 Mc. The satellite was launched in a north-to-south orbit. The Soviet Union also disclosed that it would send additional experimental spheres into the upper regions of the earth's atmosphere in the near future. This latest achievement in the present technical revolution is of outstanding scientific interest and commands our respect.

(34) *World IGY data centers*—The Russian data centers for the International Geophysical Year are being set up in two cities, Moscow and Novosibirsk. The sub-center of Moscow will house all information gathered during the 18-month IGY in the fields of aurora and airglow, ionospheric physics, solar activity, and cosmic rays. The sub-center at Novosibirsk will handle the fields of meteorology, geomagnetism, longitude and latitude, glaciology, oceanography, seismology, and gravity. All information at any center will be exchanged with the other two centers. A second world center is operated by several nations in Western Europe and the Pacific. It consists of the following sub-centers: Geomagnetism, Denmark and Japan; aurora, Sweden and Great Britain; airglow, France and Japan; ionosphere, Great Britain and Japan; solar activity, Switzerland, Italy, Great Britain, France, German Federal Republic, and Australia; cosmic rays, Sweden and Japan; glaciology, Great Britain; meteorology, World Meteorological Organization; and seismology, International Central Seismological Bureau, Strasburg. The sub-centers established in the United States were previously reported in this JOURNAL (Vol. 62, No. 3, p. 497, 1957).

(35) *New IGY Bulletin*—The first "IGY Bulletin" (No. 1, July 1957), issued by the National Academy of Sciences by its U. S. National Committee for the International Geophysical Year, appeared in August 1957. The purpose of this monthly Bulletin is to present current information on the IGY program of interest to scientists and particularly to geophysicists.

(36) *Publication of a discussion by the Royal Astronomical Society on the solar burst of February 23, 1956*—A résumé of the discussion held by the Royal Astronomical Society, February 22, 1957, is published in "The Observatory," Vol. 77, No. 898, pages 88-98. The first part deals with ionospheric changes associated with the solar cosmic-ray burst, while the second part with solar-cycle variation of the ionizing radiations.

(37) *Publication of papers delivered at Conference on Rock Magnetism*—A symposium of the papers presented at the International Conference on Rock Magnetism, in the Department of Physics at Imperial College, London, during November 1956, has been published in "Advances in Physics" (quarterly supplement of the Philosophical Magazine), Vol. 6, Nos. 22 and 23, 1957. The conference was held under the auspices of the International Union of Pure and Applied Physics, and under the chairmanship of Prof. P. M. S. Blackett.

(38) *Polish magnetic observatory rebuilt*—The magnetic observatory on the Hel Peninsula, which was destroyed near the end of the last war, has been rebuilt by the Institute of Geophysics of the Polish Academy of Sciences and continuous operation began on July 1, 1956. The Hel observatory is equipped with a set of three la Cour variometers with quick-run recording.

(39) *New officers, Society of Exploration Geophysicists*—The Society of Exploration Geophysicists have elected the following 1957-1958 officers to serve beginning November 11, 1957: president, O. C. Clifford, Jr., Dallas, Texas, chief geophysicist of the Atlantic Refining Company; vice-president, Ben F. Rummerfield, Tulsa, Oklahoma, executive vice-president of the Century Geophysical Corporation; secretary-treasurer, Howard E. Itten, Fort Worth, Texas, president of Empire, Geophysical, Inc. Dr. L. Y. Faust, Tulsa, Oklahoma, of Amerada Petroleum Corporation, was elected editor. The 27th annual convention of the Society was held at Dallas, Texas, November 10-14, 1957. It included discussion of the International Geophysical Year and international geophysics—pure science and practical applications.

(40) *Record balloon flight*—Launched from Crosby (near Brainerd), Minnesota, on August 19, 1957, under Air Force project "Man High," a huge 200-foot diameter plastic balloon, with Air Force Major David G. Simons suspended in a gondola below, reached a height of about 100,000 feet. After 32 hours aloft, landing was made safely at Ellendale, North Dakota. The next step in the Air Force project may be a four- or five-man balloon trip to similar altitudes in a large gondola.

(41) *New 1958 journal, "The Physics of Fluids"*—The American Institute of Physics is starting the publication (bimonthly) of a new journal, "The Physics of Fluids," in January 1958. It will be devoted to original contributions to the physics of fluids covering kinetic theory, statistical mechanics, structure and general physics of gases, liquids, and other fluids, as well as certain basic aspects of physics of fluids bordering geophysics, astrophysics, biophysics, and other fields of science. The Editor is Dr. F. N. Frenkiel (Applied Physics Laboratory, The Johns Hopkins University, Silver Spring, Maryland). Subscription information can be obtained from the American Institute of Physics, 335 East 45th Street, New York 17, New York.

(42) *Geomagnetic activities of the United States Coast and Geodetic Survey*—IGY World Data Center A for the disciplines of geomagnetism, seismology, and gravity has been established, and the first data from several countries have already been received.

Captain E. B. Roberts, Chief of Geophysics Division, Mr. J. H. Nelson, Chief of Geomagnetism Branch, and Mr. D. G. Knapp, Research Section of Geomagnetism Branch, attended the Toronto meeting of the International Union of Geodesy and Geophysics.

Mr. A. J. Bilik began a magnetic survey of repeat stations in the western United States.

(43) *Personalia*—Dr. *Joseph Kaplan*, Chairman of the U. S. National Committee for the International Geophysical Year 1957-58, has been elected to membership in the National Academy of Sciences.

Dr. *K. E. Bullen*, Chairman of the Australian National Committee for the International Geophysical Year 1957-58, spoke to 16 local sections of the Society of Exploration Geophysicists on a tour that covered most of the United States and part of Canada during September and October, 1957.

We regret to record the death on August 13, 1957, at Oslo, Norway, of Prof. *Carl F. M. Störmer*, Norwegian mathematician and geophysicist, at the age of 83. He was a world-famed specialist on polar aurora, having devoted the greater part of his life to the study while associated with Oslo University. In 1903, the witnessing of Prof. Kristian Birkeland's remarkable experiments on cathode rays in the field of a magnetic sphere, and his theory of the aurora as caused by cathode rays from the sun, led Prof. Störmer to become interested in this fascinating problem. He published in 1907 a paper on the motion of a single electric particle in the field of a magnetic dipole, and as a first approximation this gave promising explanations of a series of auroral phenomena (arc with ray structure). He realized the necessity of combining researches on the aurora with those of terrestrial magnetism, radio researches of the ionosphere, and studies of sunspots and the solar corona. He published more than 240 papers.

It is with regret also that we learned of the death on August 21, 1957, at Oslo Norway, of Dr. *Harald U. Sverdrup*, distinguished oceanographer and meteorologist, at the age of 68. He was born in Sogndal, Norway, on November 15, 1888. He participated importantly in the scientific work of a number of polar expeditions, such as the "Maud" Expedition, 1917-1925, and the "Nautilus" in 1931. From 1926 to 1930, he was a Research Associate of the Carnegie Institution of Washington. In Norway, he was associated with the Bergen Museum, and later with the Chr. Michelsen Institute. He was Director of the Scripps Institution of Oceanography, La Jolla, California, from 1936 to 1948, and following that Director of the Norsk Polarinstitutt, Oslo.

Rev. *Charles E. Deppermann*, Jesuit scientist of Manila Observatory, died in Manila on May 8, 1957, at the age of 68. He devoted most of his life to work in the Philippines, beginning service as Chief of the Seismological Division in the Philippine Weather Bureau in 1926. He became Director in 1946. His recent years were spent in rebuilding the observatory at Baguio, and he devoted an increasing amount of his efforts to seismology.

Dr. *Carl-Gustav Rossby*, of the University of Stockholm, Sweden, and Director of the Stockholm Meteorological Institute, died in Stockholm on August 19, 1957, at the age of 59. He was well known in the United States, having taught meteorology at the Massachusetts Institute of Technology from 1928 to 1941, and from 1939 to 1941 was Assistant Chief in Charge of Research of the U. S. Weather Bureau. He also taught meteorology at the University of Chicago. He was instrumental in the development of the Meteorological Institute in Sweden, in which he became a professor in 1947. Dr. Rossby made many notable contributions to meteorology.

(44) *Corrigendum*—Dr. Lewis E. Miller called attention to an error in his paper, " 'Molecular weight' of air at high altitudes," page 357, September 1957 issue of this JOURNAL. Eq. (25) should contain the factor 10^7, and in the next line a factor of 10^7 should follow the number 8.31439.

LIST OF RECENT PUBLICATIONS

BY W. E. SCOTT

Department of Terrestrial Magnetism,
Carnegie Institution of Washington,
Washington 15, D. C.

(Received October 10, 1957)

A—*Terrestrial Magnetism*

AKASOFU, S. On the geomagnetic micropulsations. Rep. Ionosphere Res. Japan, **10**, No. 4, 227-249 (1956).

AKIMOTO, S. Magnetic properties of ferromagnetic oxide minerals as a basis of rock-magnetism. Adv. Phys., **6**, No. 23, 288-298 (1957). [Presented at the International Conference on Rock Magnetism, London, November 1956. Some 21 additional papers are also listed herewith.]

ALEXANDER, N. S., AND C. A. ONWUMECHILLI. Variation of the horizontal force near the magnetic equator. Nature, **180**, 191-192 (July 27, 1957). [Letter to Editor.]

ASAMI, E. A palaeomagnetic consideration on the remanent magnetism of the basalt lavas at Kawajiri-misaki, Japan. Kyoto, J. Geomag. Geoelectr., **8**, No. 4, 147-155 (1956).

BABCOCK, H. W. Identification of solar "M" regions with unipolar magnetic regions. Astroph. J., **126**, No. 1, 224 (1957). [Note.]

BALSLEY, J. R., AND A. F. BUDDINGTON. Remanent magnetism of the Russell Belt of gneisses, northwest Adirondack Mountains, New York. Adv. Phys., **6**, No. 23, 317-322 (1957).

BATES, L. F. Ferromagnetic domains. Endeavour, **16**, No. 63, 151-160 (1957).

BELSHÉ, J. C. Palaeomagnetic investigations of carboniferous rocks in England and Wales. Adv. Phys., **6**, No. 22, 187-191 (1957).

BELSHÉ, J. C. Recent magnetic investigations at Cambridge University. Adv. Phys., **6**, No. 22, 192-193 (1957).

BLACKETT, P. M. S. Lectures on rock magnetism. [Being the second Weizmann Memorial lectures, December 1954.] Weizmann Science Press of Israel, Jerusalem, 131 pp. (1956).

BLACKMAN, M., G. HAIGH, AND N. D. LISGARTEN. A new method of observing magnetic transformations. Nature, **179**, 1288-1290 (June 22, 1957).

BLUNDELL, D. J. A paleomagnetic investigation of the Lundy Dyke swarm. Geol. Mag., **94**, No. 3, 187-193 (1957).

BRYNJÓLFSSON, A. Studies of remanent magnetism and viscous magnetism in the basalts of Iceland. Adv. Phys., **6**, No. 23, 247-254 (1957).

BUCHA, V. The results of magnetic measurements on points of 2nd order in the Czech lands for the epoch 1955.0. Geofysikálni abornik 1956, Československa Akademie Věd, No. 50, 572-576 + 3 charts (1957). [English summary.]

BUCHA, V. The normal geomagnetic field of the vertical component in the Czech lands for the epoch 1950.0. Geofysikálni abornik 1956, Československa Akademie Věd, No. 51, 597-600 (1957). [English summary.]

CHAPMAN, S. The lunar and solar daily variations of the horizontal geomagnetic vector at Greenwich, 1848-1913 (with an appendix on the lunar daily variation of magnetic declination at Pavlovsk and Sitka). Göttingen, Abh. Akad. Wiss., Math.-Phys. Kl., No. 3, 48 pp. + 16 Figs. (1957). [Miscellaneous reprint No. 80, High Altitude Observatory, Boulder, Colorado.]

CHRISTOFFEL, D. A. The effect of grain size on the magnetothermal properties of ferrites. Proc. Phys. Soc., B, **70**, No. 450, 623-625 (1957). [Research note.]

CLEGG, J. A., E. R. DEUTSCH, C. W. F. EVERITT, AND P. H. S. STUBBS. Some recent palaeomagnetic measurements made at Imperial College, London. Adv. Phys., **6**, No. 22, 219-231 (1957).

COLLINSON, D. W., K. M. CREER, E. IRVING, AND S. K. RUNCORN. Palaeomagnetic investigations in Great Britain. I. The measurement of the permanent magnetization of rocks. Phil. Trans. R. Soc., A, **250**, No. 974, 73-82 (1957).

Comites des Observatoires, Association Internationale de Geomagnetisme et d'Aeronomie "A.I.G.A." Description des observatoires geomagnetiques. Institut Royal Meteorologique de Belgique, 58 pp. (juillet 1957).

Creer, K. M. Palaeomagnetic investigations in Great Britain. IV. The natural remanent magnetization of certain stable rocks from Great Britain. Phil. Trans. R. Soc., A, **250**, No. 974, 111-129 (1957).

Creer, K. M. Palaeomagnetic investigations in Great Britain. V. The remanent magnetization of unstable Keuper Marls. Phil. Trans. R. Soc., A, **250**, No. 974, 130-143 (1957).

Creer, K. M., E. Irving, and S. K. Runcorn. Palaeomagnetic investigations in Great Britain. VI. Geophysical interpretation of palaeomagnetic directions from Great Britain. Phil. Trans. R. Soc., A, **250**, No. 974, 144-156 (1957).

Doell, R. R. Crystallization magnetization. Adv. Phys., **6**, No. 23, 327-332 (1957).

du Bois, P. M. Comparison of palaeomagnetic results for selected rocks of Great Britain and North America. Adv. Phys., **6**, No. 22, 177-186 (1957).

Einarsson, T. Magneto-geological mapping in Iceland with the use of a compass. Adv. Phys, **6**, No. 22, 232-239 (1957).

Gebhardt, R. L. Fredericksburg three-hour-range indices *K* for April to June, 1957. J. Geophys. Res., **62**, No. 3, 479 (1957).

Gorter, E. W. Chemistry and magnetic properties of some ferrimagnetic oxides like those occurring in nature. Adv. Phys., **6**, No. 23, 336-361 (1957).

Graham, J. W. The role of magnetostriction in rock magnetism. Adv. Phys., **6**, No. 23, 362-363 (1957).

Graham, J. W., A. F. Buddington, and J. R. Balsley. Stress-induced magnetizations of some rocks with analyzed magnetic minerals. J. Geophys. Res., **62**, No. 3, 465-474 (1957).

Graham, K. W. T., and A. L. Hales. Palaeomagnetic measurements on Karroo dolerites. Adv. Phys., **6**, No. 22, 149-161 (1957).

Griffiths, D. H., R. F. King, and A. E. Wright. Some field and laboratory studies of the depositional remanence of recent sediments. Adv. Phys., **6**, No. 23, 306-316 (1957).

Haigh, G. Observations on the magnetic transition in hematite at −15°C. Phil. Mag., **2**, No. 19, 877-890 (1957).

Hines, C. O. On the geomagnetic storm effect. J. Geophys. Res., **62**, No. 3, 491-492 (1957). [Letter to Editor.]

Hurbanovo Geomagnetic Observatory. Results of geomagnetic observations at the Hurbanovo Observatory, 1953-1954. Slovenska Akadémia Vied, 121 pp. (1956). [In years before 1948, known as Stará Ďala or O'Gyalla.]

Irving, E. Directions of magnetization in the carboniferous glacial varves of Australia. Nature, **180**, 280-281 (Aug. 10, 1957).

Irving, E. Palaeomagnetic investigations in Great Britain. III. The origin of the palaeomagnetism of the Torridonian sandstones of north-west Scotland. Phil. Trans. R. Soc., A, **250**, No. 974, 100-110 (1957).

Irving, E. Rock magnetism: a new approach to some palaeogeographic problems. Adv. Phys., **6**, No. 22, 194-218 (1957).

Irving, E., and R. Green. Palaeomagnetic evidence from the Cretaceous and Cainozoic. Nature, **179**, 1064-1065 (May 25, 1957).

Irving, E., and S. K. Runcorn. Palaeomagnetic investigations in Great Britain. II. Analysis of the palaeomagnetism of the Torridonian sandstone series of north-west Scotland. Phil. Trans. R. Soc., A, **250**, No. 974, 83-99 (1957).

Janáčková, A. Secular variation of declination on the territory of Bohemia and Moravia. Geofysikálni abornik 1956, Československa Akademie Věd, No. 52, 607 + *D* isoporic chart (1957). [English summary.]

Kato, Y., and T. Watanabe. A survey of observational knowledge of the geomagnetic pulsation. Sci. Rep. Tôhoku Univ., **8**, No. 3, 157-185 (1956).

Kraiński, W. Note on the method of calculating QHM magnetometer measurements. Acta Geophys. Polonica, **5**, No. 2, 116-117 (1957). [English summary.]

Morais, J. C. Observations of terrestrial magnetism made on the west coast of India by J. João de Castro in 1538-1539. Mem. Not. public. Mus. Lab. Min. Geol. Univ. Coimbra, No. 46, 1-8 (1956).

Nagata, T., and T. Rikitake. Geomagnetic secular variation during the period from 1950 to 1955. Kyoto, J. Geomag. Geoelectr., 9, No. 1, 42-50 (1957).

Nagata, T., S. Uyeda, and M. Ozima. Magnetic interaction between ferromagnetic minerals contained in rocks. Adv. Phys., 6, No. 23, 264-287 (1957).

Nagata, T., T. Yukutake, and S. Uyeda. On magnetic susceptibility of olivines. Kyoto, J. Geomag. Geoelectr., 9, No. 1, 51-56 (1957). [Contrib. Div. Geomag. Geoelectr., Geophys. Inst., Tokyo Univ., Ser. II, No. 66.]

Nagata, T., S. Akimoto, S. Uyeda, Y. Shimizu, M. Ozima, and K. Kobayashi. Palaeomagetic study on a quarternary volcanic region in Japan. Adv. Phys., 6, No. 23, 255-263 (1957).

Nairn, A. E. M. Palaeomagnetic collections from Britain and South Africa illustrating two problems of weathering. Adv. Phys., 6, No. 22, 162-168 (1957).

Néel, L. Action de champs magnétiques successifs de caractère aléatoire sur l'aimantation des substances ferromagnétiques. Paris, C.-R. Acad. sci., 244, No. 20, 2441-2446 (1957).

Niemegk, Adolph-Schmidt-Observatoriums für Erdmagnetismus. Jahrbuch 1954 mit wissenschaftlichen Mitteilungen. Geomagnetisches Institut, Potsdam, 129 pp. (1957). [Published under the auspices of the German Academy of Sciences, Berlin.]

Parry, J. H. The problem of reversed magnetizations and its study by magnetic methods. Adv. Phys., 6, No. 23, 299-305 (1957).

Praus, O. Das elektromagnetische Wechselfeld eines Horizontaldipols auf der Oberfläche einer geschichteten Erde. Geofysikální abornik 1956, Československa Akademie Věd, No. 57, 669-680 (1957).

Rikitake, T. Some comments on J. S. Chatterjee's "Induction in the core by magnetic storms and earth's magnetism." J. Geophys. Res., 62, No. 3, 493-494 (1957). [Letter to Editor.]

Rikitake, T., and S. Sato. The geomagnetic D_{st} field of the magnetic storm on June 18-19, 1936. Bull. Earthquake Res. Inst., 35, Pt. 1, 7-21 (1957).

Rimbert, F. Sur l'aimantation rémanente anhystérétique des ferrimagnétiques. Paris, C.-R. Acad. sci., 245, No. 4, 406-408 (1957).

Romaña, A., J. Bartels, and J. Veldkamp. International data on magnetic disturbances, first quarter, 1957. J. Geophys. Res., 62, No. 3, 475-478 (1957).

Runcorn, S. K. The sampling of rocks for palaeomagnetic comparisons between the continents. Adv. Phys., 6, No. 22, 169-176 (1957).

Shuleikin, V. V., and L. A. Korneva. Geomagnetic effects of oceanic and monsoon-path electric circulations. Doklady Akad. Nauk USSR, 76, 49-52 and 57-60 (1951); 80, 879-880 (1951); 107, 679-682 (1956). [Translation by E. R. Hope, Directorate of Scientific Information Service, Defence Research Board of Canada, Pub. No. T 247 R, June, 1957.]

Sigurgeirsson, Th. Direction of magnetization in Icelandic basalts. Adv. Phys., 6, No. 22, 240-246 (1957).

Singh, L. "Satellite-electron" theory of ferromagnetism, antiferromagnetism and related phenomena. Naturwiss., 44, Heft 15, 417-418 (1957).

Sinno, K. On the origin of the long-lived solar corpuscular streams which appeared last solar cycle. Rep. Ionosphere Res. Japan, 10, No. 4, 250-260 (1956).

Slichter, L. B. Remarks relative to Maxwell's formula for the magnetic susceptibility of disseminated material. Adv. Phys., 6, No. 23, 333-335 (1957).

Spighel, M. Réalisation d'un magnétomètre et d'un mesureur de gradient de champ magnétique. J. Phys. Radium (Physique Appliquée), 18, No. 7, 108A-111A (1957).

Sugiura, M., and S. Chapman. A study of the morphology of magnetic storms—moderate magnetic storms. University of Alaska, Geophysical Institute, Final Rep. No. AF 19(604)-1732, 54 pp. mim. (June 30, 1957). [Research sponsored by the Air Force Cambridge Research Center.]

Thellier, E. Résultats récents des recherches sur le champ magnétique et géologique. Conclusions fermes et déductions risquées. Astronomie, 71, 177-196 (Mai 1957).

University of Alaska. The solar and lunisolar daily variations of the geomagnetic field at Sitka, 1902-1952. Geophysical Institute, College, Alaska, Final Rep. No. AF 19(604)-503,

123 pp., mim. (April 1957). [Research sponsored by the Geophysics Research Directorate of the Air Force Cambridge Research Center.]

Whitham, K., and E. I. Loomer. Irregular magnetic activity in northern Canada with special reference to aeromagnetic survey problems. Geophysics, 22, No. 3, 646-659 (1957).

Wohlfarth, E. P. The anhysteretic magnetization of permanent magnetic alloys. Phil. Mag., 2, No. 18, 719-725 (1957).

Yokouchi, Y. A characteristic of the *Dst*-variation observed at Kakioka. Rep. Ionosphere Res. Japan, 10, No. 4, 261-263 (1956).

Zmuda, A. J. Extrapolation of geomagnetic field components along a radius from the center of the earth. Trans. Amer. Geophys. Union, 38, No. 3, 306-307 (1957).

B—*Terrestrial Electricity*

Burkhart, K. Die Fortschritte der erdmagnetischen Messtechnik. Phys. Bl., 13, Heft 6, 250-258 (1957).

Isikawa, H. Lightning mechanism and atmospherics radiation. Kyoto, J. Geomag. Geoelectr., 8, No. 4, 136-146 (1956).

Kirkman, J. R., and J. A. Chalmers. Point discharge from an isolated point. J. Atmos. Terr. Phys., 10, Nos. 5/6, 258-265 (1957).

Kitagawa, N. On the electric field-change due to the leader processes and some of their discharge mechanism. Pap. Met. Geophys., 7, No. 4, 400-414 (1957).

Kitagawa, N. On the mechanism of cloud flash and junction or final process in flash to ground. Pap. Met. Geophys., 7, No. 4, 415-424 (1957).

Large, M. I., and E. T. Pierce. The dependence of point-discharge currents on wind as examined by a new experimental approach. J. Atmos. Terr. Phys., 10, Nos. 5/6, 251-257 (1957).

Michnowski, St. Point discharges in the interchange of electric charge between the earth and the atmosphere. Acta Geophys. Polonica, 5, No. 2, 123-134 (1957). [English summary.]

Vidal, J. M. Contribucion al estudio de la conductibilidad eléctrica del aire y de los núcleos de condensación. Rev. Geofísica, Madrid, 15, No. 60, 441-447 (1956).

C—*Cosmic Rays*

Aly, H. H., and C. J. Waddington. The flux of primary cosmic ray α-particles over Sardinia. Nuovo Cimento, 5, No. 6, 1679-1684 (1957).

Barkow, A. G., B. Chamany, and R. E. McDaniel. Thin down and breakup of a large Z cosmic ray primary. Nuovo Cimento, 6, No. 1, 125-129 (1957).

Burbidge, G. R. Acceleration of cosmic-ray particles among extragalactic nebulae. Phys. Rev., 107, No. 1, 269-271 (1957).

Clark, G., J. Earl, W. Kraushaar, J. Linsley, B. Rossi, and F. Scherb. An experiment on air showers produced by high-energy cosmic rays. Nature, 180, 353-356 (Aug. 24, 1957), and 406-409 (Aug. 31, 1957).

Cranshaw, T. E., and W. Galbraith. Observations on extensive air showers—I. Apparatus; II. Time variations in the energy region of 10^{17} eV. Phil. Mag., 2, No. 18, 797-803 and 804-810 (1957).

Cranshaw, T. E., W. Galbraith, and N. A. Porter. Observations on extensive air showers. III. The distribution of charged particles. Phil. Mag., 2, No. 19, 891-899 (1957).

Fergusson, G. J., and G. J. McCallum. The cosmic ray flare of 23 February 1956 and its effect on the New Zealand radiocarbon dating equipment. N.Z. J. Sci. Tech., B, 38, No. 6, 577-587 (1957).

Korff, S. A. The origin and implications of the cosmic radiation. Amer. Scientists, 45, No. 4, 281-300 (1957).

McDonald, F. B. Note on primary cosmic ray proton and alpha flux near the geomagnetic equator. State University of Iowa, Dept. Physics, Pub. No. SUI-57-9 (rec'd July 30, 1957).

Neher, H. V. Cosmic rays near the north geomagnetic pole in the summers of 1955 and 1956. Phys. Rev., 107, No. 2, 588-592 (1957).

Nerurkar, N. W. An interpretation of the solar anisotropy of primary cosmic radiation. Proc. Indian Acad. Sci., A, 45, No. 5, 341-361 (1957).

O'Brien, B. J., and J. H. Noon. Measurement of the alpha particle flux at 41°N geomagnetic latitude using nuclear emulsions. Nuovo Cimento, 5, No. 6, 1463-1468 (1957).

Parker, E. N. Acceleration of cosmic rays in solar flares. Phys. Rev., 107, No. 3, 830-836 (1957).

Porter, N. A., T. E. Cranshaw, and W. Galbraith. Observations on extensive air showers. IV. The lateral distribution of penetrating particles. Phil. Mag., 2, No. 19, 900-909 (1957).

Shimooda, H. Solar and interplanetary magnetic field. I. The general magnetic field. Pub. Astr. Soc. Japan, 8, Nos. 3-4, 95-107 (1956).

Van Allen, J. A., and J. R. Winckler. Spectrum of low-rigidity cosmic rays during the solar flare of February 23, 1956. Phys. Rev., 106, No. 5, 1072-1073 (1957).

D—*Upper Air Research*

Allcock, G. McK. A study of the audio-frequency radio phenomenon known as "dawn chorus." Aust. J. Phys., 10, No. 2, 286-298 (1957).

Bailey, D. K. Disturbances in the lower ionosphere observed at VHF following the solar flare of 23 February 1956 with particular reference to auroral-zone absorption. J. Geophys. Res., 62, No. 3, 431-463 (1957).

Bauer, S. J. A possible troposphere-ionosphere relationship. J. Geophys. Res., 62, No. 3, 425-430 (1957).

Besprozvannaya, A. S., and V. A. Lovçova. State of the ionosphere in the high latitudes according to observational data for Tiksi Bay. Tr. Arctic Research Institute, Northern Sea Route Authority, Ministry of Marine, USSR, 46 pp., mim. (1956). [Translation by E. R. Hope, Directorate of Scientific Information Service, Defence Research Board of Canada, Pub. No. T 250 R, July 1957.]

Bickel, J. E. A method for obtaining LF oblique-incidence reflection coefficients and its application to 135.6-kc/s data in the Alaskan area. J. Geophys. Res., 62, No. 3, 373-381 (1957).

Blevis, B. C. Ionospheric studies by the lunar radar technique. Nature, 180, 138-139 (July 20, 1957). [Letter to Editor.]

Booker, H. G., and W. E. Gordon. The role of stratospheric scattering in radio communication. Proc. Inst. Radio Eng., 45, No. 9, 1223-1227 (1957).

Brittin, W. E. Equilibrium and transport in a fully ionized gas. University of Alaska, Geophysical Institute, College, Alaska, Geophys. Res. Rep. No. 3, 135 pp., mim. (April 1957). [Thesis in partial fulfilment of requirements for degree of Doctor of Philosophy.]

Chapman, S. The electrical conductivity of the ionosphere: A review. Nuovo Cimento, sup., 4, No. 4, 1385-1412 (1956). [International meeting on "Propagation of radio waves in the ionosphere," Venice, August 18-21, 1955.]

Chubb, T. A., H. Friedman, R. W. Kreplin, and J. E. Kupperian, Jr. Lyman alpha and X-ray emissions during a small solar flare. J. Geophys. Res., 62, No. 3, 389-398 (1957).

Davidson, M. Origin of meteor streams. Nature, 179, 1063 (May 25, 1957).

Dieminger, W., and H. G. Möller. Echo sounding experiments with variable frequency at oblique incidence. Nuovo Cimento, sup., 4, No. 4, 1532-1545 (1956). [International meeting on "Propagation of radio waves in the ionosphere," Venice, August 18-21, 1955.]

Dodson, H. W., and E. R. Hedeman. Résumé of visually and photographically observed solar activity at time of 200-Mc/s noise storms near 1954 solar minimum. Astroph. J., 125, No. 3, 827-830 (1957). [Note.]

Ehmert, A., und K. Revellio. Solare Ultrastrahlung und ionosphärische D-Schicht am 23. Februar 1956. Zs. Geophysik, 23, Heft 3, 113-134 (1957).

Ellis, G. R. Low-frequency radio emission from aurorae. J. Atmos. Terr. Phys., 10, Nos. 5/6, 302-306 (1957).

Gerson, N. C. The ionized aurora. Nuovo Cimento, sup., 4, No. 4, 1562-1571 (1956). [International meeting on "Propagation of radio waves in the ionosphere," Venice, August 18-21, 1955.]

Gregory, J. B. The relation of forward scattering of very high frequency radio waves to partial reflection of medium frequency waves at vertical incidence. J. Geophys. Res., 62, No. 3, 383-388 (1957).

Hakura, Y. On the disturbances of radio propagation along the north polar route. J. Radio Res. Lab. Japan, 4, No. 16, 101-110 (1957).

Haselgrove, J. Oblique ray paths in the ionosphere. Proc. Phys. Soc., B, 70, No. 451, 653-662 (1957).

Haurwitz, B., J. London, G. M. Sepúlveda, and M. Siebert. Solar activity and atmospheric tides. J. Geophys. Res., 62, No. 3, 489-491 (1957). [Letter to Editor.]

Hawkins, G. S., and D. F. Winter. Radar echoes from overdense meteor trails under conditions of severe diffusion. Proc. Inst. Radio Eng., 45, No. 9, 1290-1291 (1957). [Correspondence.]

Hines, C. O., and E. L. Vogan. Variations in the intrinsic strength of the 1956 Quadrantid shower. Can. J. Phys., 35, 703-711 (1957).

Houston, R. E., Jr. 75 kc/s change in phase height instrumentation and data. Pennsylvania State University, Ionosphere Res. Lab., Sci. Rep. No. 93, 68 pp., mim. (May 1, 1957).

Jackson, J. E. Effect of oblique propagation paths upon the NRL rocket studies of the ionosphere. Washington, D. C., Naval Research Laboratory, Upper Atmosphere Res. Rep. No. 29, 15 pp. (July 23, 1957).

Jastrow, R., and C. A. Pearse. Atmospheric drag on the satellite. J. Geophys. Res., 62, No. 3, 413-423 (1957).

Jones, I. L., B. Landmark, and C. S. G. K. Setty. Movements of ionospheric irregularities observed simultaneously by different methods. J. Atmos. Terr. Phys., 10, Nos. 5/6, 296-301 (1957).

Kivel, B., H. Mayer, and H. Bethe. Radiation from hot air. Part I. Theory of nitric oxide absorption. Annals of Physics, 2, No. 1, 57-80 (1957).

Landmark, B. The fading of radio waves reflected from the *E* layer. J. Atmos. Terr. Phys., 10, Nos. 5/6, 288-295 (1957).

Leighton, H. I. Field-strength variations recorded on a VHF ionospheric scatter circuit during the solar event of February 23, 1956. J. Geophys. Res., 62, No. 3, 483-484 (1957). [Letter to Editor.]

Lejay, P. La mesure des vents ionosphériques. Paris, C.-R. Acad. sci., 245, No. 3, 253-257 (1957).

Luscombe, G. W. Delayed signals in ionospheric forward-scatter communication. Nature, 180, 138 (July 20, 1957). [Letter to Editor.]

Manning, L. A., and V. R. Eshleman. Discussion of the Booker and Cohen paper, "A theory of long-duration meteor echoes based on atmospheric turbulence with experimental confirmation." J. Geophys. Res., 62, No. 3, 367-371 (1957).

Mariani, F. Some considerations on temperature effects in the upper atmosphere. Nuovo Cimento, sup. 4, No. 4, 1579-1585 (1956). [International meeting on "Propagation of radio waves in the ionosphere," Venice, August 18-21, 1955.]

Matsushita, S. Relations among radio absorbing regions, geomagneic bay-disturbances and slant-E_s in auroral latitudes. Kyoto, J. Geomag. Geoelectr., 8, No. 4, 156-160 (1956). [Letter to Editor.]

Miller, L. E. "Molecular weight" of air at high altitudes. J. Geophys. Res., 62, No. 3, 351-365 (1957).

Murcray, W. B. A possible auroral enhancement of infra-red radiation emitted by atmospheric ozone. Nature, 180, 139-140 (July 20, 1957). [Letter to Editor.]

Naismith, R. Some properties of the meteoric *E*-layer used in radio wave propagation. Nuovo Cimento, sup., 4, No. 4, 1413-1421 (1956). [International meeting on "Propagation of radio waves in the ionosphere," Venice, August 18-21, 1955.]

Nakamura, J. Latitude effect of night airglow. J. Geophys. Res., 62, No. 3, 487-488 (1957). [Letter to Editor.]

Nicolet, M. The aeronomic problem of helium. Ann. Géophys., 13, No. 1, 1-21 (1957).

Niwa, S., S. Watanabe, H. Saito, T. Sasaki, Y. Fujii, and M. Minowa. Results of experiments on VHF overland propagation beyond the radio horizon. J. Radio Res. Lab. Japan, 4, No. 16, 111-122 (1957).

Omholt, A. The red and near-infra-red auroral spectrum. J. Atmos. Terr. Phys., 10, Nos. 5/6, 320-331 (1957)

Parker, E. N. The gross dynamics of a hydromagnetic gas cloud. Astroph. J., 3, Sup. No. 27, 51-76 (1957).

Pope, J. H. Diurnal variation in the occurrence of 'dawn chorus.' Nature, 180, 433 (Aug. 31, 1957). [Letter to Editor.]

Radio Research Board, Department of Scientific and Industrial Research. Radio research 1956. Report of the Radio Research Board and the report of the Director of Radio Research. H. M. Stationery Office, London, iv + 47 (1957). [Some of the selected items of research reported on are as follows: IGY preparations; semiconductors and transistors; forecasting radio transmission conditions; the ionosphere and the propagation of HF and VHF waves; the troposphere and the propagation of VH and UHF waves; radio meteorology; and measurement of atmospheric noise.]

Rawer, K. The ionosphere. Frederick Ungar Publishing Co., New York, 202 pp. (1957). 24 cm. Bd. [Brought up to date by the author, this is an English translation by Ludwig Katz of the German original, "Die Ionosphäre," 1952. Desirable addition to the composite literature on the subject of the ionosphere. Very few books have treated the subject completely, and thus there is always need for such a presentation.]

Sato, T. Disturbances in the ionospheric *F*2 region associated with geomagnetic storms. II. Middle latitudes. Kyoto, J. Geomag. Geoelectr., 9, No. 1, 1-22 (1957).

Schmerling, E. R. The reduction of *h'-f* records to electron-density-height profiles. Pennsylvania State University, Ionosphere Res. Lab., Sci. Rep. No. 94, 51 pp., mim. (June 1, 1957).

Srirama Rao, M., and B. Ramachandra Rao. Analysis of fading records from four spaced receivers for ionospheric wind measurements. J. Atmos. Terr. Phys., 10, Nos. 5/6, 307-317 (1957).

Stewart, D. T. A spectrophotometric investigation of the airglow. J. Atmos. Terr. Phys., 10, No. 5/6, 318-319 (1957).

University of Alaska. Atmospheric ozone at College, Alaska. Geophysical Institute, College, Alaska, Final Rep. No. AF 19(604)-1817, 46 pp. mim. (April 1957). [Research sponsored by the Geophysics Research Directorate of the Air Force Cambridge Research Center.]

Villard, O. G., Jr., S. Stein, and K. C. Yeh. Studies of transequatorial ionospheric propagation by the scatter-sounding method. J. Geophys. Res., 62, No. 3, 399-412 (1957).

Warwick, J. W. Flare-connected prominences. Astroph. J., 125, No. 3, 811-816 (1957).

Warwick, J. W., and H. Zirin. Rocket observation of X-ray emission in a solar flare. Nature, 180, 500-501 (Sept. 7, 1957). [Reply by T. A. Chubb, H. Friedman, R. A. Kreplin, and J. E. Kupperian, Jr., follows, pp. 501-502.] [Letters to Editor.]

Watts, J. M. Complete night of vertical-incidence ionosphere soundings covering frequency range from 50 kc/s to 25 Mc/s. J. Geophys. Res., 62, No. 3, 484-485 (1957). [Letter to Editor.]

Weiss, A. A. Meteor activity in the southern hemisphere. Aust. J. Phys.,10, No. 2, 299-309 (1957).

Wheelon, A. D. Relation of radio measurements to the spectrum of tropospheric dielectric fluctuations. J. Appl. Phys., 28, No. 6, 684-693 (1957).

Wheelon, A. D. Refractive corrections to scatter propagation. J. Geophys. Res., 62, No. 3, 343-349 (1957).

Wilcox, J. B., and E. Maple. Audio-frequency fluctuations of the geomagnetic field. U. S. Naval Ordnance Laboratory, White Oak, Md., NAVORD Rep. No. 4009, 102 pp., mim. (July 9, 1957).

E—*Radio Astronomy*

Akabane, K. Some features of solar radio bursts at around 3000 Mc/s. Pub. Astr. Soc. Japan, 8, Nos. 3-4, 173-181 (1956).

Barrow, C. H., T. D. Carr, and A. G. Smith. Sources of radio noise on the planet Jupiter. Nature, 180, 381 (Aug. 24, 1957). [Letter to Editor.]

de Groot, T. Short duration transients in solar noise. Nature, 180, 382 (Aug. 24, 1957). [Letter to Editor.]

Denisse, J.-F., J. Lequeux, et E. Le Roux. Nouelles observations du rayonnement du Ciel sur la longueur d'onde 33 cm. Paris, C.-R. Acad. sci., 244, No. 25, 3030-3033 (1957).

Dieter, N. H. Observations of neutral hydrogen in M 33. Pub. Astr. Soc. Pacific, 69, No. 409, 356-357 (1957). [Note.]

ELSMORE, B. Radio observations of the lunar atmosphere. Phil. Mag., 2, No. 20, 1040-1046 (1957.)
FIROR, J. A radio telescope. QST, 41, No. 9, 32-36 (1957).
GIBSON, J. E. Thermal radiation of the Moon at 0.86-cm wavelength. Naval Research Laboratory, Washington, D C., NRL Rep. No. 4984 (formerly NRL Rep. No. 4124), 21 pp. (Aug. 29, 1957).
KAZÈS, I. Étude de la scintillation du Soleil observée sur la longueur d'onde de 3.2 cm. Paris, C.-R. Acad. sci., 245, No. 6, 636-639 (1957).
KAZÈS, I., ET J. L. STEINBERG. Étude de la scintillation du Soleil observée avec plusieurs antennes sur la longueur d'onde de 3.2 cm. Paris, C.-R. Acad. sci., 245, No. 7, 782-785 (1957).
LILLEY, A. E. The absorption of radio waves in space. Sci. Amer., 197, No. 1, 48-55 (1957).
MULLER, C. A. 21 cm absorption effects in the spectra of two strong radio sources. Astroph. J., 125, No. 3, 830-834 (1957). [Note.]
MULLER, C. A., AND G. WESTERHOUT. A catalogue of 21-cm line profiles. Bull. Astron. Inst. Netherlands, 13, No. 475, 151-195 (1957).
RYLE, M. The Mullard Radio Astronomy Observatory, Cambridge. Nature, 180, 110-112 (July 20, 1957).
SCHEUER, P. A. G. A statistical method for analysing observations of faint radio stars. Proc. Cambridge Phil. Soc., 53, Pt. 3, 764-773 (1957).
SCHMIDT, M. Spiral structure in the inner parts of the galactic system derived from the hydrogen emission at 21 cm wave length. Bull. Astron. Inst. Netherlands, 13, No. 475, 247-268 (1957).
TAKAKURA, T. Polarized bursts and noise storms of solar radio emission. I. Mechanism of emission. Pub. Astr. Soc. Japan, 8, Nos. 3-4, 182-206 (1956).
THOMSON, J. M. An attempt to detect linearly polarized radio emission from the galaxy. Nature, 180, 495-496 (Sept. 7, 1957). [Letter to Editor.]
VAN DE HULST, H. C. (Ed.). Radio astronomy (International Astronomical Union Symposium No. 4 held at the Jodrell Bank Experimental Station near Manchester, August 1955). University Press, Cambridge, 409 pp. (1957).
WESTERHOUT, G. Intensités relatives des quatre principales radiosources observées sur la longueur d'onde 22 cm; note sur la radiosource Sagittarius A. Paris, C.-R. Acad. sci., 245, No. 1, 35-38 (1957).

F—*Earth's Crust and Interior*

BARTA, G. About the periodic variation of the gravity field. Geofiz. Közl., Budapest, 5, No. 4, 7-13 (1956). [English abstract.]
BULLEN, K. E., AND T. N. BURKE-GAFFNEY. Evidence relating to the earth's inner core from hydrogen bomb explosions in 1954. Nature, 180, 49-50 (July 6, 1957). [Letter to Editor.]
CHANDRASEKHAR, S. The thermal instability of a rotating fluid sphere heated within. Phil. Mag., 2, No. 19, 845-858 (1957).
DOYLE, H. A. Seismic recordings of atomic explosions in Australia. Nature, 180, 132-134 (July 20, 1957).
EWING, J. I., C. B. OFFICER, H. R. JOHNSON, AND R. S. EDWARDS. Geophysical investigations in the eastern Caribbean: Trinidad shelf, Tobago through Barbados ridge, Atlantic Ocean. Bull. Geol. Soc. Amer., 68, No. 7, 897-912 (1957).
GARLAND, G. D. The figure of the earth's core and the non-dipole field. J. Geophys. Res., 62, No. 3, 486-487 (1957). [Letter to Editor.]
HOLSER, W. T., AND C. J. SCHNEER. Polymorphism in the earth's mantle. Trans. Amer. Geophys. Union, 38, No. 4, 569-577 (1957).
HONDA, H. The mechanism of the earthquakes. Sci. Rep. Tôhoku Univ., Ser. 5, Geophysics, 9, sup., 1-46 (July 1957).
MARSHALL, R. R. Isotopic composition of common leads and continuous differentiation of the crust of the earth from the mantle. Geochim. et Cosmochim., 12, No. 3, 225-237 (1957).
MASON, R. G. A small-scale field investigation of motion near the source. Geophys. Prospecting, 5, No. 2, 121-134 (1957).
OLIVER, J., AND M. EWING. Higher modes of continental Rayleigh waves. Bull. Seis. Soc. Amer., 47, No. 3, 187-204 (1957).

Tilton, G. R., G. L. Davis, G. W. Wetherill, and L. T. Aldrich. Isotopic ages of zircon from granites and pegmatites. Trans. Amer. Geophys. Union, **38**, No. 3, 360-371 (1957).

Tokarski, J. Clay minerals as possible palaeogeographic indices. Bull. Acad. Polon. Sci., Cl. 3, **5**, No. 4, 437-449 (1957).

Wetherill, G. W. Radioactivity of potassium and geologic time. Science, **126**, 545-549 (Sept. 20, 1957).

G—*Miscellaneous*

Bishop, R. O. Chromospheric emission and its dependence on latitude. Mon. Not. R. Astr. Soc., **116**, No. 6, 593-607 (1956).

Bray, R. J., R. E. Loughhead, V. R. Burgess, and M. K. McCabe. Observations of a new type of flare. Aust. J. Phys., **10**, No. 2, 319-323 (1957). [Short communication.]

Granger, C. W. J. A statistical model for sunspot activity. Astroph. J., **126**, No. 1, 152-158 (1957).

Heywood, H. Solar energy: A challenge to the future. Nature, **180**, 115-118 (July 20, 1957).

Menzel, D. H. Some advances in solar research. Sky and Telescope, **16**, No. 10, 464-467 and 476 (1957).

Nicolet, M. The International Geophysical Year. Nature, **180**, 7-10 (July 6, 1957). [Lists distribution of stations by country, by discipline, geographically, and geomagnetically.]

Pagel, B. E. J. A model atmosphere for the solar limb based on continuum observations. Mon. Not. R. Astr. Soc., **116**, No. 6, 608-623 (1957).

Waldmeier, M. Der Lange Sonnenzyklus. Zs. Astroph., **43**, 149-160 (1957). [Astron. Mitt., Eidgen. Sternwarte, Zürich, No. 209, 1957.]

Waldmeier, M. Ein neuer Effekt chromosphärischen Eruptionen. Naturwiss., **44**, Heft 16, 439 (1957).

Waldmeier, M. Provisional sunspot-numbers for April to June, 1957. J. Geophys. Res., **62**, No. 3, 479 (1957).

URSI MEETS IN BOULDER

More than 500 distinguished radio scientists from 26 countries were in Boulder, Colorado, from August 22 to September 5, to exchange technical information, coordinate their research programs on an international basis, and recommend future courses of scientific action.

They were there to attend the 12th General Assembly of the International Scientific Radio Union (URSI) at the invitation of the U.S.A. National Committee of URSI and the National Academy of Sciences.

Local hosts to the delegates and observers were the Boulder Laboratories of the National Bureau of Standards, the University of Colorado, the High Altitude Observatory, and the City of Boulder.

In charge of local arrangements were two Boulder Laboratories scientists: Kenneth A. Norton, chief of the radio propagation engineering division; and Alan H. Shapley, chief of the sun-earth relationships section. Serving as chairman of general arrangements was Dr. J. Howard Dellinger, former chief of the NBS Central Radio Propagation Laboratory and now a radio consultant in Washington, D.C.

Established in 1919 by a group of far-seeing scientists assembled in France, who then recognized the international scope of radio research, URSI met for the second time within 30 years in the United States. The second General Assembly was held in Washington, D.C., in 1927.

With its vital role in fostering world-wide collaboration, URSI can claim significant achievements, derived not only from general assembly discussions, but from the permanent URSI Commissions that conduct continuous studies in the major fields of research.

Radio Measurement Methods and Standards

At the meeting in Boulder, some interesting results were reported before the seven commissions. Five sessions were held in Commission I on Radio Measurement Methods and Standards that dealt with (*a*) frequency standards, particularly atomic frequency-standards, (*b*) standard frequency transmissions and time signals, (*c*) power and field-strength measurements, and (*d*) physical measurements based upon radio techniques. In connection with these topics, certain resolutions were adopted or reaffirmed. The international president and vice president of Commission I, Dr. B. F. Decaux, France, and Mr. W. D. George, of the NBS Boulder Laboratories, presided over the sessions, which generally began with a summary by an organizing international reporter.

Frequency and time standards were introduced by Dr. L. Essen, Great Britain. Quartz-crystal resonators continue to be used as working standards and improved performance has been obtained at very low temperatures. The greatest developments have been observed in atomic frequency standards, such as the ammonia MASER and the cesium beam standard. The latter is in regular use in the U.S.A. and the United Kingdom. Dr. Essen described the cesium beam standard in use for the last two years in the United Kingdom. Dr. J. M. Richardson, NBS Boulder

Laboratories, described results obtained with oxygen as a possible atomic frequency standard. Discussions were heard on the MASER, the Atomichron, and a proposed resolution concerning the frequency of a particular resonance in cesium.

Mr. George summarized developments in standard frequency transmission and time signals, and reported on some of the work done at the CCIR Assembly held in 1956 at Warsaw. There are 14 stations in the world broadcasting standard frequencies and time signals, and more are being planned in the frequency bands allotted for this purpose. In some areas, the problem of mutual interference becomes more serious, The nature of the interference was discussed and various proposals to relieve the situation were offered in an adopted recommendation. The use of VLF and ground-wave transmission is being considered to reduce the errors which are introduced during propagation at high frequencies during short-interval intercomparisons.

At the session on measurement of rf power and field strength, Drs. J. A. Saxton and H. E. M. Barlow, of United Kingdom, reported on numerous developments in microwave power measurements during the last three years, including torque vane wattmeters, film bolometers, differential air thermometers and calorimeters, and rf power meters employing the Hall effect. Mr. Glenn F. Engen, NBS Boulder Laboratories, gave a status report on the NBS microcalorimeter. Mr. Robert S. Kirby, NBS Boulder Laboratories, obtained adoption of a resolution to distinguish between the terms field intensity and field strength.

At other sessions, Prof. P. Grivet, France, summarized the work, which lead to a revised resolution on the velocity of electromagnetic waves. He also discussed other physical measurements, for example, magnetic fields, by high frequency techniques. Dr. Issac Koga, Japan, presented a paper on "Determination of the elastic and piezoelectric constants of quartz." Dr. Moody C. Thompson, NBS Boulder Laboratories, described a system for phase stabilization of klystrons. Mr. M. C. Selby, NBS Boulder Laboratories, delivered a paper on standardization of RF quantities, and obtained adoption of a resolution providing for tabulation of ranges and accuracies needed in the measurement of various electrical quantities.

Because of the wide interest in MASER, a joint session was held with Commission VII, Radio Electronics. A number of authoritative talks were given on MASER's.

The adopted resolutions will foster international cooperation in the improvement of radio measurement methods and standards. One resolution recommended international intercomparison of atomic frequency standards. It was felt that such a comparison would be beneficial now, in spite of the fact that a carefully defined atomic or molecular resonance is expected to be the same everywhere. The existing resolution calling for international comparison of microwave power standards was reaffirmed, and it was noted that with the submission by Japan of a calibrated bolometer mount that intercomparison is actually under way in the NBS Radio Standards Division.

Tropospheric Radio Propagation

The first few sessions of Commission II on Radio Tropospheric Propagation under the chairmanship of Dr. Smith-Rose, England, were devoted to a discussion

of within-the-horizon propagation over irregular terrain and special refraction, reflection, and obstacle gain effects in beyond-the-horizon propagation of VHF and UHF. A few meetings were devoted mainly to the discussion of turbulent scattering (forward-scatter), both theory and observation. A paper originating at the Swedish Research Institute of National Defence was of particular interest. It discussed mixed-path propagation from 20 to 80 Mc/s, and showed that, in general, a maximum height gain, on the order of 7 db above that expected over a smooth earth, is encountered just prior to reaching the top of a hill, going from land towards water; and that recovery of over-water field-strength amplitudes occurs 25 to 30 wavelengths distant from the shore-line towards fresh water. Dr. J. A. Saxton, of the Department of Scientific and Industrial Research, England, noted that within-the-horizon field strengths fall below the smooth earth field at higher and higher frequencies, on the average, and suggested this may be because antennas intervisible over a smooth earth are not intervisible over actual terrain.

Mr. W. S. Ament, of the Naval Research Laboratory, commented on the periodicity of water waves observable in near, diffraction, and duct fields over water, but not in scatter fields. Dr. Archie Straiton, of Texas University EERL, presented data showing the deterioration of the horizontal polarization reflection coefficient with increasing frequency over water, while Dr. Peter Beckmann, of Czechoslovakia, presented a theory depending upon random orientation of reflecting surfaces which agrees well with experimental results.

Major contributions to the technical sessions were in two fields: (1) Correlating radio and meteorological parameters, with the work of Anderson, Smyth, Trolese, and Bean in the U. S., Josephson and Eklund of Sweden, and Ikegami and Furutsu of Japan receiving the most attention; and (2) in the field of extra-diffraction propagation, where a number of lively discussions took place on competing theories. The structure of the atmosphere is still not sufficiently well understood to decide between the various theories on the basis of their underlying assumptions.

Ionospheric Radio Propagation

Because of the close relation between the work of the URSI and the IGY and the timeliness of the General Assembly, one complete day was devoted to discussion of the IGY program. The general morning session consisted of an address by Sir Edward Appleton, of the University of Edinburgh, Scotland, on the background and importance of the IGY. Reports on the status of the networks of observing stations that are being established within the various scientific disciplines were also given. In the afternoon, the commissions individually considered the IGY activities in their particular fields. Commission III on Ionospheric Radio Propagation, under the chairmanship of Dr. D. F. Martyn, Australia, heard reports on: The uniform interpretation and reduction of ionosphere vertical soundings; the reduction of vertical-sounding data to true-height profiles; World Days and Special World Interval program; measurement of ionosphere absorption; drift measurements; back-scatter studies; and recent ionosphere results from the Antarctic.

The first regular technical session of the Commission concerned phenomena of the lower ionosphere. Chairman A. H. Waynick, of Pennsylvania State Uni-

versity, summarized the many techniques that have become available in recent years for study of this interesting but complex region of the upper atmosphere. The physical processes of the lower ionosphere were discussed theoretically from the point of view of neutral particles by Dr. Marcel Nicolet, Belgium. Australian observations were given of reflections from many heights between 54 and 100 km of 1.75-Mc radio signals. These observations were supplemented by similar findings by German and U. S. investigators. Another important technique for obtaining information about the lower ionosphere involves the measurement of the absorption of high-frequency cosmic noise. A discussion of this work was led by Dr. C. G. Little, Geophysical Institute, College, Alaska.

Of the remaining technical sessions, perhaps the joint whistler meeting and the session on rocket investigation attracted the most attention. A highlight of the whistler discussion was the report by Dr. R. A. Helliwell, of Stanford University, that man-made radio signals had, for the first time, been successfully propagated via whistler paths from the northern to the southern hemispheres. This development is important for two reasons: (1) A new, and perhaps very reliable, means of long-distance communication is suggested; and (2) this type of propagation will almost certainly give very valuable information on the nature of the very high atmosphere—far above the ionosphere.

Dr. Herbert Friedman, of the Naval Research Laboratory, presented a comprehensive paper on recent rocket findings. His measurements, made from rockets at altitudes up to about 200 miles, show that there is enough energy in the X-ray spectrum (from 10Å to 1000Å) to produce the E region of the ionosphere and suggests that this X-radiation may be due to a 500,000°K corona. Dr. J. C. Seddon, also of Naval Research Laboratory, showed early results from the first rockets fired in the auroral zone (Ft. Churchill, Canada), which indicate that considerably greater electron densities exist in the lower ionosphere at these latitudes compared to White Sands, New Mexico. Dr. W. H. Pfister, of the Air Force Cambridge Research Center, presented rocket observations that tend to show that preferred levels for ionization exist in the E region at about 101, 106, and 112 km. Two other investigators indicated that their observations independently support the idea of preferred ionization heights and, in fact, agree quite well with Pfister's results on levels.

Radio Noise of Terrestrial Origin

In Commission IV on Terrestrial Radio Noise, under the chairmanship of J. A. Ratcliffe, England, it was agreed that valuable information regarding the nature of the ionosphere can be determined utilizing atmospherics as a source of signals, and by interpreting waveforms of the same sferic recorded at different ranges from the original lightning discharge. This type of analysis appears to be more fruitful than earlier work based on differences in waveform types.

Workers at the Boulder Laboratories described a method of calculating the reflection coefficient of the ionosphere using sferics waveforms recorded at ranges of 500 km or less.

Frederick Horner and C. Clarke, of the British Radio Research Station, have studied the use of waveform recording in the possible location of thunderstorms

from a single station. The complex nature of many of the echo-type waveforms which are used for estimating the distance of the source greatly increases the difficulty of applying the technique in a rapid routine operational manner. F. W. Chapman, at King's College, London, has continued his waveform and spectral work in the frequency range of 40 c/sec to 16 kc/sec, using magnetic tape recording. New results include the identification of two distinct types of slow component in some atmospherics. An analysis has been made on the polarity and other characteristics of these components in relation to the nature of the source and the propagation path. The laws of propagation of radio waves at frequencies down to 40 c/sec have been derived. Arrangements are being made to facilitate the simultaneous recording of waveforms at several stations in Europe and to identify subsequently the corresponding waveforms on the different records. This type of cooperative program has been advocated by the URSI for many years, and it has been planned for the IGY.

It has been observed that atmospheric clicks frequently precede the reception of whistlers. Of a very large number of atmospherics, only a very small number succeed in producing audible whistlers. These observations suggest the interesting possibility that the lightning discharges in atmospherics associated with whistlers possess some special characteristics. There was a discussion on the relation between the frequency spectra of atmospherics and the likelihood of a whistler. A suggestion was made that lightning flashes in a mountainous area differ from those occurring over flat land and that there also are differences between those occurring over land and over water. It seems possible that these differences may be associated with whistler-producing ability of the flashes. Mr. H. E. Dinger, of the Naval Research Laboratory, for instance, said he has never been able to record whistlers from atmospherics of local storms over land, but has recorded whistlers from atmospherics of local storms over water. Workers at the Boulder Laboratories have recorded waveforms of sferics which produce whistlers and found that they are characterized by a large amount of energy at frequencies near 5 kc. On one occasion, all of the lightning discharges which were producing whistlers occurred over water. On other occasions, lightning discharges occurring over land, as well as water, have been observed to produce whistlers. Dr. M. G. Morgan, of Dartmouth, and others have observed vertical lightning flashes over land that evidently produced whistlers of the long variety.

Also discussed was work being done in measuring radio noise from 15 kc to 20 Mc that originates largely in lightning flashes. General agreement has been reached on what characteristics of the noise should be measured, and considerable progress has been made in the last few years in the measurement and description of the amplitude characteristics of atmospheric noise. Useful relationships have been found between the amplitude characteristics and the interference caused by noise to many types of radio service, and during the IGY there will be widespread measurements of the noise amplitude at stations throughout the world. In addition to the 16-station network of the CRPL, noise recording stations will also be operated by a number of other countries, including Japan, Germany, the United Kingdom, and the U.S.S.R.

Recordings of the atmospheric noise obtained by these stations are expected

to provide information of great value in the solution of the more general problems of radio communication, as well as in the study of propagation.

Radio Astronomy

The quantity and quality of papers presented at Commission V on Radio Astronomy proved this field to be a dynamic and fast growing area of research in many countries. Dr. M. Laffineur, France, was chairman of the session.

At the session on techniques of reception, Dr. W. N. Christiansen, of Australia, described a new "Mills Cross" interferometer, consisting of 64 parabolas, each 19 feet in diameter, and arranged in two crossed arms, each 1,240 feet long. The instrument is being operated at 1,420 Mc/s, and its narrow "pencil beam" can be made to scan the solar disk television-wise and produce a complete picture of the radio sun at this operated frequency. Dr. A. Hewish, of the Cavendish Laboratory in England, spoke on a new technique of "getting something for nothing," namely, aperture synthesis. Using this technique, it is possible to make an electronic computer replace a large portion of the array of aerials usually required for the study of discrete radio sources.

The session on large aerials was marked by the great number and variety of instruments which are in use, in construction, or in planning stages. The most impressive of these is still the mammoth 250-foot-diameter paraboloid at Manchester, England. The completion of this instrument and results of the first measurements were described by Prof. A.C.B. Lovell, director of the Manchester Radio Astronomy group. This instrument is made of 800 tons of steel. It is driven by a total of 400 horsepower electric motors, with a drive accuracy of one minute of arc.

The sun continues to interest many radio astronomers and other groups also, as its influence on the earth becomes better and better understood. Here the radio astronomer copes with rapidly and widely varying radio emissions over great range of frequencies. But his efforts have been rewarded by the understanding of the sun's atmosphere which his results have provided. Dr. J. F. Denisse, France, gave a very interesting interpretation of the origin of long-duration solar radio-noise storms. He believes they originate in clouds of ionized gas shot out from the sun and supported high in its atmosphere by the sun's magnetic field. Theoretical physicist Prof. T. Gold, of Harvard, reported that this explanation fitted in well with his own theories.

Many surveys of discrete radio sources are in progress, with a notable difference in results between British and Australian workers that points up the need for better resolving power, that is, larger antennas.

A joint meeting with Commission VI again pointed out the utility of using extra-terrestrial radio sources to study the earth's ionosphere by observing the scintillation and refraction of radio stars.

The profound contributions made by radio astronomy to the study of our own and other galaxies was the subject of another session. Studies of the hydrogen-line emission at 1,420 Mc/s, with particular emphasis on the velocities of approach and recession indicated by the Doppler shift of the frequency, have enabled astronomers to verify the spiral structure of the galaxy.

Many reports of observations of the moon, planets, and comets filled another session. J. H. Trexler, of the Naval Research Laboratory, described moon-echo experiments with a 220-foot parabola, built into the ground and operating on a frequency of 10 to 300 Mc/s. He found that the echoes are reflected almost entirely from a relatively small area of the moon's surface facing the earth. This was confirmed by British work. A tape recording of conversation and cw signals reflected from the moon with remarkable fidelity proved most interesting. B. S. Yaplee, of the Naval Research Laboratory, has measured the distance to the moon so accurately that the principal errors are caused by lack of accurate knowledge of the earth's radius and the electron density between here and the moon.

A portion of the session called "Comet Comments" was devoted to very brief reports of attempts to observe the comet Orend-Roland and several others. Most of the results were negative, with a couple of interesting exceptions that will bear checking in the future.

Thermal radiation measurements of Venus, Niers, and Jupiter have been made by C. Mayer, of Naval Research Laboratory.

Radio Waves and Circuits

Commission VI on Radio Waves and Circuits was presided over by Samuel Silver, of the University of California. It largely concerned theory. In an introductory paper on diffraction and scattering theory, Dr. H. O. (Kip) Siegel, of the University of Michigan, presented some forward-looking ideas on scattering of electromagnetic waves from bodies with rotational symmetry. He indicated that many useful formulas can be obtained for complicated situations by extending certain classical problems. For example, the solution for the nose on back-scattering from the tip of a finite cone can be deduced from the infinite cone solution with the reflection from the base of the cone considered as a correction. The important correction term is obtained from an examination of the classical solution for a two-dimensional wedge.

Siegel's paper opened the way for a lively controversy as to the nature of the resonance phenomena occurring when the base of the cone was comparable in size to the wavelength. Dr. J. B. Keller, of New York University, attempted to show that some of the features of the back-scattering could be explained on the basis of his geometrical theory of diffraction.

The back-scattering from a circular loop was discussed by V. H. Weston, of the University of Toronto. He presented an exact solution in terms of toroidal wave functions, even though Maxwell's equation is non-separable in toroidal coordinates. Prof. Erik Hallen, of Sweden, pointed out that the solution for the thin circular loop has been known for many years, and it was possible to obtain a solution for the thick ring in terms of spherical wave functions for the far scattered field without using the toroidal coordinates. There was some discussion on the physical behavior of the ring in the resonance region and its similarity with the resonance effects for a finite cone.

Dr. H. E. Barlow, of England, presented the leading paper in the session on surface waves. He gave a useful and interesting account of the recent ideas on electromagnetic surface waves. Such waves are trapped at the interface of two

media, such as the surface of the ground, or may be guided along dielectric coated conductors or corrugated metal plates. The subject has been surrounded by controversy since 1909, when Sommerfeld presented an 80-page treatise in *Annalen der Physik*. Dr. Barlow showed that many of the features possessed by surface waves can be explained by simple physical arguments. In discussion following this paper, Dr. B. van der Pol, of Holland, indicated that if the source dipole in the Sommerfeld problem is energized by a transient current, the mathematical structure assumes a relatively simple form and the role of the controversial surface wave is clearly displayed.

Dr. S. A. Schelkunoff, of the Bell Telephone Laboratories, made some very pertinent remarks concerning the location of the poles and the branch point in the Sommerfeld integral. Further comments were made by N. Marcuvitz, of Brooklyn Polytechnic Institute, who made an eloquent plea to bury the Sommerfeld problem once and for all. The general consensus of opinion was that, while the classical problem has now been adequately solved, the extension to other types of surface waves which have very different features has lead to many misconceptions. The need for unifying the approach and terminology was stressed, and to this end a working party was formed to prepare a review of the whole subject before the next General Assembly. The members chosen by Prof. George Sinclair, of Canada, were Drs. Barlow (England), H. Bremmer (Holland), Cullen (England), Marcuvitz (U.S.A.), L. A. Veinstein (U.S.S.R.), and J. R. Wait (U.S.A.).

The radiation from surface waves was also considered. Jean Paul Simon, of Paris, disclosed some very recent advances in the design of the surface-wave antennas. The novelty lies in launching the surface waves on a structure with a modulated phase velocity. For certain conditions, it was found possible to produce very narrow beam widths with low side lobes from physically realizable structures. An example is the "cigar antenna," consisting of a dielectric rod with concentric metal disks of varying sizes. Some remarks concerning the mathematical aspects of such tapered surface-wave antennas were made by F. J. Zucker, of the Air Force Cambridge Research Center, who expounded on the concept that modulated surface waves can be analyzed in terms of (spacial) side bands in analogy to amplitude modulation in the time domain.

In the session on "Transition from Field Theory to Circuit Theory and to Optics," Prof. Chu (M.I.T.) described field solutions of Maxwell's equations, obtained by adding to the Poisson (static) solution a series expansion in powers of $j\omega$. The first term of the series gives the lumped circuit property. The subject is covered in "E.E. 6.03 Notes" by Chu, Tech. Store, M.I.T., Cambridge, Mass. Prof. van der Pol stated that the same method was published in 1922 or 1923 by Brillouin in *Radio Electricitie*. Prof. C. Manneback (Belgium) described his thesis done at M.I.T. in the 1920's, in which a Heaviside impulse-function approach led to the same results as Brillouin's and Chu's work in the frequency domain. Manneback also referred to the question of radiation. His results on radiation differed from those of Steinmetz's book on transients. Prof. van der Pol said the present topic was well known in the 1920's, and emphasized the duality of time-domain and frequency-domain formulations. He mentioned the thesis of Lenz done in collaboration with Sommerfeld, in which the lump circuit property of a coil was

developed from field theory. Prof. P. Grivet, of the University of Paris, France, suggested that a minimum theory for fields might yield circuit theory from another point of view.

Dr. Wu, from Harvard, described his corrections to the geometrical optics cross-section, using a series in ka. Prof. Morris Kline (NYU) mentioned the solution of Maxwell's equations in a power-series of $(1/j\omega)^n$ which reduces to geometrical optics for certain values of ω.

Dr. Veinstein (USSR) discussed group and phase velocity in a lossy medium. The audience pointed out that an appendix of Brillouin's book on old quantum theory discussed this subject. Congress Internationale d'Electricite, No. 100 7g 32-V.I was mentioned. Prof. J. B. Keller suggested that an integral transform would yield the group velocity in the presence of losses. This required the method of steepest descent when loss was present, but was straightforward with no loss.

Radio Electronics

Commission VII, devoted to radio electronics and embracing the entire range of electron physics, was under the chairmanship of Prof. G. A. Woonton, Canada.

Prof. P. W. Allis gave a comprehensive review of electron oscillations in gas discharges, treating growth and decay of plasma waves excited by electron beams. This topic is important, both for microwave devices and for ionospheric physics. Dr. L. S. Nergaard discussed the physics of the cathode, of importance in improving the life and efficiency of electron tubes.

Dr. J. R. Pierce introduced the session on the source and nature of noise in electron beams, of great significance in improving the performance of traveling wave amplifiers and oscillators. The theory of this noise builds on the theory of shot noise in the low-frequency diode, introduces transit time effects, velocity spread effects, and the propagation and growth of spare charge waves in the beam, interacting with neighboring electromagnetic fields. The present state of the field is that enough is known to be highly useful in the design of low-noise tubes, but too little is known for a satisfying understanding of all the phenomena involved.

Dr. Wm. Shockley reviewed physical principles of semiconducting devices for radio application. Also reported in this session was progress in understanding noise in semiconductors and semiconductor devices. In the earlier days of the transistor, electrical noise of the $1/f$ spectral distribution, often called "flicker effect," was a severe limitation on the usefulness of the device. Now, however, the magnitude of this noise, associated largely with macroscopic surface and volume conditions, has been greatly reduced, even below the level of shot noise, so that in some applications the transistor is less noisy than any available electron tube.

Perhaps the session which evoked the greatest interest was the one on the MASER, led by Prof. C. H. Townes, and held jointly with the other commissions. In this session, the entire field of non-equilibrium quantum mechanical devices was opened for consideration. As has been adequately reviewed elsewhere, a MASER is a quantum mechanical system which has been prepared in a non-equilibrium state, by virtue of which it may be stimulated by radiation of the proper frequency to emit coherently at this frequency, thus amplifying the original radiation or even sustaining oscillations. Two outstanding properties of great

practical advantage which these systems can be made to exhibit are extremely low noise figure as an amplifier, and extremely high spectral purity as an oscillator. Experimentally attained effective noise figures of -2 db (limited mainly by the temperature of the input circuit components) and spectral purities of one part in 10^{12} were reported for certain devices, with the theoretical expectation of much further improvement. Emphasized during the session was the huge variety of schemes for obtaining MASER action, from the simple two-energy level beam MASER through solid state two- or three-level MASER's depending on paramagnetic effects, adiabatic fast passage, and ferromagnetic effects. The availability of a low-noise figure amplifier is of great interest to the radio astronomers, who have already reached practical limits of sensitivity from antenna size and observation time, and who are able to increase sensitivity in detecting low-temperature radiations from outer space only by improving the noise figures of their amplifiers.

Contributed by
Technical Information Office,
BOULDER LABORATORIES, NATIONAL BUREAU OF STANDARDS,
U. S. DEPARTMENT OF COMMERCE,
Boulder, Colorado.
(Received November 18, 1957)

NOTICE

When available, single unbound volumes can be supplied at $6 each and single numbers at $2 each, postpaid.

Charges for reprints and covers

Reprints can be supplied, but prices have increased considerably and costs depend on the number of articles per issue for which reprints are requested. It is no longer possible to publish a schedule of reprint charges, but if reprints are requested approximate estimates will be given when galley proofs are sent to authors. Reprints without covers are least expensive; standard covers (with title and author) can be supplied at an additional charge. Special printing on covers can also be supplied at further additional charge.

Fifty reprints, without covers, will be given to institutions paying the publication charge of $8 per page.

Alterations

Major alterations made by authors in proof will be charged at cost. Authors are requested, therefore, to make final revisions on their typewritten manuscripts.

Orders for back issues and reprints should be sent to Editorial Office, 5241 Broad Branch Road, N.W., Washington 15, D. C., U.S.A.

Subscriptions are handled by The Editorial Office, 5241 Broad Branch Road, N.W., Washington 15, D. C., U.S.A.

CONTENTS—Concluded